UNIVERSITAT POLITÈCNICA DE CATALUNYA BARCELONATECH

PhD program in Natural Resources and Environment

Air quality inside city public commuting buses:

physico-chemical and biological characterisation

A thesis submitted by

Amaia Fernández Iriarte

Barcelona, May 2023

Supervisors:

Dr. Teresa Moreno Pérez

(IDAEA-CSIC)

Dr. Fulvio Amato

(IDAEA-CSIC)

Tutor:

Dr. M. Montserrat Solé Sardans

(EPSEM-EMIT)

idaea INSTITUTE OF ENVIRONMENTAL ASSESSMENT AND WATER RESEARCH

EXCELENCIA SEVERO OCHOA

CSIC CONSEJO SUPERIOR DE INVESTIGACIONES CIENTÍFICAS

This thesis was carried out supported by the Spanish Ministry of Economy, Industry and Competitiveness with FEDER funds (BUSAIR CGL2016-79132-R). Grateful to Transports Metropolitans de Barcelona (TMB) for their cooperation throughout the whole project and to Laval University from Quebec, Canada, for the technical support and for the internship where bioaerosol samples were analysed (PCR, sequencing, endotoxins). Funding from the Generalitat de Catalunya (AGAUR 2017 SGR41) is also acknowledged. As well as some travel expenses for A FI were provided through CD Discovery Grant (National Sciences and Engineering Council of Canada-NSERC).

ACKNOWLEDGEMENTS

Me gustaría agradecer a todas las personas que he tenido cerca el apoyo que he sentido durante el largo recorrido de la tesis. A las que ya estaban y las que han venido.

Pero antes de eso, lo primero de todo a mis directores, Teresa Moreno y Fulvio Amato, por haberme dado esta oportunidad, por todo lo que me habéis enseñado y sobre todo a Tere, por haber continuado conmigo incluso en los momentos más difíciles. Gracias a todo el grupo EGAR. A Rai, por el logo tan chulo que hizo para mi estudio. Además de la oportunidad que he tenido de poder hacer estancias en el extranjero, las que me han enseñado mucho profesionalmente y también personalmente. Han sido unas experiencias inolvidables. I would like to thank, first, to Caroline Duchaine, it was a really good experience to be in your lab. I have learned a lot about microbiology, it was a pleasure to be working with you and all the members of your lab (Hamza, Jodelle, Joanie, Pamela…). You have been very helpful not only inside the lab, but also after work, I have had a really good moment with you! Also, to Helsinki… it was a hard experience, but I have learned a lot about myself. Thanks people!

A pesar de toda la ayuda profesional que haya podido tener, sin mi familia y seres queridos esto no hubiera podido salir adelante. En especial quiero dedicar esta tesis a una persona muy importante, la persona por la que he sacado fuerzas de donde ya creía que no había, a ti, Aita, mila esker erakutsi didazun guztiagatik espero det zure eredua jarraitu ahal izatea, beti zaitut nerekin. Noski, nere amari baita ere, bizitako momento zail honetatik aurrera egiteko indarrak atera eta sostengu izaten ari dena. Nire ahizpari, Maider, oso pertsona garrantzitsua izan dena prozesu guzti honetan, berarekin kontatu ahal izan dudalako presentzialki. Eskerrik asko familia!

Nire amoñari ere eskerrak eman nahi dizkiot, zaintzen gaituen modua ezin hobea delako, eta asko ikasi behar dugu hortik. Gainontzeko familiari ere, izeba-osabak (Ana, Ainhoa, Karmele, Alberto, Juanjo, Mikel eta Leti) eta lehengusinak (Maria, Leire, Ander, Marco, Jon eta Leire) beti gertu sentitzen zaituztet. Amama, aitaita eta aitona, zuek ere lagundu didazue honeaino iristen.

Nire lagun minari, Ane Adellac, berarekin hitz egitea osasungarria delako, eta nire bizitzako pilaretako bat delako. Patri eta Ane, zuei ere eskertu nahi dizuet, beti alboan egon zaretelako. Ane Iturbide eta Petrillari ere, bizitza zeharo aldatu egin zaigu! Gehien alaitzen nauen pertsonari, indarrak eman eta momento hau arinagoa izaten laguntzen didana, Iker, zuk errexagoa egiten duzu.

Bartzelonan, bizitako momentuak ez ditut inoiz ahaztuko, Dani, Eugenia, Marta, Alejandra, Agus, Jorge, eta nire ahizparen zirkuluari ere eskertu nahi diot, oso momentu onak bizitu ditudalako zuekin, errepikatuko nituzkeenak. Masterreko lagunei ere, Maria Pau, Albert, Pedro, Laurak, Sandra, Rai, Marc, Andreu… Zuekin batera Bartzelona ezagutzen hasi nintzen. Sonia eta Albari ere, naiz eta urruti bizi beti gertu sentitzen zaituztet!

Nire pisukideei ere eskertu nahi diet, hasteko Xec eta Annari, hauek ere laguntza handikoak izan dira. Julia eta Noeliari baita ere, erreflexio handiak izan ditugu. Hortik ere Ariadna, nire sirena, berari ere eskertu nahi diot, gertuko pertsona sentitu dudana.

Eta iritsi direnei, bereziki nire arima bixkiei, Claudia eta Inma, zuekin bai denari buruz hitz egin daitekeela, habéis sido un descubrimiento y aunque haya distancia de por medio, sé que esta relación perdurará. Bestalde, nire ofizinako lagun guztiei, beti laguntzeko prest eta irrifarre bat atera nahiean egon direnak, Marta Vía, Jesús Yus eta Adolfo. Gainera ere María Izquierdo eta Garay Sosari, beti prest laguntzeko egon direnak.

Nire psikologari, Letiri, yogako irakasleari, Vanessari, eta masajistari, Maiteri, ere eskertu nahi diet, aurrera pausoak ematen laguntzen didatenak. Azkenik nere lagun berriei, Celso eta Kepa, mila esker zuekin konpartitzen dudan ostiral bakoitzari. Ez gera egoera on batengatik ezagutu, baina konexioa hasieratik sortu zen, eta orain nire familiakoak bihurtu zarete. Ekoliderretan ere ezagutu ditudan kide guztiei, eta Leireri bereziki, bi gauzak konpaginatzen lagundu eta beti aurpegi eta hitz onekin goxatzeagatik. Mila esker!

Barcelona, May 2023

ABSTRACT

People living in urban areas usually spend a considerable amount of their daily time commuting, with most public transport journeys in the EU (56 %) made using bus systems. The commuting bus system in Barcelona is particularly interesting from an air quality viewpoint. The city transport operator (*Transports Metropolitans de Barcelona*, TMB) is actively in the process of renovating its bus fleet and so currently has a mixture of buses powered by different engines. Of additional interest is the fact that the distinctive city geography, with its sloping coastal piedmont means that buses following "vertical" routes through the city, moving up and down the piedmont, may well have different emission patterns from those operating along "horizontal" routes parallel to the coastline.

Despite the undoubted efficiency of bus travel, several studies have revealed poor air quality on bus indoor environment. Several of these studies have concluded that a significant portion of air pollutants in buses is due to self-pollution. More obvious influences include opening windows during driving, starting up and idling of the bus, and opening bus doors, all of which can produce higher in-bus exposures, although background concentrations may also have a significant role. We have reached the stage where the available information needs to be overviewed and compared in a well-focussed and comprehensive study aimed at identifying the effects of as many variables as possible.

The primary objective of this PhD Thesis is to make a comprehensive multidisciplinary benchmark study of indoor commuting bus air quality, identifying the factors that control the concentrations of inhalable particles, pollutant gases and bioaerosols inside public buses in Barcelona. This was achieved by following a methodology involving physical measurements, chemical analyses, and data analysis.

Given the fact that the BCN bus fleet is in the process of active renovation, only buses in operation since 2005 were included in the study. The TMB fleet has a total of 1140 vehicles (39 % diesel, 34 % compressed natural gas, 27 % hybrid and 1 % electric (EV)), and 101 routes covering a total length of 830 km with 2590 bus stops. An intensive measurement campaign in the Barcelona bus system was performed in two campaigns. The campaigns for this Thesis were conducted in a warmer (May – September 2017) and a colder (November 2017 – March 2018) periods being defined according to the TMB annual ventilation protocols to ascertain seasonal differences, to provide maximum contrast in weather, and therefore ventilation conditions. Buses of each fuel-type were selected by pairs (along vertical, horizontal, and other mixed routes) for simultaneous return trips through the city

by two commuters. Simultaneous journeys of approximately two hours duration (one way and return) were performed, each carrying a rucksack filled with the same selection of air quality monitoring equipments. Number and size of quasi-ultra fine particles (QUFP), black carbon (BC), $PM_{2.5}$, PM_{10}, CO_2, CO, NO_2 and O_3 (on-line) and filters for chemical analyses and bioaerosols were measured to characterise PM, investigating its variability, to better understand the main factors controlling it, and therefore the way to improve air quality. Outdoor ambient concentrations were measured concurrently at an urban background station (UB), which was used as a reference site. Measurements inside the buses were performed in 11 lines in Barcelona.

Results showed that air quality inside buses is a mixture of different variables. This might be associated to differences in the age of the bus, outdoor air quality, the zones transited (traffic), ventilation, passenger densities, self-pollution, routes (sloped (vertical) vs. levelled (horizontals)). In the Barcelona bus system, the ancillary measurements indicated that no significant differences were observed between the middle and rear positions inside a bus, allowing to place them in the middle. Mean values of the pollutants were 2 (QUFPN) to 2.5 (BC and $PM_{2.5}$) times higher than urban background concentrations. In general, electric vehicles are characterized by the lowest QUFPN, BC and $PM_{2.5}$ values, whereas diesel buses show the highest ones, although there are wide ranges and much interquartile overlap between all the different fuel/engine type buses. QUFP size modes were very similar inside all the buses, being a useful indicator for the relative amount of fresh traffic-related particle emissions inside a road vehicle. BC concentrations all align around the same median value, with the only exception for diesel buses, whose BC average and top values are visibly higher than those of the other buses, that could be related to self-pollution. Air quality measured as number concentrations of QUFP inside buses can be noticeably influenced by city background levels in outside air, infiltration of traffic emissions at highly polluted locations. Individual journeys record BC levels punctuated by transient peaks that can exceed 10 times average background. Such peaks in mass concentrations inside buses coincide with road traffic hotspots, tunnels, and urban background levels. As seen with QUFP number concentration and BC levels, average $PM_{2.5}$ mass concentrations inside buses can be strongly affected by outdoor urban background air quality. $PM_{2.5}$ average concentration breathed while travelling by tourist bus for example can be less than 50 % below normal on clear, clean winter days with low levels of urban background pollution. The vertical routes and diesel buses (non-tourist) showed the highest concentrations of QUFPN and BC, being horizontal routes mean/median concentrations 25-30 % lower than vertical routes, mainly related to the slopes that generates more tailpipe emissions due to the extra effort of the

engine (exhaust emissions), and friction in the brakes and wheels wear out (non-exhaust emissions), contributing to self-pollution. Furthermore, most of the pollutants concentrations in the warmer period were higher, but $PM_{2.5}$ was higher in the colder period. Concentrations of CO_2 inside buses depend directly on the number of passengers, and therefore are influenced by outside air entry through doors and windows, and the ventilation system. CO_2 levels can then be considered a good proxy of the correct ventilation and the circulation between indoor and outdoor air.

Chemically, $PM_{2.5}$ inside buses showed organic compounds being dominated by alkanes and aromatics. OC was the most abundant element followed by EC, on average OC/EC = 3.4. The trace elements with highest enrichment inside buses $PM_{2.5}$ were Zn and Cu, followed by Zr, Ti, Mn, Cr, Ni, Sb, Sn, V, Sr, Pb, Hf, Ce, and La. The distributions of the relative contributions of the different components to the bulk $PM_{2.5}$ were similar at the compared pairs of different fuel/engine type buses. Taken overall, EV buses show relatively lower average concentrations of many $PM_{2.5}$ components compared to diesels. $PM_{2.5}$ chemistry for each of these two seasons is quite different, with the winter samples being noticeably richer in mineral dust and slightly more carbonaceous, including a quite spectacular enrichment in Cu and Sb. Summer is noticeably richer in Na, Mg, V, Ni, Cr and SO_4^{2-}, greater influence of marine aerosols contaminated by shipping emissions in summer. Vertical routes showed on average higher concentrations of carbon content and mineral dust than horizontal ones. Elements such as Cu and Sb (especially), Mg and K also occur in in > 50 % higher inside buses running along V routes. Reflecting greater use of brakes on the routes with higher gradient. A source apportionment analysis by PMF allowed the identification of two main sources. One from passenger emissions, such as textile fibres and skin flakes (46 %) dominated by OC, and the other, infiltrated vehicle exhaust and brake wear particles (19 %). Road and urban dust, regional sulphate and shipping and industrial metalliferous particles sources were also identified.

Low concentrations of total airborne bacteria were detected inside the buses of Barcelona. 80 % of relative abundance of *Actinobacteria* and *Proteobacteria* were the most abundant phyla inside all the fuel type buses and in both floors of tourist buses. The presence of humans was the main source of contamination of bacteria inside the buses. Differences between seasons were observed, relative abundance of the different taxonomic genera decreases from summer to winter. The air exchange in this microenvironment should be always optimized to reduce commuters' exposure to potentially harmful microbes. Hence, control actions on this source are essential to achieve better air quality inside the bus.

RESUMEN

Las personas que viven en zonas urbanas suelen dedicar una parte considerable de su tiempo diario a desplazarse, y la mayoría de los viajes en transporte público en la UE (56 %) se realizan utilizando sistemas de autobuses. El sistema de autobuses urbanos de Barcelona es especialmente interesante desde el punto de vista de la calidad del aire. El operador de transporte de la ciudad (Transports Metropolitans de Barcelona, TMB) está renovando activamente su flota de autobuses, por lo que actualmente cuenta con una mezcla de autobuses propulsados por diferentes motores. También es interesante el hecho de que la peculiar geografía de la ciudad, con su piedemonte costero en pendiente, hace que los autobuses que siguen rutas "verticales" a través de la ciudad, subiendo y bajando por el piedemonte, puedan tener patrones de emisión diferentes de los que operan a lo largo de rutas "horizontales" paralelas a la línea de costa.

A pesar de la indudable eficiencia de los viajes en autobús, varios estudios han revelado la mala calidad del aire en el interior de los autobuses. Varios de estos estudios han llegado a la conclusión de que una parte significativa de los contaminantes del aire en los autobuses se debe a la autocontaminación.

El objetivo principal de esta Tesis Doctoral es realizar un estudio multidisciplinar exhaustivo de referencia sobre la calidad del aire en el interior de los autobuses, identificando los factores que controlan las concentraciones de partículas inhalables, gases contaminantes y bioaerosoles en el interior de los autobuses públicos de Barcelona. Para ello se ha seguido una metodología que incluye mediciones físicas, análisis químicos y análisis de datos.

Dado que la flota de autobuses de BCN está en proceso de renovación activa, sólo se incluyeron en el estudio los autobuses en funcionamiento desde 2005. La flota de TMB cuenta con un total de 1140 vehículos (39 % diésel, 34 % gas natural comprimido, 27 % híbridos y 1 % eléctricos (EV)), y 101 rutas que cubren una longitud total de 830 km con 2590 paradas de autobús. Se realizó una campaña de medición intensiva en el sistema de autobuses de Barcelona en dos campañas. Las campañas para esta Tesis se llevaron a cabo en un periodo más cálido (mayo - septiembre 2017) y otro más frío (noviembre 2017 - marzo 2018) siendo definidos de acuerdo con los protocolos anuales de ventilación de TMB para determinar las diferencias estacionales, para proporcionar el máximo contraste en el clima, y por lo tanto en las condiciones de ventilación. Se seleccionaron autobuses de cada tipo de combustible por parejas (a lo largo de rutas verticales, horizontales y otras mixtas) para viajes simultáneos de ida y vuelta a través de la ciudad por parte de dos viajeros. Se realizaron viajes

simultáneos de aproximadamente dos horas de duración (ida y vuelta), llevando cada uno de ellos una mochila cargada con la misma selección de equipos de control de la calidad del aire. Se midieron el número y el tamaño de las partículas cuasi ultrafinas (QUFP), carbono negro (BC), $PM_{2.5}$, PM_{10}, CO_2, CO, NO_2 y O_3 (en línea) y los filtros para análisis químicos y bioaerosoles con el fin de caracterizar las PM, investigar su variabilidad, comprender mejor los principales factores que las controlan y, por tanto, la forma de mejorar la calidad del aire. Las concentraciones ambientales en el exterior se midieron simultáneamente en una estación de calidad del aire de fondo urbano (UB), que se utilizó como lugar de referencia. Las mediciones en el interior de los autobuses se realizaron en 11 líneas de Barcelona.

Los resultados mostraron que la calidad del aire en el interior de los autobuses es una mezcla de distintas variables. Esto podría estar asociado a diferencias en la edad del autobús, la calidad del aire exterior, las zonas transitadas (tráfico), la ventilación, las densidades de pasajeros, la autocontaminación, las rutas (verticales frente a horizontales). En el sistema de autobuses de Barcelona, las mediciones auxiliares indicaron que no se observaban diferencias significativas entre las posiciones central y trasera del interior de un autobús, lo que permitía situarlas en el centro. Los valores medios de los contaminantes fueron de 2 (QUFPN) a 2.5 (BC y $PM_{2.5}$) veces superiores a las concentraciones de fondo urbano. En general, los vehículos eléctricos se caracterizan por presentar los valores más bajos de QUFPN, BC y $PM_{2.5}$, mientras que los autobuses diésel muestran los más altos, aunque existen amplios rangos y mucho solapamiento intercuartílico entre todos los autobuses de distinto tipo de combustible/motor. Los modos de tamaño de QUFP fueron muy similares dentro de todos los autobuses, siendo un indicador útil de la cantidad relativa de emisiones de partículas frescas relacionadas con el tráfico dentro de un vehículo de carretera. Las concentraciones de BC se alinean todas en torno al mismo valor medio, con la única excepción de los autobuses diésel, cuyos valores medios y máximos de BC son visiblemente superiores a los de los demás autobuses, lo que podría estar relacionado con la autocontaminación. La calidad del aire medida como concentraciones numéricas de QUFP en el interior de los autobuses puede verse notablemente influida por los niveles de fondo de la ciudad en el aire exterior, la infiltración de las emisiones del tráfico en lugares muy contaminados. Los viajes individuales registran niveles de BC puntuados por picos transitorios que pueden superar 10 veces la media de fondo. Estos picos en las concentraciones de masa en el interior de los autobuses coinciden con puntos conflictivos del tráfico rodado, túneles y niveles de fondo urbano. Como se ha visto con la concentración de número de QUFP y los niveles de BC, las concentraciones medias de masa de $PM_{2.5}$ en el interior de los autobuses pueden verse muy afectadas por la calidad del aire de fondo urbano exterior. Las concentraciones medias de $PM_{2.5}$

respiradas durante un viaje en autobús turístico, por ejemplo, pueden ser inferiores al 50 % de lo normal en días claros y limpios de invierno con bajos niveles de contaminación urbana de fondo. Las rutas verticales y los autobuses diésel (no turísticos) mostraron las mayores concentraciones de QUFPN y BC, siendo las rutas horizontales concentraciones medias/medianas un 25-30 % inferiores a las rutas verticales, principalmente relacionadas con las pendientes generando más emisiones por el tubo de escape debido al esfuerzo adicional del motor (exhaust) que generan más fricción en los frenos y desgaste de las ruedas (non-exhaust), contribuyendo a la autocontaminación. Además, la mayoría de las concentraciones de contaminantes en el periodo más cálido fueron más altas, pero las $PM_{2.5}$ fueron más altas en el periodo más frío. Las concentraciones de CO_2 en el interior de los autobuses dependen directamente del número de pasajeros y, por tanto, se ven influidas por la entrada de aire exterior a través de puertas y ventanas y por el sistema de ventilación. Así pues, los niveles de CO_2 pueden considerarse un buen indicador de la correcta ventilación y circulación entre el aire interior y el exterior.

Químicamente, las $PM_{2.5}$ en el interior de los autobuses mostraban compuestos orgánicos dominados por alcanos y aromáticos. El OC fue el elemento más abundante seguido del EC, con una media OC/EC = 3.4. Los oligoelementos con mayor enriquecimiento dentro de las $PM_{2.5}$ de los autobuses fueron Zn y Cu, seguidos de Zr, Ti, Mn, Cr, Ni, Sb, Sn, V, Sr, Pb, Hf, Ce y La. Las distribuciones de las contribuciones relativas de los distintos componentes a las $PM_{2.5}$ a granel fueron similares en los pares comparados de autobuses de distinto tipo de combustible/motor. En conjunto, los autobuses eléctricos muestran concentraciones medias relativamente más bajas de muchos componentes de $PM_{2.5}$ en comparación con los diéseles. La química de las $PM_{2.5}$ en cada una de las dos estaciones es bastante diferente, siendo las muestras de invierno notablemente más ricas en polvo mineral y ligeramente más carbonosas, incluyendo un enriquecimiento bastante espectacular en Cu y Sb. El verano es notablemente más rico en Na, Mg, V, Ni, Cr y SO_4^{2-}, mayor influencia de los aerosoles marinos contaminados por las emisiones del transporte marítimo en verano. Las rutas verticales mostraron por término medio mayores concentraciones de contenido en carbono y polvo mineral que las horizontales. Elementos como el Cu y el Sb (especialmente), el Mg y el K también aparecen en > 50 % más en el interior de los autobuses que circulan por rutas V. Esto refleja un mayor uso de los frenos en las rutas con mayor pendiente. Un análisis de reparto de fuentes realizado por PMF permitió identificar dos fuentes principales. Una procedente de las emisiones de los pasajeros, como fibras textiles y escamas de piel (46 %) dominada por OC, y la otra, partículas infiltradas de los gases de escape de los vehículos y del desgaste de los frenos (19 %). También se identificaron fuentes de polvo urbano y de

carretera, de sulfatos regionales y de partículas metalíferas industriales y del transporte marítimo.

Se detectaron bajas concentraciones de bacterias totales transportadas por el aire en el interior de los autobuses de Barcelona. El 80 % de la abundancia relativa de Actinobacteria y Proteobacteria fueron los filos más abundantes en el interior de todos los autobuses de tipo combustible y en ambas plantas de los autobuses turísticos. La presencia humana fue la principal fuente de contaminación bacteriana en el interior de los autobuses. Se observaron diferencias entre estaciones, la abundancia relativa de los diferentes géneros taxonómicos disminuye de verano a invierno. El intercambio de aire en este microambiente debería optimizarse siempre para reducir la exposición de los viajeros a microbios potencialmente dañinos. Por lo tanto, las acciones de control sobre esta fuente son esenciales para lograr una mejor calidad del aire en el interior del autobús.

CONTENTS

LIST OF TABLES AND FIGURES

ACRONYMS

#/cm³	Unit of QUFPN (number of particles per cubic centimeter)
µg/m³	Unit of $PM_{2.5}$ and BC (micrograms per cubic metre)
µm	Micrometres
AB	All buses
AC	Air-conditioning
Al_2O_3	Aluminium oxide
amu	atomic mass unit
As	Arsenic
Ba	Barium
BaP	Benzo(a)pyrene
BC	Black carbon
BT	Tourist bus blue route
BTEX	It is an acronym that stands for Benzene, Toluene, Ethylbenzene, and Xylenes. These compounds are some of the Volatile Organic Compounds (VOCs)
C_6H_6	Benzene
Ca	Calcium
Cd	Cadmium
CFC	Closed-faced cassettes
Chao1	Richness estimator of bacteria in a sample
CNG	Compressed natural gas
CO	Carbon monoxide
CO_2	Carbon dioxide
COVID-19	A virus, *SARS-CoV-2*
CRT	Continuously Regenerating
Cu	Copper

DALYs	Disability-adjusted life-years
DL	Detection limits
DPF	Diesel particulate filters
E. coli	*Escherichia coli*, a bacterium
EC	Elemental carbon
EC	European Commission
equiv./m³	Microbial concentrations were expressed in *E. coli* genome equivalent/m³
EU	European Union
EU/m³	Endotoxin concentrations were expressed as endotoxin units per cubic meter of air
EURO	Emissions from road vehicles have been controlled by European legislation since the 1970s. To meet the increasingly stringent requirements of the legislation, vehicle manufacturers have continually improved engine technologies and have introduced various emission-control systems. Control on road traffic emissions is carried out by means of the EURO certification since 1992
EV	Electric
FASTQ	Is a text-based format for storing both a biological sequence (usually nucleotide sequence) and its corresponding quality scores
Fe	Iron
GA	Geometric average
GC	Gas chromatograph
genomes/m³	Unit to count bacterium concentration
GF	Glass fibre
GPS	Global Positioning System
GVW	Gross vehicle weight
HCNG	Hybrid of CNG
HD	Hybrid of diesel
Hx or H	"Horizontal" routes

ICP-AES	Inductively Coupled Plasma - Atomic Emission Spectrometry
ICP-MS	Inductively Coupled Plasma - Mass Spectrometry
IQR	Interquartile range
K	Potasium
KED	Kinetic energy discrimination
Kinetic-QCL™	Kinetic-QCL™ is a quantitative, kinetic assay for the detection of Gram-negative bacterial endotoxin
LAL	Limulus Amebocyte Lysate
LEZ	Low Emission Zone
Mg	Magnesium
Mn	Manganese
MSD	Mass spectrometry detector
Na	Sodium
NDIR	Non-dispersive infrared
NH_3	Ammonia
NH^{4+}	Ammonium
Ni	Nickel
nm	Nanometres
NO_2	Nitrogen dioxide
NO_3^-	Nitrate
NO_X	Nitrogen oxides
O_3	Ozone
OC	Organic carbon
OTUs	Operational taxonomic units
PAH	Polycyclic aromatic hydrocarbons
Pb	Lead
PD	Phylogenetic diversity
PM	Particulate matter

PM_{10}	Particles with an aerodynamic diameter between 2.5 and 10 μm
$PM_{2.5}$	Particles with an aerodynamic diameter less than 2.5 μm
PMF	Positive Matrix Factorization
PN	Particle number
ppm	Parts per million
qPCR	qPCR stands for quantitative polymerase chain reaction and is a technology used for measuring DNA using PCR (Polymerase chain reaction is a laboratory technique for rapidly producing (amplifying) millions to billions of copies of a specific segment of DNA, which can then be studied in greater detail. PCR involves using short synthetic DNA fragments called primers to select a segment of the genome to be amplified, and then multiple rounds of DNA synthesis to amplify that segment
QUFP	Quasi-ultrafine particle (10-300 nm)
QUFPN	Quasi-ultrafine particle number
r	Ratio
Rj	Recovery rates
RT	Tourist bus red route
Sb	Antimony
SCR	Selective catalytic reduction
SCRT	CRT + SCR
SD	Standard deviation
SIC	Secondary inorganic compounds
Sn	Tin
SO_2	Sulphur dioxide
SO_4^{2-}	Sulphate
SOx	Sulphur oxides
Sr	Strontium
T60	Teflon-coated borosilicate glass fibre
TBin	Inside tourist bus or down-floor or lower floor or downstairs

TBout	Outside tourist bus or upper floor or open top floor or upstairs
TD	Thermal desorption
Ti	Titanium
TMB	Transports Metropolitans de Barcelona
TRAPs	Traffic related air pollutants
UB	Urban background
UFP	Ultra-fine particle
V	Vanadium
VOCs	Volatile organic compounds
Vx or V	"Vertical" routes
Zn	Zinc

GLOSSARY

Actinobacteria	Phylum and class of Gram-positive bacteria that can be ubiquitously distributed in both terrestrial and aquatic ecosystems
Bioaerosols	Biological material that can be found in the atmosphere as airborne (pollen, spores, microorganisms and vegetal or insect debris, among others)
Boxplot	A simple way of representing data on a plot in which a rectangle is drawn to represent the second and third quartiles, usually with a vertical line inside to indicate the median value. The lower and upper quartiles are shown as horizontal lines either side of the rectangle
Bradyrhizobium	Bacterium inside Genera taxonomic category (nitrogen atmospheric fixator)
Brevundimonas	Bacterium inside Genera taxonomic category (related to human)
Burkholderia	Bacterium inside Genera taxonomic category (organic matter recycling)
Chitinophagaceae	Bacterium isolated from freshwater sediment
Chloroplast	Bacterium inside Genera taxonomic category (ubiquitous)
Cladosporium sp.	Fungi or hyphae (good marker for outdoor contamination and is a common indoor fungus)
Coarse particles	Particles with a larger aerodynamic diameter than 2.5 μm, $PM_{2.5-10}$
Corynebacteriaceae	Bacterium inside Genera taxonomic category (ubiquitous)
Corynebacterium	Bacterium inside Genera taxonomic category (human skin or body)
Crustal matter	Mineral dust
Cutibacterium	Bacterium inside Genera taxonomic category (human skin or body)
Deinococcus-Thermus	Bacterium inside Phylum taxonomic category (bacterial phylum)
Dermacoccaceae	Bacterium inside Genera taxonomic category (related to human)
Endotoxins	Are a component of the outer membrane of Gram-negative bacteria, which can be pathogen
Enhydrobacte	Bacterium inside Genera taxonomic category (related to human)
Enhydrobacter	Bacterium inside Genera taxonomic category human skin microbiota, plants, environmental bacteria, and some of them can be opportunistic pathogen for human

Ferruginibacter	Bacterium inside Genera taxonomic category from the family of *Chitinophagaceae*
Fibrobacteres	Bacterial Phylum (ruminant animal stomach)
Fine particles	Particles with an aerodynamic diameter less than 2.5 μm, $PM_{2.5}$
Fusobacteria	Bacterial Phylum (related with aquatic ecosystem, human oral microbiome, or widespread in the environment)
Genus level	A genus is a taxonomic rank comprised of species grouped based on shared attributes (having similar structures or distinct characteristics) or being phylogenetically related. It is one of the eight major taxonomic ranks in the biological classification of living things. It is below the family and above the species
Geodermatophilaceae	Bacterium inside Genera taxonomic category (ubiquitous)
Intracellular particles	Particles smaller than 40 nm in size
Kocuria	Bacterium inside Genera taxonomic category (ubiquitous)
Mann–Whitney *U* test	In statistics, it is a nonparametric test of the null hypothesis that, for randomly selected values X and Y from two populations, the probability of X being greater than Y is equal to the probability of Y being greater than X. It can also be called the Mann–Whitney–Wilcoxon (MWW/MWU), Wilcoxon rank-sum test, or Wilcoxon–Mann–Whitney test
Massilia	Bacterium inside Genera taxonomic category (related to human)
Methylobacterium	Bacterium inside Genera taxonomic category (human skin microbiota, plants, environmental bacteria, and some of them can be opportunistic pathogen for human)
Microbacterium	Bacterium inside Genera taxonomic category (ubiquitous)
Mucilaginibacter	Bacterium inside Genera taxonomic category (human skin microbiota, plants, environmental bacteria, and some of them can be opportunistic pathogen for human)
Nanoparticles	Particles smaller than 30 nm in size
Neisseria	Bacterium inside Genera taxonomic category (human microbiota)
Nitrospirae	Bacterial Phylum (related with aquatic ecosystem, human oral microbiome, or widespread in the environment)
Nocardia	Bacterium inside Genera taxonomic category (encountered in soils around the world rich in organic matter
Outlier	An outlier is a single data point that goes far outside the average value of a group. Outliers may be exceptions that stand outside individual samples of populations as well.

Paracoccus	Bacterium inside Genera taxonomic category (environmental)
Patescibacteria	Bacterial Phylum (related with aquatic ecosystem, human oral microbiome, or widespread in the environment)
Penicillium/Aspergillus sp.	Fungi or hyphae (markers of water damages (flood), condensation and humidity)
Planctomycetes	Bacterial Phylum (related with aquatic ecosystem, human oral microbiome, or widespread in the environment)
Prevotella	Bacterium inside Genera taxonomic category (human skin or body)
Primary aerosols	Aerosols that are directly emitted
Proteobacteria	The largest bacterial Phylum, with six classes and over 116 families
Proxy	In statistics, a proxy or proxy variable is a variable that is not in itself directly relevant, but that serves in place of an unobservable or immeasurable variable.
Pseudomonas	Bacterium inside Genera taxonomic category (related to human)
Rhizobium	Bacterium inside Genera taxonomic category (human skin microbiota, plants, environmental bacteria, and some of them can be opportunistic pathogen for human)
Roseomonas	Bacterium inside Genera taxonomic category (human skin microbiota, plants, environmental bacteria, and some of them can be opportunistic pathogen for human)
Rubellimicrobium	Bacterium inside Genera taxonomic category (ubiquitous)
Secondary aerosols	Aerosols that are formed in the atmosphere
Self-pollution	Contamination present inside the moving vehicle as being a result of emissions from the bus itself
Sphingomonas	Bacterium inside Genera taxonomic category (environmental)
Spirochaetes	Bacterial Phylum (related with aquatic ecosystem, human oral microbiome, or widespread in the environment)
Staphylococcus	Bacterium inside Genera taxonomic category (human microbiota)
Stomatobaculum	Bacterium inside Genera taxonomic category (isolated from the human dental plaque)
Streptococcus	Bacterium inside Genera taxonomic category (related to human)
Taxa	Taxon (singular) and taxa (plural), any unit used in the science of biological classification, or taxonomy. Taxa are arranged in a

	hierarchy from kingdom to subspecies, a given taxon ordinarily including several taxa of lower rank
Verrucomicrobia	Bacterial Phylum (related with aquatic ecosystem, human oral microbiome, or widespread in the environment)

CHAPTER 1: INTRODUCTION

1. INTRODUCTION

1.1. Urban Air Pollution

Air pollution is defined as a mix of substances that exists in the ambient air due to natural or man-made sources and may have harmful effects on human health and/or the environment (Mészáros 1999; EC, 2008).

Currently 55 % of the world's population lives in urban areas, a number that is expected to increase to 68 % by 2050 (UN DESA, 2019). High levels of urbanization are related to serious air pollution problems, affecting human health and well-being (Banzhaf et al., 2014). Therefore, the quality of the air breathed in this environment is of utmost importance for the inhabitants, and thus atmospheric pollution research has increased considerably, due to its high importance for both environmental and health policies. This requires an increase in knowledge of the different factors and processes that are involved: the sources emitting pollutants into the atmosphere, their transport, the chemical and physical transformations and deposition of the pollutants, and their effects. Urban air quality is affected by many anthropogenic sources including industry, construction and demolition, emissions from homes and businesses, and especially traffic. It is reported that over 70–80 % of air pollution in mega cities in developing nations is attributed to vehicular emissions caused by a large number of older vehicles coupled with poor vehicle maintenance, inadequate road infrastructure and low fuel quality (Molina and Molina, 2002; Badami, 2005; Anjaneyulu et al., 2006; Molina et al., 2007; Wang et al., 2010; Singh et al., 2018). The most critical pollutants responsible for deteriorating urban air quality are nitrogen oxides (NO_X), ozone (O_3), carbon monoxide (CO), particulate matter (PM) and volatile organic compounds (VOCs).

Regarding gaseous pollutants, NO_x are produced from the reaction of nitrogen and oxygen gases in the air during combustion at high temperatures. They are produced from fuel combustion processes, and are mostly emitted by power stations, vehicles, and industrial and domestic combustion processes, but in the cities the road transport is the major cause. In addition, NO_x contributes to the formation of PM and ground level ozone, the latter being a pollutant harmful for human health, that is not directly emitted to the atmosphere, but rather formed because of chemical reaction between NO_x and VOCs under the stimulation from sunlight. NO_x can deteriorate the respiratory system and cause inflammation of the airways at high levels (EEA, 2019). Long term exposure, on the other hand, can decrease lung function and increase the response to allergens.

CO is a highly toxic, colourless, odourless, and tasteless air pollutant. CO is produced in the incomplete combustion of fossil fuels such as gasoline, natural gas, oil, coal, and wood. Thus, the largest anthropogenic source of CO is related to vehicle emissions, therefore being a problem in high traffic locations.

VOCs can evaporate at ambient temperatures as they are compounds that have low boiling point. These compounds are harmful to human health (EPA, 2022). Sources of VOCs include fuels, oil-dissolving solvents, paints, cosmetics, varnishes, waxes, cleansers, disinfecting, and glues. They can be also produced from smoking and burning of fuel.

Particles in the atmospheric environment, in addition to those occurring in gaseous form, constitute a major class of pollutants (Morawska and Salthammer, 2003), affecting air quality and, in turn, ecosystem and human well-being with major health effects like respiratory diseases, cardiovascular functions and lung cancer. The concentration of PM ($PM_{2.5}$, particles with an aerodynamic diameter less than 2.5 μm; and PM_{10}, particles with an aerodynamic diameter between 2.5 and 10 μm) is a metric most often used to indicate the quality of air in urban environments.

1.1.1. Formation processes and emission sources

Aerosols are a suspension of solid and/or liquid particles in a fluid. In the case of atmospheric aerosols, this fluid is the air (Seinfeld and Pandis, 2006). These particles, also known as particulate matter, can be originated from a wide variety of anthropogenic stationary and mobile sources as well as natural sources. Particles may be directly emitted (primary aerosols) or formed in the atmosphere (secondary aerosols) because of chemical reactions between gaseous components (gas-to-particle conversion), between gaseous components and pre-existing particles (condensation), or between different pre-existing particles (coagulation; Warneck, 1988). The chemical and physical properties of PM vary greatly with time, region, climate/meteorology, and source category. The atmosphere contains particles of size ranging from a few nanometres (nm) up to hundreds of micrometres (μm) in diameter, which consist of a variety of chemical compounds (Hinds, 1999). Depending on their lifetime, the particles observed at a location can be both of local origin or the product of the transport over distances of hundreds to thousands of kilometres. Ambient particles can adversely affect human health (WHO, 2021) and drive many key aspects of the atmospheric and climate systems, such as cloud formation (IPCC, 2001). Moreover, the primary parameters that determine their role in atmospheric

processes and their environmental and health effects are their concentration, size, structure, chemical composition, density, surface area, and optical properties (Finlayson-Pitts and Pitts, 2000; Pöschl, 2005).

PM can originate from different sources that can be:

- Natural sources: processes which generate natural emissions such as volcanic and marine emissions, biological processes, forest fires (natural) or sand and dust storms.

- Anthropogenic sources: generated by human activities. The main sources of anthropogenic emissions are industry, motorized transport, power generation, agriculture and cattle industry and biomass burning. (Karagulian et al., 2015).

Urban air pollution refers to the air pollution experienced by people living in urban areas however it is important to consider that we spend most of our daily hours in indoor environments (WHO, 2005), either living, commuting, or working where the main cause of air pollution is inefficient fuel combustion from rudimentary technologies used for cooking or heating. A summary of main outdoor and indoor sources is listed in Table 1.1.

Table 1.1. Sources of atmospheric particulate matter.

Outdoor sources:	**Indoor sources:**
Natural • Biological materials (plant fragments, microorganisms, pollen, etc.) • Wildfires • Sea spray • Volcanic eruptions • Wind-driven resuspension of road, soil, and mineral dust • Lightning Anthropogenic • Fuel combustion • Non-road Transportation • Road traffic (exhaust and non-exhaust emissions) • Industrial activities • Construction and demolition activities • Agricultural activities	• human occupants, i.e. skin, hair, etc. • plants, pets • cleaning and vacuuming • building materials • combustion (biomass burning, candles, incense, smoking) • cooking • maintenance products

1.1.2. Size distribution

Aerosols can be formed by different processes, nucleation (nucleation of new particles from low vapour pressure gases emitted from sources or formed in the atmosphere by chemical reactions), condensation (condensation of low-vapour pressure gases on existing particles), coagulation (coagulation of particles, the weak bonding of two or more particles into one larger particle) or mechanical processes. These formation processes (can be one or several) will define their physical (size distribution, shape, density, etc.) and chemical (composition) characteristics (Mészáros, 1999).

The aerosol size distribution is usually a result of one or several particle modes (i.e., peaks in the size distribution), which can be related with distinct particle formation mechanisms. There are four formation mechanisms for the particle modes (Fig. 1.1): nucleation, Aitken, accumulation and coarse. In nucleation mode, particles can be directly emitted like primary particles, such as a fraction of exhaust vehicle emissions, or they can be new particles formed from gas-to-particle conversion (main gas precursors H_2SO_4, NH_3 and VOCs).

The Aitken mode contains the particles formed by condensation and coagulation and particles directly emitted by combustion as soot (Wehner and Wiedensohler 2003, Kulmala et al. 2004, Steinfeld and Pandis 2006). The particles that belong to nucleation and Aitken modes are a small percentage of the total mass of airborne particles (Seinfeld and Pandis, 2006).

The accumulation mode usually attributes to most of the aerosol surface area and most of the aerosol mass (Seinfeld and Pandis, 2006). It includes combustion, smog particles, marine organic and coagulated nucleation/Aitken mode particles (Hinds 1999, Steinfeld and Pandis 2006, Rodríguez et al. 2007). As before mentioned, particles are originated from primary emissions and gas-to-particle conversion, chemical reactions, condensation of low-volatility vapours, and coagulation of multiple small particles (Fig. 1.1. (c)). They do not reach the coarse mode as particles coagulation kinetics is usually slow, hence, they have a relatively long lifetime in the atmosphere (Harrison et al. 2000, Kumar et al. 2010). They can be removed by cloud activation and precipitation processes; they are very small for sedimentation.

The coarse mode (> 2.5 μm) is mainly composed by primary particles generated by mechanical processes and usually human-made, and mineral dust or sea salt particles, including windblown dust and mechanically generated anthropogenic particles, large salt particles from sea spray, and pollen (Harrison et al. 2000, Raes et al. 2000, Steinfeld and

Pandis 2006). These particles are large, and as their sedimentation velocity is large, their lifetime in the atmosphere is short and they impact on surfaces.

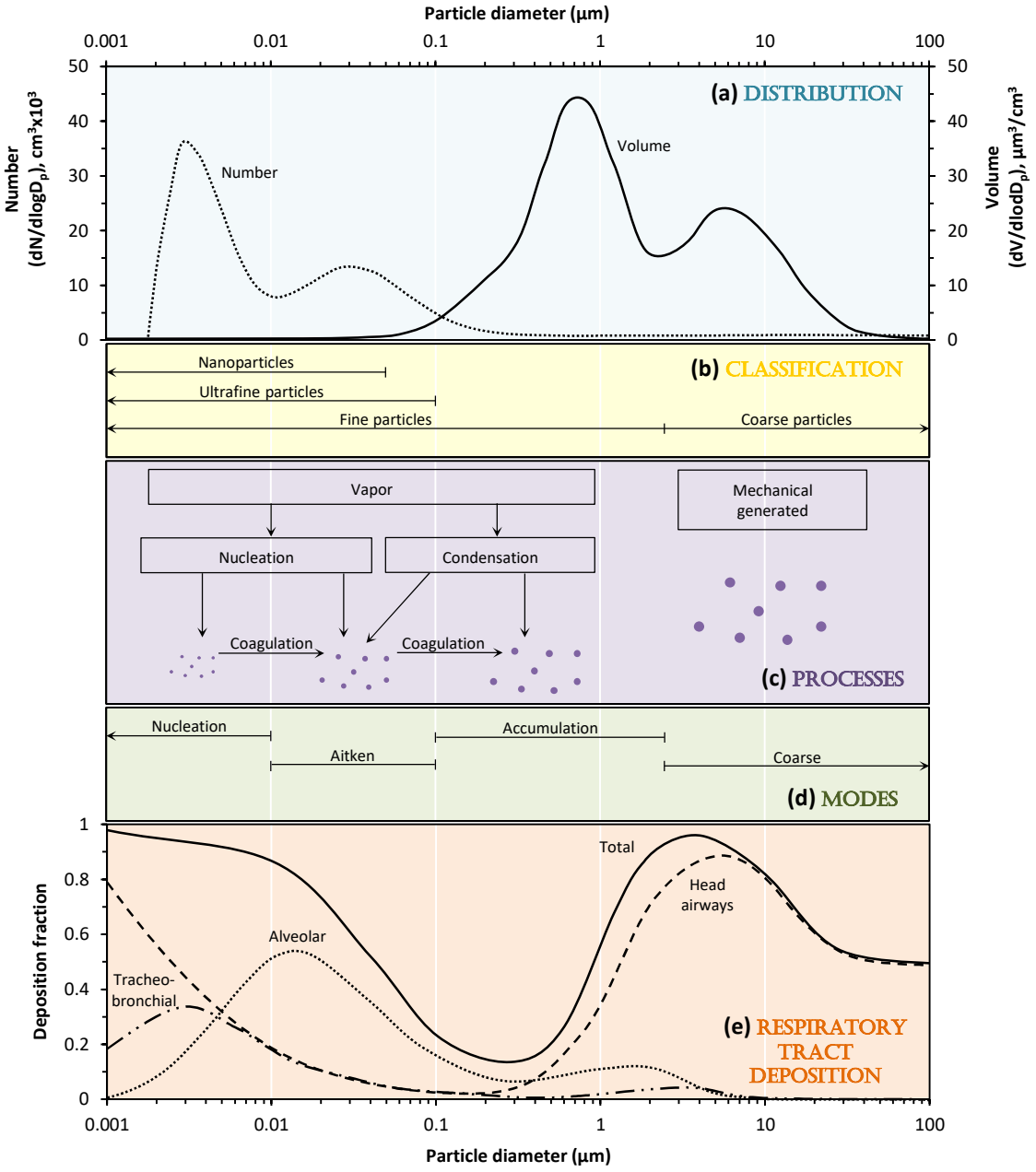

Figure 1.1. Composite picture of (a) typical atmospheric aerosol particle number and volume distributions (adapted from (Seinfeld and Pandis, 2006) (b) particles classification, (c) formation processes of particles, (d) particles modes and (e) fractional deposition of inhaled particles in the human respiratory tract (adapted from (ICRP, 1994) as a function of particle diameter.

The size distribution of an aerosol is usually a result of one or several particle modes, which can be related with distinct particle formation mechanisms (Fig. 1.1). Atmospheric aerosols are classified depending on their size in four different groups, nanoparticles (the smallest ones from 1 nm to 50 nm), ultrafine particles (UFP, from nanoparticles to 100 nm), fine particles (particles with an aerodynamic diameter less than 2.5 μm, $PM_{2.5}$) and coarse particles (particles with a larger aerodynamic diameter than 2.5 μm, $PM_{2.5-10}$) (Seinfeld and Pandis, 2006). The sources and formation mechanisms of those particles generally will be different. In terms of physics, chemistry, measurement, or health effects of aerosols it is important to identify and difference those particles, since the mechanisms to remove them from the air, their chemical and optical composition, their formation processes and their deposition patterns in the respiratory tract will be different (Seinfeld and Pandis, 2006). In the present study, these UFP have been named as quasi-ultrafine particles (QUFP 10-300nm).

When considering sources, ultrafine primary particles, mostly emitted by vehicle exhaust in urban areas, show two different modes referred to the size distribution, nucleation and Aitken modes. Particle emissions (25 –400 nm) from gasoline cars are up to two orders of magnitude lower than those from diesel cars (Wehner et al., 2009) with mean diameters in the nucleation mode. The nanoparticles (< 30 nm) formed from diesel exhaust emission are normally semivolatile, and can contain unburned fuel, unburned lubricating oil and sulphate, and form during dilution and cooling of exhaust gases (Mariq et al., 2007; Rodriguez et al., 2007; Olivares et al., 2007; Casati et al., 2007). However, in the coarse fraction related to traffic, several studies have indicated that a significant part of the road traffic emissions are non-exhaust emissions namely brake wear, road wear, tyre wear and road dust resuspension (Wåhlin et al., 2006; Schauer et al., 2006; Kupiainen, 2007; Amato et al., 2009).

Construction and demolition works are an important source of air pollution in urban areas contributing mostly to the coarse fraction of PM. Apart from emissions of high concentrations of dust (typically from soil, stone, cement and wood) in a diffuse and fugitive way, an important flow of heavy vehicles that transport materials or residues from the construction site can also be concentrated (GuideBook - Measures to improve urban air quality, 2017). This type of emission can reach high concentrations of pollutants and they are usually generated in populated areas or close to the population.

Regarding natural aerosols, bacterial aerosols are dispersed into the air through various sources (such as soil, plants, and water) and through the activities of animal, human, and

industrial activities, all of which may occur in urban environments (Bragoszewska et al., 2017). The size distribution of the bioaerosol depends on the type of microorganisms, the age of the spores and nutrient medium, the humidity, the difference in the rate of spore aggregation, and the type of particles related to the spores, such as dust. In general, bioaerosol diameters range from 0.3 to 100 μm (aerodynamic diameter), that is including the breathable size of 1 to 10 μm (Cox and Wathes, 1995). It should be noted that bioaerosol particles are usually attached to other particles for transportation, such as peeling skin, soil, dust, saliva, or water droplets.

1.1.3. Urban Aerosol Composition

The composition of urban air will be different depending on where it is geographically and topographically located. The main components of atmospheric particulate matter are mineral dust, sea salt or marine aerosol, carbonaceous aerosols (organic and elemental carbon), secondary inorganic compounds (SIC) (sulphate, SO_4^{2-}; nitrate, NO_3^-; and ammonium, NH^{4+}) and trace elements (Putaud et al., 2010).

Mineral dust (or crustal matter) is the major component (44 %, of global planetary emissions, Duce, 1995; IPCC, 2001; Prospero et al., 2002) of the total particle matter in the atmosphere. The major chemical components are Al, Ca, Si, Fe, Ti, K and Mg, but important trace elements include many metals and rare earth elements. In urban areas, road dust as a main PM source consists mainly of mineral particles and it can be a mixture of pavement and dust deposited in the pavement, carbonaceous particles (from tyres and traffic exhaust emissions deposited on the road) and metals (Fe, Cu, Sb, Ba from brakes, Ti, Rb, Sr from pavement, and Zn from tyres, (Wåhlin et al., 2006; Schauer et al., 2006; Thorpe and Harrison, 2008; Amato et al., 2009).

The ocean is the main source of marine aerosol, and its particles are mainly in the coarse fraction. Its major component is NaCl (Warneck, 1988) with smaller amounts of other components such as SO_4^{2-}, Mg^{2+}, Ca^{2+} and K^+ (White, 2008). There can also be found trace elements like Al, Co, Cu, Fe, Mn, Pb, V and Zn (Seinfeld and Pandis, 1998; Mészáros, 1999).

Carbonaceous aerosols, even if they contribute in a small (2 to 5 %) fraction to global planetary emissions (IPCC, 2001), it is one of the most abundant fractions in urban areas (~20–70%; Hama et al., 2022). They are a complex mixture of substances that contain carbon atoms, classified in two major fractions as organic carbon (OC) and elemental carbon

(EC) (Engling and Gelencsér, 2010). In industrial and urban areas 80 % of the carbonaceous species can be found in the finer fractions, with a size range < 0.1 μm, usually in the nucleation and Aitken modes (Harrison and Yin, 2008). The main emission sources of EC are road traffic (mostly diesel engines), specific industrial processes, biomass combustion and residential and domestic emissions. Moreover, bioaerosols (pollen, spores, microorganisms and vegetal or insect debris, among others) can contribute to increase the levels of organic carbonaceous aerosols. However, in urban and industrial areas anthropogenic sources of OC prevail (Rodríguez et al., 2002; Lonati et al., 2005; Viana et al., 2006).

Trace elements comprise only a small proportion of PM mass, but their negative impacts on human health and ecosystems have attracted considerable attention because of their toxicity and bioaccumulation by inhalation and deposition (Kampa and Castanas, 2008; Pan and Wang, 2015). They can be diagnostic of specific sources in the atmosphere and can therefore aid in source apportionment (Grobéty et al., 2010; Lim et al., 2010; Querol et al., 2007; Sternbeck et al., 2002; Thorpe and Harrison, 2008).

Secondary inorganic compounds are generated through a series of chemical reactions and physical processes involving precursor gases emitted from natural or anthropogenic sources (Giere and Querol, 2010; Squizzato et al., 2013). These are referred to the main inorganic compounds in the atmosphere: sulphate, nitrate and ammonium. The precursor gases emitted from natural sources can be, marine dimethyl-sulphide and volcanic SO_2, and the anthropogenic ones, NO_X, sulphur dioxide (SO_2), ammonia (NH_3) (Giere and Querol, 2010; Squizzato et al., 2013).

The bioaerosols are biological material that can be found in the atmosphere as airborne. They can be comprised of bacterial cells (as *Cutibacterium* or *Paracoccus*), cellular fragments, fungal spores or hyphae (as *Cladosporium* and *Aspergillius*), viruses, by-products of microbial metabolism and pollen grains (Encyclopedia of Microbiology, 2009). They can be generated by natural or anthropogenic activities in both indoor and outdoor spaces. Some activities that generate bioaerosols outdoors are wind, rain and wave splashing, spray irrigation, wastewater treatment activities, cooling towers and air treatment water spray systems, and agricultural processes such as harvesting and farming. However, indoor bioaerosols will be generated and dispersed by human and mechanical activities. High concentrations can be produced in industrial, manufacturing and biofermentation processes. Coughing and talking can be a source of bioaerosols, where some of them may be infectious, as it has been seen with *SARS-CoV-2* (COVID-19). Ventilation, air conditioning (AC), heating, cleaning (such as dust removal) and water spray devices (humidifiers) can

lead to the transport bioaerosols in the air. Current knowledge on the distribution of bacteria in the atmosphere is still limited by the fact that most of the bioaerosol studies carried out so far have applied only culture-based techniques (Mancinelli and Shulls 1978; Shaffer and Lighthart 1997; Fang et al. 2007).

1.1.4. Environmental and health effects

Exposure to ambient air pollution, mostly from PM, is the single largest environmental health risk at global level (Forouzanfar et al., 2015). There is no evidence of a safe level or a threshold below which no adverse health effects occur (Di et al., 2017), thus effective management of air quality aiming to achieve World Health Organization (WHO) Guidelines levels is necessary to reduce health risks to a minimum. Globally, it is the sixth risk factor for disability-adjusted life-years (DALYs), (Forouzanfar et al., 2016a) contributing to 7.6 % of total mortality (4.2 million premature deaths in 2016) (WHO, 2021; OECD, 2017). Over 80 % of EU (the European Union) population is exposed to harmful levels of air pollution, inducing more than half million premature deaths and more than 100 million DALYs (Forouzanfar et al., 2016b; EEA, 2019). Moreover, new studies have emerged indicating that the burden of disease is probably even larger than considered showing a role of ambient air pollution in the development of very important chronic conditions such as diabetes and obesity and also in the deceleration of cognitive development in children (Eze et al., 2014; Brunekreef et al., 2015; Sunyer et al., 2015; EEA, 2019). The health burden is expected to increase due population ageing and growth. Currently, the EU economic cost of deaths and diseases due to air pollution accounts for 1.44 trillion €. In no less than 10 EU countries, this cost is at or above 20 % of the national gross domestic product (Economic Cost of the Health Impact of Air Pollution in Europe, 2015).

There is by now a huge body of scientific evidence demonstrating that the human population is suffering a self-inflicted environmental health crisis in which urban air quality is being severely compromised by road transport emissions (e.g., Morawska et al., 2008; Kumar et al., 2014, 2018; Kelly and Fussell, 2015; Steiner et al., 2016; Nieuwenhuijsen et al., 2018; Pope, 2020). Traffic is the main source of air pollutants in cities, and since urban citizen already represent most of the total world population (https://data.worldbank.org/indicator/SP.URB.TOTL.IN.ZS, UN Population Division), the effects of breathing vehicle gas and particulate emissions have become one of our most challenging environmental health problems (Cepeda et al., 2017; Hoek et al., 2013; Kelly and Zhu, 2016; Heal et al., 2012; Rivas et al., 2014). Current estimates of the effects of air

pollution on human longevity (Lelieveld et al., 2020) calculate millions of deaths worldwide annually brought forward, a health insult similar in scale to smoking-related diseases, with road traffic being the main culprit. These health effects are most associated with particles measuring around 100 nm or less (UFP; Kumar et al., 2014; Krecl et al., 2017). Indeed, key to understanding the pervasiveness of our 21st century urban air pollution problem is that the extremely fine size of most inhaled traffic aerosols means that they can translocate from the lung to the systemic circulation so that "air pollution can harm nearly every organ in the body, and PM is the main offender" (Schraufnagel, 2020). In this size range the particles are low in mass (PM) but high in number (PN) concentrations, and most are small enough (< 100 nm) to enter cells by endocytosis and express their toxicity by impacting on intracellular redox state and disrupting cellular processes (Burello and Worth, 2011). Intracellular particles < 40 nm in size have even been shown to be capable of passing from the cell cytoplasm into the nucleus (Panté and Kann, 2002), with their elevated surface/volume ratio offering greatly enhanced biological reactivity (Auffan et al., 2009). The very smallest particle sizes approach atomic scales, the so-called "ultrasmall nanoparticles" of Hewitt et al. (2020) and including the traffic "nanocluster aerosols" of Rönkkö et al. (2017), giving them the ability to mimic biological macromolecules and so potentially interfere with cell machinery. In the context of traffic pollutants then, increasing recognition of the complexities of particle bioreactivity at UFP size levels demands improved understanding of the patterns of particle size ranges being inhaled.

Bioaerosols including bacteria, fungi and endotoxins are airborne biological particulate matter that can affect living beings through infectious, allergic, toxic, and irritating processes. Endotoxin inhalation may cause dry cough and shortness of breath accompanied by decreased lung function, fever reactions and malaise, and sometimes headache and joint aches occurring within a few hours of exposure (Lehtinen et al. 2013).

1.1.5. Air quality regulations

The European Commission (EC) defines the acceptable limits (standards) of ambient concentrations of atmospheric pollutants (EEA, 2020). A series of air pollutants are regulated by EU directives, such as particulate matter, NO_2, SO_2, lead (Pb), CO, benzene (C_6H_6), O_3, arsenic (As), cadmium (Cd), nickel (Ni) and benzo(a)pyrene (BaP) (Tab. 1.2). The 2008/50/EC Directive established the criteria to locate monitoring sites, their type and number and the measurement reference methods. Urban sites must be in background areas that represent exposure level of citizens. Urban traffic sites must be located near roads with high traffic inside the cities to measure direct pollution of both traffic and non-traffic

sources. Industrial sites must be located inside industrial areas to measure the local impact of industrial emissions. Finally, measurements must be undertaken also at background rural/regional sites that are in areas far from any direct anthropogenic pollution source to provide information on background levels of pollutants at a regional scale. This information is necessary to evaluate the increments in the levels of urban, industrial or traffic hotspots and to evaluate the contribution of long-range transport of atmospheric pollutants.

The 1999/30/EC Directive established an annual mean limit value of 40 μg/m^3 for PM_{10} and a daily limit value 50 μg/m^3 not to be exceeded more than 35 times per year. The Air Quality Directive 2008/50/EC did not change this limit value but establishes also limit and target values for $PM_{2.5}$ applied both to hotspots and background sites, together with exposure reduction targets and exposure concentration obligations for urban backgrounds. Moreover, the Directive 2008/50/EC establishes $PM_{2.5}$ limit and target values also for background and hotspot sites. Compliance with air quality limit values depend of course on multiple factors: anthropogenic emissions, natural contributions, atmospheric process, but also monitoring site location.

Short-term action plans from Member States may provide effective measures to control and, where necessary, suspend activities which contribute to the risk of the respective limit values or target values, or alert threshold being exceeded. Those action plans may include measures in relation to motor-vehicle traffic, construction works, ships at berth, and the use of industrial plants or products and domestic heating. In December 2019, as part of the European Green Deal (COM (2019) 640), the European Commission committed to enhancing air quality and bringing EU air quality standards closer to the WHO's recommendations. The WHO's recommendations were last updated in September 2021 (WHO, 2021), and this objective of aligning with the latest scientific findings was confirmed in the zero pollution action plan (COM (2021) 400). The zero pollution action plan has a vision for 2050 to decrease air (and water and soil) pollution to levels that are no longer considered harmful to human health and natural ecosystems, while adhering to our planet's limits, thus creating a toxic-free environment. Moreover, two of the 2030 targets are air-related: reducing the health effects of air pollution (premature deaths) by more than 55%, and reducing the share of EU ecosystems where air pollution endangers biodiversity by 25%. Stricter air quality standards would also contribute to Europe's Beating Cancer Plan's objectives (COM (2021) 44). The Beating Cancer Plan confirms the need to reduce ambient air pollution, which causes, amongst others, lung cancer. Additionally, the European Commission declared in the European Green Deal that it would enhance air quality monitoring, modelling, and planning.

Elevated health risks are associated with living next to roads, due to high concentrations of UFP, CO, NO_2, black carbon (BC), polycyclic aromatic hydrocarbons (PAH), and some metals (WHO, 2013). In addition, reduction of traffic emissions has been deaccelerated during the last two decades due to the promotion of diesel vehicles, their non-attainment to EURO standards for NOx and the lack of regulation for non-exhaust traffic emissions such as brake wear, road abrasion, tyre wear and road dust resuspension.

While cities are moving towards more sustainable mobility to improve ambient air quality, by promoting public transportation, they should also concern about the quality of the air commuters are exposed to during their commuting in public transport. Several studies have reported air pollutant levels in urban areas to be up to four times higher during road traffic rush hours than at other times of the day (Knibbs et al., 2011; Yu et al., 2012), and so encouraging increased use of public transport is one of the more obvious potential strategies aimed at improving the quality of the air we breathe in the city.

Table 1.2. Current legislation on air quality. Standard introduced by the Directive 2008/50/EC. Source: "Air quality in Europe- 2020 report".

Pollutant	Concentration	Averaging period	Legal Nature	Permitted exceedances per year
$PM_{2.5}$	25 µg/m³*	1 year	Target value entered into force 1.1.2010	n/a
	25 µg/m³		Limit value entered into force 1.1.2015	
	20 µg/m³		Indicative limit value entered into force 1.1.2020	
PM_{10}	50 µg/m³	24 hours	In force**	35 days
	40 µg/m³	1 year	In force**	n/a
NO_2	200 µg/m³	1 hour	Limit value entered into force 1.1.2010***	18 hours
	40 µg/m³	1 year	Limit value entered into force 1.1.2010***	n/a
SO_2	350 µg/m³	1 hour	In force	24 hours
	125 µg/m³	24 hours	In force	3 days
Pb	0.5 µg/m³	1 year	In force	n/a
CO	10 mg/m³	Maximum daily (8 hours mean)	In force	n/a
Benzene	5 µg/m³	1 year	Limit value entered into force 1.1.2010	n/a
Ozone	120 µg/m³	Maximum daily (8 hours mean)	Target value entered into force 1.1.2010	25 days averaged over 3 years
As	6 ng/m³	1 year	Target value entered into force 31.12.2012	n/a
Cd	5 ng/m³	1 year	Target value entered into force 31.12.2012	n/a
Ni	20 ng/m³	1 year	Target value entered into force 31.12.2012	n/a
PAH	1 ng/m³ (as Benzo(a)pyrene conc.)	1 year	Target value entered into force 31.12.2012	n/a

* *Standard introduced by the Directive 2008/50/EC.*

** *Under the Directive 2008/50/EC the Member State can apply for an extension until three years after the date of entry into force of the Directive 2008/50/EC (i.e. May 2011) in a specific zone. Request is subject to assessment by the Commission.*

*** *Under the Directive 2008/50/EC the Member State can apply for an extension of up to five years (i.e. maximum up to 2015) in a specific zone. Request is subject to assessment by the Commission.*

1.1.6. Contribution of commuting to personal exposure

Hundreds of millions of people in the world spend part of their workday commuting through a city (≈ 8 % of the daily time) inhaling atmospheric pollutants (Borghi et al., 2020). In many cases these urban journeys provide a disproportionate percentage of the individual's average daily exposure to inhalable pollutants, and recognition of this fact is reflected in a large body of scientific literature on commuting and air pollution that goes back over 50 years (e.g., Haagen-Smit, 1966; Cepeda et al., 2017). The number of such publications has accelerated in recent years, accompanied by an increasingly wide recognition of the serious insult to human health inflicted worldwide by inhaling contaminated urban air. Given the sometimes radical differences in atmospheric microenvironments experienced by city travellers using different transport modes, many of these publications have turned their attention specifically to air quality found inside moving vehicles (e.g. Alameddine et al., 2016; Fruin et al., 2011; Hudda et al., 2011, 2012; Hudda and Fruin, 2018; Jo and Yu, 2001; Leavey et al., 2017; Lee et al., 2015; Madl et al., 2015; Moreno et al., 2015; Tartakovsky et al., 2013; Xing et al., 2018; Yang et al., 2015; Zhu et al., 2007). In the context of legislative demands imposed by environmental authorities, the main focus of these studies has been on PM_{10} and $PM_{2.5}$ mass, PN, concentrations of gaseous pollutants such as NOx, CO, and CO_2 and, more recently, VOCs.

Given the high relevance of traffic emissions in urban air quality, a large fraction of daily dose to air pollutants is inhaled during commuting, even if it takes less than 2 hours per day, especially in high vehicle-density areas. During their regular journeys, commuters can receive up to 30 % of their inhaled daily dose of BC, and approximately 12 % of their daily $PM_{2.5}$ personal exposure, (Dons et al., 2011, Dons et al., 2012, Fondelli et al., 2008; Chaney et al., 2017).

In addition, the interior of the bus can also be considered a place of health risks due to the constant contact with passengers among whom some can be ill or disease carriers (Nowakowicz-Dębek et al. 2017). To date, bioaerosols have been measured in several transport microenvironments, such as public restrooms, public hospitals, houses, subway commuting and workplaces (Gołofit-Szymczak and Górny 2010; Ghosh et al. 2015; Lee et al. 2016; Triadó-Margarit et al. 2016). Important factors that can modify bioaerosol concentrations in an indoor environment, as for the chemical pollutants, is the ventilation type and AC system (Sowiak et al. 2018). Thus, previous studies inside households, university rooms, cars, and other indoor spaces, have probed that the use of AC systems when not well designed or maintained can become an additional source of fungal aerosols

introduced into indoor air (Hamada and Fujita 2002; Almoffarreh et al. 2016). It was shown that the first 10 min of AC powered on are the ones in which the fungal concentration emitted is the highest (Hamada and Fujita 2002; Jo and Lee 2008). However, Sowiak et al. (2018) evaluated ventilation differences between 30 same type buses (10 of them with natural ventilation and 20 with AC) and showed that there is no strong evidence that AC system is an additional source of indoor air contamination with fungi.

1.2. Air quality in public buses

Public transport is a good way to reduce congestion and environment and health-harming emissions in urban areas, especially when they run on alternative, cleaner fuels. The European Commission strongly encourages the use of public transport as part of the mix of modes which each person living or working in a city can use. Buses, as other commuting modes, are an important microenvironment for environmental exposure. Most public transport journeys in the EU (56 %) are made using bus systems (http://www.uitp.org/key-eu-statistics) which means 32.1 billion passenger journeys per year. There are 892,861 buses in circulation on Europe's roads today. In 2016, 40,380 new buses and coaches were registered throughout the EU. They are also more accessible for people who is in a wheelchair o for baby carts.

In Barcelona, public transport is used every day by more than a half of the city commuters, almost 3 million, on journeys lasting from 30 to 60 minutes every working day (data from Ajuntament de Barcelona, 2018).

1.2.1. Bus powertrains and exhaust emissions

Emissions from road vehicles have been controlled by European legislation since the 1970s. To meet the increasingly stringent requirements of the legislation, vehicle manufacturers have continually improved engine technologies and have introduced various emission-control systems. Control on road traffic emissions is carried out by means of the EURO certification since 1992. The stages are typically referred to as EURO I, EURO II, EURO III, EURO IV, EURO V and EURO VI for Heavy Duty Vehicles. Emissions from diesel engines (Tab. 1.3) used in vehicles of gross vehicle weight (GVW) over 3.5 t were first regulated in 1988 with the introduction of the original ECE 49 Regulation. Vehicles (or, rather, engines) complying with ECE 49 and earlier are all classified as ‘conventional’. Directive

91/542/EEC, implemented in two stages, brought two sets of reduced emission limits, valid from 1992 to 1995 (Stage 1 — Euro I) and from 1996 to 2000 (Stage 2 — Euro II). Directive 1999/96/EC Step 1 (Euro III) was valid from 2000 and introduced a 30 % reduction of all pollutants relative to Euro II. The same Directive included an intermediate step in 2005 (Euro IV), and a final step in 2008 (Euro V). The Euro V standards are very strict, requiring a reduction in NOx of more than 70 % and a reduction in PM of more than 85 % compared with the Euro II standards. This will be achieved with engine tuning and oxidation catalysts for PM control, and selective catalytic reduction (SCR) for NOx control.

Latest emission limits at a Euro VI level have enforced since the 2013/14 period, with a 50 % reduction in PM and a further 80 % reduction in NOx over Euro V, with the addition of a cold start cycle. European Green Deal will develop stricter emissions standards (Euro VII) for all petrol and diesel vehicles. To ensure vehicles on EU roads are clean over their lifetime, the proposed rules will consider new vehicle technologies and ensure emissions are measured in real-time. This initiative is part of the EU's commitment to accelerate the shift to sustainable and smart mobility. It is planned for Fourth quarter 2021 (https://ec.europa.eu/info/law/better-regulation/have-your-say/initiatives/12313-Development-of-Euro-7-emission-standards-for-cars-vans-lorries-and-buses).

Table 1.3. European regulation for pollutants exhaust emission from public buses.

Type	*Technology*	*CO*	*NMVOC*	*NOx*	*N_2O*	*NH_3*	*Pb*	*CO_2 lube*	*$PM_{2.5}$*
Units		g/km	g/km	g/km	g/km	g/km	g/km	g/km	g/km
Notes			Given as THC-CHA	Given as NO_2 equivalent				due to lube oil	$PM_{2.5}$= PM_{10}= TSP
Urban CNG buses	Euro I - 91/542/EEC I	8.400	0.371	16.500	n.a.	n.a.	2.89E-05	1.860	0.0200
	Euro II - 91/542/EEC II	2.700	0.313	15.000	n.a.	n.a.	2.68E-05	1.590	0.0100
	Euro III - 2000	1.000	0.052	10.000	n.a.	n.a.	2.37E-05	1.590	0.0100
	EEV	1.000	0.045	2.500	n.a.	n.a.	2.37E-05	n.a.	0.0050
Urban Buses Standard	Conventional	5.710	1.990	16.500	0.029	0.0029	1.90E-05	2.650	0.9090
	Euro I - 91/542/EEC I	2.710	0.706	10.100	0.012	0.0029	1.61E-05	2.050	0.4790
	Euro II - 91/542/EEC II	2.440	0.463	10.700	0.120	0.0029	1.55E-05	1.480	0.2200
	Euro III - 2000	2.670	0.409	9.380	0.001	0.0029	1.62E-05	0.861	0.2070
	Euro IV - 2005	0.223	0.022	5.420	0.012	0.0029	1.54E-05	0.265	0.0462
	Euro V - 2008	0.223	0.022	3.090	0.032	0.0110	1.54E-05	0.265	0.0462
	Euro VI	0.223	0.220	0.597	0.040	0.0090	1.54E-05	0.265	0.0023

*Urban Buses Standard: Diesel

The environmental impact of buses can vary greatly according to the vehicle type, energy consumed and the style of use. The use of hybrid and electric vehicles is becoming more common in cities, however, most engines powering buses are still fuelled by diesel. Conventional diesel engines can be noisy and emit high concentrations of NOx and PM, although a few options are available to reduce emission levels below current Euro standards. Continuously Regenerating Trap (CRT) and diesel particulate filters (DPF) can be used to reduce PM emission from buses including UFP (up to 90-95 % in the case of DPF; PTEG, 2009) and SCR filters reduce NOx emissions (up to 50-90 %; PTEG, 2009). Thus, two generations of SCRT (CRT + SCR), have been implemented in some urban bus fleets such as London and Barcelona to reduce both NOx and PM emissions (Fig. 1.2).

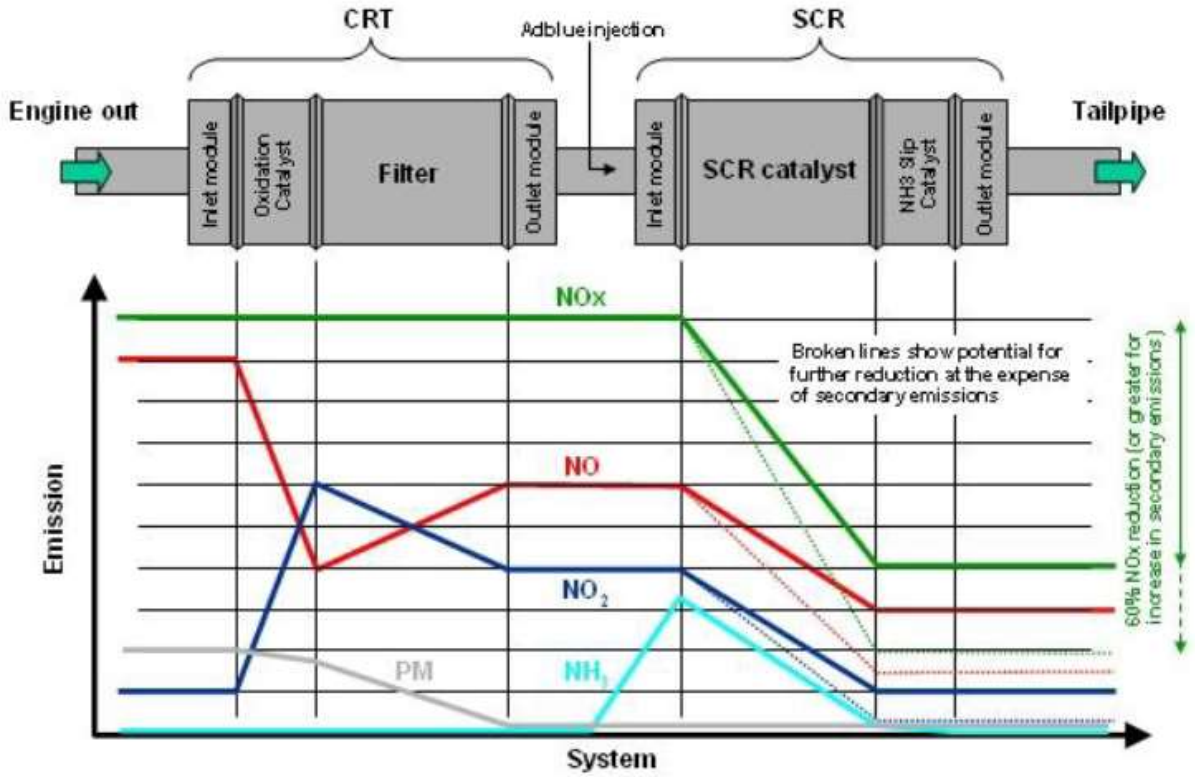

Figure 1.2. Operation of SCRT filters for treatment of exhaust gases in three stages: Stage 1: CRT reduces NO and PM (red and grey lines); Stage 2: Adblue injection (NH_3, light blue line); Stage 3: SCR reduces NOx (green, red, and blue lines). (Source: TMB).

The use of alternative fuels such as compressed natural gas (CNG; also, a frequently utilised bus fuel), hybrid buses (hybrid of diesel (HD) or hybrid of CNG (HCNG)) and electric (EV) buses, could result in a significant reduction of emissions and environmental impact. CNG can be produced from biogas but is typically produced from fossil-fuel sources and comprises a mixture of propane and butane. A major advantage of using CNG over traditional diesel buses, is the reduction of harmful tailpipe emissions (mainly methane)

including PM, which are almost negligible (although this depends on the passenger load) and emitting less NO_2 (80 % lower; PTEG, 2009), but emitting higher CO concentrations. Hybrid buses (increasingly common in the urban transport systems) can use either diesel (HD) or natural gas (HCNG) aided by an electric motor and emit lower concentrations of NOx than diesel buses as they consume less fuel, although not as low as CNG buses (Bradley, 2002). Electric buses produce no tailpipe emissions but depending on the proportion and type of fossil fuels used to generate electricity, carbon, nitrogen, and sulphur oxides emissions will be produced. HCNG buses demonstrate up to around a 30 % reduction in the use of CNG fuel, compared to standard CNG buses.

In urban areas buses can make an important contribution to emissions of NOx and primary NO_2 as retrofitting heavy duty vehicles offer the possibility of reducing emissions of key pollutants such as NOx and particulate matter relatively quickly and cheaply compared for example to the purchase of new vehicles. The long service life and slow fleet turnover of heavy-duty vehicles encourages authorities to consider options such as retrofitting older vehicles to bring about rapid reductions in emissions.

1.2.2. Factors controlling air quality inside buses

Several are the factors that influence the air quality to which passengers are exposed while travelling inside an urban bus. For the traveller outdoors the most important of these factors is proximity to the sources of traffic emissions, whereas for the commuter inside a bus exposure to traffic related air pollutants (TRAPs) will depend primarily on the air exchange rates (e.g., Zhu et al., 2002; Durant et al., 2010; Fruin et al., 2011; Leavey et al., 2017; Lee et al., 2015). Some factors such as engine type, retrofit, ventilation, driving style and maintenance conditions will determine the air quality inside buses. External weather conditions or technologies within the vehicle, such as brake and tire wear, road abrasion, fuel, interior coatings, and materials, are also responsible for the indoor air quality (Nowakowicz-Dębek et al. 2017). It will also influence the time that the passenger stays inside the bus, and the sources near to it. Several studies have concluded that a significant portion of air pollutants in buses is due to self-pollution (Adar et al., 2007; Behrentz et al., 2004; de Nazelle et al., 2012; Yang et al., 2015). More obvious influences include opening windows during driving, starting up and idling of the bus, and opening bus doors, all of which can produce higher in-bus exposures (Asmi et al., 2009; Hammond et al., 2007; Zhang and Zhu, 2010), although background concentrations may also have a significant role.

Knibbs and de Dear (2010) observed that when wind speed was lower, the ambient $PM_{2.5}$ concentrations increased and the measurements inside buses were well correlated with the concentrations measured in fixed-site monitoring stations.

Several studies have reported air pollutant levels in urban areas to be up to four times higher during road traffic rush hours than at other times of the day (e.g., Knibbs et al., 2011; Yu et al., 2012), and so encouraging increased use of public transport as one of the more obvious potential strategies aimed at improving the quality of the air we breathe in the city. Traveling by bus on low traffic roads can help reducing by 10-30 % the exposure to primary pollutants (CO and NO_X), while no evidence has been found regarding pollutants with a secondary component (NO_2, PM_{10} and $PM_{2.5}$) (Hertel et al., 2008), also a 5-20 % reduction for the exposure to secondary pollutants and 10-30 % for primary pollutants has been observed when traveling outside of traffic peak hours. Thus, the choice of the route travelled by the bus affects the internal concentration and therefore the exposure of the passengers.

Sowiak et al. (2018) evaluated ventilation differences between 30 same type buses (10 of them with natural ventilation and 20 with AC) and showed that there is no strong evidence that AC system is an additional source of indoor air contamination with fungi. Few buses in this study showed higher concentrations of fungi in AC buses. In both, AC buses and non-AC buses, the presence of allergenic fungi genera Aspergillus, Penicillium and Cladosporium section were confirmed.

1.2.3. Air pollutant levels and chemical/biological composition

Some studies have already reported that air quality experienced by travellers when inside the bus could be affected by elevated concentrations of different pollutants, including BC, PM, PN, CO_2, NO_2, VOCs or O_3 (Kaur et al. 2005; Knibbs and de Dear 2010; Molle et al. 2013; Lim et al. 2015; de Nazelle et al. 2017). In terms of PN, most inhalable traffic particles fall into the UFP size range (Morawska et al., 2008), with diesel buses providing an especially potent pollutant source (Kaur et al., 2007; Knibbs and de Dear, 2010; Kingham et al., 2013) and comparing unfavourably with, for example, gas or electric powered buses (Zuurbier et al., 2010; Dons et al., 2011; Ragettli et al., 2013). Rivas et al. (2017) found that travelling inside London transport buses provided the highest exposure levels of PN and BC, compared to the rest of commuting modes. $PM_{2.5}$ mass concentration has also been reported to be higher inside buses than in taxis in Florence, with a mean value of 56 ± 15 $\mu g/m^3$ and 39 ± 15 $\mu g/m^3$, respectively; while the corresponding concentrations recorded

simultaneously at the urban background were half (Fondelli et al. 2008). Kingham et al. (2013) showed that both PM_1 and PN levels were higher in buses compared to the car, bike (on-road and off-road) and metro.

In London, Kaur et al. (2005) has recorded highest PN inside buses (1013647 #/cm^3) whilst walking was the lowest (67773 #/cm^3) while for $PM_{2.5}$ they have measured 34.5 μg/m^3 inside buses, being the highest concentration inside taxis and lowest while walking, 41.5 and 27.5 μg/m^3, respectively. Conversely, Ragettli et al. (2013) observed the lowest PN concentrations inside CNG buses, 4188 #/cm^3, compared with the measurements done inside cars, tram, or walking. In Arnhem, the Netherlands, Zuurbier et al. (2010), showed that diesel buses obtained the highest mean value of BC, 9 μg/m^3 close to car 8.8 μg/m^3 while electric ones achieved the lowest one 5.1 μg/m^3 and found PN concentrations were highest inside diesel buses (38500 #/cm^3) and for cyclists along a high-traffic intensity route (46600 #/cm^3) and lowest in electric buses (29200 #/cm^3).

Adams et al. (2001) measured higher air pollution levels in open-back buses than in closed buses, and Hammond et al. (2007) measured three to four times higher (< 0.1μm; UFP) in diesel buses than in compressed natural gas buses or buses with oxidation catalysts.

To our knowledge, the highest $PM_{2.5}$ concentrations inside buses (517 μg/m^3, Goel et al., 2015) was recorded in Delhi (India) and the lowest (7.5 ± 2 μg/m^3, Ham et al., 2017) in Sacramento (California). Understanding the role of different factor affecting air pollutants concentrations in buses and therefore commuters' exposures is important to draw measures and strategies to reduce any health consequence related to such exposure.

When talking about the chemical composition of particles inside buses there are not many studies in the literature. Moreno et al. (2015) identified Al and Ti in relatively high concentrations, due to the unusually high amount of paving work activity during sampling. The distinctive mixture of enriched metals inside the bus showed enhanced levels of Sb and, to a lesser extent, Cu and Ba, probably from the braking system as typically shown at kerbside sites (Amato et al., 2014). According to this study, the bus traveller may inhale perhaps ten times more Ti or Sb during the daily commute, depending on the route chosen to move through the city.

Bioaerosols have also become an issue of public health and there is a lack of data on microbiological composition of air particularly in public transportation, despite the fact they can be key locations for the transmission of pathogens (Robertson et al., 2013). A major source of airborne bacteria in public buses derives from coughing, sneezing, talking, and

breathing (Johnson & Morawska, 2009), or simply emitted from the whole body thanks to thermal differences and consequent air convection leading to shedding of skin bacteria (Fox et al., 2010). Ribosomal rDNA sequences from bacteria can be used as a biomarker of airborne colonisation by bacteria, with the quantification of 16S ribosomal DNA having been used in several studies to estimate the concentration of bacteria present in indoor air (Veillette et al., 2013, Blais-Lecours et al., 2015).

1.2.4. Gaps in current knowledge

The studies described in section 1.2.2 and 1.2.3 have contributed to characterise the air in bus systems. The key parameters covered included mass and number concentration, BC, CO, and CO_2. Notwithstanding, certain gaps in the current knowledge have been identified:

- Despite the number of studies, most of them focused on the variations in PM mass concentration and the measurements have been done during a short period of time and in a reduced number of buses. Therefore, there is a need for extensive studies of entire bus systems, covering the vast diversity of lines and powertrain types.

- Studies including a global comprehension of air quality including PMx, PN, BC, VOCs, NOx, CO, CO_2 and bioaerosols inside buses, are lacking in the literature and the investigation of factors affecting the bus interior environment and the pollutants concentration, such as the ventilation with the use of AC or windows open needs to be actualised.

- The PM chemical composition study was limited to a small number of buses and a much more detailed dataset is necessary before a definitive comparison between indoor air in buses and other forms of transport can be made. This is necessary to understand the sources influencing the air quality inside buses.

- There is a lack of data on concentration and biological composition of bioaerosols in the air in various public places and particularly in public transportation, despite the fact they can be key locations for the transmission of pathogens (Robertson et al., 2013).

- There are still relatively few data available that specifically address such real-time variations in exposure of individuals to air pollution microenvironments during

commuter travel within the city, and there is consequently little awareness among the public of how their choices in commuter travel may be affecting their health.

1.3. Objectives

Considering all this, the main and specific objectives of this PhD are:

- To measure and interpret temporal and spatial variations in the concentration of $PM_{2.5}$, ultrafine particle number and size, black carbon (BC), CO_2, VOCs, bioaerosols and endotoxins (in collaboration with Prf. C. Duchaine, University of Laval) concentrations inside diesel (EURO IV and EURO V), natural gas (CNG), hybrid of diesel (HD) and of natural gas (HCNG) and electric (EV) public buses, in order to understand their differences.

- To evaluate differences in the chemical composition of $PM_{2.5}$ samples (in quartz fibre filters using portable Personal Environmental Monitors) collected while commuting in the different buses to identify their sources.

- To determine the source contribution with a Positive Matrix Factorization (PMF) receptor modelling analysis.

- To evaluate air quality in the new network system with "vertical" and "horizontal" routes, identifying for example if higher bus emissions affect the inside of the bus while travelling in routes involving climbing a sloping city surface.

- To investigate the impact of parameters such as ventilation (AC and natural ventilation), infiltration, number of passengers and location in the bus.

- To develop a comprehensive analysis of exposure for bus commuters in the city of Barcelona, identifying major factors influencing the bus (including fuel-type, route, ventilation), and identifying most polluted routes/buses to propose opportune remediation measures.

CHAPTER 2: METHODOLOGY

2. METHODOLOGY

The description of the methodology applied in this Thesis includes firstly a description of the study area and the sampling sites where measurements were carried out, followed by detailed information on the instrumentation used. Finally, a description of the chemical and biological analyses and data treatment tools applied is provided.

2.1. Monitoring sites

All measurements were done in Barcelona, which is the second largest city of Spain with 1.6 million inhabitants (3 million considering the metropolitan area). It lies along the western Mediterranean, and it is delimited by two river basins and a hill range in the West. The city is densely populated (15880 inhabitants/km^2) and has the largest vehicle density in Europe (6000 vehicles/km^2). Despite the municipal public transportation network being well developed, 25 % of travels performed by commuters are made by private vehicles, with a significant contribution from/to the metropolitan area (Ajuntament de Barcelona, 2016). Despite the recent Diesel gate, and the implementation of a Low Emission Zone (LEZ), diesel engines are still an important share of the circulating fleet in the Province of Barcelona. Consequently, the city suffers from poor air quality in terms of particulate matter (PM) and NO_2, mostly due to road traffic emissions, although other significant contributions to PM levels are originated from industries, harbour, and urban works (Amato et al., 2016). Moreover, the low wind speed and the dense urban built environment, with so-called "street canyons", hampers the dispersion of traffic pollutants.

Measurements were performed in the municipal bus fleet of Barcelona city managed by the TMB (Transports Metropolitans de Barcelona) company. As a reference background site, the Palau Reial (UB) urban air quality monitoring station, was used; this site belongs to the official air quality network of the local government.

Barcelona public bus system

The Barcelona public bus system is an extensive network that includes 1140 vehicles and 101 routes covering a total length of 830 km with 2590 bus stops. It has been built up progressively since 1906 and the system carries around 203 million of passengers per year (TMB, 2018).

The fleet is composed by different type of buses (different brands, motors…) with variable size. There are standard buses of 12 meters, articulated of 18 meters, biarticulated of 24 meters and minibuses of 7 meters. More common are the standards and the articulated ones, with capacity for 60 and 100 passengers respectively, spread among all fuel type, while the biarticulated are only in hybrid diesel buses, with capacity for 140 passengers (only in the line H12 that goes across the whole Gran Via avenue in Barcelona). Minibuses and microbuses for 22 passengers are used in the Neighbourhood Bus service. TMB also has tourist open top double-decker buses with an upper floor wide open to outdoor air, and a lower floor which, although ventilated via stairs leading to the open top floor, is more confined.

The bus fleet in 2018, when the sampling was done and before the implementation of LEZ, was composed by 5 different types of powertrains (Fig. 2.1 and Fig. 2.2 and Table 2.1): 39 % diesel (EURO I to EURO VI), 34 % compressed natural gas (CNG), 27 % hybrid (26 % hybrid diesel (HD) and 1 % hybrid compressed natural gas (HCNG)) and 1 % electric (EV). In addition, the fleet includes three touristic routes ran by diesel EURO IV buses. According to the bus dimensions, 55 % are standard buses, 31 % articulated buses, 2 % minibuses, 5 % microbuses and 7 % two-floors tourist buses.

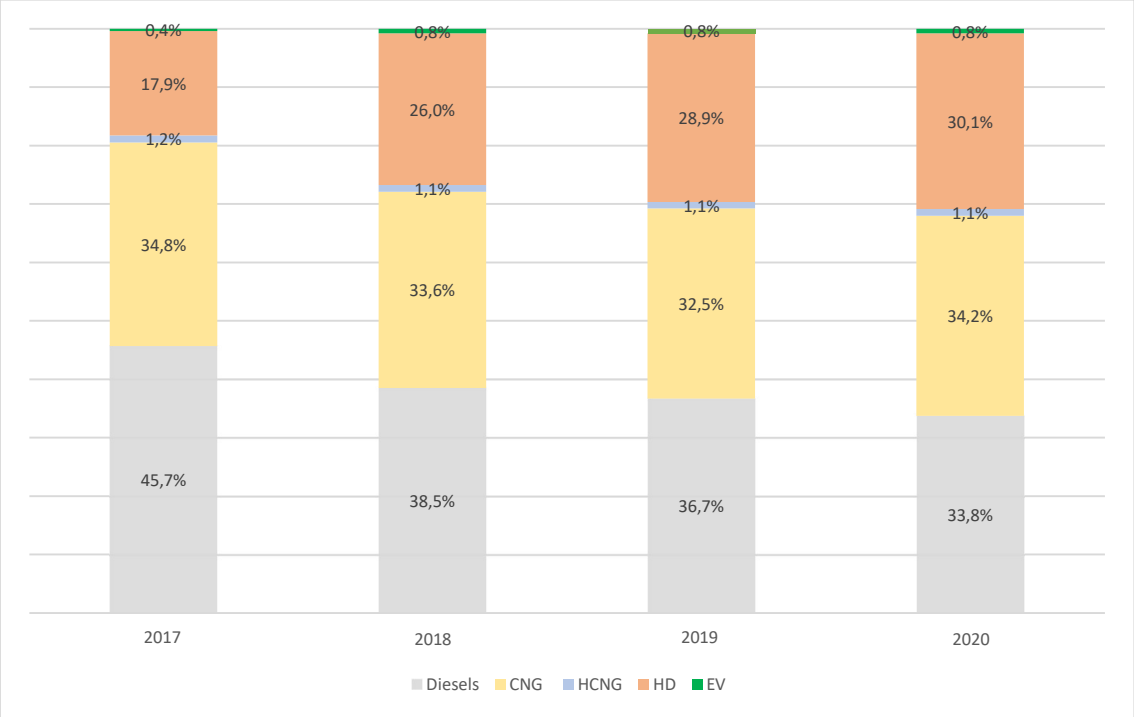

Figure 2.1. Variation of buses distribution from the fleet of TMB in five different years: 2017-2020. The sampling was done between 2017-2018. Data from TMB Dades bàsiques - Basic data www.tmb.cat. Diesels: 496-439, CNG: 378-383, HCNG: 13, HD: 194-296 and EV: 4-9.

Table 2.1. Number of buses per powertrain and year, from the year when the study started until now. Source: www.tmb.cat.

	2017	2018	2019	2020
Total fleet	1085	1140	1157	1134
Diesels	496	439	425	383
CNG	378	383	376	388
HD	194	296	334	341
HCNG	13	13	13	13
EV	4	9	9	9

Figure 2.2. Different fuel/engine type buses from the fleet of TMB and the tourist buses.

Almost all the routes run from 5 am to 11 pm every day, and all buses are equipped with an air-conditioning system (AC), working in spring and summer. During autumn/winter no AC is used, except for fully electric buses. In summer, there are two kinds of AC (TMB personal communication):

1. 100 % recirculation. 63 % of the studied buses have this type of air circulation. It is the most common type, without air renewal, except when the doors are open, which happens

approximately every 2 minutes. On the other hand, it has a very important recirculation rate through the filters. The AC turbines, which move the air inside the bus, move 3400 m^3/hour in their average speed. If we consider the volume of a bus as 68,54 m^3 (2.4 m width, 2.4 m height and 11.9 m length), the air is recirculated 50 times/hour approximately, or which is the same, the air is recirculated completely every 1.2 minutes.

2. 50 % recirculation. 18.5 % of the studied buses have this type of circulation. It has trapdoors for taking air from the exterior, which is mixed with the recirculated air (maximum 50 % outdoor air). According to the AC system manufacturers for urban buses, no forced infiltration of outdoor air is implemented, due to the frequent opening of the doors.

As energy saving policy, since 2018 the bus network is progressively changing from a radial to an orthogonal shape, so that we can distinguish between "vertical" routes (Vx), running from the coast uphill, and "horizontal" routes (Hx), parallel to the coastline (Fig. 2.3).

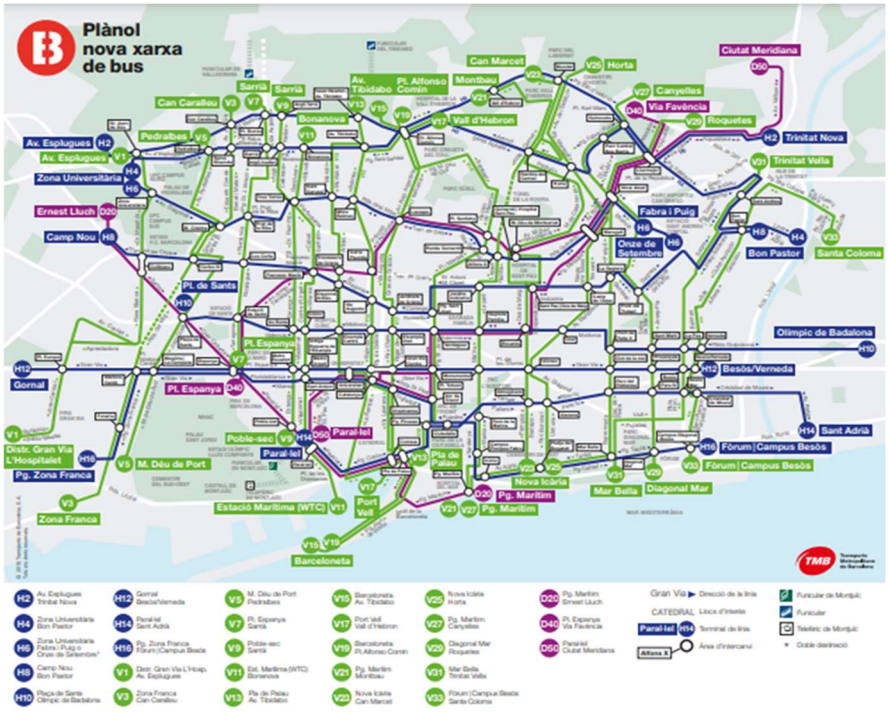

Figure 2.3. The new bus network established in 2018, ensuring that the routes have an orthogonal shape.

2.2. Sampling campaigns

2.2.1. Bus measurements

Different sampling campaigns were performed inside buses: a position study and an infiltration study before the main measurements, followed by a 10-months commuting study and finally an intermodal study (which is explained in section 2.6.) comparing different commuting modes.

Position study

Pollutant concentrations inside bus can vary in space (Moreno et al. 2015), thus before performing the commuting study, simultaneous measurements were carried out in one middle and one rear seat of the same bus, for each type of bus, to explore such variability and decide the most appropriate position for doing all measurements during the Thesis. Simultaneous measurements of quasi-ultrafine particle number (QUFPN, 10-300nm) concentration and black carbon (BC) were performed each journey (8 days in total), during a round trip along the whole length of the bus route (2 h approximately). The lines studied were 32 (EURO IV bus), 33 (HD bus), 34 (EV bus), 54 (CNG bus), 68 (HCNG bus) and H4 (EURO V bus). Three consecutive sampling days were performed in line 33, whereas only one day was done in the rest of the lines. Instruments for measurements were transported in a trolley, for the middle position, and in a backpack in the case of the rear position (Fig. 2.4). The measurements were carried out during the morning, after rush hour, on weekdays.

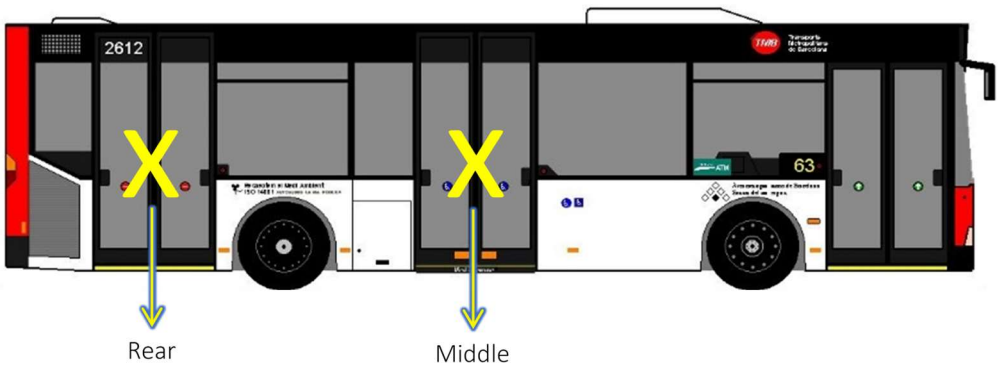

Figure 2.4. Different positions in which measurements have been carried out.

Commuting study

The commuting study was carried out between May 2017 and March 2018 in two different campaigns: "summer campaign" (from May 2017 to September 2017) with air conditioning, and "winter campaign" (from November 2017 to April 2018) without air conditioning. Only routes operated by two or more different powertrain types were selected. Measurements were performed in 11 different routes (H4, H12, H16, V3, V13, 7, 19, 34, 39, 47 and 60) and two tourist routes (blue and red), and 6 different powertrains were studied: EURO IV, EURO V), HD, CNG, HCNG and EV) (Fig. 2.5 and Fig. 2.6).

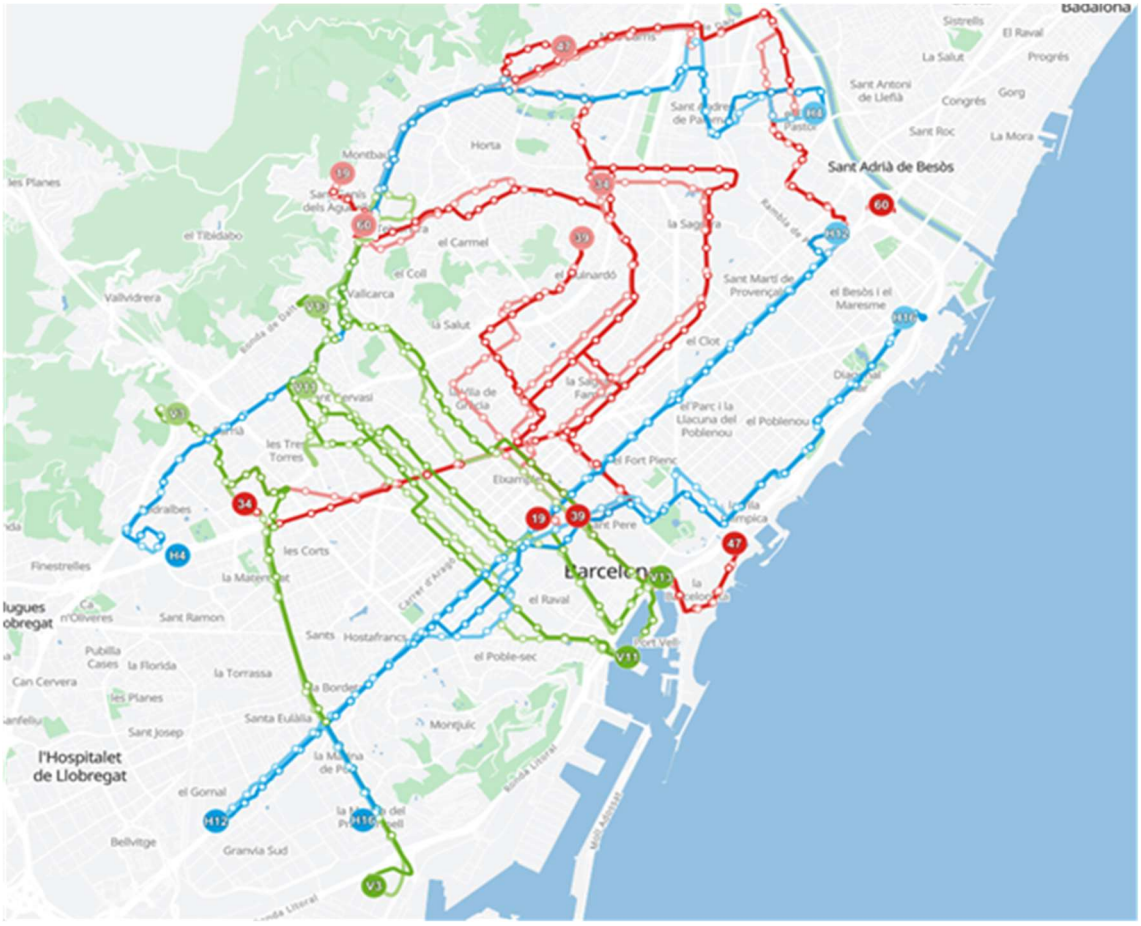

Figure 2.5. Overall map of the bus lines under study. In blue the horizontal lines, starting with "H", in green the vertical lines starting with "V" and in red the rest of the lines.

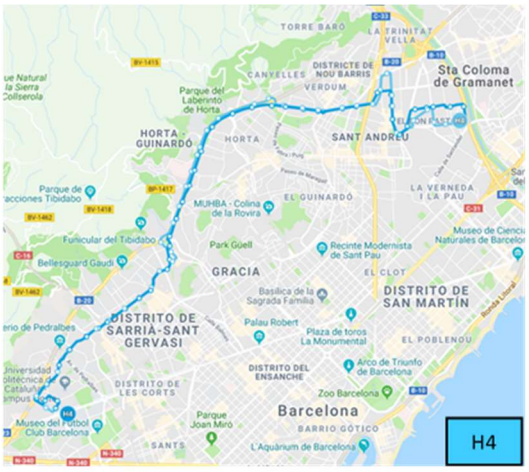

EURO V and HD

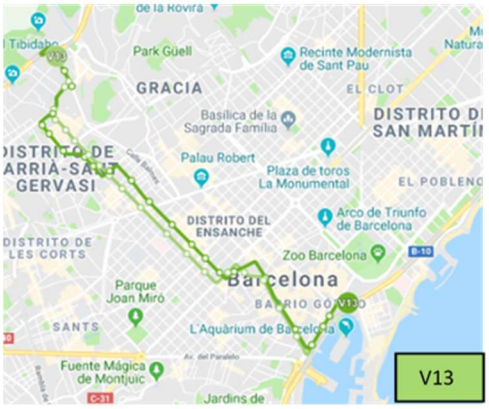

EURO V and HD
EURO IV and EURO V

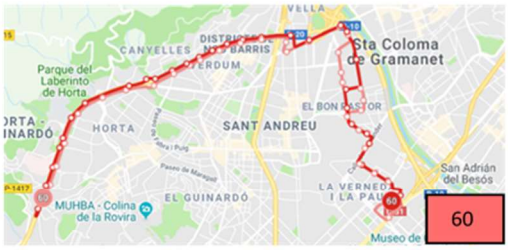

EURO IV and EV

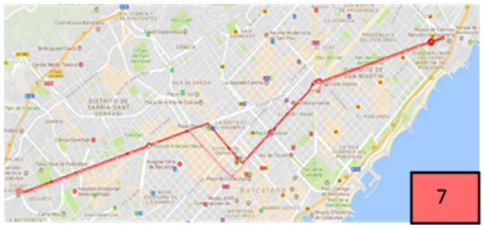

EURO V and HD

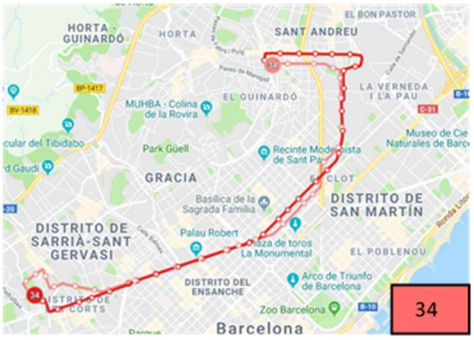

EURO V and EV
HD and EV

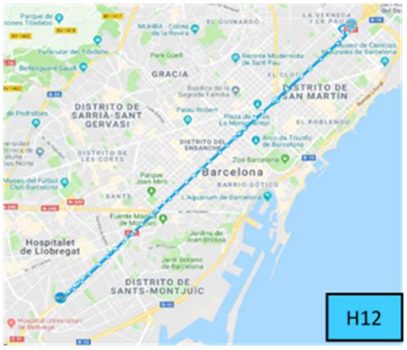

CNG and HD

EURO V and EV
HD and EV

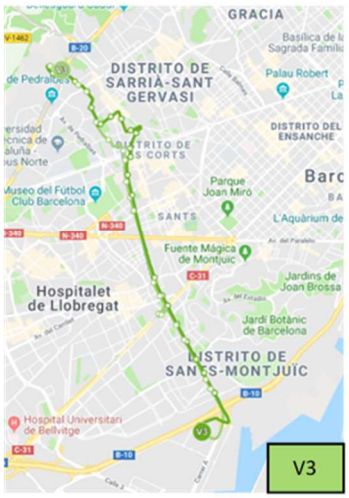

EURO V and CNG
EURO IV and CNG

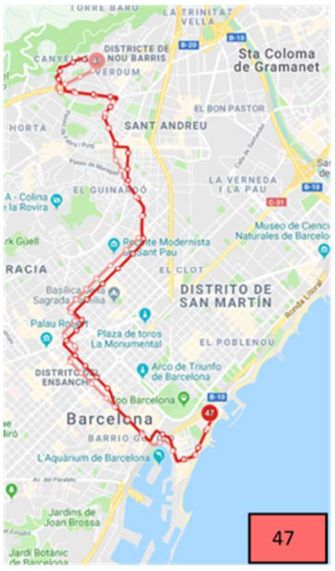

EURO IV and HD

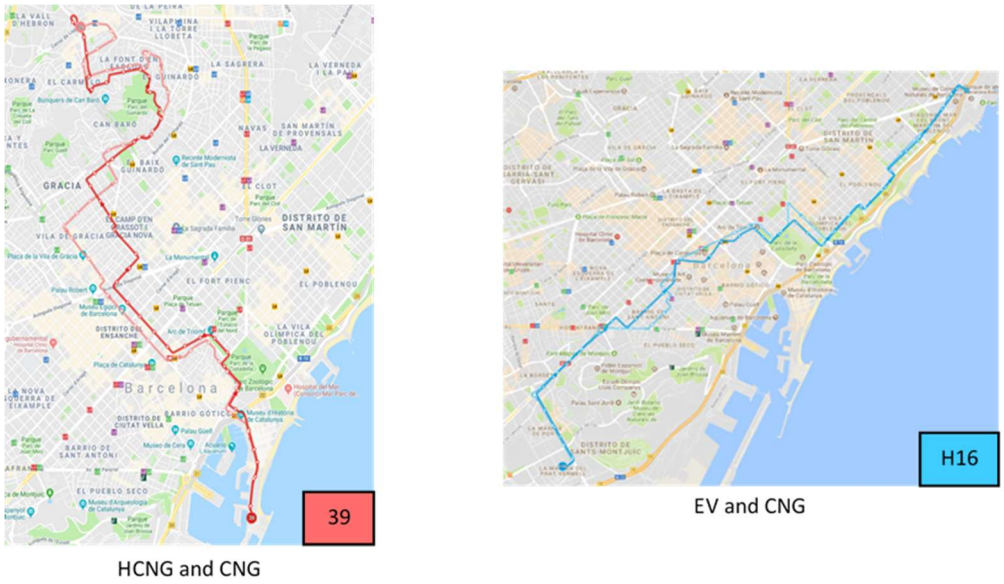

Figure 2.6. Detailed routes and operating buses.

Each route was studied in 3 different consecutive working days, and it was repeated in summer and winter (Table 2.2). Tourist buses were Euro IV, and two different lines were chosen: "red" (more southerly, including Montjuic Hill) and "blue" (mostly north of the Diagonal) routes (Fig. 2.7).

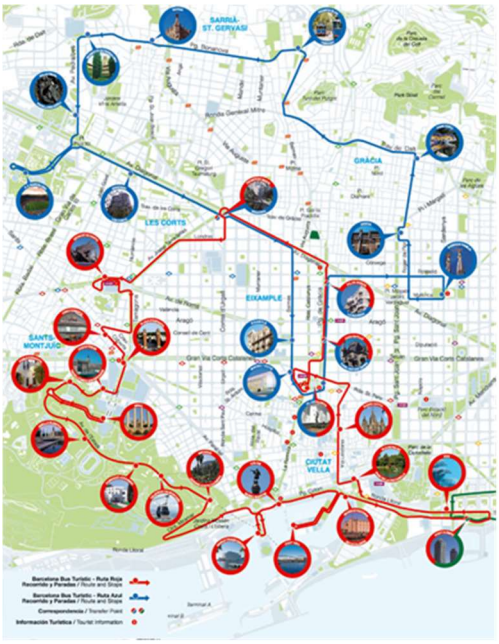

Figure 2.7. Blue and red routes of the tourist bus of TMB in which sampling were done.

Table 2.2. Bus pair comparisons made per each commuting study including information of each line and date. V = "Vertical" (coast to mountain) routes; H = "Horizontal" (coast-parallel) routes. Other bus routes (19, 34, 39, 47, 60) run along more mixed trajectories. Bus types are diesel EURO IV and V, hybrid diesel (HD), natural gas (CNG), hybrid natural gas (HCNG) and electric (EV). The tourist buses run using diesel EURO IV engines along "red" (more southerly, including Montjuic Hill) and "blue" (mostly north of the Diagonal) routes.

	SUMMER		WINTER	
Bus pair	Line	Date	Line	Date
EURO V vs EURO IV	V13	10, 11 May	V3	16, 17 Jan.
EURO V vs HD	V13	16, 17 May	H4	14, 15 Nov.
EURO V vs CNG	V3	30, 31 May.	V3	1, 12 Dec.
EURO V vs EV	34	14, 15 Sep.	-	-
EURO IV vs HD	47	10, 12 July	19	14, 15 Dec.
EURO IV vs CNG	V17 vs V11	20, 21 Sep.	V3	23, 24 Nov.
EURO IV vs EV	-	-	60	10, 12 April
HD vs CNG	H12	18, 19 Jul.	H12	26 Feb., 1 Mar.
HD vs EV	34	23, 24 May	34	27, 28 Mar.
CNG vs HCNG	39	13, 14 Jun.	39	10, 11 Jan.
CNG vs EV	H16	8, 9 Jun.	H16	19, 20 Feb.
Tourist inside vs outside	Blue	20, 21 Jun.	Blue	23, 24 Jan.
Tourist inside vs outside	Red	26, 27 Jun.	Red	30, 31 Jan.

Air quality instrumentation was carried in a trolley (Fig. 2.8) that was placed in the middle of the bus, where baby carts and wheelchairs are located during a round trip along the whole length of the bus route.

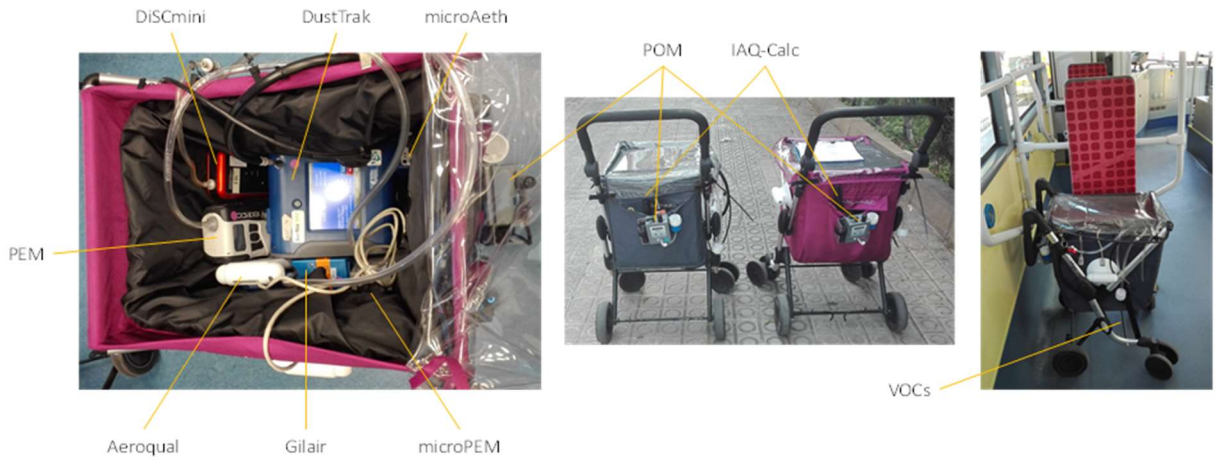

Figure 2.8. The equipment carried out in each sampling day inside buses.

For tourist buses the two commuters travelled in the same bus, one in the upper floor (which is open to outdoor air) and the other in the lower floor (which is more enclosed, but it is also ventilated through the stairs that connected it with the upper floor) (Fig. 2.9).

Figure 2.9. The sampling equipment inside tourist bus. In the left, the trolley that went in the lower floor, and in the right, the bag that went in the upper floor.

The total duration of the trip depended on the length of the route, being a round trip of 2 h approximately. The instruments were set at a 30-second time resolution. The measurements were carried out during the morning on weekdays, after 8:00 h and ending

at 14:00 h, depending on the route and the line chosen, and they were performed three consecutive days, if possible, at each of the selected lines, providing 6 h of sampling, approximately. A total of 288 routes were made, 72 trips per campaign.

A manual record of the timing, location, progress, and any special events during each journey (road crossing, bus stops, roadworks, getting in and out of the vehicle, etc.) was performed by each commuter. The bus identifier number (the ID number of buses) and the position of open windows was also recorded.

2.3. Air quality instrumentation

2.3.1. Portable equipment

Off-line instruments

For $PM_{2.5}$ sampling and chemical composition determination, 37 mm quartz fibre filters (Pallflex® Air Monitoring Filters, Pall, LifeScience) were used in the Personal Environmental Monitor (761-203B PEM, SKC) low volume sampler connected to a 10 L/min pump (Leland Legacy, SKC) (Fig. 2.10). The PEM allowed both measurement of average $PM_{2.5}$ concentration and the chemical analysis of the particles collected on the filters during 6 h. Each PEM filter was used during 3 consecutive days of sampling to achieve enough sample to be analysed. Quartz fibre filters were heated in an oven at 200°C during a minimum of 4 h to eliminate the organic impurities before sampling, conditioned for at least 48 h at 20 °C and 50 % relative humidity and then weighted before and after sampling by means of a microbalance (Model XP105DR, Mettler Toledo). Filters were kept individually in petri slides and stored at ambient temperature. The gravimetric $PM_{2.5}$ mass concentrations were determined dividing the weight difference between the blank and sampled filter by the volume of air sampled.

Figure 2.10. PEM and SKC pump used to sample $PM_{2.5}$ fraction for chemical analysis.

Volatile Organic Compounds (VOCs) were sampled using stainless steel cartridges (89 mm length x 6.4 mm O.D. x 5 mm I.D, Markes International Ltd., Llantrisant, UK) custom packed with 3 successive sections of activated graphitized BC adsorbents, 80 mg of Carbopack B absorbent, 180 mg of Carbopack and 180 mg of Carbopack X (Supelco Inc., Bellefonte, PA) for the analysis of the different compounds. The cartridges were pre-conditioned at 320°C with helium (5 N quality) flow at 100 mL/min for 2 h and conditioned before each sampling at 335 °C with same helium flow for 30 min. The clean cartridges were capped with inch brass long-term storage caps with PTFE ferrules and storage in free-VOC ambient until its use. For active sampling the cartridges were coupled to a low-flow pump through a single air inlet port of Pocket Pump Air (SKC Ltd., Blandford Forum, UK) (Fig. 2.11) with constant flow compensation at 20 mL/min for 6 h. The sampling pump was calibrated with a Defender 510L Calibrator (BIOS, Drycal, NJ, USA) before and after each sampling.

Figure 2.11. The cartridge and the pump used to measure VOCs inside buses.

Bioaerosol and endotoxin samples were collected on 37 mm glass fibre (GF) filters, with 0.8 µm pore size, loaded in closed-faced cassettes (CFC, SKC), which were connected to personal air sampling pumps (Gilian GilAir-5, Sensidyne, LP) previously calibrated with DryCal DC-2 flowmeter (BIOS, Drycal, NJ, USA) (Fig. 2.12). The sampling was done for 2 h/day during two consecutive days at a flow rate of 5 L/min filters. Filters were then kept in a 4°C fridge and send to Centre de Recherche de l'Institut Universitaire de Cardiologie et de Pneumologie de Québec (IUCPQ), Université Laval in Québec City, for analysis.

Figure 2.12. Gilair.

On-line instruments

$PM_{2.5}$ concentrations were continuously monitored by means of a light-scattering laser photometer DustTrak (Model 8533, TSI), a desktop instrument able to provide real-time measurements of particulate matter on a 90° light scattering sensor (Fig. 2.13) over a wide concentration range (0.001 – 150 mg/m^3) in real-time. This method combines photometric measurement to cover the mass concentration range and a single particle detection measurement to be able to size discriminate sampled aerosol (TSI, 2012). Prior to each sample cycle the monitor was zero-checked in accordance with manufacturer's guidelines. The time resolution was selected for 30-seconds. This equipment is easy to use and is normally taken in mobile campaigns, however frequent artefact jumps in the time-series of PM concentrations have been observed (Rivas et al., 2017).

Figure 2.13. DustTrak.

Particle number concentrations in the range 10^3 – 10^6 #/cm^3 were monitored using a DiSCmini (Testo) (Fig. 2.14) that also records the size of the particles in a range of 10 – 300 nm (modal value) and 10 – 700 nm (absolute value). The DiSCmini principle is based on particles positive unipolar charging by using a corona charger. Following particle charge, excess of ions is removed in an ion trap, and particles are detected in two stages by electrometers (diffusion and filter), allowing for particle sizing and counting. DiSCmini has high-time resolution of up to 1 second, but lower precision than a SMPS or CPC, with deviations of up to 30 %. It is sensitive to the temperature and relative humidity, and the data could be erroneous at high temperatures.

Figure 2.14. DiSCmini.

Black carbon (BC) concentrations were monitored using a microAeth® AE51 aethalometer, a pocket-sized BC aerosol monitor which provides aerosol BC concentration in real-time in µg/m^3 (Fig. 2.15). It measures the rate of change in absorption of transmitted light due to continuous collection of aerosols deposited on a filter. The air sample is collected on T60 (Teflon-coated borosilicate glass fibre) filter media, with the data being recorded in an internal flash memory operating on a 30 second time resolution. The flow rate was set up to 0.10 L/min for measurements. The instrument can operate continuously for up to 24 hours on a single battery charge, and the filter lifetime is dependent on concentration and flow rate settings. In our case the filter was

Figure 2.15. MicroAeth.

changed after 24 h of operation. It has a measurement resolution of 0.001 μg/m^3 and precision of ±0.1 μg/m^3.

CO_2 levels were monitored by means of an IAQ-Calc™ indoor air quality meter (Model 7545, TSI) which contains a non-dispersive infrared (NDIR) sensor for CO_2 in a range from 0 to 5000 ppm with accuracy of ± 3.0 % of reading or ± 50 ppm (Fig. 2.16). The instrument includes an electrochemical sensor for CO in a range from 0 to 500 ppm with accuracy of ± 3.0 % of reading or ± 3 ppm. The instrument also measures temperature and relative humidity by a thermistor (range from 0 to 60 °C with an accuracy of ± 0.6 °C), and a thin-film capacitive sensor (range of 5 to 95 %; accuracy ± 3.0 %), respectively.

Figure 2.16. IAQ-Calc.

In addition, a Global Positioning System (GPS; GARMIN eTrex® 20x) was always used to monitor geographic position of the bus every second (Fig. 2.17). Additionally, the operator recorded manually the time in which the bus was circulating or stopped.

Figure 2.17. GPS.

2.3.2. Rreference instrumentation

For comparison purposes, outdoor ambient concentrations were measured concurrently at the urban background station of Palau Reial (41°23′14″ N, 02°06′56″ E). This station is co-operated jointly by CSIC and Generalitat de Catalunya (local air quality manager).

Off-line instrument

Reference $PM_{2.5}$ samples were collected using an automatic sequential High-Volume Sampler (HVS, Model CAV-A/MSb, MCV) equipped with a $PM_{2.5}$ inlet (PM_{10}25/UNE model, built according to the European Norm: EN 14907) with a specific nozzle plate one for $PM_{2.5}$ (Fig. 2.18). This instrument was used to correct the data of the Grimm, the reference instrument that measures PMx on-line, it is explained below. The sampler operates at a sampling flow rate of 30 m^3/h. The air flow passes through the inlet and goes through the nozzles, where the speed

Figure 2.18. MCV.

increases. Then, for $PM_{2.5}$, the particles larger than 2.5 μm in diameter impact and adhere on a plate impregnated with vaseline and the smaller ones pass through and are collected on quartz fibre filter (150 mm diameter; Pallflex).

On-line instruments

Figure 2.19. Grimm.

PM_X concentrations were measured with the laser aerosol spectrometer (Environmental Dust Monitor, Model EDM180, Grimm; Fig. 2.19). Particle size is determined from the number of single particle counts registered in each channel, by a 15-channel pulse height analyser, and it is converted to mass units using a particle density-based equation thus obtaining size-resolved PM mass concentrations. This instrument measures particles of diameters between 0.3 and 15 μm. The data measured was corrected with the data of the MCV. In this study only the $PM_{2.5}$ mass concentrations were used in order to correct the data measured with the DustTrak.

Figure 2.20. CPC.

This instrument was used to calibrate the measurements obtained by DiSCmini in the Thesis. PN concentrations were measured with Water-based Condensation Particle Counters (GP-WCPC, TSI Model 3787 (range 5-800nm)) (Fig. 2.20) are designed to optically detect particles < 300 nm (Liu 1976, Stolzenburg and McMurry 1991). They are based on liquid (e.g., butanol, water) condensation on to the particles in order to increase their size up to a point where they can be optically detected (Agarwal and Sem 1980). The CPC used in this Thesis was butanol based and provided time resolved and size-integrated particle concentration data.

Environmental conditions like temperature and relative humidity (RH) were also measured. The location of the outdoor sampling stations is shown in Figure 2.22.

2.4. Sample treatment and chemical and biological analyses

2.4.1. Chemical analyses

$PM_{2.5}$ filters

After sampling filters were stored in the same conditions of 20 °C and 50 % RH for 24 hours and then weighted twice, every 24 h. Sample weight was calculated subtracting the blank weight from sampled weight.

Once the gravimetric determination was performed for a total of 48 samples, they were chemically analysed. First, a 1.5 cm^2 punch from the centre of the filter was cut to analyse organic and elemental carbon (OC, EC) by a thermal-optical technique using a Lab OC/EC Aerosol Analyser (Sunset Laboratory Inc.).

The remaining part of the filter was acid digested into a Teflon reactor using a mix of HF:HNO_3 (2.5: 1.25 mL) and then kept into an oven at 90 °C for 12 h (Querol et al., 2001). After cooling, 1.25 mL of $HClO_4$ were added. The acid solutions were then completely evaporated by placing the open reactors onto a laboratory hot plate (digital hotplate SD 500, Stuart) at 240 °C. The dry residue, was redissolved with 1.25 mL HNO_3 to make up a volume of 25 mL with Milli-Q grade water, resulting a solution of 5 % HNO_3. This solution was then chemically analysed by means of Inductively Coupled Plasma Atomic Emission Spectrometry (ICP-AES: IRIS Advantage TJA Solutions, THERMO) to determine major elements (such as Al, Ca, K, Na, Mg, Fe, P, S) and Mass Spectrometry (ICP-MS: X Series II, THERMO) to determine trace elements (Li, Ti, V, Cr, Mn, Co, Ni, Cu, Zn, Ga, Ge, As, Se, Rb, Sr, Y, Zr, Nb, Mo, Cd, Sn, Sb, Ba, La, Ce, Pr, Nd, Hf, W, Pb, Bi, Th, U, among others). For quality control of the analytical procedure an external calibration was carried out using 1633b Standard Reference Material (Trace Elements in Coal Fly Ash, NIST). For that, a small amount (0.01 g) of 1633b Standard Reference Material loaded on a similar fraction of blank quartz filter was also analysed. These external standards have a matrix like that of the samples and cover the entire range of expected concentrations, forming the calibration lines (0.5-100 ppb). The reference material analysis assures the quality of the results permitting the identification of possible analytical or calibration errors. Recovery rates and detection limits are listed in Table 2.3.

Table 2.3. Recovery rates (Rj) and detection limits (DL) obtained per each element analised. a) summer campaign and b) winter campaign.

a) Summer						
Element	**Certified value**	**SD**	**Mean value found**	**SD**	**Rj**	**DL**
µg/g						
Al	15.0500	0.2700	15.212	0.0107	101 %	0.5581
Ca	1.5100	0.0600	1.514	0.0091	100 %	0.5363
Fe	7.7800	0.2300	7.948	0.0029	102 %	0.3117
K	1.9500	0.0300	1.935	0.0129	99 %	0.5279
Na	0.2010	0.0030	0.165	0.0334	78 %	0.7680
Mg	0.4820	0.0080	0.470	0.0020	97 %	0.2209
P	0.2300	-	0.249	0.0021	108 %	0.2344
S	0.2075	0.0011	0.178	0.0050	84 %	0.5218
Ba	0.0709	0.0027	0.065	0.0019	90 %	0.1975
Cu	0.0113	0.0003	0.011	0.0003	93 %	0.0315
Mn	0.0130	0.0002	0.012	0.0001	96 %	0.0085
Ni	0.0010	0.0002	0.008	0.0023	188 %	0.2352
Pb	0.0068	0.0001	0.006	0.0008	85 %	0.0844
Sr	0.1041	0.0014	0.106	0.0000	102 %	0.0052
Ti	0.7910	0.0140	0.778	0.0004	98 %	0.0407
V	0.0296	0.0004	0.030	0.0001	103 %	0.0125
Zn	0.0210	0.0000	0.017	0.0019	76 %	0.1928
ng/g						
Ti	7910.0	0.003	7902.012	3.907	100 %	0.0386
V	295.7	0.008	292.721	1.264	99 %	0.0198
Cr	198.2	4.700	169.122	5.499	83 %	0.0588
Mn	130.0	0.001	124.266	0.826	95 %	0.0095
Ni	120.6	1.800	81.726	22.299	52 %	0.2343
Cu	112.8	2.600	103.384	6.363	91 %	0.0663
Zn	210.0	-	178.728	13.713	83 %	0.1383
Sr	1041.0	14.000	1022.639	0.443	98 %	0.0057
Zr	-	-	156.203	9.765	-	0.1133
Nb	-	-	22.391	0.000	-	0.0032
Cd	0.8	0.006	0.710	0.254	87 %	0.0042
Sn	-	-	5.632	0.328	-	0.0048
Sb	6.0	-	5.541	0.107	92 %	0.0034
Ba	709.0	27.000	607.298	15.845	83 %	0.1727
La	94.0	-	92.036	0.055	98 %	0.0033
Ce	190.0	-	190.389	0.101	100 %	0.0034
Nd	120.6	-	86.994	0.049	61 %	0.0033
Gd	13.0	-	17.792	0.058	127 %	0.0033
Dy	17.0	-	16.294	0.110	96 %	0.0034
Hf	6.8	-	4.540	0.619	50 %	0.0074
Pb	68.2	1.100	63.592	0.271	93 %	0.0043
Bi	-	-	0.869	0.000	-	0.0032
U	8.8	0.360	6.498	0.189	65 %	0.0039

b) Winter						
Element	**Certified value**	**SD**	**Mean value found**	**SD**	**Rj**	**DL**
µg/g						
Al	15.0500	0.2700	15.159	0.0534	101 %	0.1360
Ca	1.5100	0.0600	1.489	0.0038	99 %	0.1087
Fe	7.7800	0.2300	7.803	0.0043	100 %	0.0842
K	1.9500	0.0300	1.890	0.0337	97 %	0.1058
Na	0.2010	0.0030	0.213	0.0190	106 %	0.0872
Mg	0.4820	0.0080	0.480	0.0021	100 %	0.0822
P	0.2300	-	0.235	0.0017	102 %	0.0821
S	0.2075	0.0011	0.207	0.0041	100 %	0.0868
Ba	0.0709	0.0027	0.067	0.0011	94 %	0.0046
Cu	0.0113	0.0003	0.011	0.0006	95 %	0.0122
Mn	0.0130	0.0002	0.014	0.0002	104 %	0.0045
Ni	0.0010	0.0002	0.015	0.0026	193 %	0.0049
Pb	0.0068	0.0001	0.004	0.0008	34 %	0.0136
Sr	0.1041	0.0014	0.098	0.0001	93 %	0.0039
Ti	0.7910	0.0140	0.771	0.0003	97 %	0.0060
V	0.0296	0.0004	0.030	0.0008	102 %	0.0116
Zn	0.0210	0.0000	0.023	0.0028	107 %	0.0051
ng/g						
Ti	7910.0	0.003	7893.802	1.122	100 %	0.0670
V	295.7	0.008	288.274	0.306	97 %	0.0067
Cr	198.2	4.700	201.317	2.921	102 %	0.0512
Mn	130.0	0.001	131.542	0.232	101 %	0.0105
Ni	120.6	1.800	167.230	0.338	128 %	0.1965
Cu	112.8	2.600	112.275	8.754	100 %	0.0771
Zn	210.0	-	239.926	3.777	112 %	0.1848
Sr	1041.0	14.000	1040.239	0.218	100 %	0.0175
Zr	-	-	183.729	7.427	-	0.0729
Nb	-	-	26.495	0.000	-	0.0031
Cd	0.8	0.006	0.453	0.250	23 %	0.0040
Sn	-	-	6.446	0.036	-	0.0041
Sb	6.0	-	5.976	0.112	100 %	0.0052
Ba	709.0	27.000	753.174	1.203	106 %	0.1854
La	94.0	-	103.132	0.018	109 %	0.0056
Ce	190.0	-	194.568	0.053	102 %	0.0120
Nd	120.6	-	82.909	0.025	55 %	0.0049
Gd	13.0	-	17.467	0.016	126 %	0.0047
Dy	17.0	-	18.668	0.016	109 %	0.0061
Hf	6.8	-	7.390	0.599	108 %	0.0061
Pb	68.2	1.100	67.279	0.280	99 %	0.0052
Bi	-	-	0.837	0.000	-	0.0031
U	8.8	0.360	9.155	0.030	104 %	0.0062

Volatile Organic Compounds (VOCs) analyses

Volatile organic compounds (VOCs) were measured in 16 buses air, 46 samples in total. To analyse the samples, the same methodology as detailed in Moreno et al. (2019) was used. The VOCs trapped in the cartridges were analysed by the thermal desorption (TD) equipment Ultra 50:50 Multi-tube Auto-sampler/Thermal Desorber Unity Series 2 (Markes International Ltd, Llantrisant, UK) coupled to a gas chromatograph (GC) with mass spectrometry detector (MSD). Compounds were desorbed from the cartridges at 300 °C for 5 min with a helium carrier gas flow of 40 mL/min to the focusing trap (U-T11GPC-2S; Markes International Ltd.) at −20 °C. Afterwards, the trap was heated to 300 °C for 5 min with a carrier gas flow of 7.5 mL/min and transferred of the analytes into analytical column initiated the GC run. The GC was equipped with a DB-5MS UI capillary column (length 60 m, internal diameter 0.32 mm, film thickness 1 μm, Agilent J&W GC columns). Helium (5Ngrade) was the carrier gas at a flow of 1.5 mL/min (constant flow mode). The GC oven temperature program for VOCs started at 40 °C (10 min initial hold time), then increased to 150 °C at 5 °C/min and 210 °C at 15 °C/min (10 min final hold time). A transfer line heated to 280 ° C carried the compounds from the GC to the electron impact source of MSD. The source and quadrupole temperatures were 230 °C and 150 °C, respectively. The MSD acquired data in scan mode with a range 30 to 380 atomic mass units (amu).

2.4.2. Biological analyses

A total of 100 bioaerosol samples were kept in a 4 °C fridge until being sent to the University Institute of Cardiology and Pulmonology of Quebec - Laval University for analysis of total bacteria and fungi concentrations and endotoxins.

For this, each glass-fibre filter was placed in a 50 mL sterilized falcon tube that was eluted with 20 mL of the extraction solution (saline water, 0.9 % NaCl, containing 0.025 % of Tween 20, Sigma-Aldrich, P2287) (Fig. 2.21). After 60 min of vortexing at 4 °C (Multi-Pulse Vortexer, Glas-Col, Terre Haute, Ind.), each sample was centrifuged (Centrifuge 5810R, Eppendorf) for 10 min at 5000 rpm (2800 G-force or RCF) and 4 °C to pellet the debris. A volume of 1 mL of debris free aliquot was taken for endotoxin assay. The rest of the supernatant was filtered, to concentrate all the microbial cells as described in Mbareche et al. (2019), and was used to analyse total bacteria, *Penicillium/Aspergillus*, and *Cladosporium* fungi. Both aliquots were stored at -20 °C freezer, until their analysis.

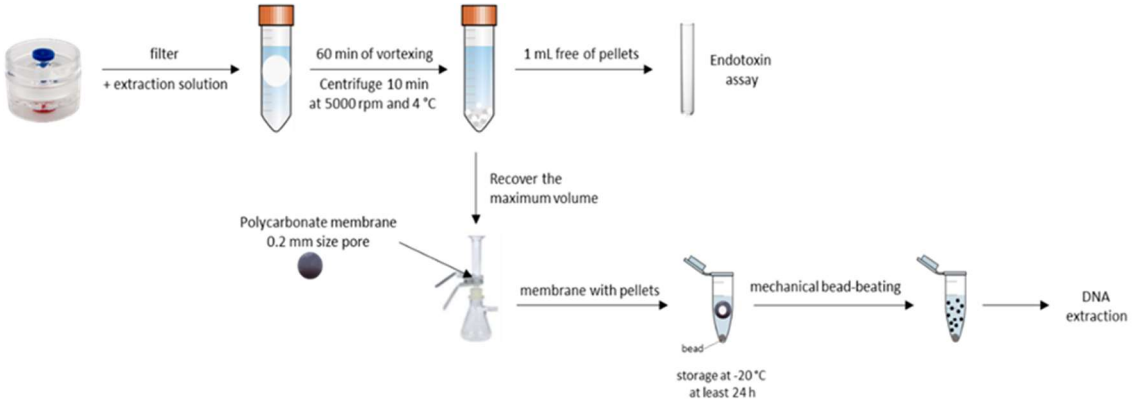

Figure 2.21. Filter treatment diagram to obtain aliquots for endotoxin assay and DNA extraction, with its prior cells concentration protocol.

2.4.2.1. Microbial concentration measurement by qPCR

DNA extraction was performed on pellets obtained from the previous step, using a Qiagen commercial DNasay kit (Qiagen, Canada) according to the protocol established by the manufacturer. Concentrations of total bacteria, *Penicillium/Aspergillus* and *Cladosporium* sp. were assessed by quantitative Polymerase Chain Reaction (qPCR). Primers, probes, master mix preparation and thermoprotocols are described in Table 2.4. All master mixes were prepared using iQ Supermix 1X (BioRad, Canada). Standard curves were prepared by diluting in series DNA from *Escherichia coli* (ATCC 25922), *Aspergillus fumigatus* colonies (isolated from peatland/air samples) and *Cladosporium* sp. (colony isolated from indoor air)

for total bacteria, *Penicillium/Aspergillus* and *Cladosporium* sp. qPCR respectively. All qPCR runs were performed using thermal cycler CFX96™ Real Time System (BioRad, Canada) for 40 cycles (Table 2.4). Data were analysed using the software CFX Manager version 3.1 (BioRad, Canada). Microbial concentrations were expressed in *E. coli* genome equivalent/m^3, *A. Fumi* genome equivalent/m^3, *Clado* genome equivalent/m^3 for total bacteria, *Penicilium/Aspergillus* sp. and *Cladosporium* sp. respectively.

Table 2.4. Primers/probes, master mix composition and the thermoprotocol used for each analysis (total bacteria, *Penicillium*/*Aspergillus* and *Cladosporium* sp.).

Target Primers/probe	**Master mix composition**	**Temperature cycles**	**Reference**
Total bacteria (16S rDNA) EUBf: [5′-GGTAGTCYAYGCMSTAAACGT-3′] EUBr: [5′-GACARCCATGCASCACCTG-3′] EUBP: FAMa-5′-TKCGCGTTGCDTCGAATTAAWCCAC-3′ IBTMFQb] EUBP: FAMa-5′-TKCGCGTTGCDTCGAATTAAWCCAC-3′ IBTMFQb]	Primers (F+R): 50 µM Probe: 10 µM iQ SuperMix: 10 µL DNA template: 5 µL Water: 4.5 µL Final volume: 20 µL	Initial denaturation: 95°C, 3 min Denaturation: 95°C, 20 s Hybridization and elongation: 62°C, 60 s	Bach et al. 2002
***Penicillium/Aspergillus* (18S rDNA)** PenAspF1: 5'- CGG AAG GAT CAT TAC TGA GTG-3' PenAspR1: 5'- GCC CGC CGA AGC AAC-3' PenAspP1mgb: 5'-FAM-CCA ACC TCC CAC CCG TG-TAMRA-3'	Primers (F+R): 50 µM Probe: 10 µM iQ SuperMix: 10 µL DNA template: 5 µL Water: 4.5 µL Final volume: 20 µL	Initial denaturation: 94°C, 3 min Denaturation: 94°C, 15 s Hybridization and elongation: 60°C, 60 s	EPA, 2019
***Cladosporium sp.* (18S rDNA)** Clado-TaqMan-PF: 5'- CCTCAACGTCAGTTATTACAT -3' Clado-TaqMan-PR: 5'- ACCTAGACAGTATTTCTAGCCT -3' Clado-TaqMan-PB: 5'-FAM-CTACTCCAATGGTTCTAATATTTTCCTCTC -BHQ-3'	Primers (F+R): 50 µM Probe: 10 µM iQ SuperMix: 10 µL DNA template: 2 µL Water: 7.5 µL Final volume: 20 µL	Initial denaturation: 95°C, 5 min Denaturation: 95°C, 10 s Hybridization and elongation: 60°C, 60 s	Zeng et al. 2006

Standard curve preparation

DNA from *E.coli* (#ATCC: 35218) was extracted using the Qiagen commercial kit (Qiagen, Mississauga, Ontario, Canada), QIAamp® DNeasy PowerLyzer PowerSoil Kit according to the manufacturers' recommendations. DNA per tube was assessed to calculate the volume to be suspended in TE buffer for 5×10^5 copies of genome/µL. Then, 10 µL aliquots were prepared. From this point, serial dilutions were made to achieve a standard curve from 10^0 to 10^6 copies per reaction. The results of the concentration of total bacteria have been expressed in terms of *E. coli*.

MiSeq Illumina® Sequencing

The amplification of targeted genes, equimolar pooling, and sequencing were performed at the Plateforme d'analyses génomiques (IBIS, Université Laval, Québec, QC, Canada). The 16S rRNA V6-V8 region was amplified using the sequence-specific regions described in Comeau et al. (2011) using a two-step dual-indexed PCR approach, specifically designed for Illumina® instruments, San Diego, California, United States. The gene-specific sequence was first fused to the Illumina® TruSeq sequencing primers and PCR was carried out in a total volume of 25 µL containing 1 × Q5 buffer (NEB, Ipswish, MA, USA), 0.25 µM of each primer, 200 µM of each of the dNTPs, 1 U of Q5 High-Fidelity DNA polymerase (NEB) and 1 µL of template DNA. PCR reactions were purified, checked for quality on a DNA7500 Bioanalyzer chip (Agilent®, Santa Clara, CA, USA) and then quantified spectrophotometrically with the Nanodrop® 1000 (Thermo Fisher Scientific, Waltham, MA, USA). Barcoded amplicons were pooled in equimolar concentrations for sequencing on the Illumina® MiSeq machine.

2.4.2.2. Endotoxin assay

The debris-free aliquot obtained from filter extraction was used for endotoxin quantification using a Limulus Amebocyte Lysate (LAL) Kinetic-QCL® kit Kinetic Chromogenic LAL Assay (Lonza, Walkersville, Maryland, USA) according to the protocol established by the manufacturer.

Endotoxins from *Escherichia coli* O55:B5 were used as a standard. An inhibition/enhancement test was performed prior to measurement (Hollander et al. 1993). Runs were performed using a plate reader (Synergy H1 Hybrid Multi-Mode Reader, BioTek, Winooski, VT, USA) and data were analysed using the software Gene5 2.00 (BioTek, Winooski, NH, USA). Endotoxin concentrations were expressed as endotoxin units per cubic meter of air (EU/m^3).

Sample preparation

First, samples and the endotoxin quantification reagents (Lonza) had to reach room temperature. After that, samples were vortexed for 30 min in a maximum speed (Vortex Genie 2), and they were diluted in endotoxin-free borosilicate tubes with LAL reagent water. The plate was filed with 100 µL of each, dilution, in duplicate, and in one of each duplicate a 10 µL spike of 5 EU/mL was added, to assess a potential inhibition of the enzymatic reaction, also in blanks. 100 µL of standards and negative controls were added. Using Gen5TM software, some parameters were set: 150 s of time between readings (Delta t), 405 nm of wavelength, 200 nm of Delta m0D, 40 number of reads and DO 0.2 reaction time. While the incubation time, Kinetic-QCL™ reagent (Lonza, K50-643) was reconstituted adding 2.6 mL of LAL reagent water (Lonza, W50-640), and mixed gently to homogenize the solution to avoid any foam formation, when coated with the endotoxin-free side of the parafilm and aluminium foil. With a multichannel pipette, 100 µL of Kinetic-QCL™ reagent were added in each well. That step had to be immediate, due to the reaction activation, and the plate was put inside the reader without the lid.

Standard curve preparation

E. Coli O55:B5 Endotoxin solution (50 EU/mL) was used as a concentrated standard. It was vortexed for 15 min prior its use. Standard curve was prepared with solutions of 5, 0.5, 0.05 and 0.005 EU/mL concentrations. And as in the rest of standard curve preparations cascade dilutions was done with a minute of vortexing between each dilution and adding 0.9 mL of LAL reagent water to each of them.

2.5. Data processing

2.5.1. Portable equipment data correction

Intercomparisons were performed between the portable equipment, carried inside buses, and the reference instruments at the urban background (UB) station of Palau Reial, before and after each commuting study (Fig. 2.22).

Figure 2.22. Location of Palau Reial reference background station in Barcelona (on the left) and the station (on the right).

Portable measurement equipment calibration consists in comparing and documenting device's measurement against a traceable reference standard equipment. Calibration is important to be confident in the validity of the measurements, to ensure higher performance of the instrument. The reference equipment is calibrated by technicians from the company that produces it. In Table 2.5a (for summer campaign) and table 2.5b (for winter campaign) are summarized the information corresponding to the comparation and correction of each of the portable equipment used to measure the air pollutants inside buses against the reference equipment. The reference equipment with which the comparison was made is indicated, as well as the correction values used for each of the portable equipment.

The intercomparisons were carried out during 8 consecutive days. The resolution of the reference instrumentation was 30 min for the Grimm and 5 min for the CPC. In the case of the measurements with the Dusttrak several problems were encountered as already mentioned by Rivas et al. (2017), so those corrections were not applied. Thus, Dusttrak measurements shown in this Thesis are not corrected against reference equipments, and therefore data available for $PM_{2.5}$, should be considered as semiquantitative. Values are showed only to compare $PM_{2.5}$ behaviour between the different conditions analysed.

Table 2.5. Information corresponding to the calibration of each portable equipment used to measure air pollutants inside the buses (equipments A and B) against the reference equipment. a) summer campaign and b) winter campaign.

a)			***SUMMER***					
			BUS A			***BUS B***		
Parameter	**Portable equipment**	**Reference equipment**	**Slope**	**Offset**	**R^2**	**Slope**	**Offset**	**R^2**
QUFPN	DiSCmini (Testo)	CPC (GP-WCPC, TSI Model 3787 (range 5-800nm))	1.2293	792.48	0.9071	1.1985	699.96	0.9139
BC	microAeth® AE51 aethalometer	Corrected against another microAeth® AE51 aethalometer	Ref.			1.0155	11.42	0.8121
$PM_{2.5}$	DustTrak (Model 8533, TSI)	GRIMM (Environmental Dust Monitor, Model EDM180) corrected with HVS, Model CAV-A/MSb, MCV	0.4354	51.72	0.8977	0.5825	4.68	0.8969
CO_2	IAQ-Calc™ (Model 7545, TSI)	Corrected against another IAQ-Calc™ (Model 7545, TSI)	1.4263	- 66.21	0.8089	Ref.		
T	IAQ-Calc™ (Model 7545, TSI)	GRIMM (Environmental Dust Monitor, Model EDM180)	0.702	4.24	0.7615	0.7884	2.53	0.8331

b)			***WINTER***					
			BUS A			***BUS B***		
Parameter	**Portable equipment**	**Reference equipment**	**Slope**	**Offset**	**R^2**	**Slope**	**Offset**	**R^2**
QUFPN	DiSCmini (Testo)	CPC (GP-WCPC, TSI Model 3787 (range 5-800nm))	0.6638	781.05	0.5208	0.609	1168.3	0.511
BC	microAeth® AE51 aethalometer	corrected against another microAeth® AE51 aethalometer	Ref.			1.0155	11.42	0.8121
$PM_{2.5}$	DustTrak (Model 8533, TSI)	GRIMM (Environmental Dust Monitor, Model EDM180) corrected with HVS, Model CAV-A/MSb, MCV	0.2888	5.30	0.9074	0.3454	5.27	0.9064
CO_2	IAQ-Calc™ (Model 7545, TSI)	corrected againts another IAQ-Calc™ (Model 7545, TSI)	1.4263	- 66.21	0.8089	Ref.		
T	IAQ-Calc™ (Model 7545, TSI)	GRIMM (Environmental Dust Monitor, Model EDM180)	0.702	4.24	0.7615	0.7884	2.53	0.8331

2.5.2. Statistical analyses

Real-time data statistical analyses

Statistical analyses were performed for QUFPN and BC to see the significant differences between different kind of variables. Values of each pollutant were compared between each fuel, per pairs, using the Wilcoxon rank-sum (Mann–Whitney) tests. Statistical analysis was performed in Stata SE 12 (StataCorp LLC, College Station, Texas, USA). For that, ventilation conditions were considered: AC on or off and windows closed or opened.

Bioaerosol statistical analyses

Statistical analyses were performed to see if there were significant differences between both sampling seasons, bus fuel type differences and differences between inside and outside tourist bus. They were run in Prism version 8.0 (GraphPad) and different tests were applied: Mann Whitney test to see if there were significant differences between both sampling seasons, Kruskal-Wallis test for bus fuel type differences, Wilcoxon matched-pairs signed rank test for differences between inside and outside tourist bus.

For alpha diversity measures, the normality was verified using the D'Agostino and Pearson omnibus normality test. The assumption of data normality was not fulfilled. Non-parametric Mann-Whitney U tests (two-tailed) were performed to highlight that there are significant differences in diversity measures between the groups of samples. A p-value ≤ 0.05 was considered statistically significant. All the results were analysed using the software GraphPad Prism 5.03 (GraphPad Software, Inc., San Diego, California, United States). Detailed information about the performance of the test is presented in the multivariate section of the results. The non-parametric Mann-Whitney U test was used to ascertain whether differences in Operational Taxonomic Unit (OTU) abundances were statistically significant between the group of samples. To test OTU differential abundance, the null hypothesis was that the populations of the two groups of samples were collected from have equal means.

Regarding Bioinformatics, it was applied to EURO IV, EURO V, HD and GNG, as they had enough bacterial concentration and EV and HCNG were excluded due to small number of samples with that bacterial load. Briefly, after de-multiplexing the raw FASTQ (is a text-based format for storing both a biological sequence (usually nucleotide sequence) and its corresponding quality scores) files, the reads generated from the paired end sequencing

were combined using the make.contigs script from mothur (Schloss et al. 2009). Quality filtering was also performed with mothur, using the screen.seqs script to discard homopolymers, reads with ambiguous sequences, and reads with suspiciously short lengths. Similar sequences were gathered to reduce the computational burden, and the number of copies of the same sequence was displayed to monitor the abundance of each sequence. This de-replication step was performed with VSEARCH (Rognes et al. 2016). The sequences were then aligned with the bacterial reference SILVA core alignment using the QIIME script align_seqs.py (Caporaso et al. 2011). OTUs, with a 97 % similarity cut-off, were clustered using the UPARSE method implemented in VSEARCH. UCHIME was used to identify and remove the chimeric sequences (Edgar et al. 2011). QIIME was used to assign taxonomy to OTUs based on the SILVA database reference training dataset for taxonomic assignment and to generate an OTU table. A metadata-mapping file was produced that includes information about air samples. The microbial diversity analyses, including statistical analyses, conducted in this study, were achieved using QIIME plugins in version 1.9.0 as described in QIIME scripts (http://qiime.org/scripts/).

2.5.3. Source apportionment of $PM_{2.5}$

After the complete chemical characterisation of $PM_{2.5}$, a receptor model was applied to determine and quantify the sources. This was carried out by means of the Positive Matrix Factorization (PMF) software (US–EPA PMF v5, Paatero and Tapper, 1994; Amato et al., 2009), using relevant criteria (see Paatero and Hopke, 2003) that allowed selection of 11 strong species (OC, EC, Ca, Fe, Mg, SO_4^{2-}, Mn, Cu, Sr, Sn, Sb) and 10 weaker species (Al_2O_3, K, Na, Ti, V, Ni, Zn, Ba, La and Pb). This multivariate receptor model provides estimates of the chemical composition of PM associated with different sources and the mass contribution attributed to each source. PMF factorizes the chemical composition matrix X, containing n samples (rows) with m species (columns), into two submatrices, the chemical profiles F and the time series G, so that p different sources of emissions or secondary components are identified, and their contribution is quantified. The residual E matrix corresponds to the fraction of X not explained by the solution (Eq. 2.1).

$$X = GF + E \qquad \textbf{Equation 2.1}$$

The G and F matrices are adjusted until a minimum for the objective function Q for a given number of factors p is found (Eq. 2.2):

$$Q = \sum_{i=1}^{n} \sum_{j=1}^{m} \left(\frac{e_{ij}}{\sigma_{ij}} \right)^2$$ **Equation 2.2**

The data matrix was uncensored (i.e. negative) so that below detection and zero limit values were included in the analyses to avoid a bias in the results (Paatero, 2007).

For the PMF analyses the species uncertainties were calculated according to Escrig et al. (2009). The source apportionment was applied using the sum of all chemical species analysed, as the total variable hence excluding the non-determined mass due to humidity and heteroatoms. The selection of the species included in the model was done according to their signal to noise ratio, the percentage of samples above detection limit and the significance of the species (knowledge of its presence in possible PM sources).

CHAPTER 3:
RESULTS AND DISCUSSION

3. RESULTS AND DISCUSSION

All the data collected inside buses were divided into selected sub-groups by differences in powertrain (diesel (EURO IV and EURO V), hybrid diesel (HD), natural gas (CNG), hybrid of natural gas (HCNG), and electric (EV)), "seasonal differences" with AC on or off, type of route (vertical vs horizontal and "other routes"), as well as the tourist buses upper floor (outside) and lower floor or downstairs (inside). Equivalent data were collected simultaneously at the Palau Reial urban background monitoring site (UB). Different contaminants were analysed inside the buses, and they were divided into different subgroups: levels, chemistry and bioaerosols.

The number of days in which the sampling took place covered two campaigns 1st from May to September 2017 and the 2nd one from November to March 2018. As a result of these field campaigns an unprecedented amount of data on bus AQ was obtained, not only from standard urban commuting vehicles but also from open top double decker tourist buses.

Position study. Ancillary measurements: Equipment location

The ancillary measurements carried out to choose the most appropriate position to place the equipment inside the buses, indicate that no significant differences exist in the concentrations of QUFPN and BC between the middle and rear seats of the same bus (Fig. 3.1). This led to the decision to always place the monitoring equipment in the middle position at the centre of the bus, this being the most spacious and comfortable interior location. The slope obtained for QUFPN (data in 10 s resolution) was of 1.03 and R^2=0.84 and for BC (data in 30 s resolution) the slope was 0.95 and R^2=0.95.

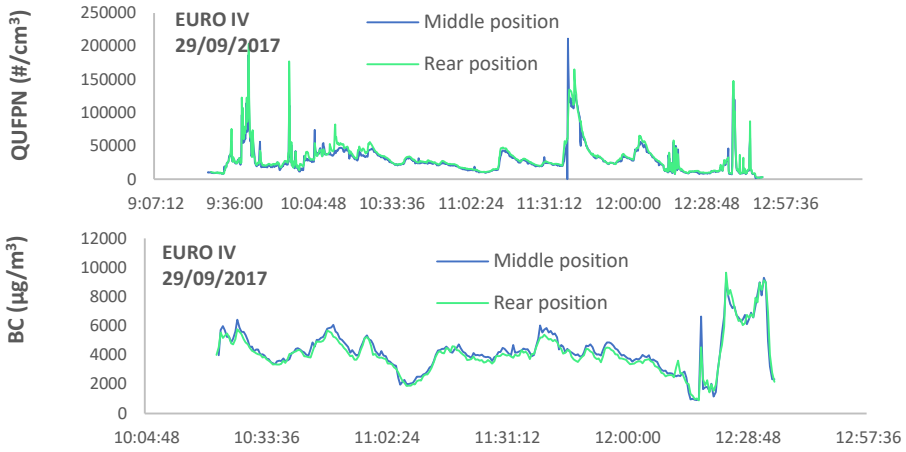

Figure 3.1. Example of QUFPN and BC concentrations comparing two different positions of the same bus (middle and rear).

3.1. Levels. Analysing general results

In this section, the concentrations recorded by the equipment measuring on-line is explained. These data are summarized in Table 3.1. presented with mean, median, and standard deviation (SD) of the reference station (UB), all buses (AB), vertical routes (V), horizontal routes (H), the different powertrain types, AC on, AC off, and tourist buses (inside and outside) for the whole campaigns. *n* indicates the number of measured journeys that could be analysed or interpreted.

Table 3.1. Average and median values of quasi-ultrafine particle number (QUFPN: 10-300 nm) concentrations and size, and BC and $PM_{2.5}$ mass concentrations measured inside buses during the monitoring campaign. "All buses" refers to commuting buses (not tourist services) and these are subdivided into different routes, engine types, and whether the air conditioning was recorded to be on (summer months only) or off. All values corrected against reference equipment except $PM_{2.5}$. SD: Standard Deviation, n: number of trips.

		UB	AB	AB/ UB	Vertical route	Horizontal route	Diesel nontourist	Non-diesel	AC on	AC off	Tourist inside	Tourist outside
QUFPN (#/cm³)	*n*				*40*	*30*	*62*	*50*	*58*	*54*	*12*	*12*
	Mean	17,391	34,511	1.98	38,720	28,543	37,776	30,463	37,233	26,278	47,092	49,196
	Median	16,232	28,250	1.74	32,368	22,899	29,883	26,225	29,913	22,045	37,142	31,303
	S.D.	5,737	24,906	4.34	29,063	21,108	29,930	18,675	28,258	18,202	34,315	66,864
QUFP size (nm)	*n*				40	30	63	50	58	54	12	12
	Mean	47	42	0.90	43	43	41	44	47	39	41	41
	Median	43	43	1.00	44	43	42	44	47	39	42	42
	S.D.	4.6	6.7	1.44	6.6	6.6	7.0	6.2	8.3	5.5	7.3	9.7
BC (μg/m³)	*n*				38	29	57	50	57	50	11	12
	Mean	2.2	5.6	2.5	6.6	5.1	6.1	5.1	5.0	5.7	6.8	6.2
	Median	2.0	5.2	2.5	6.2	4.6	5.6	4.6	4.5	5.5	6.0	4.9
	S.D.	1.0	2.9	2.8	3.5	2.7	3.1	2.8	2.7	2.8	3.7	4.2
$PM_{2.5}$ (μg/m³)	*n*				40	29	57	50	57	54	9	11
	Mean	13.7	33.7	2.4	36.1	33.4	32.4	35.1	29.7	37.5	40.1	41.9
	Median	13.7	31.7	2.3	35.6	32.3	31.1	32.4	28.3	35.7	39.9	40.9
	S.D.	2.2	12.2	5.6	12.9	8.2	11.4	13.5	8.4	14.9	9.2	14.0
CO_2 (ppm)	*n*				40	30	58	45	53	50	11	9
	Mean	-	936	-	694	754	869	1023	1015	905	470	452
	Median	-	865	-	682	743	809	930	905	864	454	444
	S.D.	-	293	-	180	213	242	330	334	242	41	44

Mean values of the pollutants listed in Table 3.1. were 2.0 (QUFPN) to 2.5 (BC and $PM_{2.5}$) times higher than urban background concentrations measured simultaneously during each bus journey. Vertical routes and diesel (non-tourist) buses recorded highest median values of QUFPN and BC, as it was expected since they are traffic tracers (Moreno et al., 2015; Ham

et al., 2017; Liu et al., 2019; Amato et al., 2016; Zhang and Zhu, 2010; Ham et al., 2017; Morawska et al., 2008). Inside vertical routes buses, higher concentrations were measured, as the engine needs more power going uphill, and therefore more emissions. The frequency of pollutant peaks of QUFPN and BC measured in the buses is reflected by consistently lower median values, this being most obvious in the open top of the tourist buses ("Tourist outside": mean/median = 1.6) where passengers were most exposed to transient traffic-related pollutant spikes. Median values for ultrafine particle sizes were remarkably consistent at around 42-44 nm, except for a wider spread (39-47 nm) revealed by comparing AC on (47 nm) with AC off (39 nm) conditions. CO_2 highest mean concentration was measured inside non-diesel buses (1023 ppm) and lowest in tourist buses (470 and 452 ppm, inside and outside, respectively).

Figure 3.2 shows number concentrations of quasi-ultrafine particles (10-300nm modal diameter) measured using the DiSCmini, comparing the various groups separated in Table 3.1. Note the relatively low values recorded by the urban background station, the interquartile range (IQR) data from which do not overlap with that of "All buses". Lowest mean/median values measured inside buses were in the Horizontal routes sub-group (28,543 / 22,899 #/cm^3) and are 25-30% lower than mean/median values in Vertical routes (38,720/32,368 #/cm^3).

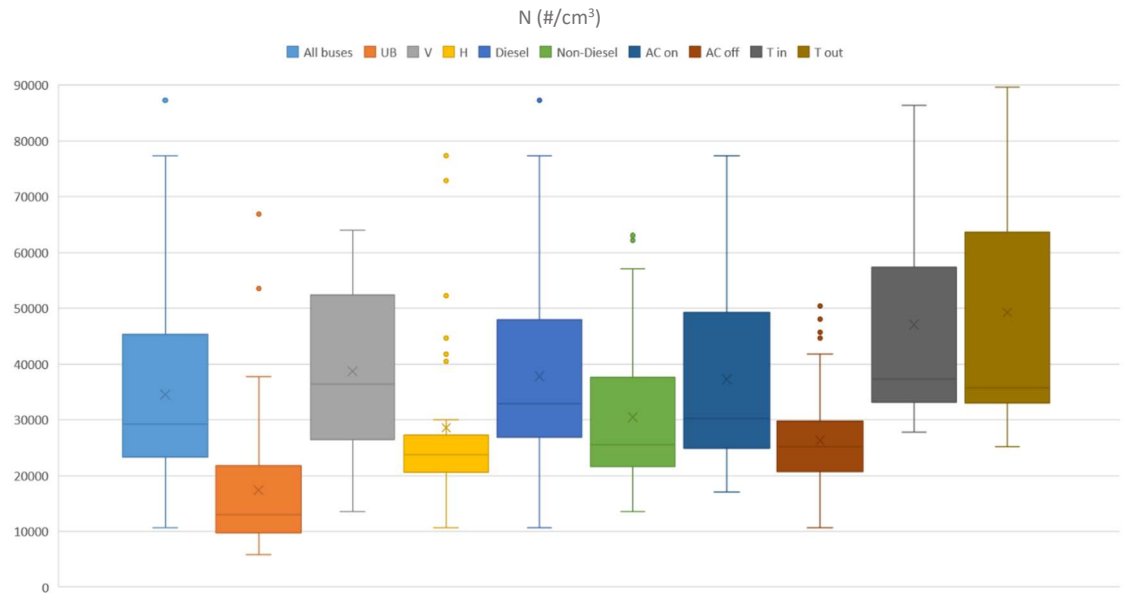

Figure 3.2. Boxplot for number concentrations (N) of particulate matter < 300 nm in diameter (quasi-ultrafine particles QUFP). Mean values marked as crosses and median values as horizontal lines. Interquartile range (IQR) represented as coloured rectangles. Outliers (mean values, which are explained in section 3.1.4.) marked as coloured dots. "All buses" excludes tourist buses; UB = urban background; V = vertical routes; H = horizontal routes; Tin/Tout = open-topped tourist buses inside (downstairs) and outside (upstairs).

All data groups record overlapping IQR values for QUFP sizes between 34 and 50nm, with little difference between mean and median concentrations (Table 3.1; Fig. 3.3). This size range seems to be typical of the peak size distribution of airborne ultrafine particles found inside buses and is sometimes referred to as "aged traffic" PM to distinguish it from finer "fresh traffic" size modes <25nm (compare Moreno et al., 2020).

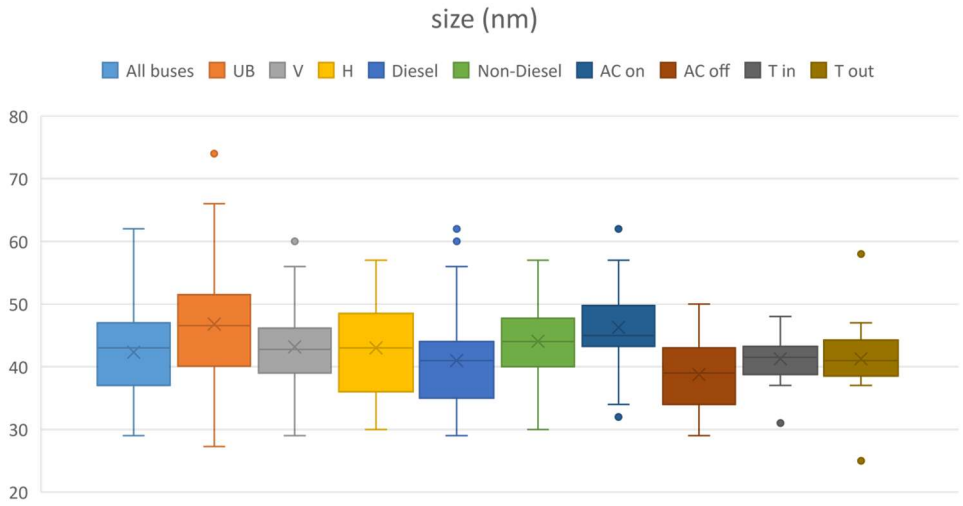

Figure 3.3. Average sizes of particulate matter < 300nm. Outliers (which are explained in section 3.1.4.) marked as coloured dots are as follows: Urban Background 8 June 74nm; Vertical route, diesel, AC on 17 May EURO V 60nm; AC on 23 May bus 34 hybrid diesel 32nm; Tourist inside downstairs (in) 28 June 31nm, Tourist outside upstairs (out) 28 June 25nm and 26 June 58nm.

Levels of BC inside buses averaged 5.6 µg/m^3, with most measurements lying within an IQR of 4-7 µg/m^3 (Table 3.1). In contrast, equivalent measurements taken at the Palau Reial urban background site recorded average concentrations of 2.2 µg/m^3, demonstrating the important contribution of incompletely combusted hydrocarbon fuels sourced from road traffic exhaust within the city. Somewhat higher average and median BC values for vertical route and diesel bus, as compared to horizontal route and non-diesel buses, are revealed on the BC boxplot (Fig. 3.4), although there is overlap between all bus sub-group IQRs.

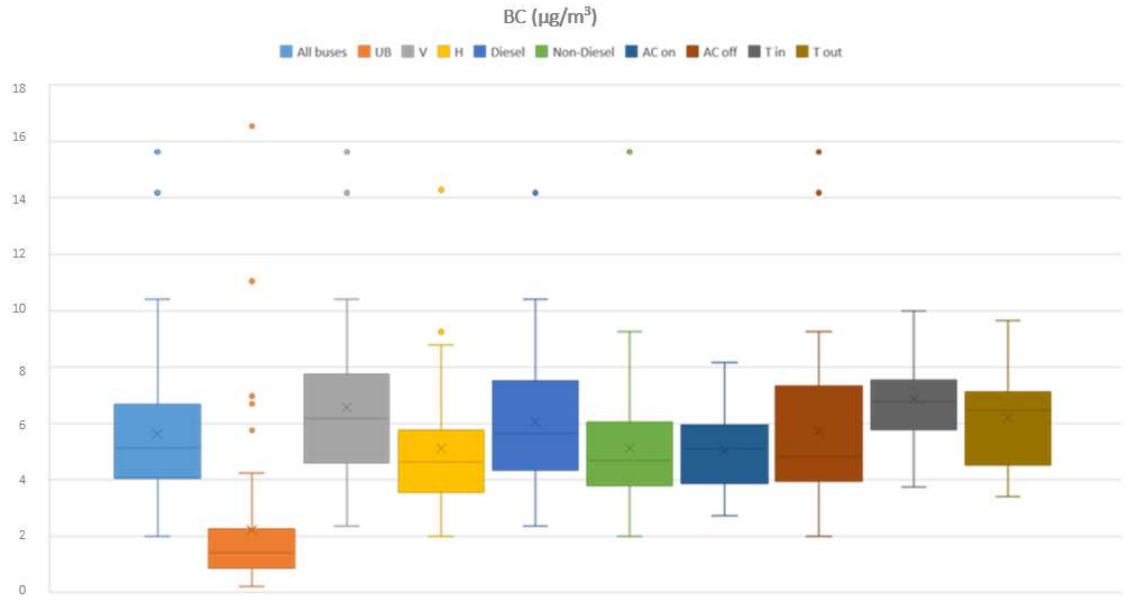

Figure 3.4. Ranges of black carbon concentrations measured inside buses and in urban background. Outliers (which are explained in section 3.1.4.) marked as coloured dots are as follows: All buses: 24 Nov natural gas V3 15.6 µg/m³; 1 Mar hybrid diesel H12 14.6 µg/m³; 24 Nov EURO IV V3 14.2 µg/m³; Urban Background: 24 November 16.5 µg/m³; 24 January 11.0 µg/m³, 16 November 6.7 µg/m³; 23 November 5.8 µg/m³; 1 March 7.0 µg/m³; Vertical route: same as all buses; Horizontal route: same as all buses plus 1 March natural gas H12 9.6 µg/m³; AC off: same as all buses.

Average mass concentration values of $PM_{2.5}$ measured inside buses were 34 µg/m³ (uncorrected values), as compared to 13 µg/m³ in the urban background recorded simultaneously at the Barcelona Palau Reial monitoring station. Similar mean values (30-38 µg/m³) were recorded in the various sub-groups of commuter buses (Table 3.1), although rising to 40-42 µg/m³ in the tourist buses (Fig. 3.5). There is typically a strong similarity between the patterns of $PM_{2.5}$ and BC concentrations registered during a bus journey, with traffic pollution peaks being registered simultaneously by the two pollutants (this is going to be explained in section 3.1.4; Fig. 3.21).

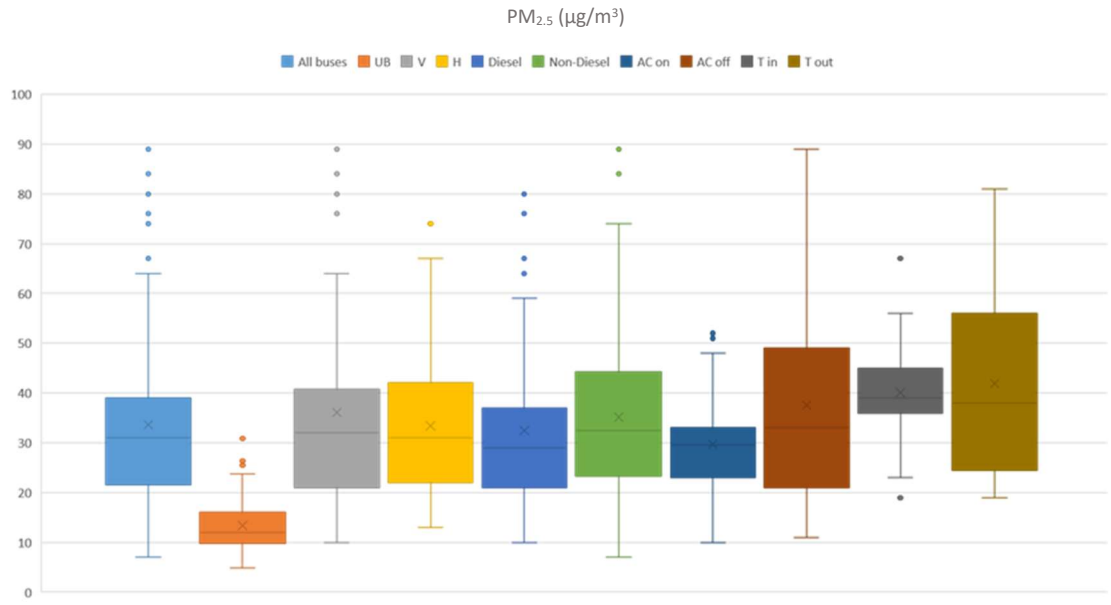

Figure 3.5. $PM_{2.5}$ mass concentration ranges measured (same sub-groups as in Table 3.1). Note the difference between urban background levels and all other values.

Although there is little difference in IQRs between the sub-groups or much deviation from the overall mean value of 34 µg/m³ (Table 3.1), there is a considerable spread of daily average mass concentrations (< 10 to > 80 µg/m³).

CO_2 was measured as a proxy of the quantity of people taking the bus. Tourist buses showed lower mean and median concentrations of quasi 300 ppm less, as they are an open area, even down on the lower inside floor, because there is always notable air exchange (this is discussed further under section 3.1.2 dealing with CO_2 levels).

Now, it is considered the concentrations of the pollutants exposure in each of the sub-groups shown in Table 3.1. Firstly, pairwise comparisons are analysed, after that "seasonal" differences are explained followed finally by differences between routes. An extra section is added with data from specific days considering the traffic-hotspots and the air quality of the urban background.

3.1.1. Impact of bus powertrain/fuel

The effect of the bus engine on exposure levels was analysed to verify whether it can be influenced by the bus itself (self-pollution). To get an overview, Figures 3.6-3.10 show the boxplots of the concentrations of QUFPN, size of QUFPN (n), BC, $PM_{2.5}$ and CO_2 measured inside the buses and tourist buses and distinguished by the engine type; the corresponding numerical results are reported in Table 3.2 including mean and median values with each SD.

The values in Figures 3.6 to 3.10 are median values, which reduce the effect of the numerous transient pollution peaks typically encountered during a bus journey.

The data are subdivided into subgroups including fuel/engine type (diesel (EURO IV, EURO V), hybrid diesel (HD), compressed natural gas (CNG), hybrid compressed natural gas (HCNG) and electric (EV)), tourist buses inside and outside, which uses EURO IV engine. In general, electric vehicles are characterized by almost the lowest QUFPN, BC and $PM_{2.5}$ values, whereas diesel buses show the highest ones, although there are wide ranges and much interquartile overlap (Fig. 3.6 to 3.10).

Table 3.2. Mean and median concentrations recorded from the sampling campaigns per each type of fuel/engine bus. n indicates the number of sampling days that were carried out in each type of bus. Measurements done at tourist buses are also compiled in average concentrations. Diesels (EURO IV and EURO V), hybrid diesel (HD), compressed natural gas (CNG), hybrid compressed natural gas (HCNG) and electric (EV).

		UB	*AB*	*EURO IV*	*EURO V*	*HD*	*CNG*	*HCNG*	*EV*	*Tourist inside*	*Tourist outside*
	n		*112*	*20*	*20*	*22*	*29*	*6*	*15*	*12*	*12*
QUFPN (#/cm³)	Mean	17,391	34,511	37,673	37,182	38,055	31,370	28,014	29,688	47,092	49,196
	Median	16,232	28,250	30,182	29,480	29,472	27,123	23,840	25,444	37,142	31,303
	SD	5,737	24,906	31,126	28,751	30,449	20,991	13,982	16,076	34,315	66,864
	n		113	20	20	23	29	6	15	12	12
QUFP size (nm)	Mean	47	42	42	42	38	44	43	44	41	41
	Median	43	43	43	43	39	44	43	44	41	42
	SD	4.6	6.7	6.8	7.3	6.9	6.3	7.3	5.7	7.3	9.7
	n		107	16	19	22	30	3	17	11	12
BC (µg/m³)	Mean	2.2	5.6	7.0	6.3	5.2	5.4	4.6	4.8	6.8	6.2
	Median	2.0	5.2	6.5	6.0	4.7	4.9	4.3	4.3	6.0	5.0
	SD	1.0	2.9	3.7	3.1	2.7	3.0	2.7	2.3	3.7	4.2
	n		111	19	20	22	28	6	16	9	11
$PM_{2.5}$ (µg/m³)	Mean	13.74	33.7	37.3	28.3	32.0	39.5	34.8	27.6	40.1	41.9
	Median	13.68	31.7	37.0	26.9	29.7	37.4	30.2	24.5	39.9	40.9
	SD	2.19	12.2	12.6	10.7	10.5	14.1	17.8	10.7	9.2	14.0
	n		103	15	20	23	24	6	15	11	9
CO_2 (ppm)	Mean	-	936	880	857	872	1015	1351	904	470	452
	Median	-	865	864	806	789	895	1241	865	454	444
	SD	-	293	220	235	270	312	426	235	41	44

The number of samples measured for each engine type was not the same, since the measurements have been done by pairs to compare two different engine bus types in the same line, and it was not always possible to compare them. The measurements were made in regular daytime schedules and under normal working conditions. Permission was needed to enter each bus to start sampling, and on each measuring day it had to be confirmed if the buses in which the sampling was going to be done were functioning or not. This involved close interaction with the local bus company TMB and was commonly influenced by the

inevitable delays and complications affecting any urban bus service in a busy city. Despite this, however, it was able to obtain data from a total of 144 days of sampling inside TMB line buses under normal working conditions. All types of buses in operation were sampled, with generally coverage except for the case of HCNG buses for which only 6 buses were used (compared to 17 EV buses, 21-23 diesel and HD, and 30 CNG). In the case of tourist buses, 12 sampling days were performed.

In figure 3.6. it can be observed that diesel buses have higher median concentrations of QUFPN than the rest of the buses, with a concentration around 30,000 #/cm^3, starting with EURO IV and ending with HD, being EURO V and HD quite similar. In contrast, the other three buses show lower concentrations, from 27,000 #/cm^3 to almost 24,000 #/cm^3, CNG and HCNG respectively.

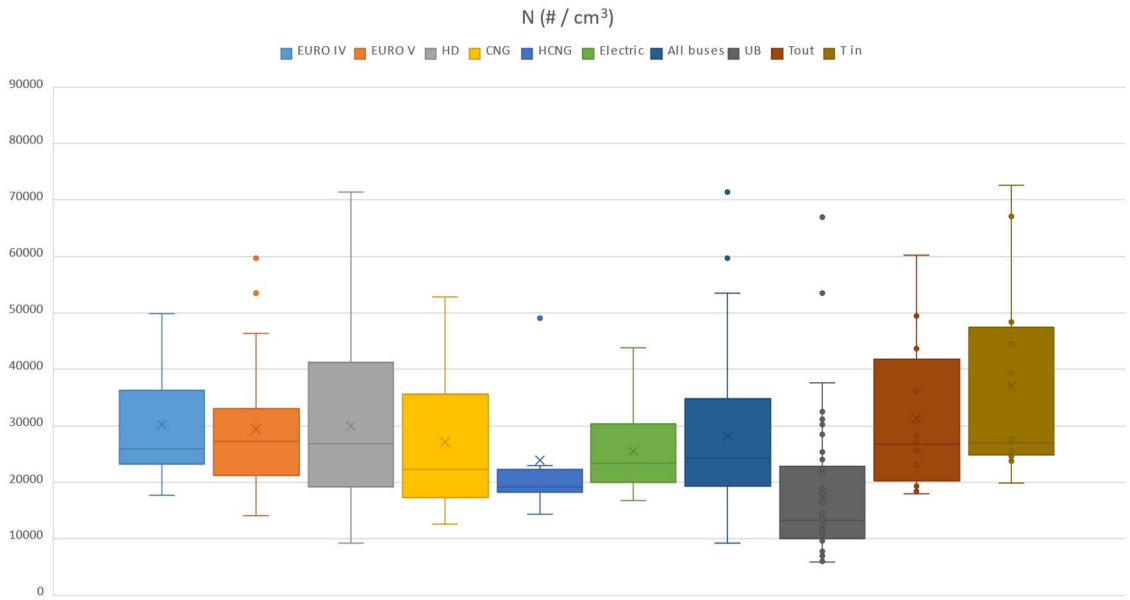

Figure 3.6. Box-and-Whisker plots for quasi-ultrafine particle concentrations (N) comparing all buses, powertrain sub-groups (diesel EURO IV, diesel EURO V, HD, CNG, HCNG and EV), tourist buses and urban background. The number of monitored journeys for each sub-group is CNG= 30, EURO V = 22, EURO IV = 20, HD = 23, EV = 17, HCNG = 6 and Tourist buses = 24.

Regarding the mean concentrations, the diesels achieve a much higher concentrations than the other buses, around 38,000 #/cm^3, with the highest concentrations occurring in the HD models inside which pollutant peaks were more concentrated and more frequent than in the rest of the buses. If looking at the concentrations in the boxplots (Fig. 3.6) a declining trend is observed from EURO V to HCNG. EURO IV and EV fall outside this trend, the first being slightly lower than the concentration of EURO V, and the concentration of the latter being a little higher than HCNG.

Regarding the mean values, the highest value was recorded as 38,055 #/cm^3 concentration in HD buses, and the lowest was 28,014 #/cm^3 (HCNG). This concentrations range is restricted and rather low compared to maximum-minimum results on bus AQ published elsewhere (1,149-95,023 #/cm^3: Knibbs and de Dear, 2010; Zurbier et al., 2010; de Nazelle et al., 2012; Kaur et al., 2006; Kumar et al., 2018; Kingham et al., 2013; Moreno et al., 2015; Zhang and Zhu, 2010; Ham et al., 2017; Molle et al., 2013; Ragettli et al., 2013; Strasser et al., 2018; Tan et al., 2017; Lim et al., 2015). The two studies performed previously in Barcelona (de Nazelle et al., 2012; Moreno et al., 2015) recorded a mean concentration around 55,000 #/cm^3, much higher than those in the present study. When analysing tourist buses concentrations, higher concentrations were measured, being 7,000 #/cm^3 higher than those analysed inside EURO IV buses. Here it was also observed that the IQR was wide in both, inside and outside tourist buses, being mean concentrations much higher than the median ones, being both 10,000 #/cm^3 higher, with 49,196 #/cm^3 outside tourist buses.

QUFP size modes vary only slightly within all the different fuel/engine bus types, between 39 (HD) and 44 nm (CNG = EV) (HD < HCNG = EURO V = EURO IV < EV = CNG) as shown in table 3.2 and figure 3.7. The average concentration of UB being higher than any of those found inside the buses, as expected, because buses are closer to fresher traffic emissions. Moreno et al. (2015), observed higher QUFP sizes inside Barcelona buses (mean 64 nm and median 63 nm), but it has to be mentioned that the equipment used by the authors was a Nanotracer (not a DiscMini) and that also it was a pilot study and the number of samples measured was lower than in this Thesis.

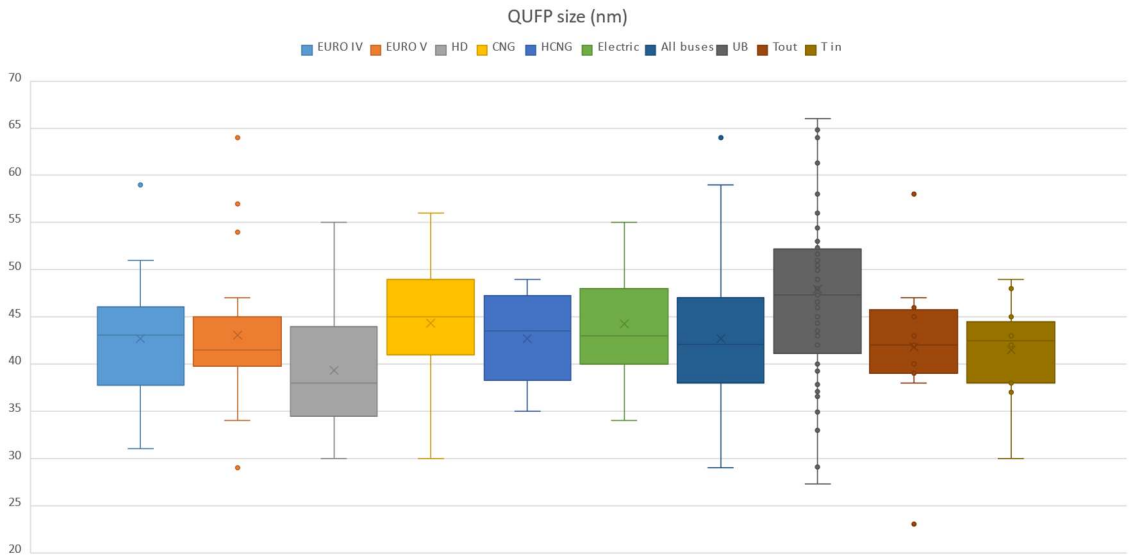

Figure 3.7. Box-and-Whisker plots for quasi-ultrafine particle sizes (nm) comparing all buses, powertrain sub-groups (diesel EURO IV, diesel EURO V, HD, CNG, HCNG and EV), tourist buses and urban background. The number of monitored journeys for each sub-group is CNG= 30, EURO V=22, EURO IV = 20, HD = 23, EV = 17, HCNG = 6 and Tourist buses = 24.

As before mentioned, in section 3.1.1, there were no differences encountered between mean and median sizes measured when comparing different fuel/engine type buses. Those size particles were referred as "aged traffic" PM. When comparing QUFP sizes with number, there is an inverse correlation between them. More specific examples are going to be explained later.

For BC concentrations all align around the same median concentrations (4.3 – 4.9 µg/m³, Fig. 3.8), with the only exception for diesel buses, whose BC average and top values are visibly higher than those of the other buses (6.5 µg/m³ in EURO IV and 6.0 µg/m³ in EURO V), this being likely related to self-pollution. It can also be seen in tourist buses, which use diesel fuel (EURO IV), and show average concentration inside buses higher than on the open upper floor (6.0 and 4.9 µg/m³, respectively).

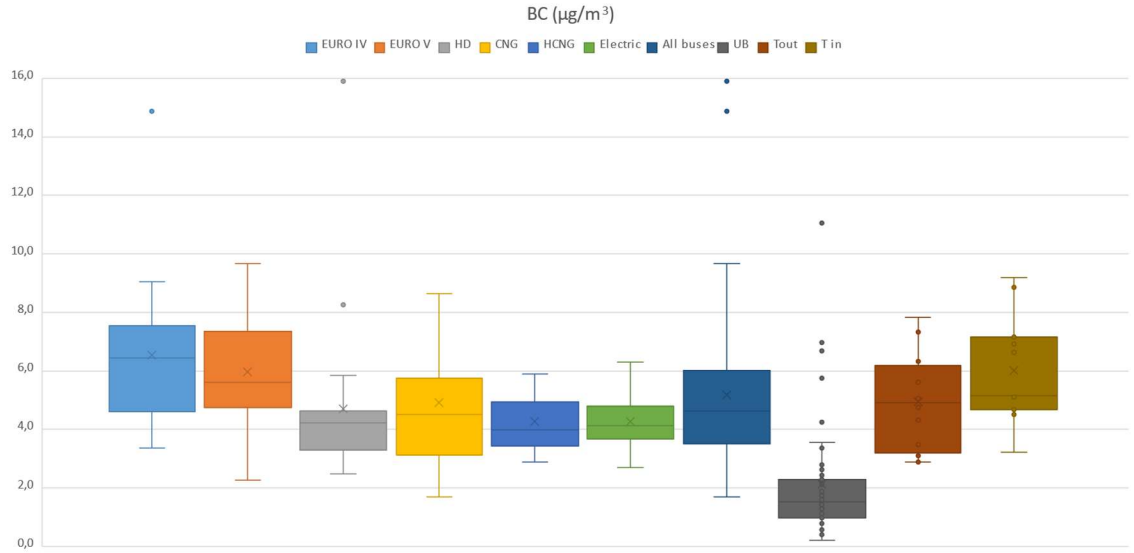

Figure 3.8. Box-and-Whisker plots for BC comparing all buses, powertrain sub-groups (diesel EURO IV, diesel EURO V, HD, CNG, HCNG and EV), tourist buses and urban background. The number of monitored journeys for each sub-group is CNG = 30, EURO V = 22, EURO IV = 20, HD = 23, EV = 17, HCNG = 6 and Tourist buses = 24.

Mean concentration within all the buses was 5.5 µg/m³, with the lowest one being 4.6 µg/m³ (HCNG) and the highest 7.0 µg/m³ (EURO IV) in the range of literature values (from 0.16 µg/m³ in Stuttgart to 11.6 µg/m³ in Hong Kong, Sabin et al., 2005; Zhang and Zhu, 2010; Moreno et al., 2015; Ham et al., 2017; Kumar et al., 2018; Fondelli et al., 2008; Dons et al., 2012; Williams and Knibbs, 2016; Vouitsis et al., 2014; Bauer et al., 2018; Tan et al., 2017; Yang et al., 2015). In Barcelona, a previous study (Moreno et al., 2015) found a similar mean concentration to that of our study (5.5 µg/m³), while de Nazelle et al. (2012) observed higher concentrations (average of 7.6 µg/m³).

Concerning $PM_{2.5}$ median concentrations two declining trends can be observed in figure 3.9 and table 3.2, varying between 25 (EV) and 37 µg/m³ (EURO IV and CNG) (EV < EURO V < HCNG = HD < CNG < EURO IV). One trend starting with EURO IV up to HD and the next would be from CNG to EV. In each trend the concentration decreases as the cleaner the vehicle is, in terms of fuel. EURO IV is the one with the highest median concentration and the highest IQR (37 µg/m³), followed by CNG with the same median concentration, but higher mean concentration (40 µg/m³). The EV shows the lowest IQR and the lowest median concentration (25 µg/m³), followed by the EURO V (27 µg/m³), having both a mean concentration of 28 µg/m³. These EV buses have a window system which is hermetically sealed, climate control is regulated by the driver, and they are equipped with regenerative braking which reduces the use of friction brakes, all of which favour reduction of outside PM infiltration, including that sourced from their own brakes. As for tourist buses, they show a fairly wide IQR, with the highest average concentration, like CNG mean concentration, being in the exterior slightly higher than that of the interior, 42 and 40 µg/m³, respectively; and the exterior one having the widest IQR.

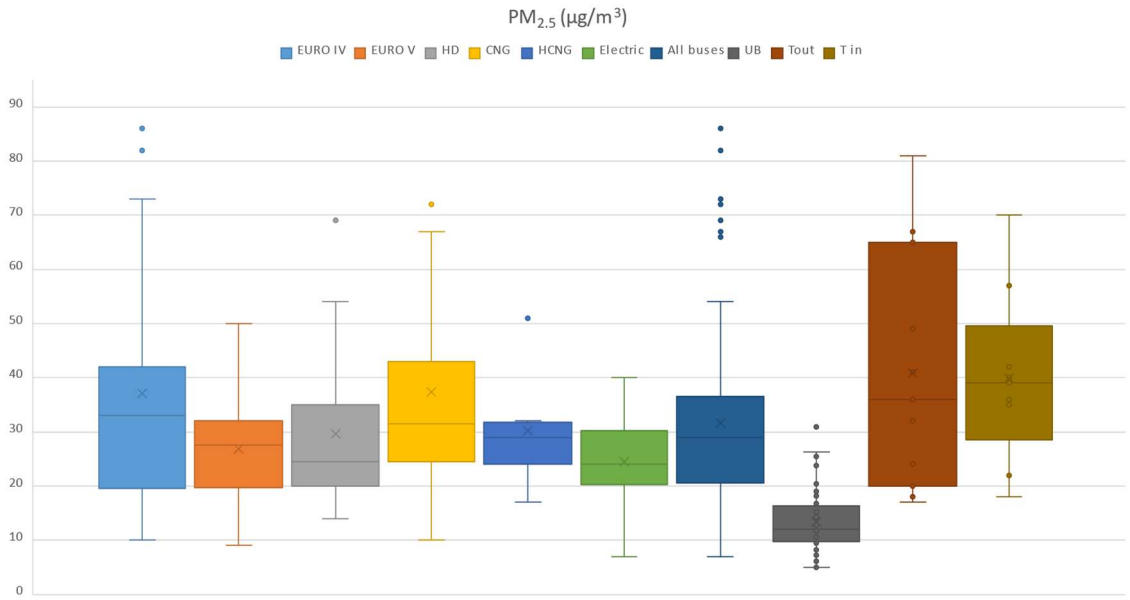

Figure 3.9. Box-and-Whisker plots for $PM_{2.5}$ comparing all buses, powertrain sub-groups (diesel EURO IV, diesel EURO V, HD, CNG, HCNG and EV), tourist buses and urban background. The number of monitored journeys for each sub-group is CNG = 30, EURO V = 22, EURO IV = 20, HD = 23, EV = 17, HCNG = 6 and Tourist buses = 24.

The mean concentration in our study was 33 µg/m³ within the range of 28 to 40 µg/m³ observed in the literature of most US and EU studies (9-64 µg/m³, Weichenthal et al., 2015; Cepeda et al. 2017; de Nazelle et al., 2017; Karanasiou et al., 2014; Ham et al., 2017; Knibbs and de Dear, 2010; Zhang and Zhu, 2010; Strasser et al., 2018). Outside this range one study

in Dublin registered 115.8 µg/m³ (McNabola et al., 2008) while concentrations up to 492 µg/m³ were found in Asia.

The concentrations of CO_2 analysed between different engine/fuel type buses (Fig. 3.10) showed that natural gas buses have the highest mean concentration. Being HCNG with the widest IQR. It is interesting to analyse it with different type of ventilation, so it is going to be explained in next section (3.1.2. Seasonal differences).

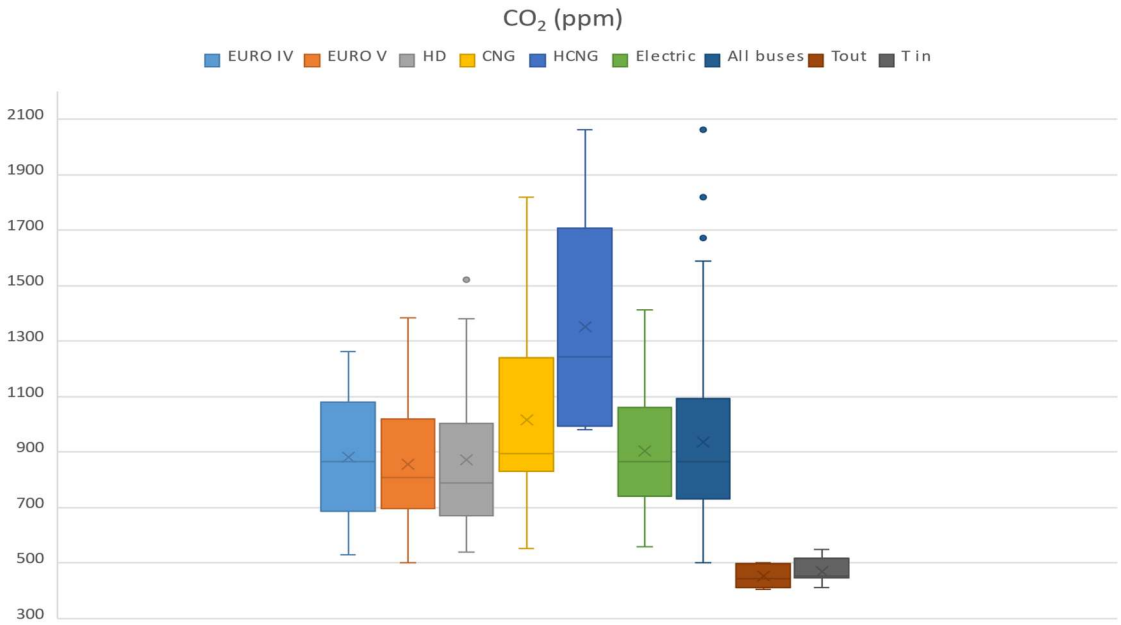

Figure 3.10. Box-and-Whisker plots for CO_2 comparing all buses and powertrain sub-groups (diesel EURO IV, diesel EURO V, HD, HCNG, CNG, EV, TB out and TB in. The number of monitored journeys for each sub-group is CNG = 30, EURO V = 22, EURO IV = 20, HD = 23, EV = 17, HCNG = 6, TBout = 12, TBin = 12.

Statistical differences are analysed between different powertrains and seasons in the section below (3.1.2. Seasonal differences).

3.1.2. Seasonal differences

The effect of the season was analysed to verify how AQ can be influenced by the air conditioning being on ("summer" months only) or off. The database registered 39 summer (warmer period, with AC, from May 2017 to September 2017) and 52 winter (colder period from November 2017 to April 2018) journeys (Table 3.3; Fig. 3.11). To obtain an overview, table 3.3. shows the mean and median concentrations measured with each SD for "summer" (AC on) and "winter" (AC off).

Table 3.3. Mean and median concentrations recorded from the sampling campaigns per each seasonal campaign: summer (AC on) and winter (AC off). n indicates the number of sampling days that were carried out in each type of bus. Measurements done at tourist buses are also compiled in average concentrations.

		UB (Summer)	*UB (Wintrer)*	*AB*	*Summer (AC on)*	*Winter (AC off)*
	n				58	54
QUFPN	Mean	17,401	17,388	30,973	37,233	26,278
(#/cm³)	Median	17,135	15,999	25,417	29,913	22,045
	SD	4,078	6,163	22,512	28,258	18,202
	n				58	55
QUFP size	Mean	52	45	42	46	39
(nm)	Median	36	45	42	47	39
	SD	2.1	5.4	6.7	8.3	5.5
	n				57	50
BC (µg/m³)	Mean	1.8	2.4	5.4	5.0	5.7
	Median	1.7	2.2	5.1	4.5	5.5
	SD	0.6	1.2	2.8	2.7	2.8
	n				57	54
$PM_{2.5}$	Mean	13.1	13.6	34	30	38
(µg/m³)	Median	12.8	13.4	32	28	36
	SD	1.8	2.2	12	8.4	15
	n				57	55
CO_2	Mean	-	-	936	1015	905
(ppm)	Median	-	-	865	905	864
	SD	-	-	293	334	242

QUFPN (mean: 37,233 vs 26,278 #/cm³; median: 29,913 vs 22,045 #/cm³) and QUFP size (mean: 46 vs 39 nm; median: 47 vs 39 nm) were recorded higher in summer, whereas BC concentration (mean: 5.0 vs 5.7 µg/m³; median: 4.5 vs 5.5 µg/m³) and $PM_{2.5}$ were higher in winter without AC (mean: 30 vs 38 µg/m³; median: 28 vs 36 µg/m³). The comparisons between different fuel type buses were done both in summer and winter, except from those between diesel buses and the EV. In the case of diesel buses, they were EURO V in summer and EURO IV in winter. When possible, the comparisons were made between the same line in each season.

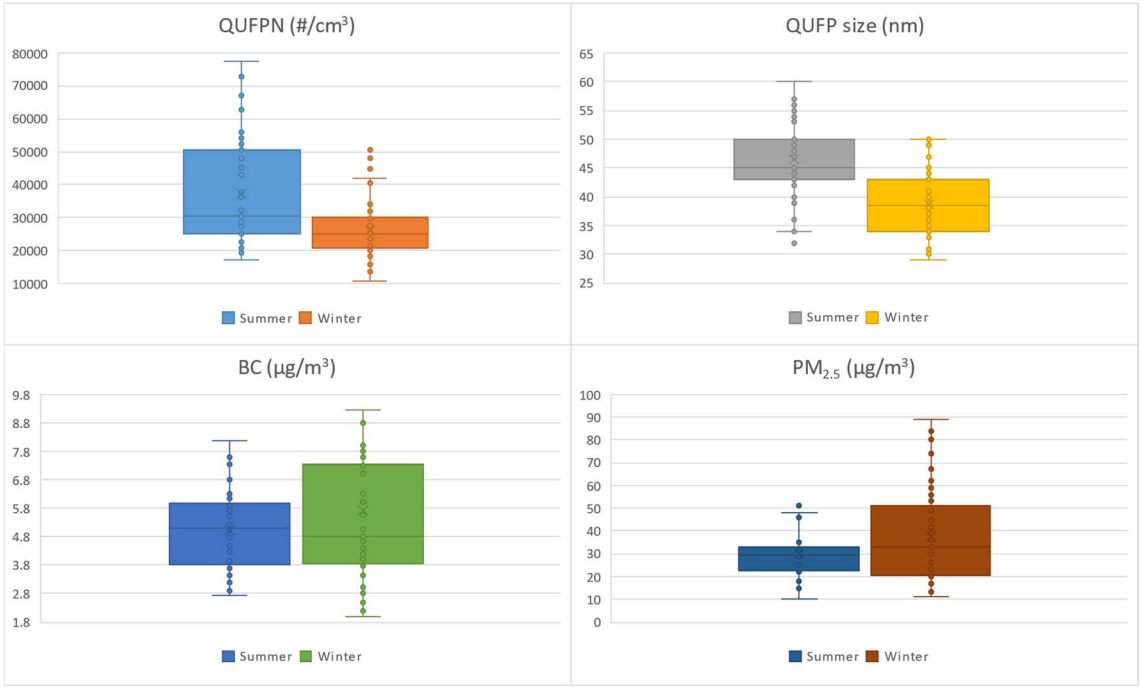

Figure 3.11. Whisker plots of concentrations and particle sizes measured during summer and winter per each type of pollutant (N and size mode of QUFP, BC and $PM_{2.5}$).

Previous studies that have analysed differences between ventilation modes include that in South Texas (Zhang and Zhu, 2010), where different pollutants (QUFPN, BC, CO and $PM_{2.5}$) were measured inside two different age school buses (1990 and 2006, both diesel). The average values of $PM_{2.5}$ were registered from 6.5 to 19.7 µg/m³, the highest values were achieved when windows were open, for both buses. When windows were open, same concentrations were recorded in both buses, 19 µg/m³, but once they were closed the concentration inside the newest was lower (10 vs 6.5 µg/m³). Regarding to N of QUFP, the values registered inside the older bus were much higher when windows were closed, and when windows were open, even if the concentration decreased, it was higher than inside the newest one. No AC was used in the study.

In Sacramento, California (Ham et al., 2017) measured QUFPN, BC and $PM_{2.5}$ and considered 3 ventilation conditions. They observed that when the recirculation mode was on, the concentrations of all the pollutants were 2 times lower than when all the windows were open or when AC (with air form outside) and windows were closed.

In Sydney (Knibbs and de Dear, 2010), mean concentrations of $PM_{2.5}$ ranged from 13.1 to 30.2 µg/m³ in mechanically ventilated buses and from 26.9 to 74.8 µg/m³ in naturally

ventilated buses. Lim et al. (2015) measured QUFPN with AC on and windows closed, registering median concentration of 17,300 #/cm^3.

European studies have showed $PM_{2.5}$ median concentrations in between the concentrations obtained in the present study, with a range between 6.2-64 $\mu g/m^3$ (Cepeda et al. 2017; de Nazelle et al., 2017; Karanasiou et al., 2014; Ham et al., 2017; Knibbs and de Dear, 2010; Zhang and Zhu, 2010; Strasser et al., 2018) being the ones with mechanical ventilation with less concentration than the ones with natural ventilation.

- *Statistical analyses*

As the number of samples measured for each engine type was not the same and given the fact that several variables influence the air quality inside a bus, a statistical analysis was carried out to see if the differences between the compared bus types were significant (Table 3.4). The non-parametric Wilcoxon rank-sum (Mann–Whitney) test was run only for simultaneous data comparing two engine types (e.g., EV vs diesel EURO IV) measured during several daily trips, if possible, in the same line, to minimise the effect of several confounders (route type, meteorology and air conditioning). However, other possible confounders may play a role such as the number of passengers and possible indoor sources (exhaled smoke, perfumes, personal care products and food), likely affecting QUFPN (and BC) levels.

First, summer data was analysed (internal air conditioning with windows closed), then winter data and finally summer and winter data altogether. Data were averaged in median values over the entire daily trip.

Table 3.4. Statistical analysis in the composition of the different powertrain types and seasons studied.

QUFPN		**Summer**				**Winter**				**Total**			
(#/cm³)		**Median**	**Z**	**p-Value**	**r**	**Median**	**Z**	**p-Value**	**r**	**Median**	**Z**	**p-Value**	**r**
EURO V vs EURO IV	EURO V	18945	24.744	0.000	0.57	50073	3.167	0.002	1.03	23600	16.027	0.000	0.66
	EURO IV	33194				51786				35863			
EURO IV vs HD	EURO IV	37042	22.185	0.000	1.57	30291	3.332	0.001	0.99	32877	18.934	0.000	1.23
	HD	23590				30520				26838			
EURO IV vs CNG	EURO IV	-	-	-	-	27265	-	0.000	1.84	-	-	-	-
	CNG					14798							
EURO IV vs EV	EURO IV	-	-	-	-	18365	-	0.000	1.04	-	-	-	-
	EV					17733							
EURO V vs HD	EURO V	64554	-8.613	0.000	2.05	31980	45.634	0.000	2.81	34419	28.922	0.000	1.72
	HD	31459				11378				20062			
EURO V vs CNG	EURO V	34320	6.968	0.000	0.88	22452	-23.917	0.000	2.61	38899	-8.618	0.000	2.01
	CNG	39138				8605				19395			
EURO V vs EV	EURO V	45950	15124	0.000	1.29	-	-	-	-	-	-	-	-
	EV	35592											
HD vs CNG	HD	41614	-27.020	0.000	2.63	18681	-12.581	0.000	0.70	25150	-12.581	0.000	1.16
	CNG	15850				26793				21627			
HD vs EV	HD	29515	-15.470	0.000	1.35	57775	-18.817	0.000	1.54	44334	-22.744	0.000	1.83
	EV	21802				37587				24215			
CNG vs HCNG	CNG	36961	-1.746	0.020	1.10	27660	-1.967	0.240	0.96	32682	0.750	0.420	1.06
	HCNG	33562				28733				30882			
CNG vs EV	CNG	21130	5.931	0.000	1.10	31601	-14.454	0.000	1.22	23777	-5.660	0.000	0.92
	EV	19129				25854				25788			
BC		**Summer**				**Winter**				**Total**			
(µg/m³)		**Median**	**Z**	**p-Value**	**r**	**Median**	**Z**	**p-Value**	**r**	**Median**	**Z**	**p-Value**	**r**
EURO V vs EURO IV	EURO V	9.24	- 0.862	0.000	0.74	-	-	-	-	-	-	-	-
	EURO IV	12.44											
EURO IV vs HD	EURO IV	14.25	11.353	0.000	2.08	12.66	16.371	0.000	1.58	12.78	20.543	0.000	1.72
	HD	6.85				7.99				7.44			
EURO IV vs CNG	EURO IV	-	-	-	-	4.04	-	0.437	1.15	-	-	-	-
	CNG					3.50							
EURO IV vs EV	EURO IV	-	-	-	-	11.85	-	0.000	1.23	-	-	-	-
	EV					9.66							
EURO V vs HD	EURO V	6.49	3.885	0.0233	1.20	5.25	0.693	0.012	1.05	5.11	-2.858	0.000	1.01
	HD	5.40				4.99				5.05			
EURO V vs CNG	EURO V	5.62	-5.389	0.000	1.34	8,85	-16.683	0.000	3.16	6.55	-15.975	0.000	1.99
	CNG	4.19				2,80				3.29			
EURO V vs EV	EURO V	10.79	12.771	0.000	1.57	-	-	-	-	-	-	-	-
	EV	6.85											
HD vs CNG	HD	4.77	2.530	0.011	0.82	6,99	-0.165	0.869	1.17	5.67	-0.165	0.870	0.96
	CNG	5.81				6,00				5.93			
HD vs EV	HD	3.25	7.995	0.000	0.78	19.92	-6.163	0.000	1.23	4.58	2.301	0.021	0.85
	EV	4.16				16.19				5.40			
CNG vs HCNG	CNG	4.87	2.331	0.049	1.11	-	-	-	-	-	-	-	-
	HCNG	4.41											
CNG vs EV	CNG	3.84	1.131	0.257	1.10	9.73	0.749	0.454	1,00	6.12	0.099	0.533	0.82
	EV	3.50				9.69				7.49			

For QUFPN all the statistical comparisons were significant (*p*-value 0.000, and 0.020 for HCNG, all of them *p*-values ≤ 0.05). Looking at the ratios (r), EURO V buses seem to be half of the concentration measured inside EURO IV buses, with the same ventilation condition (0.57 EURO V vs EURO IV). The highest ratios were observed between HD vs CNG (r = 2.63) in line H12 and EURO V vs HD (r =2.05) in line V13, but if looking at the comparison between EURO V vs CNG, in line V3, the ratio value is slightly smaller, and in that case, EURO V bus seems to be "cleaner" (r = 0.88). Other factors, beyond ventilation conditions that cannot be controlled, should also be considered while measuring or determining concentration levels inside the bus. These factors could not be eliminated or accounted for in the statistical analysis, indicating a need for more specialized studies.

For BC, most of the comparisons were significantly different, with the exception of three. The first comparison that was not significantly different was between HD and CNG (line H12, *p*-value 0.011, r = 0.82). The second one was between CNG and HCNG (line 39, *p*-value 0.049, r = 1.11). In this case, both, the statistical analysis, and the ratio value, indicate that there are no significant differences in terms of BC concentration. The last comparison was between CNG and EV buses (line H16, *p*-value 0.257, r = 1.10). However, in the case of QUFPN, the comparison that showed the greatest difference in terms of the ratio did not have a significant difference between HD and CNG, according to the statistics.

The data were also analysed statistically focusing only on the winter period. It was more complicated to collect data with the same ventilation conditions, as the AC was switched off, and only window positions were considered. During this period, the windows were generally kept closed. For QUFP data, only one of the comparisons did not show a significant difference, which was the comparison between CNG and HCNG (line 39, *p*-value 0.240, r = 0.96). For BC data, the statistical analysis indicated that, as with the summer data, three comparisons were not significantly different. Two of them were the same comparisons as for summer: HD vs CNG (line H12, *p*-value 0.869, r = 1.17) and CNG vs EV (line H16, *p*-value 0.454, r = 1.00). The comparison that was not repeated was between EURO IV and CNG (line V3, *p*-value 0.437, r = 1.15).

For the whole dataset (summer and winter trips), most of the comparisons provide statistically significant differences between the two bus types. In the case of BC, with higher levels in those buses with the 'lower' EURO category (12.78 μg/m^3 vs 7.5 μg/m^3 the highest of the rest of the powertrains). The only comparison that was not significantly different for QUFPN concentrations was between CNG and HCNG (line 39, *p*-value 0.418, r = 1.06) and for BC concentrations 2, HD vs CNG (line H12, *p*-value 0.869, r = 0.96) and CNG vs EV (line H16, *p*-value 0.533, r = 0.82).

This study did not reveal any dominant link between interior bus air quality and the type of powertrain operated by the bus. Taken overall, the amount of variation exhibited by the data, combined with variability in the number of buses measured of each fuel/engine bus type, resulted in no clear pattern emerging. Even with the measurements carried out over 3 consecutive days, the conditions were never the same, emphasizing the transient variability of the bus interior microenvironment. In addition to daily changes in weather conditions, other variables will include the age of the bus, the traffic flow, the type of powertrain, the way the vehicle is being driven and the number of passengers. Taken

together then, it was concluded that the type of powertrain operated by the bus was not the dominant AQ variable.

- *CO_2 especial section*

Concentrations of CO_2 measured in this Thesis are shown in Table 3.5 and Figure 3.12, which demonstrate how the lowest CO_2 levels were measured in open-topped tourist buses which are well ventilated by outside air and therefore provide obvious exceptions to normal "indoor" conditions inside commuter buses. In contrast, typical mean levels of CO_2 inside buses are commonly around double those of outside air although there is considerable variation, depending especially on whether windows are open (Table 3.5).

Table 3.5. Mean and median values for CO_2 (in ppm) measured in Barcelona buses. Given uncertainties over the accuracy of the measuring equipment, these data have been normalized to Barcelona background levels and are therefore best used for comparative purposes rather than as exact numbers.

	CO_2 mean	**CO_2 median**
All commuting buses	936	865
Closed windows	1030	918
Open windows	787	759
Tourist downstairs	470	454
Tourist upstairs	452	444

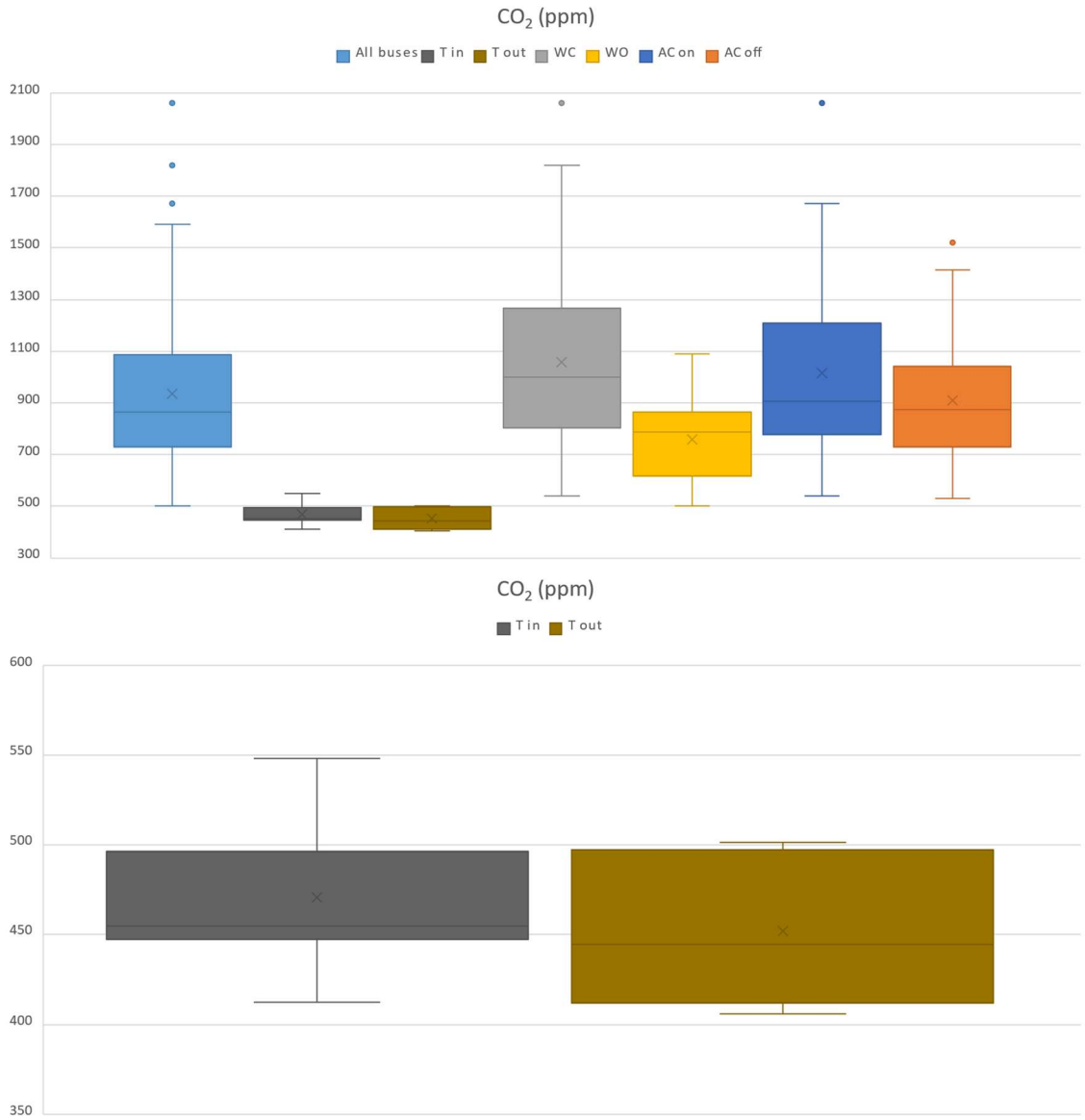

Figure 3.12. Boxplot for CO_2 concentrations mean values marked as crosses and median values as horizontal lines. Interquartile range (IQR) represented as coloured rectangles. Outliers (mean values) marked as coloured dots. All commuting buses excludes tourist buses; Tdown/Tup = open-topped tourist buses inside (downstairs) and outside (upstairs); Open and Closed Windows, and air conditioning (AC) on and off.

The concentrations of CO_2 inside a commuting bus on a weekday morning typically rise to a peak as the vehicle travels from its outward terminus to the crowded city centre and then declines as passenger numbers decrease towards the end of the route, after which the pattern is repeated on the return journey. However, the height of the peak will depend on ventilation conditions. Thus, the sub-group of buses recorded as having windows closed during the journey record higher mean and median CO_2 values than with those with at least

one window open (Fig. 3.12, Table 3.5). To demonstrate the point, a specific example which compares two buses is shown below, one operating with closed windows the other with at least one window open (16 May). Both buses stopped almost the same number of times (39, 37 stops) and ran 10-12 minutes apart the entire return journey on the same route (V13), but the bus with windows closed recorded nearly double the concentration of CO_2 (Fig. 3.13).

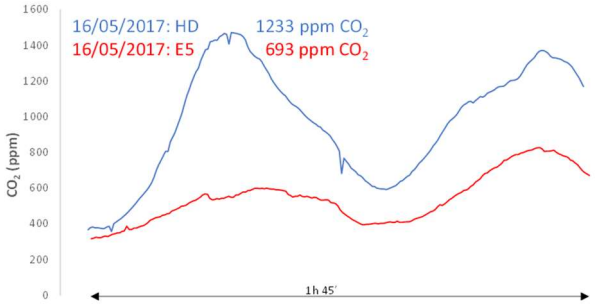

Figure 3.13. Comparison of CO_2 concentrations inside on two buses (diesel EURO V and hybrid diesel) running along route V13 the same day with windows open (EURO V) and closed (HD).

Another example illustrating the controls on CO_2 levels inside buses, in this case the direct link with passenger numbers, is presented in Figure 3.14. This compares two journeys made on the same route (H4) on the same day (14 Nov) with one bus initially 7 minutes in front of the other. On the outward journey the front bus picked up more passengers, stopping 33 times and opening 84 doors, with CO_2 levels correspondingly peaking at over 1,500 ppm. In contrast the bus behind stopped 27 times, opened 66 doors and outward CO_2 peaked at around 1250 ppm (Fig. 3.14). However, it is on the return journey that a much greater difference in CO_2 levels emerged, when the rear bus was by now running progressively closer behind and thus increasingly failing to pick up passengers (it opened only 40 doors, as compared to 95 in the front bus, on this leg of the journey). Under these conditions whereas CO_2 levels in the crowded front bus showed a similar peak to the outward journey, concentrations of the gas in the near-empty rear bus failed to reach even 600 ppm (Fig. 3.14).

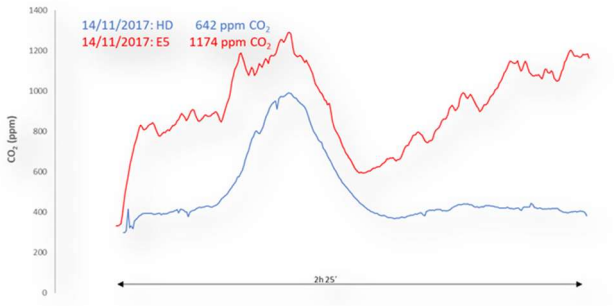

Figure 3.14. Comparison of CO_2 concentrations measured inside two buses running on route H4 the same day with clear differences on the number of passengers on the return journey (see text for details).

Concentrations of CO_2 inside buses depend directly on the number of passengers, outside air entry through doors and windows, and the ventilation system. As such, levels of this gas inside public transport vehicles are a good proxy for how much indoor air is being diluted from outside. In this context, a crowded bus operating with closed windows can record CO_2 concentrations more than 3,000 ppm, over seven times natural background.

3.1.3. Routes

The possible effect of bus route on interior air quality, was analysed by comparing three types of journey: Those running essentially horizontal and coast-parallel through the city (these routes being designated with the prefix H for "horizontal"), those operating across a considerable change of gradient between the coast and the northeast-southwest oriented hills that form the hinterland of Barcelona (prefix V: "vertical"), and those that are neither H nor V but follows some more variable route through the city ("other routes" buses 34, 39, 47, 19, and 60: "others" on Table 3.6).

To obtain an overview, table 3.6. shows the mean and median concentrations measured with each SD for horizontal routes (H, parallel to the coastline), vertical routes (V, i.e., running to and from the coastline) and other routes (others).

Table 3.6. Mean and median values recorded from the sampling campaigns per each type of route with each sd. n indicates the number of sampling days that were carried out in each type of bus. Measurements done at tourist buses are also compiled in average concentrations.

		Horizontal	*Vertical*	*Others*
n		*30*	*42*	*45*
QUFPN (#/cm³)	Mean	28,543	38,720	34,765
	Median	22,899	32,368	28,150
	SD	21,108	29,063	23,659
***QUFP size*(nm)**	Mean	43.0	43.1	40.9
	Median	43.2	43.7	41.4
	SD	6.6	6.6	6.8
BC (µg/m³)	Mean	5.12	6.56	5.10
	Median	4.59	6.21	4.62
	SD	2.72	3.46	2.64
$PM_{2.5}$ (µg/m³)	Mean	33.4	36.1	31.5
	Median	32.3	35.6	27.5
	SD	8.2	12.9	14.6

The data are subdivided into subgroups including horizontal, vertical, and other routes for QUFPN, size, BC and $PM_{2.5}$. In general, vertical route buses are characterized by the highest QUFPN, BC and $PM_{2.5}$ values, the size of the QUFPs being quite similar in the three types of routes. Lowest mean/median values measured inside buses were in the Horizontal routes sub-group (28,543 / 22,899 #/cm³) and are 25-30% lower than mean/median values in Vertical routes (38,720/32,368 #/cm³).

When analysing the data, considering all routes (Table 3.7) it can be observed that the highest concentrations were measured inside vertical route buses.

Table 3.7. Mean and median values recorded from the sampling campaigns per each type of route with each sd. In other routes (19, 34, 39, 47 and 60), horizontal routes (H12, H16 and H4) and vertical routes (V11, V13, V17 and V3). n indicates the number of sampling days that were carried out in each type of bus.

		OTHERS					*HORIZONTAL*			*VERTICAL*			
ROUTES		**19**	**34**	**39**	**47**	**60**	**H12**	**H16**	**H4**	**V11**	**V13**	**V17**	**V3**
	n	*6*	*16*	*12*	*5*	*6*	*12*	*12*	*6*	*3*	*12*	*3*	*24*
QUFPN	Mean	27521	45972	27132	30496	34667	37337	22052	23938	57324	41707	47263	33751
(#/cm³)	Median	24074	37201	23599	24233	22536	27844	20233	18342	48502	34484	40930	28135
	SD	14364	32100	12870	27251	33478	30976	11015	21561	30543	27834	28572	29522
QUFP size	Mean	39.5	39.9	41.8	47.8	36.6	42.5	47.1	35.8	43.0	47.7	45.3	40.7
(nm)	Median	39.8	40.4	41.8	49.6	37.2	42.9	46.8	36.8	43.7	48.5	46.3	41.0
	SD	5.83	6.87	6.75	8.80	5.60	7.33	6.50	5.33	5.00	7.80	8.33	6.04
BC (µg/m³)	Mean	5.67	5.00	4.05	5.94	5.81	5.80	4.15	5.83	6.80	5.90	7.08	6.80
	Median	5.25	4.52	3.79	5.56	4.72	5.05	3.79	5.39	6.50	5.34	6.28	6.61
	SD	2.50	2.38	2.04	3.38	3.92	3.86	1.64	2.57	2.71	2.68	4.12	3.89
$PM_{2.5}$	Mean	34.8	28.6	34.2	39.8	23.8	38.6	30.7	28.2	33.0	26.6	35.7	41.1
(µg/m³)	Median	30.7	24.1	29.0	39.0	22.4	37.0	29.8	27.7	32.3	25.1	35.7	41.0
	SD	14.5	14.9	17.6	13.0	8.6	9.3	6.9	8.5	8.3	8.6	10.0	16.0

Vertical routes (from coastline to the hills) record concentrations 25-30 % higher than the coast-parallel horizontal routes (Table 3.7). As before mentioned, the engine needs more power going uphill, that is one of the reasons why concentrations in vertical routes are higher, as more emissions are issued. Also suggesting that brake particles are more common in the buses operating along a significant slope.

3.1.4. Special data measurements (outliers)

a) Quasi-ultrafine particle number concentrations (QUFPN)

- *Influence of urban background (UB)*

The two UB outliers recording exceptional levels of QUFP reflect abnormally polluted winter conditions in the city on 24 November and 24 January when SMPS mean values of QUFP 10-400nm were over three times normal. During both citywide pollution events unusually, high N levels were also recorded by the DiSCmini inside the buses, as detailed below.

In the 24 November pollution episode, mean QUFPN values rise >10,000 #/cm³ above average in both buses for that day (V3 CNG bus 50,378 #/cm³ and V3 diesel EURO IV bus

45,653 #/cm³). In contrast, the same V3 bus pair was monitored 6 days later when urban background levels had dropped back to normal and recorded mean N values of just 16,279 #/cm³ (CNG) and 23,726 #/cm³ (diesel EURO IV).

In the 24 January pollution episode, the added effect of poor outside air was even more marked as this day was used to sample in an open-topped tourist bus where mean QUFPN concentrations proved to be >20,000 #/cm³ higher than the "All buses" average (lower floor 56,310 #/cm³; upper floor 59,488 #/cm³). Figure 3.15 compares QUFPN concentrations measured on the open top deck of a tourist bus during this 24 January event with those registered just the day before, when the city atmosphere was unusually clean.

Two other days during the monitoring campaign also registered notably high (although not boxplot outlier) urban background pollution levels, these being 1 March and 1 June. On these two days once again both buses registered outlier values recording unusually high levels of in-vehicle pollution.

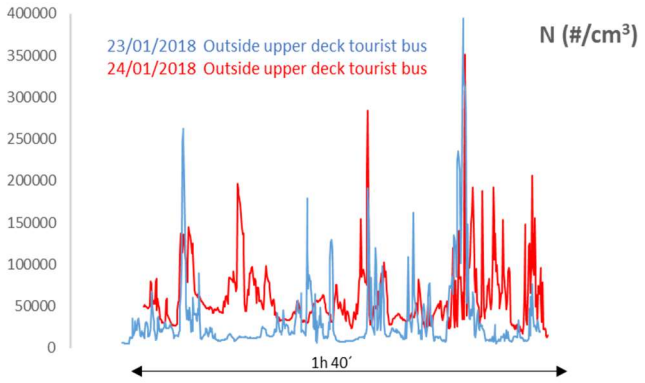

Figure 3.15. Comparison between mean number concentrations (N) of quasi ultrafine particles measured on the upper deck of an open topped tourist bus (Barcelona Blue Route) during days of low (23 January) and high (24 January) urban background levels. The peaks rising to N>100,000 record traffic congestion hotspots. The less polluted outdoor conditions on the 23 January are reflected in the lower baseline N concentrations recorded on the top deck of the bus.

On 1 March Route H12 buses (41,815 #/cm³ HD and 40,478 #/cm³ CNG) N levels were around 15,000 #/cm³ higher than the mean for their subgroup. On 1 June Route V3 both buses recorded N values of QUFP also much high than average (63,015 #/cm³ CNG and 52,240 #/cm³ diesel EURO V).

- *Influence of traffic hotspots*

Other exceptional "outlier" N concentrations of QUFP shown on Figure 3.2 are always associated with extreme peaks produced by traffic hotspots such as proximity to the urban motorways that both encircle and traverse the city (Ronda de Dalt, Meridiana, Diagonal,

Ronda de Mig, Gran Via, Ronda Litoral), or major node points such as Plaça D'Espanya and Plaça de les Glòries Catalanes. The three most prominent of these outlier values recorded inside buses, all occurred in the warmer months of the year from May to September and are detailed in the examples below.

Example 1: 87,254 #/cm^3 Route 34 on 25 May. Hybrid diesel bus recorded frequent N exceedance >100,000, several >200,000 and one exceptional peak of 631,000 #/cm^3. The peaks always coincide with busy traffic hotspots, notably crossing the Meridiana urban highway, points along the Diagonal and Avenida Sarrià, and for the extreme peak of 631,000 #/cm^3, the area around the Ronda de Mig. This hybrid diesel bus was much more polluted in QUFPN than the EV bus (N = 45,259 #/cm^3) running along the same route 10 minutes behind, and which showed only one 100,000 peak exceedances (Fig. 3.16). The reason for this is deduced to be linked to the fact that the EV bus had a more closed indoor environment (no windows can be opened and therefore all glass is fully sealed), reflected by median CO_2 levels being higher than in the hybrid diesel (Fig. 3.16). Another marked difference was in QUFP size, which averaged 31 nm in the hybrid diesel bus but 44 nm in the EV bus, suggesting the presence of more fresh exhaust in the former.

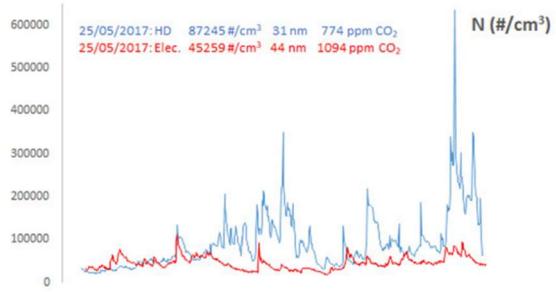

Figure 3.16. Comparison between number concentrations (N) of QUFP recorded inside a Route 34 bus pair monitored on 25 May (timings adjusted to coincide approximately with first 100,000 #/cm^{3}peak: the HD bus started the journey 9 minutes ahead of the EV bus). The hybrid diesel (HD) bus data record greater infiltration of outside ultrafine traffic pollutants, especially at traffic hotspots crossing the Meridiana, Diagonal, Avenida Sarrià and Ronda del Mig, but lower levels of CO_2 due to greater outside air exchange. The windowless indoor environment of the EV bus, and possibly the lack of self-pollution from exhaust emissions, suppress N levels for most of the journey (initially higher N values inside the EV bus may be related to the log sheet stating that someone was smoking adjacent to the bus waiting at the initial stop).

It is possible that the hybrid diesel bus was at least in part self-polluted by its own exhaust plume entering as the doors opened at bus stops. Similar observations were repeated for the two other hybrid diesel/EV bus pairs on Route 34 monitored that week (23 and 24 May),

with the EV bus again recording lower N values and higher QUFP sizes than the hybrid diesel.

Example 2: 52-77000 #/cm^3 Route H12 on 18-20 July. Cluster of three hybrid diesel buses on consecutive days sampling during typically very busy traffic along the Gran Via urban highway, especially around Plaça D'Espanya and Plaça de les Glòries Catalanes. 18 July: mean N value 77,321 #/cm^3 with several peaks exceeding 100,000 #/cm^3 including one with an 848,000 #/cm^3 extreme value.

19 July: mean N value 52,234 #/cm^3 with four peaks exceeding 100,000 #/cm^3 and a maximum peak of 161,000 #/cm^3. 20 July: 72,912 #/cm^3 with N>100,000 #/cm^3 recorded during much of the journey along the Gran Via through the city centre, reaching extreme peaks of 62,6000 #/cm^3 (outward) and 719,000 #/cm^3 (return). All these three buses were paired with natural gas-powered buses, all three of which showed much lower N values (24-28,000 #/cm^3) and larger QUFP sizes (46-53 nm versus 34-39 nm in hybrid diesel), as seen in the 25 May bus pair (Figs. 3.16 and 3.17). The outward journey for the 18 July bus pair is depicted on Figure 3.17 which demonstrates how the hybrid diesel bus interior was more contaminated by traffic emission infiltration, as reflected by higher N, smaller QUFP sizes and lower CO_2 concentrations. As with the previous example shown on Figure 3.16, there is the possibility of self-pollution by the hybrid diesel bus.

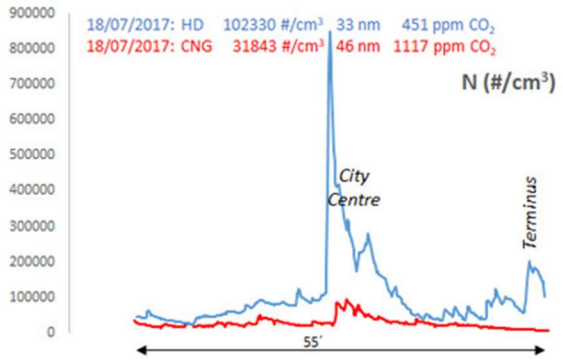

Figure 3.17. Comparison between two H12 buses (hybrid diesel HD and compressed natural gas CNG) on outward journey through city centre to terminus at Besòs-Verneda. Traffic particle emission infiltration into the HD bus at the busy city centre (Gran Via crossing Balmes and Passeig de Gracia) is most obviously reflected in a strong peak (848,000 *#/cm^3*) which is much more subdued in the NG bus. At the terminus the HD bus was left with engine running while waiting with AC on for 11 minutes, producing an increase in QUFP concentrations that briefly peaked at > 200,000 *#/cm^3*. In contrast the NG bus was running late and stopped at the terminus for only 2 minutes.

Example 3: 62,152 #/cm³ route V11 on 28 September. Natural gas bus with peaks of N>100,000 #/cm³ at busy traffic hotspots in Via Augusta (out and back) and the Drassanes area, plus a 17-minute period of high N (peaking at 271,000 #/cm³) during the uphill route along Carrer Compte d'Urgell (Fig. 3.18).

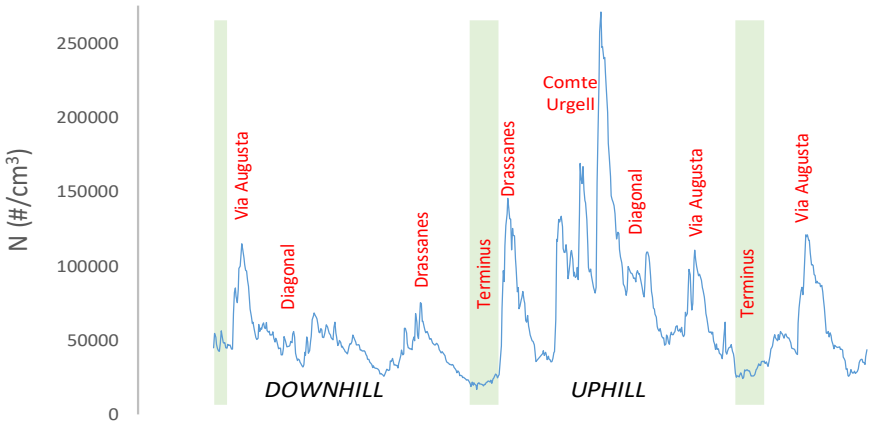

Figure 3.18. Concentrations of quasi ultrafine particles measured during a return journey on the "vertical" route in natural gas bus V11 (28 September, bus windows open). Note repetition of N peaks at traffic hotspots such as around Via Augusta, the low values of N at the termini, and the more polluted nature of the uphill journey climbing away from the sea level terminus near Drassanes to the Diagonal.

b) *Quasi-ultrafine particle size*

As the number concentration of ultrafine particles rises due to infiltration of pollutants from outside, the size mode defines a corresponding trough. This is related to the fact that the higher the concentrations of fresh traffic-related particle emissions the smaller the sizes will be. An example of this is illustrated in Figure 3.19 on which a hybrid diesel bus running along the Gran Via urban highway (Route H12) records an extreme concentration peak (> 800,000 #/cm³) and size trough (< 15nm) coinciding at a major traffic hotspot in the city centre.

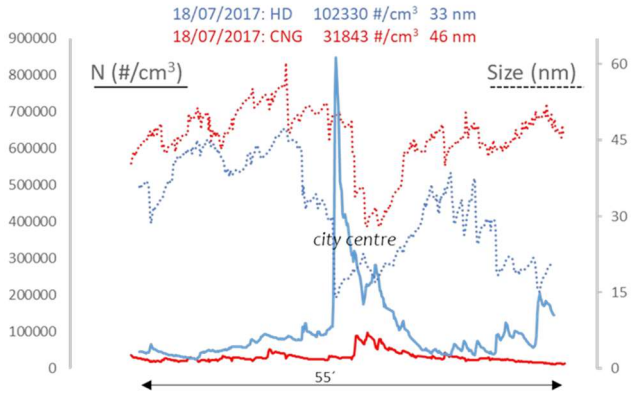

Figure 3.19. Comparison between number concentrations (N) and sizes (in nm) of ultrafine particles recorded during a return journey along the Gran Via in an H12 hybrid diesel bus. The data record very high N in the city centre on the outward journey but not on the return route on the other side of the road. This difference is attributed to the wind blowing at 15km/hr from east to west across the multilane highway, contaminating the west side (outward) with traffic emissions far more than the eastern side return). Ultrafine particle sizes vary inversely with N, falling from 45nm to 15nm at the city centre traffic hotspot.

Exceptional cases of unusually high and low mean ultrafine particle sizes deviating from the average value of 42nm were noted in the following buses:

74nm urban background. 8 June. This unusually coarse average value of background QUFP in the city coincided with very low number concentrations of QUFPN (N = 7,509 #/cm³) and BC (1.1 µg/m³) values, indicating good air quality diluted by a fresh south westerly breeze blowing at 29 km/hr across the city. This was reflected by correspondingly low N and BC values in the two buses monitored that day (natural gas 17,119 #/cm³, 49 nm and 2.7 µg/m³; EV 20,028 #/cm³, 47 nm and 3.3 µg/m³ respectively).

32nm Route 34. 23 May hybrid diesel. Unusually fine average QUFP size appears to have resulted from the impact of two traffic pollution hotspots (with correspondingly increased N values of QUFP) around the Sagrada Familia and the Ronda de Mig (Fig. 3.20).

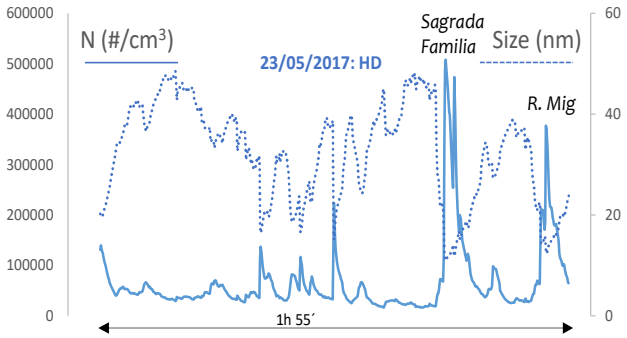

Figure 3.20. Comparison between number concentrations (N) and sizes (in nm) of ultrafine particles recorded during a return journey inside a hybrid diesel bus operating on Route 34. Note the inverse relationship between ultrafine particle size and number concentration N.

31nm route Tourist inside and 25nm Tourist outside. 28 June. This low value again coincides with unusually high N values (76,186 #/cm³) during busy traffic and is interpreted as recording enhanced levels of fresh traffic exhaust hotspots that coincide with Plaza España, the ascent of Montjuic, descent via a tunnel (extreme peak) to the congested seafront area from Colon to Port Olympic, the ascent of Via Laietana in the medieval city, and the area around Casa Batllo in the Passeig de Gracia. Urban background values for that day are not available. Coinciding average BC and $PM_{2.5}$ values recorded during the journey were not exceptional but also punctuated by prominent traffic congestion peaks (Fig. 3.21).

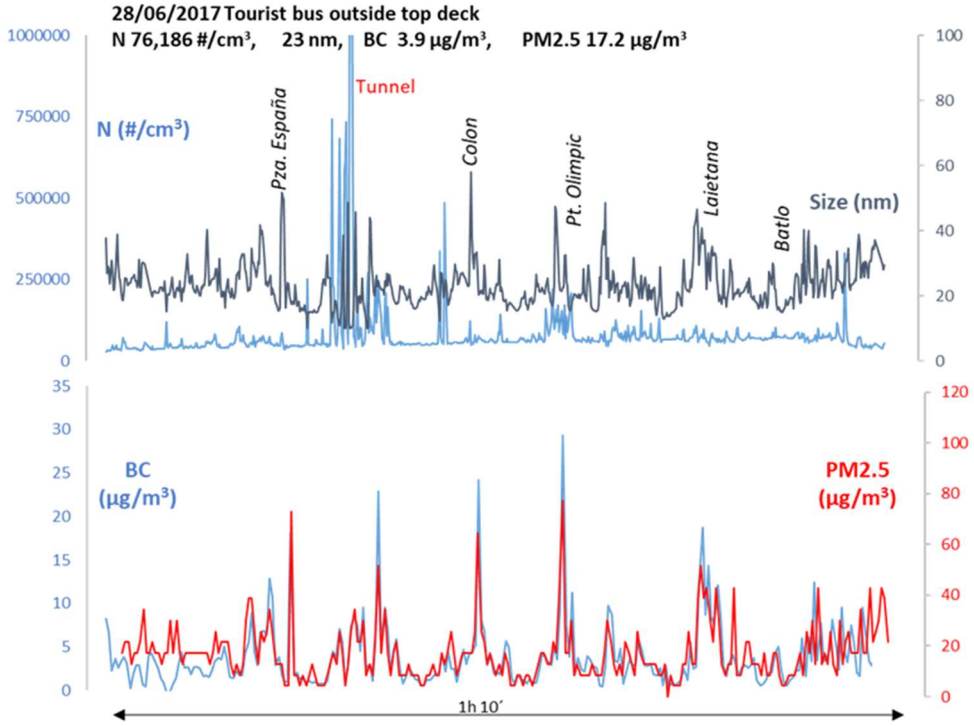

Figure 3.21. Levels of air pollutants recorded on the top open deck of a tourist bus (red route). An unusually extreme peak of QUFP number concentrations exceeding 2 million #/cm³, with corresponding trough of sizes well below 20nm, was recorded in the Montjuic tunnel. Black carbon and $PM_{2.5}$ values define similar patterns, with the peaks coinciding with traffic-congested hotspots.

c) Black carbon concentrations (BC)

The five outliers in the urban background data on Figure 3.4 record days when the city air was exceptionally polluted (24 November (16.5 µg/m^3), 24 January (11.0 µg/m^3), 1 March (7.0 µg/m^3), 16 November (6.7 µg/m^3), 23 November 5.8 µg/m^3). Two of these dates coincide with outlier BC measurements in the "all buses", "vertical", and "horizontal" groups on Figure 3.4, i.e. 24 November vertical route buses (natural gas 15.6 µg/m^3 and EURO IV diesel 14.2 µg/m^3) and 1 March horizontal route buses (hybrid diesel 14.3 µg/m^3 and natural gas 9.2 µg/m^3), all 4 of which had AC off. Details of the bus group outliers >10 µg/m^3 shown on the boxplot Figure 3.4 are as follows:

15.6 µg/m^3 route V3 on 24 November. Natural gas bus. The highest BC values coincide with a traffic hotspot (Diagonal) and a short tunnel entered for a few minutes in the Ronda del Mig south of the Diagonal, combined with the effect of a polluted urban background for that day. On the outward and return journeys BC values in the tunnel rose to peaks of 22 µg/m^3. On the return (uphill) journey the bus entered and stopped several times in the Diagonal traffic hotspot, causing BC levels to continue to rise to a peak of 39 µg/m^3. Figure 3.22 compares BC data from the natural gas bus with that from the same bus on the same route but 4 days later when urban background levels of BC had dropped from 16.5 µg/m^3 to 1.8 µg/m^3.

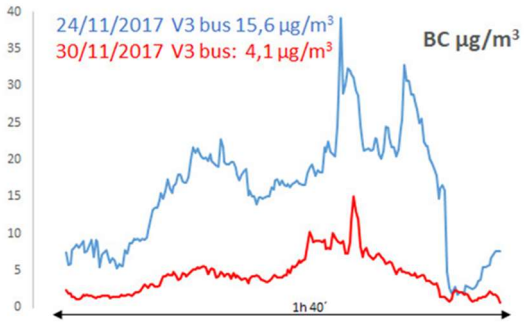

Figure 3.22. Comparison between BC concentrations (in µg/m^3) measured inside two natural gas-powered buses running on line V3 on days with very high (24 November: 16.5 µg/m^3) and low (30 November: 1.8 µg/m^3) urban background BC levels. The average in-bus values for the two journeys were: 24 November 15.6 µg/m^3, 30 November 4.1 µg/m^3. The 24 November recorded the worst pollution event affecting the city during the monitoring campaign. Both buses recorded their maximum peak in the traffic hotspot intersection between 2 urban motorways (Diagonal and Carles III).

14.3 µg/m³ route H12 on 1 March. Hybrid diesel bus. As with the above example, high BC levels associated with tunnels and traffic hotspots were superimposed on a high urban background. Levels of BC jump to 15 µg/m³ on entering a tunnel beneath the Plaça D'Espanya, after which BC concentrations remained high (15-20 µg/m³) for most of the journey, apart from another jump at the Plaça de les Glòries Catalanes traffic hotspot (to 35 µg/m³).

14.2 µg/m³ route V3 on 24 November. EURO IV diesel. Like the other bus paired on 24 November (see above) with the tunnel again causing BC levels to reach peaks of 21-22 µg/m³. The Diagonal traffic hotspot on the return (uphill) journey is less pronounced, probably because the bus stopped fewer times.

d) *$PM_{2.5}$ mass concentrations*

As with BC levels, the prominently polluted urban background day of 24 November tops the list of mean $PM_{2.5}$ concentrations (at 89 µg/m³). Other outlier days registering mean $PM_{2.5}$ concentrations >60 µg/m³ are 1 December, 18 January, 1 March, 23 November and 30 January. Urban background levels average 13 µg/m³, and only very rarely rise above 25 µg/m³ (26-32 µg/m³ on 22 to 24 of November).

Details for the high urban background $PM_{2.5}$ outlier days are as follows:

89 µg/m³ Route V3 on 24 November. Natural gas. Similar pattern to BC, with elevated urban background levels combined with traffic hotspot pollution around the Diagonal highway ($PM_{2.5}$ rising from 40 to 70 µg/m³) and the effect of open windows. Concentrations jumped to 100 µg/m³ after entering tunnel in Ronda del Mig after which PM levels inside the bus failed to dissipate (Fig. 3.23). Levels thus remained high for most of the rest of the journey, peaking at 137 µg/m³ in the Gran Via area then at 147 µg/m³ upon re-entering tunnel on the return journey, and staying at >100 µg/m³ around the Diagonal hotspot and beyond. At the upper terminus a 7 minute wait dropped $PM_{2.5}$ levels to <30 µg/m³.

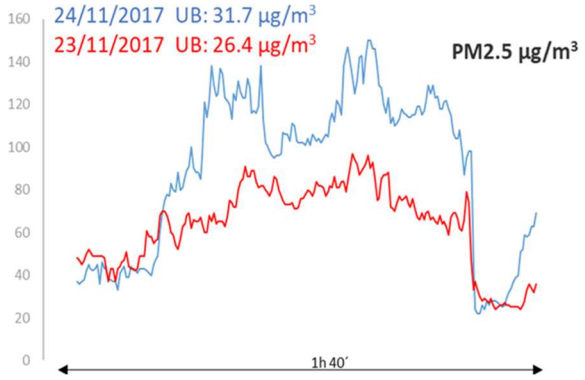

Figure 3.23. Comparison between $PM_{2.5}$ concentrations (in µg/m³) measured inside two natural gas-powered buses running on line V3 on days with very high (24 Nov.: 31.7 µg/m³) and lower (23 Nov.: 26.4 µg/m³) urban background $PM_{2.5}$ concentrations. The average in-bus values for the two journeys were: 24 Nov. 89 µg/m³, 23 Nov. 62 µg/m³. The 24 Nov. recorded the worst pollution event affecting the city during the monitoring campaign. Both buses recorded their maximum peak in the traffic hotspot intersection between two urban motorways (Diagonal and Carles III).

84 µg/m³ Route V3 on 1 December. Natural gas. Contrasts with previous example in having all windows closed (cold weather), which slightly subdued the pollution peak associated with tunnel entry. The most notable characteristic was a prominent peak in $PM_{2.5}$ at both bus termini (>100 µg/m³), when the bus waited with engines on but doors closed, suggesting the effect of self-pollution.

80 µg/m³ on 18 January, 76 µg/m³ on 24 November, 64 µg/m³ on 23 November Route V3. Diesel EURO IV in all cases and all display same pollution pattern, as seen in previous examples of V3 route. High urban background pollution on both days enhanced by traffic hotspots (up to 130 µg/m³) and tunnels (up to 125 µg/m³). At the upper terminus levels can drop to <30 µg/m³, as seen on 24 November natural gas bus pair.

74 µg/m³ route H12 on 1 March. Hybrid diesel. Levels start at around 60 µg/m³ then increase to 80 µg/m³ for the first 15 minutes without stopping the bus. Levels generally high throughout journey with three peaks: when the bus started the engines at the outward terminus (jump from 62 to 98 µg/m³) a major peak at (162 µg/m³) that corresponds with Plaza España, and another at 127 µg/m³ that is Plaza Europa.

67 µg/m³ route H12 on 1 March. Natural gas. Levels begin at 40 µg/m³ and rise gradually to >60 µg/m³ with peaks at 91 (Plaza España), 95 (Gran Via/Balmes) and 97 µg/m³ (Gran Via/Ciudad de la Justicia).

67 µg/m³ on 30 January. Tourist bus upper deck. PM levels increase because of the ascent of Montjuic, from 50 to 80 µg/m³, and stay >60 µg/m³ for the rest of the journey (Fig. 3.24).

In contrast, average levels as low as 19 µg/m^3 were recorded on 23 January during a clean, clear, sunny, cold day with excellent city AQ.

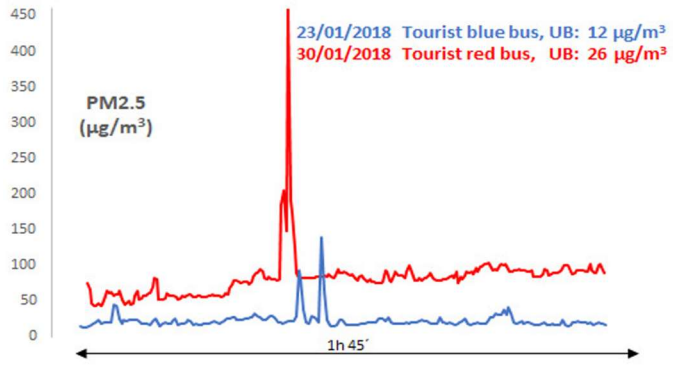

Figure 3.24. Comparison between $PM_{2.5}$ mass concentrations (uncorrected values in µg/m^3) measured in the open deck of tourist buses in a clean (23 January) and more polluted (30 January) day.

Considering all data shown above from the monitoring campaigns it can be **discussed** that air quality measured as number concentrations of QUFP inside buses can be noticeably influenced by city background levels in outside air. Transient peaks in ultrafine particle number concentrations of 100,000-1,000,000 cm^{-3} can be produced frequently inside buses due to the infiltration of traffic emissions at highly polluted locations such as the proximity to urban motorways, busy intersection crossings and roundabouts, and uphill stretches of relatively narrow, canyon-like roads.

Quais-ultrafine particle size is a useful indicator for the relative amount of fresh traffic-related particle emissions inside a road vehicle, with an inverse correlation typically existing between particle size and number of quasi-ultrafine particles.

Concentrations of BC inside buses (4-8 µg/m^3) are 2 or 3 times higher overall than those typically measured in Barcelona urban background air (2 µg/m^3) due to incompletely combusted hydrocarbon fuels sourced from road traffic exhaust within the city. Individual journeys record BC levels punctuated by transient peaks that can exceed 10 times average background. Such peaks in mass concentrations inside buses coincide with road traffic hotspots, tunnels, and urban background levels of outside air pollution in the city. In the statistical analysis was shown that self-pollution could be a significant source of QUFPN and BC exposure for commuters.

As seen with QUFP number concentration and BC levels, average $PM_{2.5}$ mass concentrations inside buses can be strongly affected by outdoor urban background air quality. $PM_{2.5}$

breathed while travelling by tourist bus for example can be less than 50% below normal on clear, clean winter days with low levels of urban background pollution. Transient peaks superimposed on this background typically show a strong coincidence between BC and $PM_{2.5}$ concentrations. Such pollution peaks in $PM_{2.5}$ encountered inside commuter buses are associated with traffic hotspots and tunnels and typically lie within the range 75-150 $\mu g/m^3$, and so can be >x10 average urban background.

Most of the pollutants, as QUFPN, N size and mean concentration of BC were recorded higher in summer, but $PM_{2.5}$ was higher in winter. Summer was expected to be cleaner as the AC is on, but this was not the case. The objective of TMB having hermetically closed windows is to control the temperature or ambient inside, but as it is an enclosed microenvironment, pollutants could be resuspended and if there is not good ventilation their concentration can become excessive.

Concentrations of CO_2 inside buses depend directly on the number of passengers, outside air entry through doors and windows, and the ventilation system. As such, levels of this gas inside public transport vehicles are a good proxy for how much indoor air is being diluted from outside. In this context, a crowded bus operating with closed windows can record CO_2 concentrations more than 3,000 ppm, over seven times natural background.

Vertical routes, as they run on a slope, are the ones registering highest concentrations. Apart from the traffic and exhaust emissions, being on a slope makes them their own materials (the rubber of the wheel, brake…) wear out more easily, contributing to self-pollution. Horizontal routes are the ones that have registered the lowest concentrations, 25-30% lower than in vertical routes.

3.2. Chemical results

The design of the PM sampling programme was based on the expectation that several factors influence air quality inside buses, but that some of these factors are likely to be more influential than others. Thus, bus pairs powered by different engines in different seasons and following different routes through the city were sampled, adding the open-topped tourist buses as an interesting "extra" to compare with normal commuting routes. Given such variety, the number of buses sampled (48) is rather small, but it is enough to make several observations. The chemical analyses of the 48 $PM_{2.5}$ samples collected during the campaigns are presented in chronological order in Table S1 (supplementary information) which also records the bus fuel-type (diesel (EURO IV, EURO V), hybrid diesel (HD), compressed natural gas (CNG), hybrid compressed natural gas (HCNG) and electric (EV)), and the bus number/route (V = "vertical"; H = "horizontal"; TB tourist bus red and blue trajectories). The analyses are further grouped into 20 "summer" (AC on with closed windows; May to September) and 20 "winter" samples (November to February), the other 8 samples were considered mixed. The data from these various sub-groups based on bus engine type, season, and route are averaged in Table 3.8. which for comparison adds the values for the average for all buses (AB) and the urban background (UB) in Barcelona during the sampling period. The chemical results of these campaigns have been published in **Fernández-Iriarte et al. (2020).**

Table 3.8. Summary of chemical analyses of $PM_{2.5}$: all bus average (AB), urban background (UB), and sub-groups based on bus engine types, season, and route (see Table TS1).

	URBAN BACKGROUND	ALL BUSES (AB)		BUS TYPE							SEASON		ROUTE		
	UB	AB	AB/UB	Diesel	HD	CNG	HNG	Electric	Tourist outside	Tourist inside	Summer	Winter	Vertical	Horizontal	Others
n		48		14	8	10	2	6	4	4	16	16	14	10	16
µg/m³															
OC	2.39	16.3	6.8	19.2	17.0	16.6	23.0	12.9	10.7	11.2	14.7	19.1	17.9	14.2	18.9
EC	1.04	4.8	4.6	6.6	4.6	4.2	4.8	3.8	4.1	2.9	4.8	5.1	6.6	4.0	4.4
CO_3^{2-}	0.35	1.6	4.5	2.0	1.2	1.8	2.3	1.4	0.5	0.7	1.4	1.7	1.9	1.1	2.0
SiO_2	0.54	2.1	3.8	2.6	1.8	2.6	4.0	1.8	0.6	0.6	0.7	4.0	2.3	1.9	2.8
Al_2O_3	0.18	0.7	4.0	0.9	0.7	0.9	1.3	0.6	0.2	0.2	0.3	1.3	0.8	0.6	1.0
Ca	0.23	1.0	4.5	1.4	0.8	1.2	1.6	0.9	0.3	0.5	1.0	1.1	1.3	0.8	1.3
Fe	0.19	1.4	7.3	1.9	0.9	1.6	1.4	1.3	0.5	0.5	1.2	1.6	2.0	1.0	1.5
K	0.11	1.0	8.8	1.6	0.5	1.1	1.5	0.9	0.5	0.6	0.9	0.9	1.6	0.4	1.2
Na	0.15	0.3	2.0	0.2	0.5	0.3	<0.1	0.3	0.4	0.4	0.4	0.2	0.1	0.3	0.4
Mg	<0.1	0.4	9.3	0.8	0.1	0.4	0.2	0.6	0.1	0.2	0.6	0.1	0.7	0.1	0.7
P	<0.1	1.2	122	3.0	0.1	0.6	0.2	1.6	<0.1	0.1	1.9	0.1	0.8	0.1	3.1
SO_4^{2-}	1.72	1.8	1.0	1.8	1.8	1.6	2.1	1.6	1.9	2.0	2.5	0.9	1.6	1.8	1.8
OC+EC	3.43	21.1	6.2	25.9	21.5	20.8	27.7	16.8	14.8	14.1	19.5	24.2	24.6	18.1	23.3
Mineral	1.65	5.5	3.3	8.0	4.0	6.0	7.9	5.1	1.7	2.0	4.6	7.5	6.2	3.6	8.2
ng/m³															
Ti	6.64	19.47	2.93	20.06	13.98	18.43	106.83	11.09	9.11	8.23	22.32	21.70	14.14	14.06	34.09
V	4.04	6.78	1.68	7.21	5.33	6.42	31.20	7.53	4.80	4.05	9.56	2.39	7.23	4.38	10.31
Cr	1.53	9.72	6.37	9.36	14.16	6.82	5.25	4.84	12.68	13.25	8.11	7.75	8.46	6.15	11.47
Mn	4.10	12.03	2.93	15.39	10.32	13.69	17.51	7.03	8.37	7.94	6.91	19.17	15.09	12.13	11.22
Ni	2.38	8.89	3.74	10.48	9.11	5.59	1.91	7.43	12.96	13.95	8.64	5.54	9.95	5.83	7.43
Cu	6.70	82.37	12.29	96.29	107.86	107.17	174.89	19.94	30.19	20.17	84.42	119.10	113.83	71.86	89.99
Zn	23.70	90.25	3.81	123.28	73.70	113.69	92.50	42.71	55.82	53.82	47.53	135.02	135.24	75.23	78.00
Sr	0.88	4.27	4.86	6.21	3.96	4.52	6.26	2.12	1.57	2.23	2.71	6.28	5.42	3.34	5.21
Zr	5.08	36.65	7.21	44.44	38.10	40.25	33.47	39.76	23.12	12.31	29.87	43.05	47.88	36.86	36.93
Sn	1.78	4.74	2.67	6.18	4.48	4.57	3.93	3.99	3.57	3.34	4.28	5.64	6.05	4.79	4.20
Sb	0.94	10.72	11.46	15.31	7.79	14.58	23.75	4.04	2.78	2.35	6.24	19.87	16.56	9.32	10.58
La	0.12	0.64	5.49	0.61	0.42	1.30	1.04	0.39	0.26	0.25	0.25	1.25	0.78	0.56	0.75
Ce	0.23	1.81	7.79	2.18	1.27	2.65	2.39	1.20	0.67	0.88	0.40	3.45	2.21	1.25	2.47
Hf	0.24	2.19	9.13	2.77	2.29	2.40	2.29	2.30	1.16	0.55	1.40	2.97	2.90	2.12	2.34
Pb	3.05	3.30	1.08	3.39	3.46	3.11	4.43	2.48	3.36	3.51	2.95	3.91	2.84	4.04	3.04
OC/EC	2.29	3.37	1.47	2.90	3.67	3.98	4.83	3.39	2.62	3.81	3.09	3.71	2.70	3.56	4.25

The data presented can be viewed as "state-of-the-art" in the sense that it is currently technically difficult to obtain gravimetric samples of inhalable particles breathed by commuters in public transport in enough quantity to allow comprehensive chemical analysis. The limitations of the personal environmental monitor used in the study meant that the same filter had to be used for three journeys (on the same route and at approximately the same time) to obtain just one chemical analysis, so that each of the results listed on Table 3.8 are an average of 6 h, collected over three days. Such logistic limitations, added to the difficulties of negotiating permission with transport companies, have perhaps inevitably resulted in very few publications on the chemistry of indoor bus air. In this context, and despite these limitations, the information presented here represents by far the largest bus air chemical database publicly available to date, involving 132 days of direct sampling inside urban commuter buses under normal working conditions.

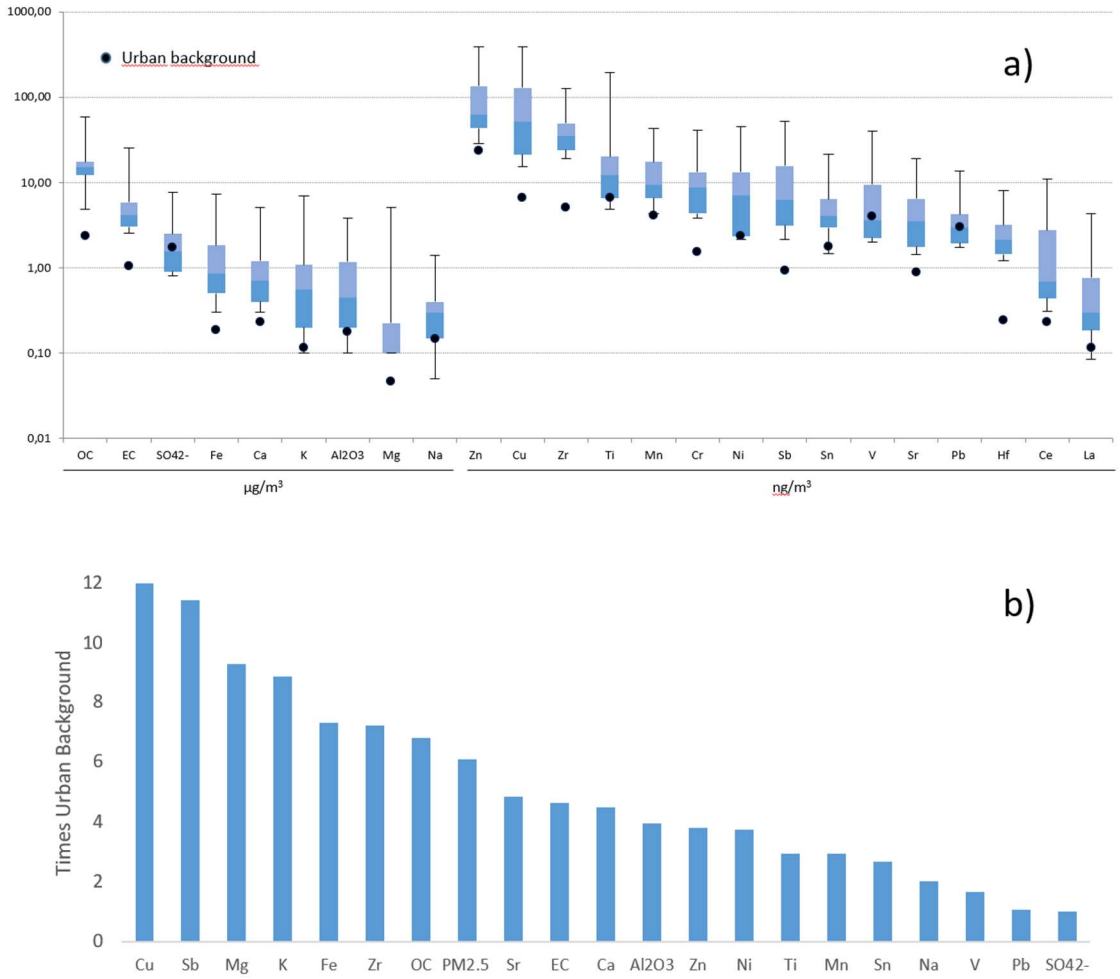

Figure 3.25. Elemental concentrations measured inside Barcelona buses and urban background. 1a. Boxplot showing concentration median, lower and upper quartiles, and ranges (vertical "whisker" bar) of major and trace elements measured from $PM_{2.5}$ sampled in buses and compared to urban background (black dot); 1b. Histogram demonstrating the relative enrichments of elements measured from $PM_{2.5}$ sampled in buses relative to Barcelona urban background.

The highest concentrations, as recorded in Table S1 and Table 3.8, and graphically presented in Fig. 3.25a, are those of OC (most values 10–20 µg/ m^3) and EC (most values 3–6 µg/m^3), followed by SO_4^{2-}, Fe, Ca, K, Al_2O_3, Mg and Na. Average OC concentrations are in general around x3 those of EC average (OC/EC = 3.4), and calculated mineral content is approximately one third that of total carbon content (EC + OC). Regarding the trace elements the highest concentrations are recorded for Zn and Cu, followed by Zr, Ti, Mn, Cr, Ni, Sb, Sn, V, Sr, Pb, Hf, Ce, and La. This distinctive inorganic trace element signature of interior bus air is further emphasised by comparing the present chemical database with levels recorded within the Barcelona UB (Table 3.8; Fig. 3.25a and b). Whereas concentrations of most elements and compounds recorded in the contaminated city road

are raised typically 2–8 times higher than UB levels (AB/UB on Table 3.8), some elements stand out as unusually enriched (both Cu and Sb > 10 times: Fig. 3.25b).

Lets consider now the PM chemistry characterising exposure in each of the bus sub-groups shown in Table 3.8, then present the results of source apportionment calculations. Finally, an examination of the pattern of VOCs present inside sixteen of the buses used during the winter campaign is shown (Table S2, supplementary information).

3.2.1. Impact of bus powertrain/fuel

Although the results reveal considerable $PM_{2.5}$ chemical variation, the majority of data fall within a relatively restricted range. In the case of EC, for example, most (73%) buses recorded levels of 3 – 7 μg/m^3 although exceptionally, concentrations as high as 19 μg/m^3 and as low as 1 μg/m^3 were reached (Table S1). Most bus pairs show similar EC concentrations, with nearly half differing by < 1 μg/m^3 and only 3 pairs differing by more than 2.5 μg/m^3 (Table 3.9). A notable exception to this general rule is a diesel EURO V/EURO IV pair (16 January) that records a difference in EC content 17 μg/m^3 (Table 3.9).

Table 3.9. Elemental Carbon concentrations (μg/m^3) in $PM_{2.5}$ sampled from bus pairs chosen for this study.

Bus pair	SUMMER		WINTER	
	Line	Elemental Carbon	Line	Elemental Carbon
Euro V vs Euro IV	V13	8.9 vs 9.5	V3	19.4 vs 2.6
Euro V vs HD	V13	6.8 vs 5.8	H4	4.9 vs 4.2
Euro V vs CNG	V3	4.5 vs 5.7	V3	4.1 vs 6.9
Euro V vs Electric	34	4.9 vs 7.2	–	–
Euro IV vs HD	47	3.5 vs 8.9	19	3.8 vs 2.9
Euro IV vs CNG	V17 vs V11	6.3 vs 3.8	V3	3.9 vs 4.7
Euro IV vs Electric	–	–	60	9.6 vs 4.9
HD vs CNG	H12	3.8 vs 3.1	H12	6.4 vs 6.4
HD vs Electric	34	3.1 vs 4.7	34	1.0 vs 0.3
CNG vs HCNG	39	3.8 vs 5.3	39	2.0 vs 4.2
CNG vs Electric	H16	2.7 vs 2.4	H16	2.7 vs 3.2
Tourist Inside vs outside	Blue	3.6 vs 6.1	Blue	2.4 vs 2.5
Tourist Inside vs outside	Red	3.8 vs 5.5	Red	1.9 vs 2.3

A similar pattern is revealed by OC concentrations, which cluster around 10 – 15 μg/m^3 and rarely (25%) exceed differences > 5 μg/m^3 between bus pairs. In the case of "mineral"

concentrations (essentially mainly a mix of silicates and carbonates: Table S1) these again show very few exceedances above 10 μg/m^3, with 92% of bus pairs showing differences below 2 μg/m^3, irrespective of whichever engine type was powering the bus.

Taken overall, the diesel buses record slightly higher average EC concentrations inside the bus when compared to CNG or EV models, this being interpreted as likely evidence for some degree of self-pollution (Table 3.9). In contrast, when compared to diesel buses the six EV buses show relatively lower average concentrations of many $PM_{2.5}$ components, but especially the metals Cu and Sb (Fig. 3.26a). These EV buses have a window system which is hermetically sealed, climate control is regulated by the driver, and they are equipped with regenerative braking which reduces the use of friction brakes, all of which favour reduction of outside PM infiltration, including that sourced from their own brakes.

The data from the tourist buses offer insight into the differences between the upper floor, which is wide open to outdoor air, and the lower floor which, although ventilated via stairs leading to the open top floor, is more confined. The data demonstrate consistently higher EC levels in the upper floor ("out" in Table S1) than in the downstairs interior ("in"). If the concentration of EC inside buses can be viewed as a proxy for traffic emissions, this would indicate that passengers travelling on the open upper deck of the bus are more exposed to traffic exhaust emissions than those below. However, it should be noted that this difference between EC concentrations upstairs and downstairs in these buses is always < 2.5 μg/m^3.

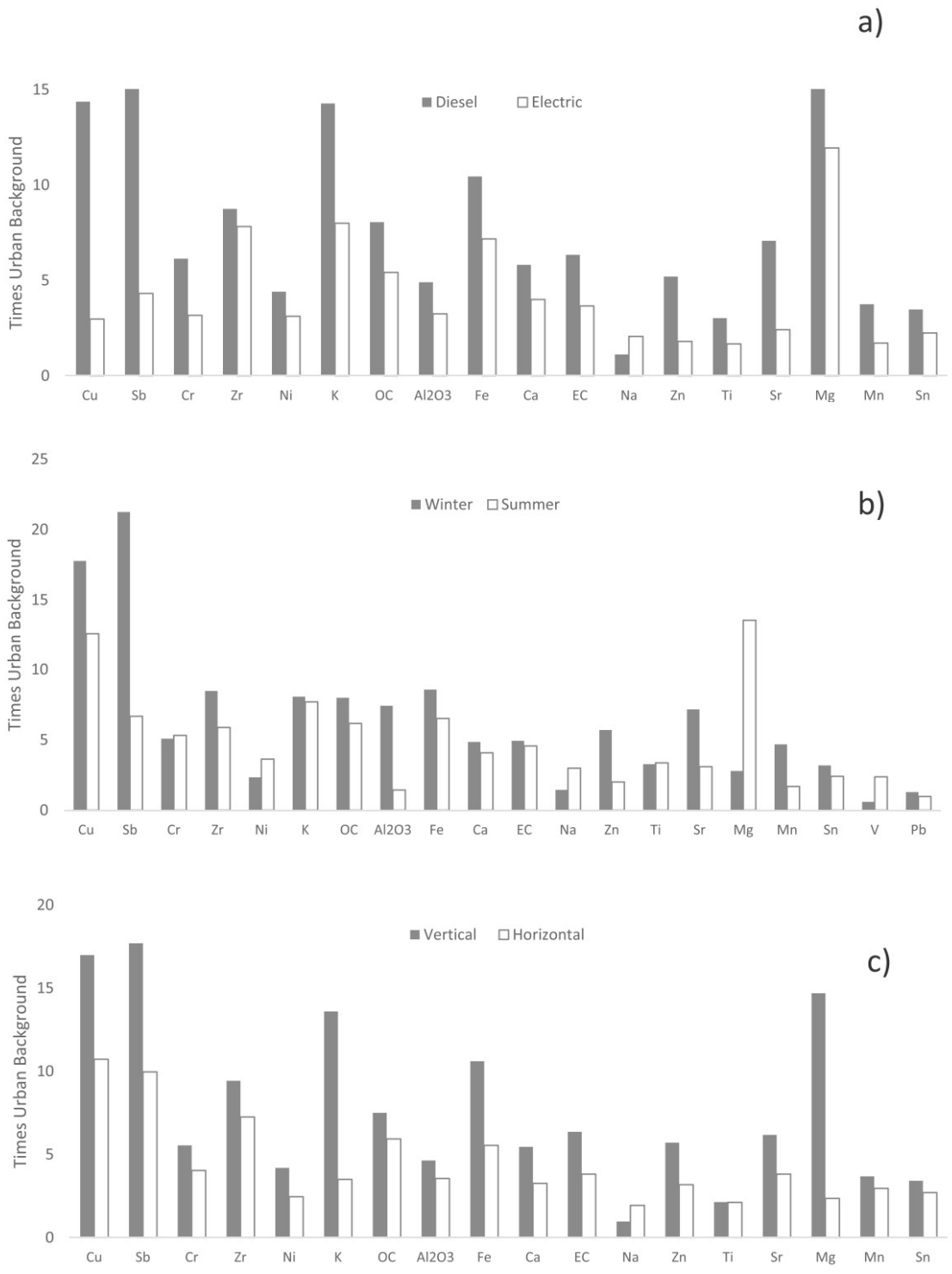

Figure 3.26. Histograms comparing Barcelona buses data with urban background in: 1a. Diesel v electric buses; 2b. Winter v summer, 2c. "Vertical" (sea-to-mountain) v "Horizontal" (coast-parallel) routes. Note the consistent especial enhancement of Cu and Sb, interpreted as sourced from brake emissions.

3.2.2. Seasonal differences

The two subgroups selected based on warmer ("summer") and cooler ("winter") seasons are listed in Table S1 and compared with UB concentrations in Fig. 3.26b. The $PM_{2.5}$ chemistry for each of these two subgroups is quite different, with the winter samples being noticeably richer in mineral dust (summer average Al_2O_3 0.3 μg/m^3; winter average 1.3 μg/m^3) and slightly more carbonaceous (summer OC + EC 19 μg/m^3; winter OC + EC 24 μg/m^3). Several trace elements occur in higher concentrations in winter, most notably Sb, Cu, Zn and Mn. The highest increase was recorded for Sb x 6.5 above UB in summer and x21 in winter. In contrast concentrations of Na, P, V, Ni, Cr, SO_4^{2-} and especially Mg were considerably lower in winter. The likely controls on these seasonal chemical differences are discussed below.

It is observed distinct difference between interior bus air chemistry of $PM_{2.5}$ in summer and winter (Fig. 3.26b). The air chemistry inside the buses sampled in summer is noticeably richer in Na, Mg, V, Ni, Cr and SO_4^{2-}. Given the coastal position of Barcelona, a city with a large and active port catering especially for cruise ships, combined with more active landward-driven sea breezes in early summer, it seems likely that this seasonal difference in chemical signature is due to a greater influence of marine aerosols contaminated by shipping emissions and to the higher summer SO_2 oxidation (Querol et al., 2001; Amato et al., 2009). Another seasonal difference is registered in winter, when most $PM_{2.5}$ elemental concentrations are not only higher inside the buses, but the chemical mix is noticeably richer in several trace metals, including a quite spectacular enrichment in Cu and Sb.

3.2.3. Routes

The "route" sub-groups listed on Table S1 and Table 3.8 have been chosen on the basis of whether they run essentially horizontal and coast-parallel through the city (these routes being designated with the prefix H for "horizontal"), whether they operate across a considerable change of gradient between the coast and the northeast-southwest oriented hills that form the hinterland of Barcelona (prefix V: "vertical"), or whether the bus is neither H nor V but follows some more variable route through the city (buses 34, 39, 47, 19, and 60: "others" on Table 3.8). Vertical routes showed on average higher concentrations of carbon content (OC + EC = 25 for V vs. 18 μg/m^3 for H), and mineral dust (6.2 V vs 3.6 μg/ m^3 H). Other elements also occur in higher concentrations in V routes, especially Cu, Sb, Mg

and K which are >50% higher in buses running along V routes (Fig. 3.26c, Table 3.8) and presumably this is likely to reflect greater use of brakes on the routes with higher gradient.

The data presented here fail to reveal any great difference in major element chemistry between the chosen bus pairs following the same route one after another, even though the buses were driven always by different engine types. Thus, the differences between bus pairs of measured OC, EC and "mineral" concentrations were most commonly < 5 $\mu g/m^3$, < 2.5 $\mu g/m^3$, and < 2 $\mu g/m^3$ respectively (Table S1). Taken overall, however, our data do suggest poorer interior bus air quality, measured as increased carbon and mineral content, is more likely to be associated with diesel buses when compared to, for example, electric buses (Fig. 3.26a). This implicates part of the PM contamination present inside the moving vehicle as being a result of emissions from the bus itself ("self-pollution"), a phenomenon well documented in previous publications (e.g. Fondelli et al., 2008; Zhang et al., 2013; Chernyshev et al., 2019).

Another, and stronger, indication of self-pollution affecting interior bus chemistry, however, emerges from a consideration of the trace element signature of the $PM_{2.5}$. One of the more striking observations repeatedly noted in this study is the ubiquity and abundance of Cu- and Sb-bearing fine particulates in bus air. Previous publications have demonstrated how these elements are good tracers for brake particles (Adamice et al., 2016; Amato et al., 2011; Grigoratus and Martini, 2015). Previous works on public transport air quality in Barcelona based on a pilot study on just three buses, also demonstrated the same enrichment in Sb and introducing a Mn, Ti, Sbx10 ternary diagram to show how bus air can be contrasted with $PM_{2.5}$ samples collected from subway and outdoor city air (Moreno et al., 2015). On Fig. 3.27 a plot with the same ternary diagram is showing the new bus database, adding the urban background data from the Palau Reial monitoring site during the sampling campaigns. The same relative enrichment in Sb and Cu inside the vehicle also strongly suggests that brake particles are more common in the buses operating along a significant slope, with the "vertical" buses (from coastline to the hills) recording concentrations > 50% higher than the coast-parallel "horizontal" buses (Fig. 3.26c, Table 3.8). Even more interesting is the fact that electric buses do not show such enrichment (Fig. 3.26a), an observation that may reflect the fact that these buses have more hermetic closure and/or that they use regenerative braking and so emit fewer brake particles. Another conclusion arising from this difference in braking patterns is that it is the brake-contaminated PM plume generated by the bus itself ("self-pollution") that is infiltrating into the bus,

presumably through open windows and when doors are opened after braking upon arrival at bus stops.

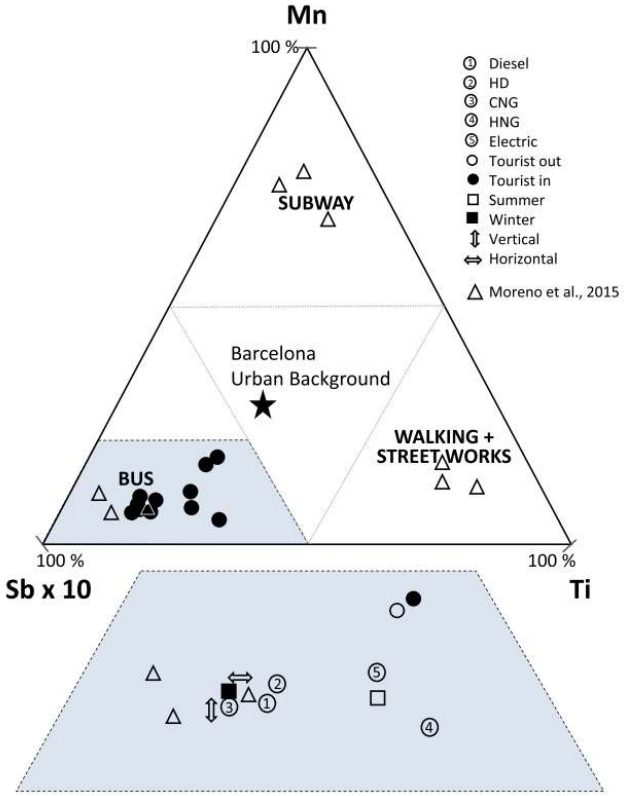

Figure 3.27. MnTiSbx10 ternary plot comparing $PM_{2.5}$ measured inside Barcelona buses, showing enrichment in Sb typical of brake PM-contaminated air. Fields for subway, walking/streetworks, and bus from Moreno et al. (2015).

The open-topped tourist buses provide a special case in that upstairs they are open to the city highway air which also enters the lower floor of the bus. This higher degree of ventilation is reflected in the fact that the $PM_{2.5}$ mass represented by OC content is relatively low in the tourist buses (11 μg/m^3) when compared to all other bus types (17–23 μg/m^3) except electric (13 μg/m^3) (Table 3.8). It is possible to also observe that those passengers travelling in the open top upper floor of the tourist bus breathe higher levels of EC, Cu and Zr, presumably sourced from fresh traffic exhaust and brake emissions (Table 3.8).

3.2.4. Source apportionment calculations

Several PMF solutions were evaluated in terms of scaled residuals, Gspace plots, profiles, and contributions. The most-reliable solution provided 6 main factors responsible for the variability of $PM_{2.5}$ and its components (Fig. 3.28):

- The first factor comprises mainly OC although it also explains a significant share of some metals such as Ti, Pb, Na, Sr, and Ca. Previous studies in Barcelona have related indoor sources of high OC concentrations (without EC) to the textile fibres and skin flakes of occupants (Amato et al., 2014; Rivas et al., 2014). This is the dominant source of $PM_{2.5}$ inside the bus (46%) increasing $PM_{2.5}$ levels by 39.6 μg/m^3 on average. In addition, this first factor is taken to include a Ca, Ti, Sr, and Na grouping like that identified as linked to a cosmetic product source in a previous study in Barcelona (Minguillón et al., 2012). The largest contributions of this first factor were found in tourist buses, probably due to the higher occupancy.

- The second factor was traced by Cu, and mainly comprises OC and EC (OC/EC = 1.8). This factor was labelled as vehicle exhaust, although it likely involves a partial contribution from brake wear as well. It is the second most important source of $PM_{2.5}$, contributing 16.3 μg/m^3 (19%) on average. Interestingly the lowest contributions were obtained for EV buses, as already described for EC, Cu and Sb. The rest of fuel-types do not register significant differences.

- The third factor was traced by SO_4^{2-} and d V (highest % of species) and was interpreted as secondary SO_4^{2-} and shipping. The mean contribution to exposure in buses was 4.8 μg/m^3 (6%). Significant differences were observed between the winter (3 μg/m^3) and summer (7 μg/m^3) campaigns, as both oxidation processes and shipping emissions reach their maximum in summer months (Querol et al., 2001; Amato et al., 2009). The association of secondary sulphate and primary vanadium in the same factor has been reported in Barcelona before, as the ammonium sulphate particles are formed from SOx emissions which are often emitted by heavy oil combustion processes (notably by shipping) containing high amount of vanadium.

- The fourth factor was traced by Mg, Fe, K and Ca, with OC as main component. This factor had a contribution in only 2 bus pairs and was practically null for the rest of the campaigns. Since the 2 bus pairs included routes and vehicles used also in other days, it was interpreted this source as local urban dust, probably some minor building activities, which affected only 2 samples.

- The fifth factor was traced by Sb, Cu, Zn, Al_2O_3 and La and was interpreted as road dust resuspension. The main components are OC, EC, and Fe, with an OC/EC ratio of 6.0. The lowest contributions of this factor were observed for EV and touristic buses, the reason for the latter remains unclear.

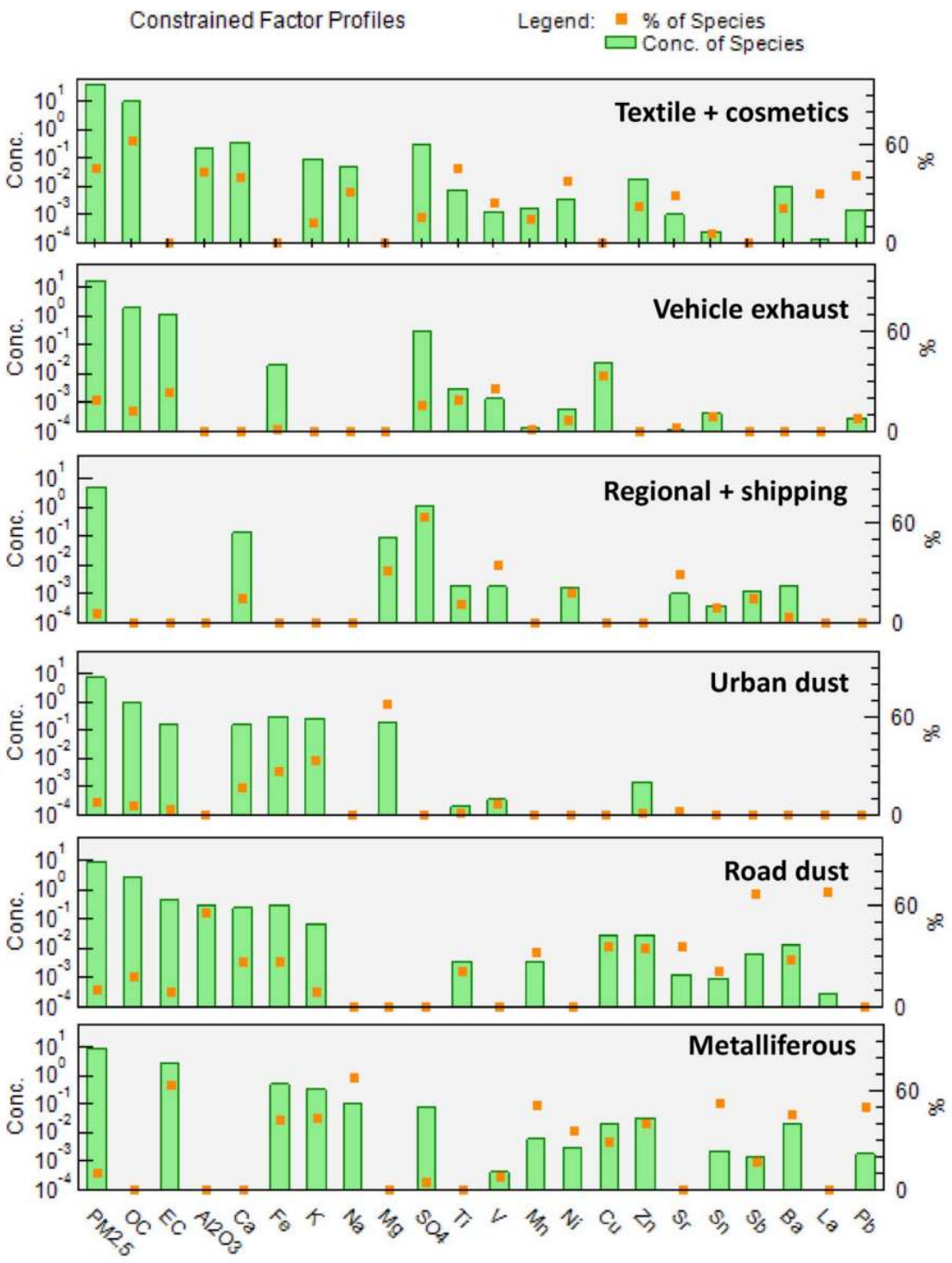

Figure 3.28. Positive matrix factorization results showing the factor profiles identified.

- The sixth factor was identified as metalliferous and accounts for most of the variance of metals originated from brake wear (Sn, Ba, Fe) and metallurgy (Mn, Pb and Zn) (Amato et al., 2009). The largest components are EC and Fe. The largest contributions were found in tourist buses, possibly due to their higher weight (higher braking emissions) and because they move mostly in the southern part of the city which is nearer to the metallurgical cluster of Baix Llobregat county.

Source apportionment data indicates that although almost half of the particles inhaled when travelling in the bus are most probably related to vehicle passenger emissions such as textile fibres and skin flakes (Amato et al., 2014; Minguillón et al., 2012; Rivas et al., 2014), independently of the bus type. The infiltration from outdoor sources such as vehicle exhaust and brake wear particles both from the same bus (self-pollution) and from other vehicles, also represents an important source of pollution (19%).

3.2.5. Volatile organic compounds

A total of 44 VOCs were quantified inside 16 buses sampled during the winter campaign (Table S2, supplementary information). The overall VOC concentrations ranged from 69.9 to 173 μg/m^3. However, bus 34 hybrid diesel was a notable exception because of the much higher concentrations (851 μg/m^3). This bus is a special case in the context of the study because it was a brand-new vehicle which was still degassing VOCs from the furnishing and coatings, including glues and other products.

Excluding the above-mentioned bus, the VOC distributions in the studied buses are rather similar. The aromatic compounds are dominant (27.5–50.2%), being mainly constituted of benzene, toluene, ethylbenzene, xylenes and trimethylbenzenes, which involve 87% of the total aromatic compounds. Toluene (10–29 μg/m^3) and m-xylene (5–17 μg/m^3) are common in all samples (Table S2). The overall BTEX (Benzene, Toluene, Ethylbenzene and Xylene) signature of indoor air in the buses is remarkably similar and generally rather low (< 70 μg/m^3). The typical distribution is predominated by toluene (10–30 μg/m^3) and followed by m-xylene (5–17 μg/m^3) > p-xylene (2–5 μg/m^3) > o-xylene (3–6 μg/m^3) > ethylbenzene (2–7 μg/m^3) and benzene (2–4 μg/m^3). These last two were both consistently present in low concentrations. Such aromatic VOCs levels can be favourably compared to other studies, for example that by Chen et al. (2011) in Changsha city, China, where mean ΣBTEX values inside buses were 464 μg/m^3 and included highly undesirable levels of benzene (69 μg/m^3). A comparable study inside buses in Bangkok found ΣBTEX concentrations of 169 μg/m^3, with 12 μg/m^3 benzene (Ongwandee and Chavalparit, 2010). A study in Taegu, Korea, reported mean ΣBTEX levels of 131 μg/m^3 inside buses and 195 μg/m^3 inside taxis, including 22 μg/m^3 and 33 μg/m^3 benzene respectively (Jo and Yu 2001). However, not all studies of VOC levels in public transport have been conducted in busy, polluted cities, as demonstrated by measurements made inside public buses operating in the relatively small and uncongested Spanish city of Pamplona where ΣBTEX concentrations of 10-22 μg/m^3 were recorded (Parra et al., 2008).

The alkanes (26.7–48.1%) constitute the second most abundant VOC group (Fig. 3.29). They are dominated by 2-methylbutane (14–36 µg/m³) followed by n-pentane (5–15 µg/m³) which are found in all samples (Table S2). About the remaining VOCs detected, only the monoterpene compound d-Limonene was present in concentrations >10 µg/m³ and this in only four buses, one of which registered 65 µg/m³ (Table S2).

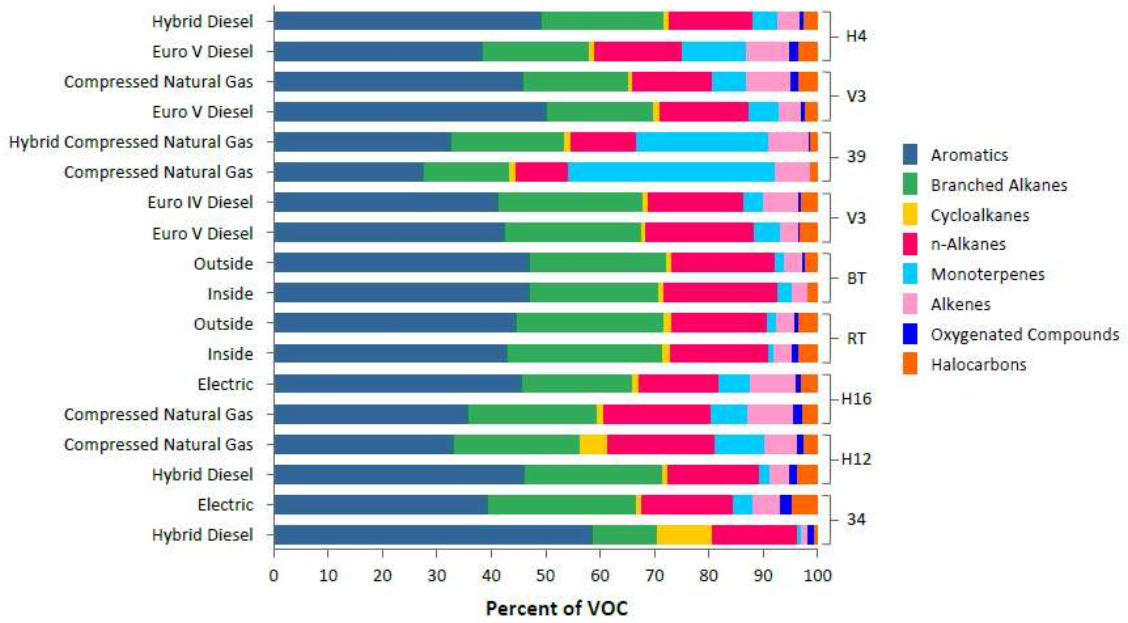

Figure 3.29. Percentages of abundances of VOCs measured in 17 Barcelona buses and a brand-new hybrid diesel bus (34) contaminated by severe interior offgassing. See Table S2 and text for details.

As mentioned above, bus 34 (a hybrid diesel) registered exceptionally high VOC concentrations that together totalled over 850 µg/m³. In this case aromatic compounds were present in higher overall concentrations (497 µg/m³: 58% of total VOCs) than the alkane/alkene subgroup (332 µg/m³; 39%). Most outstanding in the aromatic subgroup are anomalously high concentrations of the three xylene (= dimethylbenzene) isomers (especially o-xylene: these compounds were found in concentrations of 160 µg/m³). Ethylbenzene was also present in exceptional concentrations (95 µg/m³) which, like Isopropylbenzene and sec-butylbenzene, registered levels well over tenfold those in any other bus sampled (Fig. 3.29). This bus shows a completely different BTEX hierarchy from normal, with o-xylene (160 µg/m³) > ethylbenzene (95 µg/m³) > p-xylene (91 µg/m³) > toluene (44 µg/m³) > m-xylene (43 µg/m³) > benzene (5 µg/m³). In the alkane/alkene sub-group the most abundant VOC was again 2-methylbutane (92 µg/m³), as with the other buses. However, relative to levels in the other buses, the most striking alkane/alkene VOC

increases were shown by cyclohexane (86 μg/m^3), n-decane (63 μg/m^3), n-octane (12 μg/m^3), and 2,3-dimethylpentane (10 μg/m^3). Other VOCs subgroups showed much lower concentrations, although relative to the other buses, there were unusually raised levels of the monoterpene p-cymene, the organochlorine 1,1,2-trichloroethane, as well as methyl methacrylate, tetrahydrofuran, and ethyl methacrylate (Table S2). As mentioned above, this bus was brand new and the high VOC concentrations presumably reflect significant offgassing from the interior components.

Concerning VOCs, comparison of the concentrations in the inner bus atmospheres with those in open air collected in the Route Blue and Red Tourist buses, shows similar concentrations for gasoline vehicle pollutants such as benzene, toluene, ethylbenzene, xylenes, and trimethylbenzenes. Thus, the concentrations of toluene are 11–26 μg/m^3 in the external atmosphere and 10–29 μg/m^3 in the inner bus air, and total xylenes are 19–23 μg/m^3 and 11–28 μg/m^3, respectively. Traffic emissions infiltrating from outside will be also rich in alkanes, but also contain BTEX and other aromatic compounds as well as several alkanes (Yang et al., 2017). Evaporative emissions will normally favour aromatics over alkanes (Yue et al., 2017), whereas exhaust emissions of alkane and aromatic VOC are likely to be mostly toluene, 2-methylbutane and p- & m-xylenes derived from gasoline (petrol) combustion (Chin and Batterman, 2012; Montells et al., 2000).

Table 3.10. Statistical analysis in the composition of aromatic alkanes in all routes studied.

Route	Engine	Aromatics							Alkanes						
		Wilcoxon Signed Rank Test					Spearman's Correlation		Wilcoxon signed rank test					Spearman's correlation	
		25	Median	75	Z	p-Value	r_s	p-Value	25	Median	75	Z	p-Value	r_s	p-Value
H4	Hybrid Diesel	0.43	2.77	3.42	−2.856	0.004	0.996	0.000	0.95	2.04	5.18	−1.362	0.173	0.983	0.000
	Euro V Diesel	0.38	1.63	3.16					0.85	2.07	5.33				
V3	Compressed Natural Gas	0.22	1.38	2.54	−0.282	0.778	0.952	0.000	0.59	1.18	4.42	−0.533	0.594	0.917	0.001
	Euro V Diesel	0.24	1.31	2.82					0.66	1.25	4.13				
39	Hybrid Compressed Natural Gas	0.38	1.77	3.29	−1.961	0.050	0.974	0.000	0.91	1.72	5.72	−1.12	0.263	0.983	0.000
	Compressed Natural Gas	0.38	1.98	3.42					0.86	1.70	6.08				
V3	Euro IV Diesel	0.24	1.31	2.57	−2.919	0.004	1.000	.	0.81	1.45	3.96	−2.666	0.008	0.950	0.000
	Euro V Diesel	0.26	1.40	2.79					0.85	2.52	5.67				
BT	Outside	0.19	2.36	4.90	−2.856	0.004	0.991	0.000	1.13	2.76	9.16	−2.666	0.008	0.983	0.000
	Inside	0.20	2.53	6.20					1.22	2.96	10.94				
RT	Outside	0.16	1.66	4.25	−2.040	0.041	0.988	0.000	0.83	1.40	6.37	−1.244	0.214	0.939	0.000
	Inside	0.13	1.54	3.72					0.72	1.32	6.37				
H16	Electric	0.40	2.06	4.34	−0.943	0.345	0.996	0.000	0.93	1.92	7.18	−2.666	0.008	0.988	0.000
	Compressed Natural Gas	0.46	2.39	4.12					1.15	2.69	10.44				
H12	Compressed Natural Gas	0.31	2.30	3.97	−3.180	0.001	0.991	0.000	1.29	4.32	11.23	−2.666	0.008	0.77	0.009
	Hybrid Diesel	0.17	1.68	2.75					0.67	1.29	5.26				
34	Hybrid Diesel	0.27	1.64	3.32	−3.296	0.001	0.855	0.000	0.75	1.46	6.04	−2.666	0.008	0.491	0.150
	Electric	2.68	5.86	55.27					10.05	19.24	74.41				

Pairwise comparison of the concentrations of the individual VOCs found in the buses compared in each route shows statistically significant correlations for the concentrations of aromatic compounds in all routes and alkanes in all routes except 34 (Hybrid Diesel and

Electric) (Table 3.10). Despite these correlations significant statistical differences in the composition of aromatic compounds were observed in routes H4 (Hybrid and EURO V Diesel), V3 (EURO IV and V Diesel), H12 (compressed natural gas hybrid Diesel) and 34 (Hybrid Diesel, Electric). They also show significant differences when comparing between inner and external atmospheres (routes BT and RT) (Table 3.10).

The composition of alkanes shows significant differences in route V3 (EURO IV and V Diesel), H16 (Electric and CNG), H12 (CNG and Hybrid Diesel) and 34 (Hybrid Diesel and Electric), and significant differences between the inner and external atmospheres of route BT but not in route RT (Table 3.10).

Regarding the compounds related to personal care, such as the monoterpenes, these are present in higher concentrations in the inner bus atmospheres than in the external air. This is the case of p-cymene, 0.15–0.17 μg/m^3 in the outer atmosphere and 0.11–0.54 μg/m^3 in the inner atmosphere (Table S2), δ-limonene, 0.94–1.6 μg/m^3 and 0.49–65 μg/m^3, respectively, and β-ocimene, ND-0.03 μg/m^3 and ND-0.64 μg/ m^3, respectively. The same is the case of VOCs exhaled from human breath such as isoprene (Marco and Grimalt, 2015), e.g., 0.78–1.3 μg/m^3 in the external atmosphere and 0.80–10 μg/m^3 in the inner bus air. Compounds that are commonly found in furniture tissues such as methyl methachrylate are also found in higher concentrations in the inner bus atmospheres, 0.12–0.19 μg/m^3 and <LOD-0.89 μg/m^3, respectively. The organochlorinated VOCs do not show a defined trend when comparing both atmospheres (Table S2).

The obvious exception to the general rule of relatively low VOCs concentrations inside buses in Barcelona is that of the brand-new hybrid diesel bus sampled on 27 March and seriously contaminated by interior VOC off-gassing (Table S2). In this new bus many VOCs concentrations were much higher, and with a different distribution: o-xylene (160 μg/ m^3), ethylbenzene (95 μg/m^3), 2-methybutane (92 μg/m^3), p-xylene (91 μg/m^3), and cyclohexane (86 μg/m^3). However, despite the fact that levels of BTEX approached 500 μg/m^3 in this bus (over x10 higher than normal), the benzene concentrations still remained relatively subdued at 4.5 μg/m^3, below the European Union limit value of 5 μg/m^3 (EU air quality directive 2008/EC/50; Kerchich and Kerbachi, 2012) because the occurrence of this compound is related to the inputs from external air and the general pollution by traffic. Although the VOCs concentrations in this bus are much higher than what is normal for a commuter bus in Barcelona, other studies have demonstrated that levels of interior BTEX in brand new passenger vehicles can be even higher. A study of newly built coaches less than a month from the production line in China reported BTEX levels that in some cases

exceeded 8,000 μg/m^3, with the highest concentrations peaking at around 15 days after delivery (Lu et al., 2016).

It is also interesting to compare the chemical data, presented in this study, with a recent study of air quality inside Barcelona taxis (Moreno et al., 2019). The taxi interiors recorded the same "top-five" distribution of VOCs as observed inside the buses, although at significantly higher concentrations: 2-methylpentane (43–60 μg/m^3), toluene (37–56 μg/m^3), xylenes (32–50 μg/m^3, with m- » o- > p-xylene) and n-pentane (17–28 μg/m^3). This VOC signature is typical of Barcelona city roadside air and, although varying in concentration, is quite homogeneous in terms of composition. The observation that taxi interior air is higher in VOCs than bus air is consistent with the results of the Taegu study mentioned above (Jo and Yu, 2001), and likely reflects poorer air quality in the more confined breathing space inside smaller vehicles.

3.3. Bioaerosol results

3.3.1. Total bacteria quantification

Of 100 bioaerosol samples, total bacteria were detected in 94, (46 of 50 in summer: May–September and 48 of 50 in winter: November–March, **Fernández-Iriarte et al., 2021**). The detection limit of the sampling procedure was 2.5 x 10^0 equivalent *E. coli* genomes/m^3 of air, and the concentrations of samples that were below the detection limit were defined as 1.25 x 10^0 equivalent *E. coli* genomes/m^3 of air. Total bacteria concentrations in the summer: May–September campaign ranged between 1.25 x 10^0 and 3.49 x 10^4 equivalent *E. coli* genomes/m^3 of air, which correspond to a geometric average (GA) concentration of 9.63 x 10^2 ± 7.21 x 10^0 equivalent *E. coli* genomes/m^3 of air for the summer: May–September campaign (a total of 50 filters), whereas for winter: November–March total bacteria concentrations ranged between 1.25 x 10^0 and 2.28 x 10^4 equivalent *E. coli* genomes/m^3 of air, which correspond to a GA concentration of 2.63 x 10^3 ± 1.31 x 10^1 equivalent *E. coli* genomes/m^3 of air. Mann Whitney test confirmed that there are significant differences (*P-value* 0.021) between the different campaigns. In addition, Kruskal–Wallis test confirmed that there is no significant difference (*P-value* 0.273) between different types of fuel (this statistical analysis was made for all the samples, taking both campaigns into account). No statistically significant difference was noted between inside (lower floor) or outside (upper floor) the tourist bus, as demonstrated by Wilcoxon matched-pairs signed rank test and Mann Whitney test. A ventilation system working efficiently help reduce contaminants in the inside air, which could explain why inside the tourist bus had similar concentration of equivalent *E. coli* genomes compared to the open upper floor.

Total airborne bacteria geometric average concentration was approximately 1.35 x 10^3 equivalent *E. coli* genomes/m^3 lower than the one detected in the Barcelona subway system (Triadó-Margarit et al. 2016). *E. coli* genome eq. median values were highest inside EURO V and HCNG buses, while the lowest value was found inside EV buses (Fig. 3.30). As EV buses do not allow opening windows, they always have the ventilation on, which can help reducing bacterial concentration entering inside the bus with passengers (Bonetta et al. 2010; Maestre et al. 2018). *E. coli* concentrations were also lower in the tourist bus when travelling outside in the open upper floor (**Fernández-Iriarte et al., 2021**).

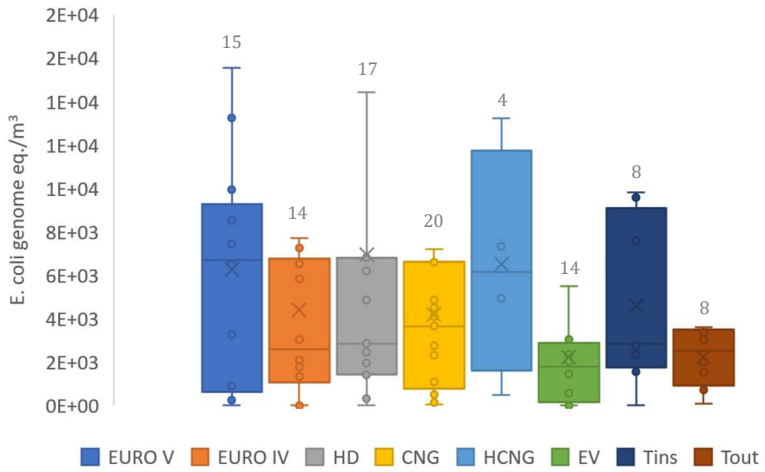

Figure 3.30. Concentrations of airborne Bacterial 16S rDNA gene copies determined by qPCR analyses for different fuel/engine type and tourist buses. The number above each of the boxes refers to the number of samples taken in each kind of fuel bus.

When analysing the total concentration clustered by campaign (summer: May–September and winter: November–March, according to TMB ventilation protocols) the bacterial load was higher in winter: November–March (Fig. 3.31), as it was expected, due to less ventilation as the AC is not functioning, as opposed to summer: May–September. Nowakowicz-Dębek et al. (2017) have analysed microorganisms inside public buses in winter, autumn, and spring, in Lublin, Poland, and showed that the highest concentration of total bacteria was detected in winter, while the lowest in spring. In contrast, for Lee and Jo (2005) in a study in Daegu, Korea, total bacteria concentration inside buses was higher in summer than in winter, however, these comparisons must be taken with care as the ‘‘summer: May–September’’ and ‘‘winter: November–March’’ periods were not the same, and the methodology for sampling was also different in each study.

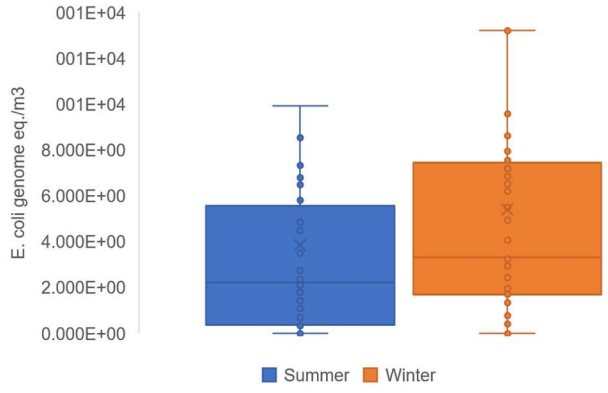

Figure 3.31. Concentrations of airborne Bacterial 16S rDNA gene copies determined by qPCR analyses for different seasons.

3.3.2. Biodiversity analysis

3.3.2.1. Powertrain/fuel type bus differences

As in 94 of 100 samples bacterial load was detected, a biodiversity study was carried out to determine the microbial diversity present in different type of buses (excluding HCNG and EV due to small number of samples with enough bacterial concentration). In the case of samples taken in tourist buses, differences between the inside and the outside can also be seen.

CNG buses were the richest in terms of the number of observed OTUs, followed by HD, EURO V and EURO IV (Fig. 3.32). The slope of the curves shows sufficient sequencing depth and good bacterial coverage in all samples, as no more OTUs were identified even with a higher number of sequences per sample.

Chao1 is a richness estimator. The higher the number of unique OTUs in a sample, the higher the value of the Chao1 index. Shannon diversity index is a measure of diversity that considers the number of species present, as well as the relative abundance of each species. PD (Phylogenetic diversity) whole tree is a measure of biodiversity which incorporates phylogenetic difference between species.

It is defined and calculated as the sum of all branch lengths of the OTUs in the group (Fig. 3.33). CNG buses were statistically the richest, the most diverse and the most branched (Mann–Whitney *U* p-value ≤ 0.05).

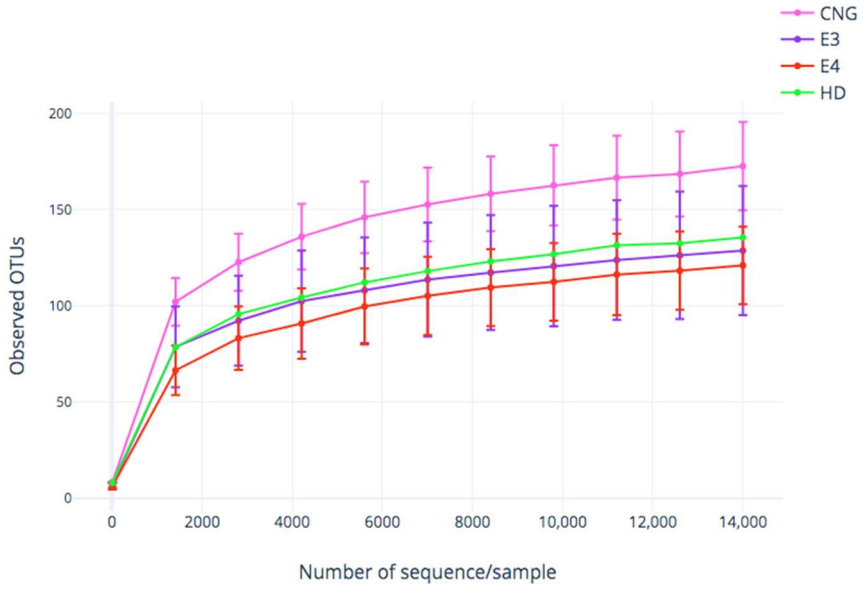

Figure 3.32. Rarefaction curves obtained from the number of observed operational taxonomic units (OTUs) and the sequences per sample for air samples from four different fuelled buses. The plateau of the curves started around 2000 sequences.

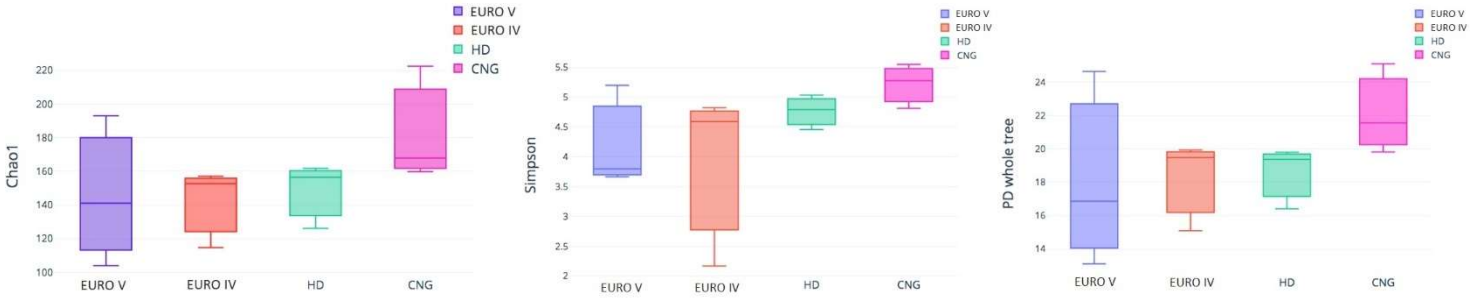

Figure 3.33. Boxplots of bacterial richness (Chao 1), bacterial diversity (Shannon and PD whole tree) for different analysed fuel type buses (EURO IV, EURO V, HD and CNG).

HD and EURO IV achieved similar results, but HD was richer and more diverse, and EURO IV had more branches. The lowest, taking the median value into account, was the EURO V. It had a wide range, but the median values were lower than the rest of the buses.

Regarding the identified taxa at the phylum level (Fig. 3.34), almost 80% of the relative abundance was covered by *Actinobacteria* and *Proteobacteria* for all the buses. *Actinobacteria* are a phylum and class of Gram-positive bacteria that can be ubiquitously distributed in both terrestrial and aquatic ecosystems. They can produce two-thirds of all the antibiotics in current clinical use that came from natural sources, as well as many anticancer, anthelmintic, and antifungal compounds, that is why these bacteria are very important for biotechnology, medicine, and agriculture (Barka et al. 2016). *Proteobacteria* is the largest bacterial phylum, with six classes and over 116 families (Parte et al. 2020). Members are Gram-negative and play a variety of roles in diverse microbial ecosystems (such as in aquatic, soil, plant, and animal niches). They can grow up on a variety of organic compounds: proteins, carbohydrates, and lipids; and contribute to the human gut microbiome functional variation (Bradley & Pollard, 2017).

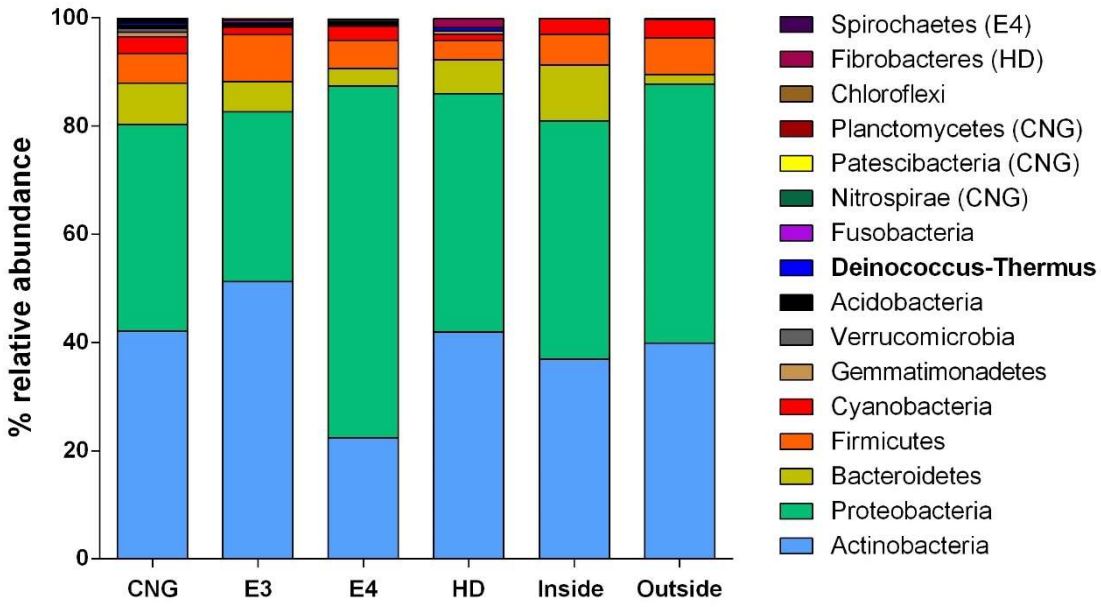

Figure 3.34. Relative abundance of Phylum taxonomic category for each kind of fuel type and tourist buses. The taxa in bold are specific to Inside buses.

Amongst the differences that were found inside the different fuel type buses, the most obvious one was *Proteobacteria* being more abundant in EURO IV compared to the others (Mann–Whitney U *p-value* ≤ 0.05), and *Deinococcus-Thermus* being detected only in the inside of the four types of buses analysed, and not present in the outside samples, which make it a potential useful marker.

Moving on to the genus level (Fig. 3.35), some substantial differences were noted. Airborne bacterial communities in Barcelona bus systems were largely dominated by a limited number of taxa, where *Cutibacterium* was the most abundant. The interior of the bus is a distinctive microenvironment where the concentration of pollutants from both outdoor environment and the ones generated internally can occur, that's why, variety of ubiquitously detected genus level taxa was regarded as the environment inside the bus can be a mixture of both, indoor and outdoor air. Six of 44 (14 %) were found to overlap between all the different fuel type buses, where two of them were detected in the six scenarios above mentioned, *Cutibacterium* and *Bradyrhizobium*. However, looking to the ones that are overlapped at least in two different fuel type buses, the percentage gets to 48 % (21 of 44). The ones encountered in all the different fuel type buses with a high relative abundance were from different sources as: human skin or body (*Cutibacterium, Corynebacterium, Prevotella*), environmental (*Paracoccus, Sphingomonas*) nitrogen atmospheric fixator

(*Bradyrhizobium*), organic matter recycling (*Burkholderia*) (Collins et al. 2004; Larsen, 2017).

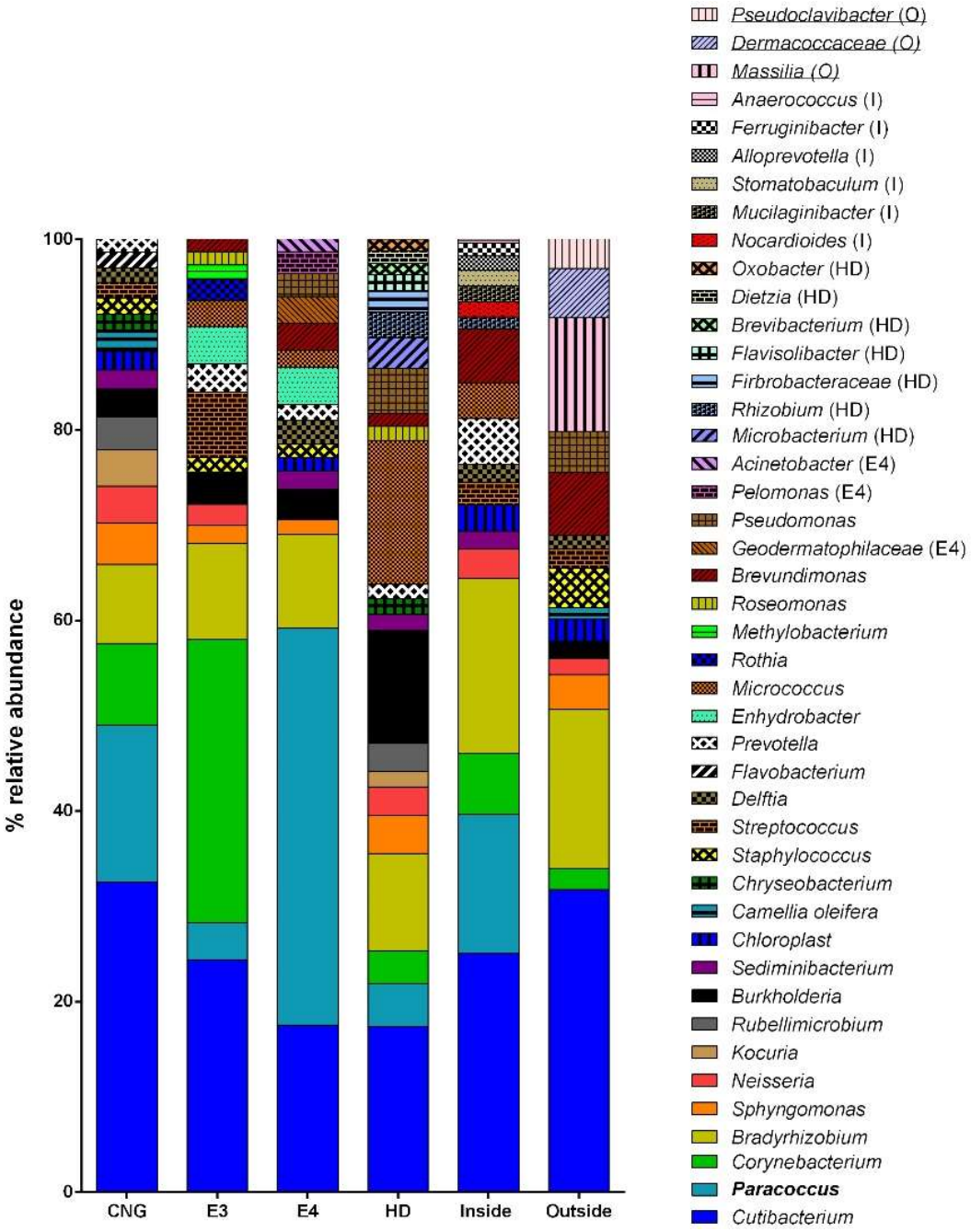

Figure 3.35. Relative abundance of Genera taxonomic category for each kind of fuel type and tourist buses. The taxa that were specific to each bus or to the outside controls are specified in parentheses. Taxa in bold was specific to inside buses.

Related to human microbiota, *Staphylococcus* and *Neisseria* were detected in 3 of the different fuel type buses and outside the tourist bus. The relative abundance of *Staphylococcus* was higher outside and *Neisseria* was higher inside CNG buses (Mann–Whitney U *p-value* ≤ 0.05). The main source of contamination of bacteria inside the buses is human, as 19 of 44 (43 %) genera taxa are related to human beings (presence in the human body, in the skin microbiota, dental plaque, blood among other human scenarios.). Note that the mentioned taxa herein are ubiquitous and can be found in other terrestrial and atmospheric environments.

It is interesting to see that *Paracoccus* and *Prevotella* were detected inside all the buses, and *Sediminibacterium* and *Micrococcus* only in some of them. *Paracoccus* is the one with the highest relative abundance, representing 40 % of genera detected inside EURO IV buses (Mann–Whitney U *p-value* ≤ 0.05). Some other taxa that were detected with high richness or abundance were *Streptococcus, Brevundimonas, Massilia* (O), *Enhydrobacte, Dermacoccaceae* (O) and *Pseudomonas* (Mann–Whitney U *p-value* ≤ 0.05). Most of them are related to human skin and some of them are opportunistic pathogens for humans.

Figure 3.36 shows the top five taxa that were differentially more abundant in each one of the four buses type compared to the others. The highest mean number of sequences of differentially abundant bacteria was found in the inside buses. *Stomatobaculum* had a mean count of sequences of 320 inside tourist buses, which doubles the highest of any of the other scenario. This bacterium is isolated from the human dental plaque (Sizova et al. 2013). *Nocardia* had a mean count of sequences of 270; these taxa are encountered in soils around the world rich in organic matter. Some species can be pathogenic causing pneumonia and nocardiosis, among other diseases (Ryan & Ray, 2004). *Ferruginibacter* also had a high mean count of sequences of 200. It is a genus of bacteria from the family of *Chitinophagaceae* which is isolated from freshwater sediment (Lim et al. 2009). In summary, the biodiversity inside buses is greatly affected by the presence of humans inside, but also by the outdoor sources at the moment of the sampling more than the fuel type.

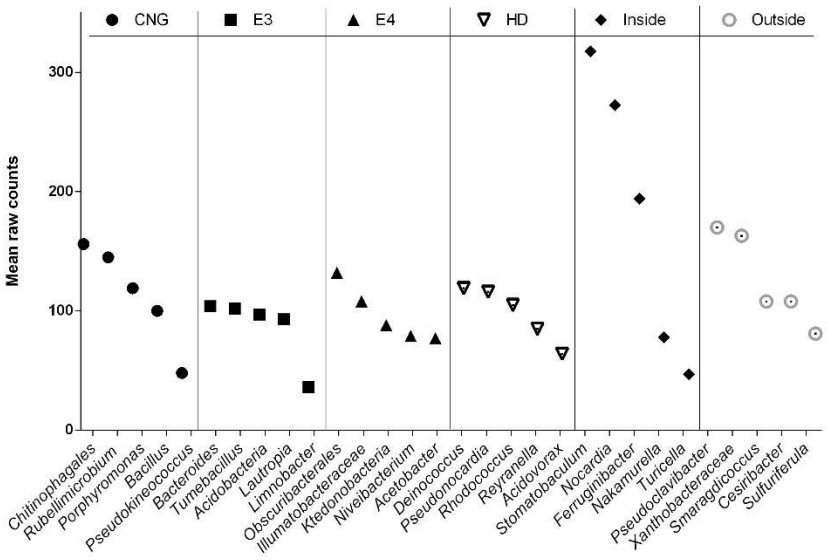

Figure 3.36. Differential abundance analysis of five taxa detected in a specific type of bus but not in the others. The mean raw counts represent the mean number of sequences identified to a particular taxa in the different groups of samples.

3.3.2.2 Seasonal differences

It is important to consider that in this work seasonal campaigns were defined according to TMB ventilation protocols, thus summer: May–September having air conditioning functioning (windows closed) compared to winter: November–March without it. The main determinants for bacterial growth are the environment, meteorological conditions, including variability between cities and seasons (Gandolfi et al. 2015). Looking at the 2 different seasons in the bus study, summer: May–September samples were the richest, and most branched. For Shannon diversity index, although the median values were close for the two seasons, summer: May–September samples were statistically richer than winter: November–March (Fig. 3.37). This agrees with previous studies showing spring and winter: November–March climatic conditions to be unfavourable for bacterial growth in air samples (Chakrawarti et al. 2020; Tignat-Perrier et al. 2020).

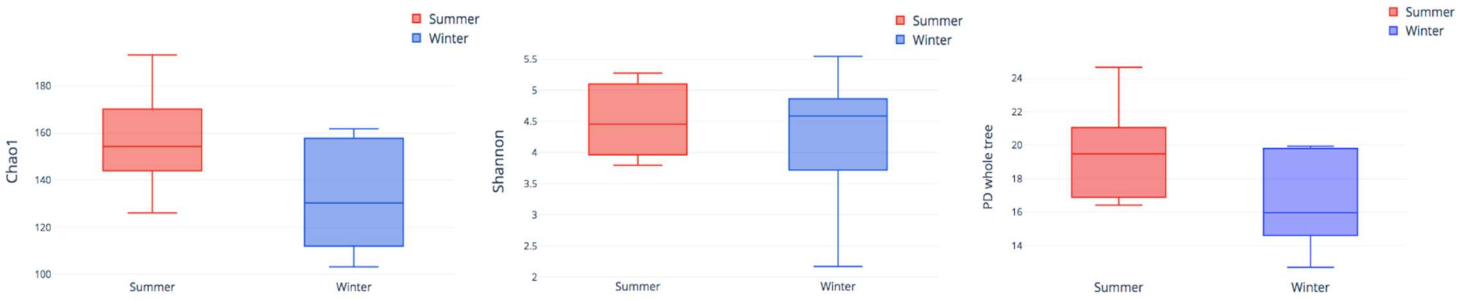

Figure 3.37. Boxplots of bacterial richness (Chao 1), bacterial diversity (Shannon and PD whole tree) for different analysed seasons (summer and winter).

The observed seasonality could be a combination between changes in meteorological conditions and changes in the contributions of individual source environments (Bowers et al. 2013; Uetake et al. 2019). Nuñez et al., (2019) suggested that the variability of airborne diversity in urban areas is mostly influenced by environmental changes, in agreement with other studies (Bertolini et al., 2013; Franzetti et al., 2011; Innocente et al., 2017) and in a less extent due to the characteristics of the local microenvironment, indicating that air temperature also has a strong influence on the composition of bacteria. Bowers et al. (2013) and Genitsaris et al. (2017) agreed in that the only meteorological variable found to be correlated with airborne bacteria composition was the temperature, but that it does not have direct control in it. Temperature was measured inside buses in the present study (not showed due to be very similar between both seasons), but it was not measured outside, where temperatures are more different between summer and winter in Barcelona. Apart from the temperature, seasonal variability is also affected by different environmental source contributions. And human pathogens that could cause respiratory diseases could be transported by the air (Abd Aziz et al., 2018; Fan et al., 2019). The bus routes in where measurements have been done are distributed all over Barcelona, going through sea environments to mountain and urban areas, which may have affected the airborne bacteria composition.

Proteobacteria and *Actinobacteria* were the most abundant Phylum as observed in the different fuel type buses achieving more than the 80 % of relative abundance in the two seasons (Fig. 3.38). *Proteobacteria* were more abundant in winter: November–March and *Firmicutes* more abundant in summer: May–September (Mann–Whitney U *p-value* ≤ 0.05). Some Phylum were exclusively detected in summer: May– September and others only in the winter: November–March, like *Fibrobacteres* that was the only one identified only in winter: November–March. *Fibrobacteres* are a small bacterial Phylum that includes many of the

ruminant animal stomach bacteria that allow degradation of plant-based cellulose (Ransom-Jones et al. 2012). The ones detected only in summer: May–September were *Verrucomicrobia, Fusobacteria, Nitrospirae, Patescibacteria, Planctomycetes* and *Spirochaetes*, most of them related with aquatic ecosystem, but also with human oral microbiome, or widespread in the environment (Chiang et al. 2018; Dewhirst et al. 2010; Gupta et al. 2013; Pollet et al. 2014; Tian et al. 2020; Zecchin et al. 2017).

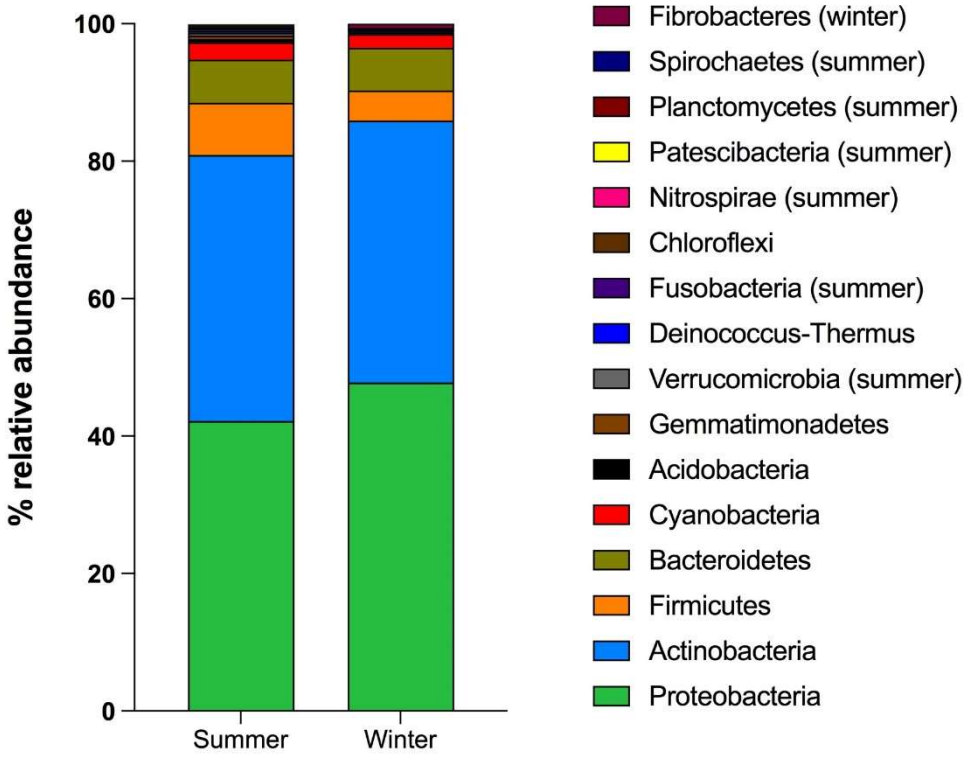

Figure 3.38. Relative abundance of Phylum taxonomic category for each season.

Moving on to the genus level (Fig. 3.39), some substantial differences were noted between the two seasons. *Corynebacterium, Bradyrhizobium, Paracoccus* and *Streptococcus* were identified in both seasons, summer: May–September and winter: November–March, but summers' relative abundance was higher (Mann–Whitney U *p-value* ≤ 0.05). Bonetta et al. (2010) identified that bacterial counts increased in summer: May–September. This study could be helpful to see if the season affects the existing taxonomic genera. Some genera were exclusively detected in summer: May–September and others only in winter: November–March. Airborne bacterial communities in Barcelona bus systems were largely dominated by a limited number of taxa, where *Corynebacterium*, *Bradyrhizobium* and *Paracoccus* were the most abundant genera in summer: May– September (Mann–Whitney U *p-value* ≤ 0.05), whereas *Paracoccus* and *Cutibacterium* were only detected in winter: November–March

with a 20% of relative abundance (Mann–Whitney U *p-value* ≤ 0.05). *Cutibacterium* is a taxonomic genera related to skin microbiota (Corvec, 2018) and *Paracoccus* is an environmental genus. Half of the genera, 13 of 26, were detected in the two seasons, being almost the 80 % of the genera in summer: May–September and almost 70% in winter: November–March. It can be observed that the relative abundance of the different taxonomic genera decreases from summer: May– September to winter: November–March.

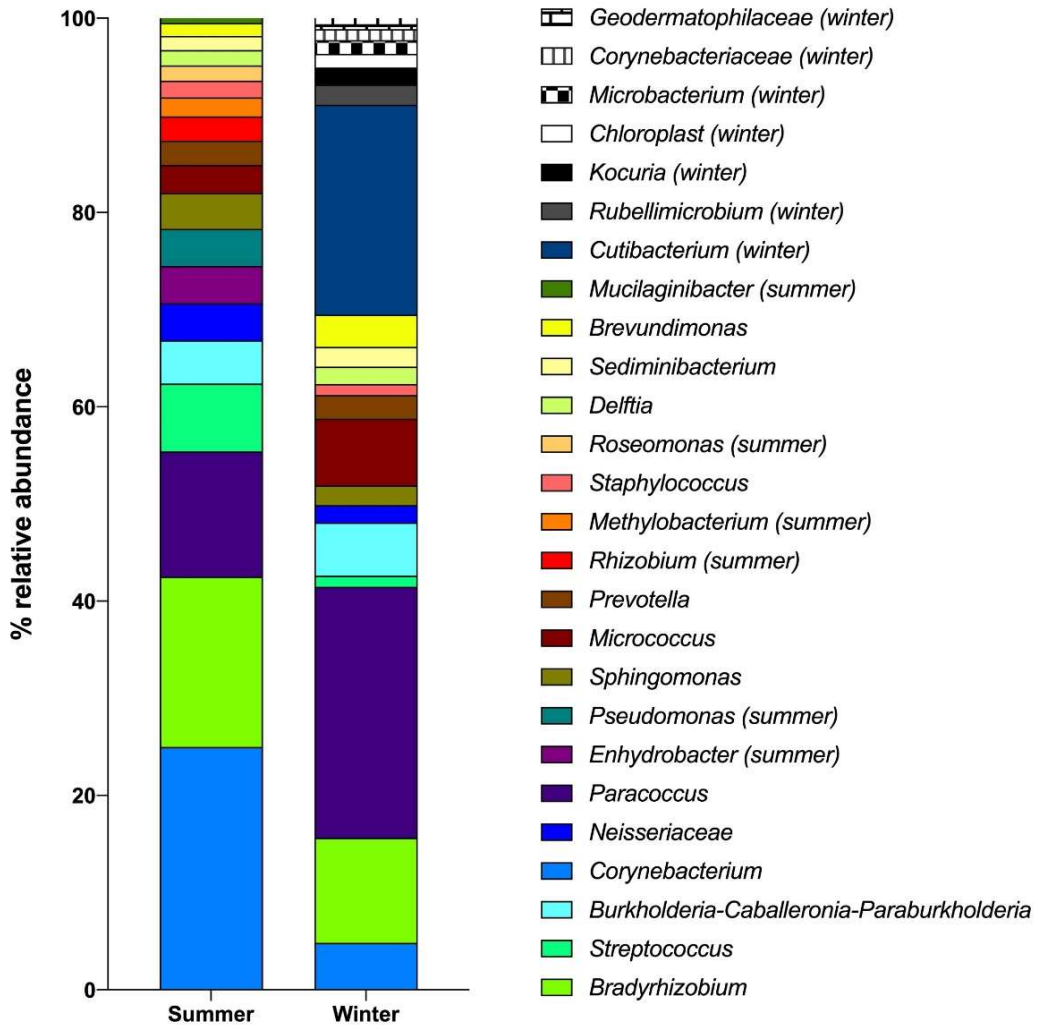

Figure 3.39. Relative abundance of Genera taxonomic category for each season. The taxa that were specific to each season, controls are specified in parentheses.

Enhydrobacter, Pseudomonas, Rhizobium, Methylobacterium, Roseomonas and *Mucilaginibacter* were only detected in summer: May–September. These genera were related to human skin microbiota, plants, environmental bacteria, and some of them can be opportunistic pathogen for human (Indra Dé et al. 2004; Leung et al. 2015; González et al. 2019; Lai et al. 2020). *Cutibacterium, Rubellimicrobium, Kocuria, Chloroplast,*

Microbacterium, Corynebacteriaceae and *Geodermatophilaceae* were the ones identified only in winter: November–March, which are ubiquitous, related to wide range of environments (soil, human commensals, plants) (Collins et al. 1983; Dastager et al. 2008; Kandi et al. 2016; Sun et al. 2015).

3.3.3. Penicillium/Aspergillus and Cladosporium quantification

Quantification of *Penicillium/Aspergillus sp.* and *Cladosporium sp.* concentrations was performed in bioaerosols to assess fungi contamination in buses. Concentrations were below detection limit for both targets in all samples. Detection limit was between 9 and 16 for *A. fumigatus* genome equiv/m^3 (median = 19 *A. fumigatus* genome equiv/m^3 for *Aspergillus/Penicillium sp.* and between 4 and 66 *Cladosporium sp.* genome equiv/m^3 (median = 8 *Cladosporium* genome equiv/m^3) for *Cladosporium sp.* depending on sample.

Penicillium and *Aspergillus sp.* are very close genetically, and are markers of water damages (flood), condensation and humidity. *Cladosporium sp.* is a good marker for outdoor contamination and is a common indoor fungus. This suggests that the air quality inside the buses in terms of the studied fungi is good.

In contrast to what was identified in the present study, Nowakowicz-Dębek et al. (2017) and Prakash et al. (2014) identified *Aspergillus sp.* as the most frequently represented fungi genera inside buses. Similar results were shown by Priyamvada et al. (2018) and Sowiak et al. (2018).

Lee and Jo (2005) have also indicated that the growth medium used in the measurement, the vehicle type and the season are related to microorganism concentration. Indeed, it could be due to the cleanliness of the bus, AC maintenance, the method of sampling, and sample treatment. All these factors can affect the concentration of the microorganism measured. However, the cited studies used culture methods, which make the comparison of concentrations with our work not valid.

It would be necessary to make a study more focused on the detection of fungi using different methods, including culture, and sequencing methods. The moment in which the AC is turned on, and the exact moment in which the windows are open could be considered as variables for future studies.

3.3.4. Endotoxins

Taking total bacteria results into account, three samples were analysed to perform an inhibition/enhancement test, including those with the highest and lowest total bacteria concentration, and one with an intermediate value. All three samples concentrations were below detection limit, with a value of 0.004 EU/m^3 and 4.445 EU/m^3. Therefore, no other samples were analysed. In addition, inhibition was detected in the suggesting an underestimation of endotoxin content (Hollander et al. 1993). However, given the relatively low sample volume (240 L of air) and the relatively low bacterial concentration and the importance of Gram-positive taxa, this result is not surprising.

CHAPTER 4: CONCLUSIONS

5. CONCLUSIONS

- Bus interior air quality is strongly influenced by road traffic emissions. Highly transient peaks in ultrafine particle number concentrations of 100,000-1,000,000 #/cm^3, BC levels of >20 μg/m^3, and $PM_{2.5}$ concentrations of > 50 μg/m^3 can occur frequently inside public buses due to the infiltration of traffic emissions.

- Outside road emission infiltration into buses is commonly most severe at highly polluted localized points within a given route, such as the proximity to urban motorways, busy intersection crossings and roundabouts, tunnels, and uphill stretches of relatively narrow, canyon-like roads. Closer attention to the atmospheric microenvironment of individual bus routes and the location of bus stops could considerably reduce passenger exposure whilst waiting and travelling.

- Quasi-ultrafine particle size is a useful indicator for the relative amount of fresh traffic-related particle emissions present inside a road vehicle, with an inverse correlation typically existing between particle size and number.

- Mean concentrations of BC particles inside buses are 2 to 3 times higher overall than those typically measured in Barcelona urban background air, lying within the range 4 - 8 μg/m^3. There is commonly a strong coincidence between BC and $PM_{2.5}$ concentrations inside a bus.

- Air quality inside buses can also be noticeably influenced by localised wind patterns and by background levels of pollution in the air outside the vehicle. Thus a "bad air quality day" across a city can increase individual exposure to pollutant particles and gases whilst travelling in public transport. In contrast, on a "good air quality day" $PM_{2.5}$ breathed while travelling by tourist bus for example can be less than 50% below normal on clear, clean winter days with low levels of urban background pollution.

- This study did not reveal any dominant link between interior bus air quality and the type of powertrain operated by the bus, although diesel buses were associated with higher levels in several cases. Further work is needed on this question, although the data so far indicate that the quality of the outdoor air and the extent to which such air could infiltrate and circulate around the bus appear to be the main factors influencing air quality on any given journey.

- Vertical routes are those in which passengers may be more exposed to higher concentrations of different pollutants. In Barcelona, vertical routes run on slopes, and that is

why the concentrations measured on this type of routes are higher, due to wear and tear on the bus itself (e.g. wheels, brakes). The horizontal routes, on the other hand, were the ones that registered the lowest concentrations, with the concentration of QUFPN being 25 - 30 % lower.

- Contrary to expectations, the highest concentrations of QUFPN were recorded in summer, and BC and $PM_{2.5}$ in winter. Based on some previous studies, summer was pretended to be cleaner as the AC is on, but it was not observed in this study.

- The chemistry of $PM_{2.5}$ measured inside Barcelona public buses is dominated by the presence of OC (typically 10–15 μg/m^3) and EC (usually 3–6 μg/m^3), followed by SO_4^{2-}, Fe, Ca, K, Al_2O_3, Mg and Na. Average OC values are around x 3 those of EC average (OC/EC = 3.4), and calculated mineral content is approximately one third that of total carbon content. Most bus pairs used in the study, following the same route but using differing bus models, show little difference in major element $PM_{2.5}$ chemistry, typically varying in EC, OC and mineral content by < 2.5 μg/m^3, < 3 μg/m^3, and < 2 μg/m^3 respectively. However, major element concentrations of $PM_{2.5}$ in bus interiors are typically 2–8 times higher than urban background levels, reflecting the compromised air quality of the traffic-contaminated city streets.

- Enhanced concentrations of certain trace metals and metalloids, notably Cu and Sb, inside the buses are attributed to the presence of brake particles entering the bus through doors and windows. In extreme cases, Sb concentrations can exceed x 20 that of urban background.

- Interior bus PM chemistry is not especially affected by the type of fuel used by the bus (with the exception of the electric and diesel bus) and can be affected by seasonal changes in ambient outdoor air. In the case of Barcelona in summer bus $PM_{2.5}$ can contain relatively higher levels of Na, Mg, V, Ni, Cr and SO_4^{2-}, attributed to the ingress of outdoor marine aerosols contaminated by port emissions and the higher SO_2 summer oxidation ratio. In winter, when air conditioning is off and city air is commonly more contaminated, the air inside the bus can be richer in mineral particles, with enhanced levels of trace metals/metalloid such as Mn, Sr, Zn, Zr, Sb and Cu.

- Interior bus air chemistry can be influenced by both route taken and bus model. Higher gradients favour the ingress of more brake particles and thus affect the chemistry of the PM being inhaled by passengers. In contrast, buses designed to use more engine-braking (such as the Barcelona electric buses) are less contaminated by their own brake PM, especially if the windows are kept closed. Open topped double decker tourist

buses are more directly exposed to fresh traffic emissions (especially on the upper floor), but enhanced air exchange rates maintain elemental PM concentrations slightly below that more typical of enclosed commuter buses.

- Based on the chemical tracers, the two main sources of particles inside the bus are deduced to be from passenger emissions such as textile fibres and skin flakes (46 %) and infiltrated vehicle exhaust and brake wear particles (19 %). Other sources include road and urban dust, regional sulphate and shipping and industrial metalliferous particles.

- The chemical signature of VOCs present in most Barcelona buses is remarkably uniform, irrespective of bus engine type, being dominated by alkanes and aromatics in the following order: 2-methylpentane (14–36 μg/m^3), toluene (10–30 μg/m^3), xylenes (10–28 μg/m^3, with m- » o- > p-xylene) and n-pentane (5–15 μg/m^3). This is the same mixture recorded inside Barcelona taxis (although inside buses VOC concentrations are usually lower than in taxis) and presumably records the ingress into the vehicle of mostly gasoline-sourced exhaust emissions from outside. Ambient benzene concentrations measured inside the buses were always < 5 μg/m^3. A notable exception to this rule occurs in new buses which can exhibit a very different, and greatly enhanced, VOC signature due to off gassing of interior coatings and materials. In this study one such bus (HD 34) recorded exceptionally high concentrations in particular of o-Xylene (160 μg/m^3), Ethylbenzene (95 μg/m^3), 2-Methybutane (92 μg/m^3), p-Xylene (91 μg/m^3), and Cyclohexane (86 μg/m^3).

- BTEX concentrations in Barcelona buses typically range from 25 to 68 μg/m^3 in a hierarchy of Toluene (10–30 μg/m^3) > m-Xylene (5–17 μg/m^3) > p-Xylene (2–5 μg/m^3) > o-Xylene (3–6 μg/m^3) > Benzene (2–4 μg/m^3) and Ethylbenzene (2–7 μg/m^3). The exceptional levels of VOC offgassing recorded in the new hybrid diesel bus produced interior BTEX concentrations closely approaching 0.5 mg/m^3, although benzene levels still remained below the European Union limit value of 5 μg/m^3.

- Total airborne bacteria inside buses was detected in low concentrations. Actinobacteria and Proteobacteria were the most abundant phyla inside all the fuel type buses and also in both floors of tourist buses, achieving almost 80% of relative abundance in all the buses. In relation to genus level, *Cutibacterium* was the most abundant one followed by *Paracoccus*, which was only detected inside buses. The main source of contamination of bacteria inside the buses is the presence of humans inside, as 19 of 44 (43 %) genera taxa are related to human being, but also by the outdoor sources at the moment of the sampling. The different type of fuel did not seem to affect airborne microbes.

However, the seasons affect inside buses, both, qualitatively and quantitatively. It can be observed that the relative abundance of the different taxonomic genera decreases from summer: May – September to winter: November –March. Fungi and endotoxins couldn't be detected in any sample.

- Bus routes in Barcelona are long enough to cross different areas in the city attributed to different airborne bacterial sources. When comparing summer: May – September and winter: November – March samples, where all types of routes were taken into account, the seasonal comparison was a mix of different sources. This could explain why most abundant airborne bacteria are the same in both seasons.

- Even if humans are the main source of bacteria inside buses, the air exchange in this microenvironment should be always optimized in order to reduce commuters' exposure to potentially harmful microbes.

CHAPTER 5:
FUTURE RESEARCH

5. FUTURE RESEARCH

This PhD Thesis has aimed to promote a better understanding in the characterisation of PM inside public buses in terms of concentration, chemical composition, source apportionment and microorganism biodiversity, considering variables such as different fuel/engine, annual season and type of routes.

Although robust results have been obtained from the work done, further research is still required to fully understand some topics not covered or not completely explored by this study. A brief list of some of the major outstanding questions and suggested future work is described hereinafter:

- To measure and interpret temporal and spatial variations in the concentration of gas pollutants inside all the fuel/engine type buses. They are difficult to measure as sensors are still not developed enough to obtain good reliable data.

- The present work studied air quality improvement measures based on ventilation settings, using pre-existent infrastructures. The installation of air purification systems within the buses may also be adopted, but further study is required to evaluate the efficiency and viability of these devices.

- In this study it was identified that the external air quality was directly affecting the air quality inside buses. Deeper studies on this matter will represent an opportunity to characterise and better understand how exactly affects the exterior pollutants concentration inside the bus environment. Further studies are required to assess the magnitude and variability of this influence among locations. Also, to better understand the influence of the outdoor weather conditions within the bus environment.

- Regarding seasonal (warmer vs. colder) variation of aerosols inside buses, in the Barcelona bus system, a more specific study would be required regarding the type of ventilation. In which the influence for example of the filters changing frequency, on the aerosols concentrations inside buses could be considered.

- It would also be interesting to measure inside buses without people, considering different variables. For example, windows and doors closed along the whole route, in order to characterise the base concentrations that could have each of the buses.

- The development of a ventilation protocol (forced or natural) considering CO_2 concentration would also be of interest.

- The accumulative amount of time that commuters spend exposed to high concentrations of pollutants throughout their lifetime, and the possible adverse health effects associated with such exposure, may be significant and is certainly worthy of further investigation.

- It would be necessary to make a study more focused on the detection of fungi using different methods, including culture, and sequencing methods. The moment in which the AC is turned on, and the exact moment in which the windows are open could be considered as variables for future studies.

- Bioaerosol samples were also characterized by environmental scanning electron microscope (ESEM, Quanta™ 450 FEG) and with a field emission scanning electron microscope (FESEM, Zeiss Sigma VP) but no bioaerosol could be identified. The characterization of bioaerosols could also be interesting for future studies.

APPENDIX

Inside 3. RESULTS AND DISCUSSION

3.2. Chemical results

Table S1. Summary of chemical analyses of $PM_{2.5}$ for all pairs analysed in each campaign, summer and winter.

	not for summer average												SUMMER											not for summer average	
ENGINE	EIV	EV	EV	HD	Elect.	HD	CNG	EV	CNG	Elect.	HCNG	CNG	EIV	EIV	EIV	EIV	EIV	HD	HD	CNG	Elect.	EV	CNG	EIV
ROUTE	(V13)	(V13)	(V13)	(V13)	(34)	(34)	(V3)	(V3)	(H16)	(H16)	(39)	(39)	(TB out)	(TB in)	(TR out)	(TR in)	(47)	(47)	(H12)	(H12)	(34)	(34)	(V11)	(V11)
DATE		10/05/17		16/05/17		23/05/17		30/05/17		08/06/17		13/06/17		20/06/17		26/06/17		10/07/17		18/07/17		14/09/17		20/09/17
µg/m³																								
$PM_{2.5}$	177.13	230.60	129.58	117.58	118.32	111.81	119.64	130.22	75.52	70.18	104.96	99.05	127.25	176.07	90.44	99.51	146.14	114.79	80.85	95.91	131.40	143.51	138.92	158.76
OC	41.1	22.3	15.1	13.8	13.1	12.9	12.9	15.5	9.7	8.9	15.1	16.1	13.9	16.5	10.1	10.9	31.5	17.0	15.2	8.2	15.8	14.6	13.9	17.0
EC	8.9	9.5	6.8	5.8	4.7	3.1	5.7	4.5	2.7	2.4	5.3	3.8	6.1	3.6	5.5	3.8	3.5	8.9	3.8	3.1	7.2	4.9	3.8	6.3
CO_3^{2-}	5.6	0.2	0.3	2.6	1.4	0.2	1.3	1.8	1.1	0.8	0.7	0.8	0.6	1.3	<0.1	0.4	1.0	1.9	0.4	0.6	3.9	4.0	4.2	4.1
SiO_2	0.3	<0.1	<0.1	0.1	0.9	<0.1	1.4	0.6	0.5	0.4	0.3	0.8	0.6	0.8	0.8	0.9	1.4	1.2	0.3	<0.1	<0.1	0.3	0.2	0.2
Al_2O_3	0.1	<0.1	<0.1	<0.1	0.3	<0.1	0.5	0.2	0.2	0.1	0.1	0.3	0.2	0.3	0.3	0.3	0.5	0.4	0.1	<0.1	<0.1	0.1	0.1	0.1
Ca	3.7	0.1	0.2	1.7	0.9	0.1	0.9	1.2	0.7	0.5	0.5	0.6	0.4	0.9	<0.1	0.3	0.6	1.3	0.3	0.4	2.6	2.7	2.8	2.8
Fe	1.2	1.0	0.5	0.8	0.6	0.2	1.9	0.9	0.4	0.2	0.6	0.5	0.6	0.6	0.5	0.5	0.4	0.5	0.6	0.3	5.5	5.5	5.3	5.4
K	0.1	<0.1	<0.1	0.2	0.1	0.1	0.2	0.4	0.1	0.2	<0.1	0.1	0.2	0.2	0.2	0.2	<0.1	<0.1	<0.1	0.3	3.7	4.3	5.2	5.9
Na	0.3	<0.1	<0.1	<0.1	<0.1	<0.1	<0.1	0.1	<0.1	<0.1	<0.1	<0.1	<0.1	<0.1	<0.1	<0.1	<0.1	1.0	<0.1	<0.1	0.2	<0.1	<0.1	<0.1
Mg	0.7	<0.1	<0.1	0.1	0.1	<0.1	0.1	0.3	0.2	0.1	0.1	0.1	0.1	0.3	0.1	0.1	0.1	0.3	0.1	0.1	2.3	4.9	2.5	2.2
P	0.2	0.1	0.1	0.1	0.1	<0.1	0.1	0.1	0.1	0.1	0.2	<0.1	<0.1	0.1	<0.1	0.1	<0.1	0.3	0.1	0.1	4.6	19.2	2.8	3.7
SO_4^{2-}	5.2	1.5	1.8	1.5	2.2	1.6	2.5	3.3	2.4	2.1	3.1	1.7	2.7	3.5	2.6	2.5	2.5	3.4	3.3	2.5	2.9	3.7	<0.1	<0.1
Mineral	5.1	0.2	0.3	2.2	2.4	<0.1	3.0	2.8	1.7	1.4	1.2	1.8	1.5	2.5	1.4	1.9	2.6	3.5	0.8	1.0	13.3	31.4	13.5	14.9
OC+EC	50.0	31.8	22.0	19.6	17.8	16.0	18.5	20.0	12.5	11.2	20.4	19.9	20.0	20.1	15.6	14.7	35.0	25.9	19.0	11.2	23.0	19.5	17.7	23.3
ng/m³																								
Ti	50.97	17.30	4.31	6.25	13.90	12.50	22.16	16.94	5.37	4.92	176.64	11.86	5.51	9.56	12.04	8.13	35.21	20.17	5.38	2.86	6.58	12.04	6.35	5.64
V	4.72	<0.10	15.65	7.95	6.55	0.94	2.66	0.25	8.99	5.94	31.20	21.91	10.92	1.89	2.65	9.58	9.90	2.54	10.34	3.41	21.13	3.59	6.03	23.88
Cr	10.25	24.67	2.83	5.27	6.35	<0.10	9.00	3.86	6.37	0.96	0.54	15.00	8.93	8.41	15.86	11.63	25.81	18.81	7.48	2.52	8.71	<0.10	6.34	12.40
Mn	16.23	13.91	5.26	3.76	7.91	5.17	18.95	11.28	5.82	2.30	11.41	7.78	8.42	9.50	7.17	6.29	3.59	6.20	5.35	3.26	7.45	4.99	6.70	9.44
Ni	10.12	32.05	3.38	13.14	13.87	0.15	12.43	25.36	6.44	7.82	2.25	19.64	13.00	18.92	17.36	13.94	10.12	4.17	3.12	1.53	6.14	<0.10	1.47	<0.10
Cu	111.64	46.34	39.12	138.18	32.06	208.34	178.28	119.84	15.00	5.84	129.23	159.80	46.22	25.99	37.62	20.67	50.83	97.72	118.67	25.75	25.21	6.89	13.63	89.89
Zn	228.26	58.04	42.42	138.89	51.97	35.52	100.25	69.55	37.04	49.48	33.93	57.39	91.58	60.67	28.43	29.48	14.96	25.87	19.76	21.77	16.98	44.69	154.16	159.22
As	0.91	<0.10	4.27	1.21	0.27	<0.10	<0.10	<0.10	2.02	0.66	6.17	4.75	2.89	<0.10	<0.10	2.26	2.06	<0.10	2.37	<0.10	7.40	<0.10	2.35	6.29
Sr	12.51	1.77	<0.10	1.41	1.02	0.33	1.80	6.49	4.14	0.83	1.77	1.17	2.32	4.47	0.51	1.66	2.16	9.96	2.04	1.86	0.58	5.06	1.87	3.83
Zr	63.67	53.01	<0.10	33.66	35.57	<0.10	41.84	33.93	7.57	<0.10	21.58	26.29	31.98	18.45	29.62	5.25	34.40	<0.10	4.94	<0.10	39.85	48.97	64.86	53.23
Nb	<0.10	3.17	<0.10	<0.10	1.49	<0.10	<0.10	<0.10	<0.10	0.93	<0.10	<0.10	1.58	<0.10	<0.10	<0.10	1.60	<0.10	<0.10	<0.10	2.14	<0.10	<0.10	<0.10
Cd	<0.10	<0.10	1.75	<0.10	<0.10	<0.10	1.43	<0.10	0.93	<0.10	<0.10	1.40	<0.10	2.61	1.23	<0.10	<0.10	<0.10	<0.10	<0.10	<0.10	0.74	0.68	<0.10
Sn	6.93	4.96	2.19	2.37	6.43	3.76	7.80	15.18	1.55	1.48	3.67	3.10	4.09	4.08	3.66	2.79	4.05	3.64	2.13	2.47	4.97	3.65	3.36	5.25
Sb	9.91	12.97	5.40	2.14	6.19	1.83	23.66	14.94	3.13	1.03	10.56	6.35	3.96	3.52	3.17	2.75	2.43	4.72	2.92	3.24	6.26	5.11	6.50	8.59
Ba	62.16	39.92	8.77	9.99	29.21	7.62	51.12	33.26	60.17	10.38	13.30	21.40	52.92	25.99	19.10	12.54	9.91	41.05	60.59	12.73	10.48	10.63	15.46	11.83
La	0.46	0.20	0.16	0.19	0.27	0.10	0.34	0.12	0.14	0.16	0.91	0.23	0.42	0.23	0.13	0.25	0.15	0.17	<0.10	<0.10	<0.10	<0.10	0.24	0.17
Ce	0.91	0.61	0.28	0.35	0.52	<0.10	0.56	0.17	0.35	0.24	0.79	0.62	0.83	0.60	0.57	0.52	0.35	0.44	0.13	<0.10	<0.10	<0.10	0.38	0.98
Nd	0.19	0.50	0.29	0.49	0.49	0.14	0.22	0.37	0.23	0.18	0.10	0.14	0.53	0.56	0.42	0.42	0.47	0.36	<0.10	<0.10	<0.10	<0.10	0.14	<0.10
Gd	0.34	0.21	0.11	0.20	0.14	<0.10	0.12	0.05	0.05	<0.10	<0.10	<0.10	<0.10	0.34	0.12	<0.10	0.21	0.24	<0.10	<0.10	<0.10	<0.10	0.25	<0.10
Dy	0.41	0.29	0.23	0.22	0.38	<0.10	0.38	0.26	0.17	0.18	<0.10	0.25	0.43	0.45	0.42	0.41	0.18	0.22	0.15	0.16	<0.10	<0.10	<0.10	0.25
Hf	3.20	3.07	<0.10	1.73	1.50	<0.10	1.65	1.61	0.34	<0.10	0.84	1.18	1.61	0.57	1.39	0.24	1.67	<0.10	0.25	<0.10	2.22	2.39	3.33	3.02
Pb	4.96	6.23	3.22	3.28	4.04	2.40	3.72	2.85	1.91	1.66	3.20	2.76	2.63	4.26	2.23	2.36	5.81	5.36	1.78	1.50	1.30	2.38	1.46	2.39
Bi	<0.10	<0.10	<0.10	<0.10	<0.10	<0.10	<0.10	<0.10	<0.10	<0.10	<0.10	<0.10	<0.10	<0.10	<0.10	<0.10	<0.10	<0.10	<0.10	<0.10	<0.10	<0.10	<0.10	<0.10
U	<0.10	0.76	0.41	0.63	0.65	0.13	0.47	0.55	0.25	0.34	<0.10	<0.10	0.46	0.63	0.54	0.59	0.43	0.38	<0.10	0.12	<0.10	<0.10	0.10	0.15

											WINTER										not for winter average			
	EV	HD	EIV	CNG	CNG	EV	HD	EIV	CNG	HCNG	EV	EIV	EIV	EIV	EIV	EIV	HD	CNG	Elect.	CNG	Elect.	HD	EIV	Elect.
	(H4)	(H4)	(V3)	(V3)	(V3)	(V3)	(19)	(19)	(39)	(39)	(V3)	(V3)	(TB out)	(TB in)	(TR out)	(TR in)	(H12)	(H12)	(H16)	(H16)	(34)	(34)	(60)	(60)
		14/11/17		23/11/17		01/12/17		14/12/17		10/01/18		16/01/18		23/01/18		30/01/18		26/02/18		19/02/18		27/03/18		10/04/18
µg/m³																								
$PM_{2.5}$	41.8	87.8	68.5	71.3	160.1	154.1	198.7	132.4	134.6	115.5	164.5	151.1	72.1	66.3	54.7	56.3	75.6	78.9	63.4	62.5	125.2	130.1	74.1	70.2
OC	15.9	12.7	8.3	12.7	29.4	17.8	26.4	21.8	27.3	30.8	8.9	22.1	11.4	8.7	7.5	8.5	21.7	18.9	13.1	17.2	10.7	15.9	17.3	16.0
EC	4.9	4.2	3.9	4.7	6.9	4.1	2.9	3.8	2.0	4.2	19.4	2.6	2.5	2.4	2.3	1.9	6.4	6.4	3.2	2.7	0.5	1.8	9.6	4.9
CO_3^{2-}	1.4	1.1	3.1	0.3	0.4	1.3	0.9	1.4	5.8	3.9	1.0	0.3	0.3	0.3	0.6	0.8	1.6	1.6	0.9	1.8	0.7	1.0	2.9	0.8
SiO_2	3.6	3.3	2.3	2.6	5.2	3.5	4.3	3.7	8.0	7.6	4.9	5.8	0.3	0.3	0.7	0.3	1.9	2.7	2.8	1.7	0.9	1.7	4.7	3.8
Al_2O_3	1.2	1.1	0.8	0.9	1.7	1.2	1.4	1.2	2.7	2.5	1.6	1.9	0.1	0.1	0.2	0.1	0.6	0.9	0.9	0.6	0.3	0.6	1.6	1.3
Ca	0.9	0.8	2.1	0.2	0.3	0.9	0.6	0.9	3.9	2.6	0.7	0.2	0.2	0.2	0.4	0.5	1.1	1.1	0.6	1.2	0.5	0.6	2.0	0.5
Fe	1.5	2.3	1.1	1.4	1.9	2.0	0.7	1.5	1.7	2.2	2.1	2.1	0.5	0.4	0.4	0.3	1.8	1.6	0.5	1.1	0.3	0.6	2.0	0.9
K	0.8	0.9	0.5	0.6	1.6	0.9	1.1	1.0	1.5	1.5	1.5	1.6	0.8	1.0	0.8	0.8	0.3	0.5	0.1	0.4	0.1	0.3	1.0	1.3
Na	0.1	<0.1	<0.1	<0.1	<0.1	0.1	0.2	0.1	0.3	<0.1	0.1	0.1	0.3	0.4	0.4	0.3	0.4	0.5	0.2	0.2	0.4	0.3	0.4	0.4
Mg	0.1	0.1	<0.1	<0.1	<0.1	0.1	0.1	0.1	0.3	0.3	0.1	0.1	0.1	0.1	0.1	0.1	0.1	0.1	0.1	0.1	<0.1	<0.1	0.2	0.2
P	<0.1	0.1	<0.1	<0.1	<0.1	0.1	<0.1	0.1	0.1	<0.1	<0.1	<0.1	<0.1	<0.1	<0.1	0.1	0.1	<0.1	<0.1	0.1	<0.1	0.1	<0.1	<0.1
SO_4^{2-}	0.6	0.7	0.6	0.7	1.0	0.5	0.6	0.6	0.8	1.0	0.8	0.1	1.1	1.0	1.1	0.9	2.1	2.1	1.0	1.1	0.1	0.9	1.7	1.3
Mineral	6.6	6.2	5.7	4.4	8.8	6.6	7.7	7.1	16.4	14.6	8.8	9.8	1.6	1.8	2.3	1.8	4.1	5.4	4.5	4.0	1.8	3.4	9.4	7.0
OC+EC	20.9	16.9	12.2	17.5	36.3	22.0	29.2	25.6	29.3	35.0	28.2	24.7	13.9	11.1	9.8	10.5	28.1	25.3	16.4	19.9	11.2	17.6	27.0	20.9
ng/m³																								
Ti	25.75	21.37	14.23	6.60	<0.10	1.76	20.20	<0.10	63.07	37.01	<0.10	17.18	7.91	7.64	10.98	7.60	14.15	27.74	13.21	19.83	<0.10	11.79	39.38	16.84
V	1.31	1.06	1.77	2.17	<0.10	<0.10	<0.10	<0.10	<0.10	<0.10	<0.10	<0.10	3.18	2.84	2.46	1.89	4.40	3.71	2.19	2.49	<0.10	10.06	3.79	1.85
Cr	3.77	16.00	1.49	<0.10	<0.10	<0.10	14.06	7.86	<0.10	9.96	<0.10	<0.10	10.84	20.47	15.07	12.50	9.72	3.65	6.15	4.87	2.01	27.80	0.69	<0.10
Mn	22.12	23.82	15.72	17.27	23.57	20.92	10.44	18.38	23.99	23.60	24.48	23.73	7.26	8.44	10.64	7.53	20.73	16.72	8.40	12.80	3.47	7.05	25.41	12.67
Ni	8.30	16.85	5.26	8.51	0.87	<0.10	17.81	1.88	1.28	1.56	0.86	5.95	6.29	16.47	15.17	6.45	<0.10	2.15	4.65	1.58	2.35	8.51	12.04	9.73
Cu	128.42	173.05	53.05	123.19	262.21	169.42	10.16	104.79	159.96	220.55	157.01	91.83	19.05	21.39	17.87	12.64	96.74	83.20	21.33	50.64	8.53	20.04	179.05	26.67
Zn	99.45	110.65	246.34	110.71	177.23	170.71	55.17	128.65	258.69	151.07	143.44	94.10	59.57	65.35	43.70	59.76	149.12	135.60	45.35	84.03	28.81	54.58	226.10	63.67
As	<0.10	<0.10	<0.10	<0.10	<0.10	<0.10	<0.10	<0.10	<0.10	<0.10	<0.10	<0.10	<0.10	<0.10	<0.10	<0.10	<0.10	<0.10	<0.10	<0.10	<0.10	<0.10	<0.10	<0.10
Sr	6.59	5.56	4.77	3.55	9.92	6.71	6.00	6.26	12.22	10.74	8.31	7.48	1.81	1.02	1.65	1.76	2.44	4.56	1.34	4.08	<0.10	<0.10	8.82	6.83
Zr	30.65	36.82	26.54	29.92	54.02	45.91	19.21	20.74	42.84	45.35	51.39	70.49	9.15	11.45	21.74	14.08	78.43	49.74	41.51	45.18	52.80	55.54	44.81	29.05
Nb	<0.10	1.47	<0.10	<0.10	<0.10	2.88	<0.10	<0.10	<0.10	<0.10	<0.10	2.22	<0.10	0.92	0.74	<0.10	1.85	<0.10	<0.10	1.79	<0.10	<0.10	1.66	1.95
Cd	<0.10	<0.10	<0.10	<0.10	<0.10	<0.10	<0.10	<0.10	<0.10	<0.10	<0.10	<0.10	<0.10	<0.10	<0.10	<0.10	<0.10	<0.10	<0.10	<0.10	<0.10	<0.10	<0.10	<0.10
Sn	8.78	9.85	4.01	5.92	7.69	6.33	3.09	2.66	3.43	4.19	7.78	4.96	4.03	4.38	2.48	2.09	8.19	6.72	3.02	3.69	1.56	2.77	9.72	6.48
Sb	20.08	25.24	10.69	22.74	33.01	33.43	5.08	17.51	27.91	36.93	27.38	20.41	1.97	1.74	2.03	1.40	14.99	11.39	3.30	7.88	2.15	5.42	25.46	5.31
Ba	45.18	61.62	29.93	45.36	63.07	54.42	26.51	47.70	122.61	73.53	66.93	58.45	14.22	19.77	19.57	18.32	83.96	170.92	16.29	147.56	<0.10	3.23	68.20	24.32
La	1.52	0.70	0.47	3.59	2.69	0.65	0.96	0.59	1.90	1.16	0.63	1.05	0.18	0.25	0.32	0.28	<0.10	<0.10	0.30	<0.10	<0.10	<0.10	1.71	0.83
Ce	5.26	2.44	1.79	6.81	8.22	2.74	2.98	2.50	6.41	3.99	3.08	4.02	0.58	0.69	0.68	1.71	<0.10	0.14	1.07	0.36	<0.10	<0.10	5.65	2.96
Nd	0.14	0.16	<0.10	<0.10	0.23	<0.10	<0.10	<0.10	0.24	0.19	<0.10	<0.10	<0.10	0.17	0.13	0.10	<0.10	<0.10	0.26	<0.10	<0.10	<0.10	<0.10	0.12
Gd	0.05	0.11	<0.10	<0.10	<0.10	<0.10	<0.10	<0.10	<0.10	<0.10	<0.10	0.11	<0.10	0.11	0.12	<0.10	<0.10	<0.10	0.10	<0.10	<0.10	<0.10	<0.10	<0.10
Dy	0.29	0.34	0.13	<0.10	<0.10	<0.10	0.32	0.23	0.38	0.35	<0.10	0.55	0.12	0.24	0.22	0.13	<0.10	<0.10	0.23	<0.10	<0.10	<0.10	0.44	0.31
Hf	2.19	2.15	1.83	1.96	4.31	3.27	1.86	1.86	3.55	3.73	3.90	4.83	0.49	0.58	1.15	0.80	4.53	2.67	2.24	2.62	3.19	3.20	3.20	2.33
Pb	4.78	2.83	1.40	1.53	<0.10	0.21	0.69	<0.10	<0.10	5.65	<0.10	<0.10	4.34	3.95	4.22	3.45	9.27	7.99	4.67	3.99	<0.10	2.07	3.08	0.73
Bi	1.26	<0.10	<0.10	<0.10	<0.10	<0.10	<0.10	<0.10	<0.10	<0.10	<0.10	<0.10	<0.10	<0.10	<0.10	<0.10	<0.10	<0.10	<0.10	<0.10	<0.10	<0.10	2.37	2.08
U	0.24	0.31	0.23	0.11	<0.10	<0.10	0.27	0.12	0.16	0.23	<0.10	0.48	0.42	0.48	0.47	0.31	<0.10	<0.10	0.35	<0.10	<0.10	<0.10	0.30	0.36

Table S2. Summary of VOCs measured in different Barcelona routes.

	Route H4		Route V3		Route 39		Route V3		Route Blue Tourist		Route Red Tourist		Route H16		Route H12		Route 34	
	14-16/11/17		1st, 12-13/12/17		10-12/01/18		16-18/01/18		23-25/01/18		30/01-1/02/18		21/01/18	31/01/18	26/02 & 1/03/18		27-28/03/18	
	Hybrid Diesel	Euro V Diesel	CNG	Euro V Diesel	Hybrid CNG	CNG	Euro IV Diesel	Euro V Diesel	Outside	Inside	Outside	Inside	Electric	CNG	CNG	Hybrid Diesel	Electric	Hybrid Diesel
Aromatics:																		
Benzene	2.8	2.6	2.5	1.9	3.2	3.2	2.3	2.3	3.7	3.9	2.8	2.8	3.1	3.8	3.9	2.6	2.4	4.5
Toluene	21	15	18	17	16	20	9.7	15	26	29	11	12	27	22	17	16	14	43
Ethylbenzene	3.1	2.6	2.3	2.2	2.9	3.2	2.1	2.2	4.9	6.6	4.1	3.7	4.0	3.9	3.4	2.7	2.7	95
o-Xylene	3.8	3.4	2.8	2.8	3.7	4.0	2.6	2.8	5.0	6.0	4.6	3.8	5.3	4.8	4.1	3.0	3.5	160
m-Xylene	8.7	6.8	6.0	6.1	7.3	8.4	5.5	6.0	14	17	11	9	11	10	9.5	7.3	7.5	43
p-Xylene	2.9	2.4	2.2	2.2	2.7	3.0	2.0	2.1	4.1	4.9	3.7	3.1	3.4	3.8	3.2	2.5	2.6	91
1,2,4-Trimethylbenzene	3.3	3.1	2.2	2.8	3.0	2.9	2.6	2.9	3.9	4.2	3.4	2.4	3.9	3.8	3.4	2.4	3.3	39
1,3,5-Trimethylbenzene	0.82	0.76	0.57	0.71	0.80	0.80	0.66	0.72	1.0	1.1	0.54	0.69	1.0	1.0	0.93	0.66	0.86	4.8
n-Propylbenzene	0.54	0.50	0.30	0.48	0.45	0.45	0.42	0.46	0.60	0.65	0.54	0.40	0.51	0.58	0.53	0.40	0.46	3.0
Isopropylbenzene	0.17	0.15	0.11	0.14	0.17	0.17	0.13	0.13	0.19	0.21	0.17	0.14	0.20	0.21	0.18	0.14	0.15	3.0
n-Butylbenzene	0.22	0.23	0.08	0.24	ND	<LOD	0.24	0.27	0.14	0.01	0.13	0.07	0.28	0.22	0.20	0.14	0.16	1.7
p-Cymene	0.50	0.43	0.26	0.23	0.53	0.50	0.23	0.23	0.17	0.18	0.15	0.11	0.44	0.54	0.34	0.17	0.31	1.4
sec-Butylbenzene	<LOD	0.10	<LOD	0.10	<LOD	<LOD	<LOD	0.09	0.06	0.07	0.05	<LOD	<LOD	<LOD	<LOD	<LOD	<LOD	1.3
Styrene	2.7	0.85	0.49	0.37	0.77	1.0	0.38	0.35	0.54	0.55	0.56	0.48	0.88	0.70	1.40	0.93	0.50	6.9
Branched alkanes:																		
2-Methylbutane	22	19	15	14	26	27	17	18	33	36	25	25	26	35	32	21	26	92
2,3-Dimethylpentane	0.81	0.71	0.51	0.49	0.85	0.79	0.50	0.63	1.1	1.2	0.79	0.78	0.90	1.0	1.3	0.62	0.69	9.9
Isooctane	0.51	0.41	0.45	0.14	<LOD	<LOD	1.1	2.6	0.61	0.65	0.50	0.48	0.58	0.98	0.43	ND	ND	0.57
Cycloalkanes:																		
Cyclohexane	1.1	0.99	0.69	0.82	1.7	1.7	0.62	0.64	1.4	1.4	1.3	1.3	1.7	1.7	7.6	0.80	1.0	86
n-Alkanes:																		
n-Pentane	8.1	7.3	5.7	5.2	9.0	9.3	5.6	6.1	12	13	8.6	8.8	9.9	13	15	7.1	9.3	29
n-Hexane	2.0	2.1	3.1	1.2	0.99	1.3	2.3	5.2	6.7	7.1	4.1	3.9	4.5	7.5	4.3	3.4	2.8	19
n-Octane	1.3	1.4	0.7	1.1	0.97	0.94	1.0	1.1	1.2	1.3	0.86	0.66	0.96	1.27	1.31	0.71	0.80	12
n-Heptane	2.3	2.1	1.4	1.7	2.4	2.3	1.5	1.8	2.8	3.0	2.0	1.95	2.26	2.69	3.05	1.79	1.91	10
n-Decane	2.2	3.4	1.2	3.0	2.0	2.9	1.9	2.5	3.4	9.0	1.40	1.05	1.92	6.32	4.87	1.29	1.46	63
Monoterpenes:																		
d-Limonene	2.7	11	4.2	3.6	30	65	2.0	3.1	1.6	3.2	0.94	0.49	6.4	8.6	12	1.1	2.7	5.8
alpha-Pinene	1.6	0.78	0.52	0.32	0.68	0.90	0.40	0.56	0.65	0.80	0.61	0.46	0.66	0.81	0.92	0.56	0.43	0.55
beta-Ocimene	0.20	0.26	0.24	0.12	0.27	0.36	0.13	0.23	0.03	ND	ND	ND	0.35	0.64	0.43	0.05	0.24	0.38
alpha-Ocimene	0.10	0.12	0.11	0.05	ND	ND	ND	0.10	ND	ND	ND	ND	0.18	0.30	0.20	ND	0.10	0.21
Alkenes:																		
Isoprene	2.3	6.3	5.3	1.8	6.8	8.2	2.8	1.1	1.3	0.95	0.78	0.80	8.7	10	5.9	1.2	3.4	5.6
trans-2-Pentene	1.2	1.0	0.85	0.76	1.6	1.6	0.94	1.0	2.0	2.2	1.4	1.4	1.5	1.9	1.6	1.0	0.94	3.0
1-Pentene	0.40	0.39	0.35	0.25	0.61	0.59	0.41	0.35	0.67	0.67	0.50	0.48	0.60	0.69	0.60	0.42	0.40	1.1
cis-Pentene	0.41	0.35	0.29	0.25	0.53	0.54	0.33	0.35	0.68	0.74	0.47	0.47	0.52	0.63	0.57	0.35	0.35	1.1
Oxygenated compounds:																		
Ethyl methacrylate	ND	ND	ND	ND	ND	ND	ND	ND	ND	ND	ND	ND	ND	ND	ND	ND	ND	3.3
Tetrahydrofuran	0.32	0.54	0.40	0.11	0.16	0.21	0.17	<LOD	0.23	0.25	0.27	0.27	0.43	0.76	0.26	0.19	0.19	3.2
Methyl methacrylate	0.15	0.64	0.28	0.13	<LOD	0.15	ND	<LOD	0.12	0.07	0.19	0.30	0.39	0.62	0.89	0.54	0.27	2.4
Isobutanol	0.07	0.33	0.24	0.19	0.14	<LOD	0.11	<LOD	0.11	<LOD	0.12	0.18	0.39	0.30	0.34	0.30	1.3	1.1
Diethyl ether	0.10	0.12	0.38	0.12	<LOD	<LOD	0.12	0.30	0.36	ND	0.27	0.20	0.16	0.60	0.21	0.15	0.36	0.21
Halocarbons:																		
Tetrachloroethylene	1.1	1.4	0.74	0.55	0.64	0.70	0.45	0.41	1.2	1.2	1.3	1.3	1.4	1.5	1.2	1.6	1.7	1.7
1,2,2-Trichlorotrifluoroethane	0.79	0.76	0.78	0.54	0.75	0.80	0.83	0.77	0.71	0.73	0.71	0.73	0.93	1.0	0.75	0.39	0.75	0.71
1,1,2-Trichloroethane	<LOD	ND	ND	ND	0.00	0.00	ND	ND	ND	ND	ND	ND	0.00	0.32	ND	ND	ND	0.66
Carbon Tetrachloride	0.32	0.48	0.62	0.44	0.34	0.38	0.46	0.41	0.43	0.35	0.43	0.46	0.67	0.82	0.60	0.31	0.59	0.43
1,2-Dichloroethane	0.09	0.15	0.14	0.10	0.00	0.00	0.14	0.12	0.18	0.10	0.27	0.26	0.65	0.54	0.28	0.24	0.33	0.33
Chloroform	0.14	0.60	0.51	0.05	0.06	0.00	0.19	0.91	0.14	0.03	0.03	0.03	0.09	0.24	0.09	0.07	0.95	0.23
Trichloroethylene	0.18	0.14	<LOD	<LOD	0.00	0.00	<LOD	0.10	0.27	0.27	0.43	0.47	0.26	<LOD	0.70	0.56	0.18	0.21
Nitriles:																		
Propionitrile	<LOD	0.07	<LOD	ND	0.00	0.16	<LOD	ND	<LOD	<LOD	0.06	<LOD	<LOD	<LOD	<LOD	<LOD	ND	0.11

Article 1

Chemistry and sources of $PM_{2.5}$ and volatile organic compounds breathed inside urban commuting and tourist buses

Amaia Fernández-Iriarte, Fulvio Amato, Natalia Moreno, Antonio Pacitto, Cristina Reche, Esther Marco, Joan O. Grimalt, Xavier Querol, Teresa Moreno
Atmospheric Environment 223, 117234
https://doi.org/10.1016/j.atmosenv.2019.117234
2020

Atmospheric Environment 223 (2020) 117234

Contents lists available at ScienceDirect

Atmospheric Environment

journal homepage: http://www.elsevier.com/locate/atmosenv

Chemistry and sources of $PM_{2.5}$ and volatile organic compounds breathed inside urban commuting and tourist buses

Amaia Fernández-Iriarte [a,c], Fulvio Amato [a], Natalia Moreno [a], Antonio Pacitto [b], Cristina Reche [a], Esther Marco [a], Joan O. Grimalt [a], Xavier Querol [a], Teresa Moreno [a,*]

[a] Institute for Environmental Assessment and Water Studies (IDAEA), Spanish Research Council (CSIC), 18-26 Jordi Girona, Barcelona, 08034, Spain
[b] Dept. of Civil and Mechanical Engineering, University of Cassino and Southern Lazio, Italy
[c] Department of Natural Resources and Environment, Industrial and TIC Engineering (EMIT), Universitat Politécnica de Catalunya (UPC), Manresa, 08242, Spain

HIGHLIGHTS

- Interior bus air chemistry can be influenced both by route taken and bus model.
- Carbon and most metal concentrations are much higher in buses than urban background.
- Enhanced levels of Cu and Sb are attributed to brake particles entering the bus.
- Inhalable PM are mostly textile fibres, skin flakes, vehicle exhaust and brake wear.
- New buses show much higher VOC signature due to off-gassing of interior materials.

ARTICLE INFO

Keywords:
Indoor air quality
Commuting
Public buses
Electric bus
Diesel bus
Tourist bus

ABSTRACT

Inhalable particulate matter (size <2.5 μm: $PM_{2.5}$) inside commuting and tourist buses moving through the city of Barcelona, Spain, was chemically analysed. The analyses show PM dominated by organic carbon (mostly 10–20 μg/m^3) and elemental carbon (mostly 3–6 μg/m^3; OC/EC = 3.4), followed by SO_4^{2-}, Fe, Ca, K, Al_2O_3, Mg, and Na, with calculated mineral content being around one third that of total carbon. Elemental carbon levels are higher inside diesel buses than those powered by natural gas or electricity, and higher in the upper floor of open-top double decker tourist buses than in the lower floor. Overall, major element concentrations inside the buses are typically 2–8 times higher than 24 h-averaged urban background levels, although some metallic trace elements, notably Cu and Sb, are exceptionally enriched due to the presence of brake particles, especially on routes involving higher gradients and therefore more brake use. In contrast, Cu and Sb concentrations in electric buses are unexceptional, presumably because these buses rely more on regenerative braking and are hermetically sealed when moving. Seasonal differences reveal PM to be more mineral in winter (Al_2O_3 1.3 μg/m^3 vs. summer average of 0.3 μg/m^3), with summer enrichment in Na, Mg, P, V, Ni and SO_4^{2-} being attributed to marine aerosols contaminated by port emissions. Source apportionment calculations identify 6 main factors: road dust resuspension, metalliferous (brake wear and metallurgy), local urban dust, secondary sulphate and shipping (6%), vehicle exhaust (19%), and an indoor source (46%) interpreted as likely related to the textile fibres and skin flakes of bus occupants. Volatile Organic Compounds measured inside all buses except one were dominated by 2-Methylpentane (14–36 μg/m^3), Toluene (10–30 μg/m^3), Xylene isomers (10–28 μg/m^3, with m- » o- > p-Xylene) and n-Pentane (5–15 μg/m^3). ΣBTEX concentrations were <70 μg/m^3, with Toluene being commonest, followed by m-Xylene, with p-Xylene, o-Xylene and Ethylbenzene each below 7 μg/m^3 and Benzene concentrations always less than the EU limit value of 5 μg/m^3. The VOCs mixture is similar to that recently reported from inside Barcelona taxis (although inside the larger volume bus VOC concentrations are lower than in the taxis) and is interpreted as providing a chemical fingerprint characterising traffic-contaminated ambient air in the city road environment. The notable exception to the VOC content was a brand new hybrid diesel bus still offgassing volatiles to such an extent that Σ(alkane + alkene + aromatic) indoor concentrations exceeded 800 μg/m^3, with ΣBTEX ten times higher than normal.

* Corresponding author.
E-mail address: teresa.moreno@idaea.csic.es (T. Moreno).

https://doi.org/10.1016/j.atmosenv.2019.117234
Received 4 October 2019; Received in revised form 16 December 2019; Accepted 17 December 2019
Available online 21 December 2019
1352-2310/

1. Introduction

Hundreds of millions of people in the world spend part of their workday commuting through a city (≈8% of the daily time) and inhaling atmospheric pollutants, including organic and inorganic compounds in the form of gases or particles. In many cases these urban journeys provide a disproportionate percentage of the individual's average daily exposure to inhalable toxins, and recognition of this fact is reflected in a large body of scientific literature on commuting and air pollution that goes back over 50 years (e.g. Haagen-Smit, 1966; Cepeda et al., 2017). The number of such publications has accelerated in recent years, accompanied by an increasingly wide recognition of the serious insult to human health inflicted worldwide by inhaling contaminated urban air. Given the sometimes radical differences in atmospheric microenvironments experienced by city travellers using different transport modes, many of these publications have turned their attention specifically to air quality found inside moving vehicles (e.g. Alameddine et al., 2016; Fruin et al., 2011; Hudda et al., 2011, 2012; Hudda and Fruin, 2018; Jo and Yu, 2001; Leavey et al., 2017; Lee et al., 2015; Madl et al., 2015; Moreno et al., 2015; Tartakovsky et al., 2013; Xing et al., 2018; Yang et al., 2015; Zhu et al., 2007). In the context of legislative demands imposed by environmental authorities, the main focus of these studies has been on PM_{10} and $PM_{2.5}$ mass, numbers of ultrafine particles (UFP), concentrations of gaseous pollutants such as NOx, CO and CO_2 and, more recently, volatile organic compounds (VOCs).

In this paper we turn our attention to a much less-studied aspect of in-vehicle air quality, namely that of the major and trace element chemistry of inhalable particles breathed by passengers using public transport. Such studies are few primarily because of the practical difficulties of obtaining enough PM sample to allow a comprehensive chemical analysis, a challenge we have overcome by using state-of-the-art portable equipment, having access to our own ICP-AES/MS geochemical laboratory, and a sampling team prepared to spend many hours inside the vehicles. Specifically, we have collected $PM_{2.5}$ samples from filters placed inside public transport buses moving through the city of Barcelona, as well as VOCs with in situ pumping and adsorption into cartridges packed with graphitized BC adsorbents, choosing different fuel-type buses, routes, and seasons of the year to investigate the main factors influencing commuting exposure to $PM_{2.5}$ pollutants. This study has been complimented by the addition of comparative chemical data from 24 h averaged $PM_{2.5}$ obtained at an urban background site in the city (Palau Reial), and by source apportionment calculations using Positive Matrix Factorization.

2. Methodology

The air quality sampling was carried out within the BUSAIR project between May 2017 and March 2018 inside public buses operated by the Metropolitan Transports of Barcelona (TMB), Spain, which carries around 203 million of passengers a year and comprises 101 lines running along a network of 830 km built progressively since 1906 (2018 TMB data). All buses are equipped with an air-conditioning system (AC) which starts functioning in spring until the end of the summer. With this in mind the sampling was divided in two different campaigns, "summer", from May 2017 to September 2017, and "winter", from November 2017 to March 2018, to observe any differences in air quality between buses with and without AC. Buses were also selected to include a range of different engine-types operating in the fleet (diesel, natural gas, electric, hybrid). In addition, buses were chosen to include lines representative of the newly-introduced route system that emphasises "vertical" (i.e. running to and from the coastline, across the sloping piedmont that defines the city surface) and "horizontal" (parallel to the coastline) trajectories.

A total of 24 bus pairs were sampled, as listed on Table 1, including two tourist bus lines (open top double-decker buses) running along the "red" and "blue" routes through the city. The bus pair would run on their normal scheduled service, one usually 10 min or so behind the other. Thus, on each sampling day, two members of the research team travelled for around 2 h along the same route but in buses of different fuel type (with the exception of the tourist buses). To take an explanatory example from Table 1, on 16 May the first bus of the chosen pair operating on "vertical" route V13 was a diesel Euro V, with a hybrid diesel being the next bus to arrive, and sampling equipment was placed inside each of these two buses for a 2-h return journey. This procedure was repeated three times on dry weekdays to ensure enough PM sample was collected for chemical analysis (i.e. 6-hour samples collected over 3 days: in the example above, on 16, 17 and 18 May). In several cases schedule changes meant that sampling could not be done on strictly consecutive days, but it was always completed (without changing the filter) during the next available weekday and at the same time in the morning. Similar logistical problems with schedule changes meant that there are two bus pairs that were not repeated in summer and winter (left blank in Table 1).

Sampling equipment inside the buses was located in the middle of the bus in the space reserved for wheelchairs and strollers, facing the central double doors. Notes were written during the sampling, recording variables such as if the AC was on or if the windows/doors were open. Ambient environmental conditions such as temperature (T) and relative humidity (RH) were also measured. Summer average T and RH inside the buses ranged between 19 and 27 °C and 38–64% in summer, and 14–25 °C and 28–45% in winter.

For $PM_{2.5}$ chemical composition determination, 37 mm quartz fibre filters (Pallflex® Air Monitoring Filters, Pall, LifeScience) were used loaded in a personal environmental monitor (761-203B PEM, SKC, usually known as portable emission monitoring system) connected to a personal air sampling pump (Leland Legacy, SKC) operating at 10 L/min. The filters were gravimetrically weighed prior to their use, having been first placed for 6 h in an oven at 200 °C (Memmert) to eliminate volatiles, and then kept at room temperature for 24 h before weighing them (XP105DR, Mettler Toledo) in an acclimatised room where T and RH are controlled to 20 °C and 50%, respectively. The same filter was used during 3 weekdays of sampling in order to achieve enough sample to be analysed. Once the sampling had been done, the filters were kept inside a box to maintain them in darkness before being subjected to the same procedure as for blank filters before weighing.

Table 1
Bus pair comparisons made per seasonal campaign including information on each line and date. V = "Vertical" (coast to mountain) routes; H = "Horizontal" (coast-parallel) routes. Other bus routes (19, 34, 39, 47, 60) run along more mixed trajectories. Bus types are diesel Euro IV and V, hybrid diesel (HD), natural gas (CNG), hybrid natural gas (HCNG) and electric. The tourist buses run using diesel Euro IV engines along "red" (more southerly, including Montjuic Hill) and "blue" (mostly north of the Diagonal) routes.

Bus pair	SUMMER		WINTER	
	Line	Date	Line	Date
Euro V vs Euro IV	V13	10, 11, 12 May	V3	16, 17, 18 Jan.
Euro V vs HD	V13	16, 17, 18 May	H4	14, 15, 16 Nov.
Euro V vs CNG	V3	30, 31 May, 1 Jun.	V3	1, 12, 13 Dec.
Euro V vs Electric	34	14, 15, 18 Sep.	–	–
Euro IV vs HD	47	10, 12, 14 July	19	14, 15, 19 Dec.
Euro IV vs CNG	V17 vs V11	20, 21, 28 Sep.	V3	23, 24, 30 Nov.
Euro IV vs Electric	–	–	60	10, 12, 13 April
HD vs CNG	H12	18, 19, 20 Jul.	H12	26 Feb., 1, 2 Mar.
HD vs Electric	34	23, 24, 25 May	34	27, 28 Mar.
CNG vs HCNG	39	13, 14, 15 Jun.	39	10, 11, 12 Jan.
CNG vs Electric	H16	8, 9, 12 Jun.	H16	19, 20, 21 Feb.
Tourist inside vs outside	Blue	20, 21, 22 Jun.	Blue	23, 24, 25 Jan.
Tourist inside vs outside	Red	26, 27, 28 Jun.	Red	30, 31 Jan., 1 Feb.

Given the fact that the sampling campaign took place over several months, all data in the study have been deseasonalised with reference to the Barcelona Urban Background station at Palau Reial (UB-PR), thus smoothing (not removing) the effect of meteorological parameters as a whole (Rivas et al., 2014). This calculation involved determination of an adjusted concentration $(C_i^j)_k{}^*$ of the i_{th} pollutant for the k_{th} day at the bus j_{th} as shown in Eq. (1):

$$(C_i^j)_k^* = (C_i^j)_k / [(C_i^{PR})_k / (\overline{C_i^{PR}})] \quad (1)$$

where $(C_i^j)_k$ is the concentration measured at the bus $(C_i^{PR})_k$ and $(\overline{C_i^{PR}})$ are the 6 h average corresponding to the 3 days kth and campaign averages at UB-PR, respectively.

A total of 48 $PM_{2.5}$ gravimetric samples collected on quartz fibre filters using the PEM samplers were chemically analysed. First of all, a 1.5 cm^2 section from the middle of the filter was cut in order to analyse organic and elemental carbon (OC, EC) by a thermal-optical technique using a Lab OC/EC Aerosol Analyser (Sunset Laboratory Inc.). The rest of the filter was acid digested with 2.5 mL of HF, 1.25 mL of HNO_3, 1.25 mL of $HClO_4$ for major and trace elements analysed using ICP-AES and ICP-MS respectively. For quality control, 0.1 g of 1633b Standard Reference Material (Trace Elements in Coal Fly Ash, NIST) was used to identify any possible analytical or calibration.

Volatile Organic Compounds were measured in 16 of the buses using stainless steel cartridges custom packed with activated graphitized BC adsorbents, using the same methodology as detailed in Moreno et al. (2019). With regard to the $PM_{2.5}$ source apportionment calculations, these used Positive Matrix Factorization software (PMF v5, Paatero and Tapper, 1994; Amato et al., 2009), using relevant criteria (see Paatero and Hopke, 2003) that allowed selection of 11 strong species (OC, EC, Ca, Fe, Mg, SO4, Mn, Cu, Sr, Sn, Sb) and 10 weaker species (Al2O3, K, Na, Ti, V, Ni, Zn, Ba, La and Pb). The data matrix was uncensored (i.e. negative) so that below detection and zero limit values were included in the analyses to avoid a bias in the results (Paatero, 2007).

3. Results

The chemical analyses of the 48 $PM_{2.5}$ samples collected during the BUSAIR campaigns are presented in chronological order in Table S1 (supplementary information) which also records the bus fuel-type (diesel (EIV, EV), hybrid diesel (HD), compressed natural gas (CNG), hybrid compressed natural gas (HCNG) and electric), and the bus number/route (V = "vertical"; H = "horizontal"; TB tourist bus red and blue trajectories). The analyses are further grouped into 20 "summer" (AC on with closed windows; May to September) and 20 "winter" samples (November to February), the other 8 samples were considered mixed. The data from these various sub-groups based on bus engine type, season, and route are averaged in Table 2 which for comparison adds the values for the average for all buses (AB) and the urban background (UB) in Barcelona during the sampling period.

The highest concentrations, as recorded in Table S1 and Table 2, and graphically presented in Fig. 1a, are those of OC (most values 10–20 μg/m^3) and EC (most values 3–6 μg/m^3), followed by SO_4^{2-}, Fe, Ca, K, Al_2O_3, Mg and Na. Average OC concentrations are in general around x3 those of EC average (OC/EC = 3.4), and calculated mineral content is approximately one third that of total carbon content (EC + OC). With regard to the trace elements the highest concentrations are recorded for Zn and Cu, followed by Zr, Ti, Mn, Cr, Ni, Sb, Sn, V, Sr, Pb, Hf, Ce, and La. This distinctive inorganic trace element signature of interior bus air is further emphasised by comparing the BUSAIR chemical database with levels recorded within the Barcelona UB-PLR (Table 2; Fig. 1a and b). Whereas concentrations of most elements and compounds recorded in the contaminated city road are raised typically 2–8 times higher than UB-PLR levels (AB/UB on Table 2), some elements stand out as unusually enriched (both Cu and Sb > 10 times: Fig. 1b).

We now consider the PM chemistry characterising exposure in each of the bus sub-groups shown in Table 2, then present the results of source apportionment calculations. Finally, we examine the pattern of VOCs present inside sixteen of the buses used during the winter campaign (Table S2, supplementary information).

3.1. Bus type

Although the results reveal considerable $PM_{2.5}$ chemical variation, the majority of data fall within a relatively restricted range. In the case of EC, for example, most (73%) buses recorded levels of 3–7 μg/m^3 although exceptionally, concentrations as high as 19 μg/m^3 and as low as 1 μg/m^3 were reached (Table S1). Most bus pairs show similar EC concentrations, with nearly half differing by < 1 μg/m^3 and only 3 pairs differing by more than 2.5 μg/m^3 (Table 3). A notable exception to this general rule is a diesel EV/EIV pair (16 January) that records a difference in EC content 17 μg/m^3 (Table 3).

A similar pattern is revealed by OC concentrations, which cluster around 10–15 μg/m^3 and rarely (25%) exceed differences >5 μg/m^3 between bus pairs. In the case of "mineral" concentrations (essentially mainly a mix of silicates and carbonates: Table S1) these again show very few exceedances above 10 μg/m^3, with 92% of bus pairs showing differences below 2 μg/m^3, irrespective of whichever engine type was powering the bus.

Taken overall, the diesel buses record slightly higher average EC concentrations inside the bus when compared to CNG or electric models, this being interpreted as likely evidence for some degree of self-pollution (Table 2). In contrast, when compared to diesel buses the six electric buses show relatively lower average concentrations of many $PM_{2.5}$ components, but especially the metals Cu and Sb (Fig. 2a). These electric buses have a window system which is hermetically sealed, climate control is regulated by the driver, and they are equipped with regenerative braking which reduces the use of friction brakes, all of which favour reduction of outside PM infiltration, including that sourced from their own brakes.

The data from the tourist buses offer insight into the differences between the upper floor, which is wide open to outdoor air, and the lower floor which, although ventilated via stairs leading to the open top floor, is more confined. The data demonstrate consistently higher EC levels in the upper floor ("out" in Table S1) than in the downstairs interior ("in"). If the concentration of EC inside buses can be viewed as a proxy for traffic emissions, this would indicate that passengers travelling on the open upper deck of the bus are more exposed to traffic exhaust emissions than those below. However, it should be noted that this difference between EC concentrations upstairs and downstairs in these buses is always <2.5 μg/m^3.

3.2. Season

The two subgroups selected on the basis of warmer ("summer") and cooler ("winter") seasons are listed in Table S1 and compared with UB-PLR concentrations in Fig. 2b. The $PM_{2.5}$ chemistry for each of these two subgroups is quite different, with the winter samples being noticeably richer in mineral dust (summer average Al_2O_3 0.3 μg/m^3; winter average 1.3 μg/m^3) and slightly more carbonaceous (summer OC + EC 19 μg/m^3; winter OC + EC 24 μg/m^3). Several trace elements occur in higher concentrations in winter, most notably Sb, Cu, Zn and Mn. The highest increase was recorded for Sb x6.5 above UB-PLR in summer and x21 in winter. In contrast concentrations of Na, P, V, Ni, Cr, SO_4^{2-} and especially Mg were considerably lower in summer. The likely controls on these seasonal chemical differences are discussed below.

3.3. Route

The "route" sub-groups listed on Table S1 and Table 2 have been chosen on the basis of whether they run essentially horizontal and coast-parallel through the city (these routes being designated with the prefix H

Table 2
Summary of chemical analyses of $PM_{2.5}$: all bus average (AB), urban background (UB), and sub-groups based on bus engine types, season, and route (see Table TS1).

	URBAN BACKGROUND	ALL BUSES (AB)		BUS TYPE						SEASON		ROUTE		
	UB	AB	AB/UB	Diesel	HD	CNG	HNG	Electric	Tourist outside	Tourist inside	Summer	Winter	Vertical	Horizontal	Others
n		48		14	8	10	2	6	4	4	16	16	14	10	16
μg/m³															
OC	2.39	16.3	6.8	19.2	17.0	16.6	23.0	12.9	10.7	11.2	14.7	19.1	17.9	14.2	18.9
EC	1.04	4.8	4.6	6.6	4.6	4.2	4.8	3.8	4.1	2.9	4.8	5.1	6.6	4.0	4.4
CO_3^{2-}	0.35	1.6	4.5	2.0	1.2	1.8	2.3	1.4	0.5	0.7	1.4	1.7	1.9	1.1	2.0
SiO_2	0.54	2.1	3.8	2.6	1.8	2.6	4.0	1.8	0.6	0.6	0.7	4.0	2.3	1.9	2.8
Al_2O_3	0.18	0.7	4.0	0.9	0.7	0.9	1.3	0.6	0.2	0.2	0.3	1.3	0.8	0.6	1.0
Ca	0.23	1.0	4.5	1.4	0.8	1.2	1.6	0.9	0.3	0.5	1.0	1.1	1.3	0.8	1.3
Fe	0.19	1.4	7.3	1.9	0.9	1.6	1.4	1.3	0.5	0.5	1.2	1.6	2.0	1.0	1.5
K	0.11	1.0	8.8	1.6	0.5	1.1	1.5	0.9	0.5	0.6	0.9	0.9	1.6	0.4	1.2
Na	0.15	0.3	2.0	0.2	0.5	0.3	<0.1	0.3	0.4	0.4	0.4	0.2	0.1	0.3	0.4
Mg	<0.1	0.4	9.3	0.8	0.1	0.4	0.2	0.6	0.1	0.2	0.6	0.1	0.7	0.1	0.7
P	<0.1	1.2	122	3.0	0.1	0.6	0.2	1.6	<0.1	0.1	1.9	0.1	0.8	0.1	3.1
SO_4^{2-}	1.72	1.8	1.0	1.8	1.8	1.6	2.1	1.6	1.9	2.0	2.5	0.9	1.6	1.8	1.8
OC + EC	3.43	21.1	6.2	25.9	21.5	20.8	27.7	16.8	14.8	14.1	19.5	24.2	24.6	18.1	23.3
Mineral	1.65	5.5	3.3	8.0	4.0	6.0	7.9	5.1	1.7	2.0	4.6	7.5	6.2	3.6	8.2
ng/m³															
Ti	6.64	19.47	2.93	20.06	13.98	18.43	106.83	11.09	9.11	8.23	22.32	21.70	14.14	14.06	34.09
V	4.04	6.78	1.68	7.21	5.33	6.42	31.20	7.53	4.80	4.05	9.56	2.39	7.23	4.38	10.31
Cr	1.53	9.72	6.37	9.36	14.16	6.82	5.25	4.84	12.68	13.25	8.11	7.75	8.46	6.15	11.47
Mn	4.10	12.03	2.93	15.39	10.32	13.69	17.51	7.03	8.37	7.94	6.91	19.17	15.09	12.13	11.22
Ni	2.38	8.89	3.74	10.48	9.11	5.59	1.91	7.43	12.96	13.95	8.64	5.54	9.95	5.83	7.43
Cu	6.70	82.37	12.29	96.29	107.86	107.17	174.89	19.94	30.19	20.17	84.42	119.10	113.83	71.86	89.99
Zn	23.70	90.25	3.81	123.28	73.70	113.69	92.50	42.71	55.82	53.82	47.53	135.02	135.24	75.23	78.00
Sr	0.88	4.27	4.86	6.21	3.96	4.52	6.26	2.12	1.57	2.23	2.71	6.28	5.42	3.34	5.21
Zr	5.08	36.65	7.21	44.44	38.10	40.25	33.47	39.76	23.12	12.31	29.87	43.05	47.88	36.86	36.93
Sn	1.78	4.74	2.67	6.18	4.48	4.57	3.93	3.99	3.57	3.34	4.28	5.64	6.05	4.79	4.20
Sb	0.94	10.72	11.46	15.31	7.79	14.58	23.75	4.04	2.78	2.35	6.24	19.87	16.56	9.32	10.58
La	0.12	0.64	5.49	0.61	0.42	1.30	1.04	0.39	0.26	0.25	0.25	1.25	0.78	0.56	0.75
Ce	0.23	1.81	7.79	2.18	1.27	2.65	2.39	1.20	0.67	0.88	0.40	3.45	2.21	1.25	2.47
Hf	0.24	2.19	9.13	2.77	2.29	2.40	2.29	2.30	1.16	0.55	1.40	2.97	2.90	2.12	2.34
Pb	3.05	3.30	1.08	3.39	3.46	3.11	4.43	2.48	3.36	3.51	2.95	3.91	2.64	4.04	3.04
OC/EC	2.29	3.37	1.47	2.90	3.67	3.98	4.83	3.39	2.62	3.81	3.09	3.71	2.70	3.56	4.25

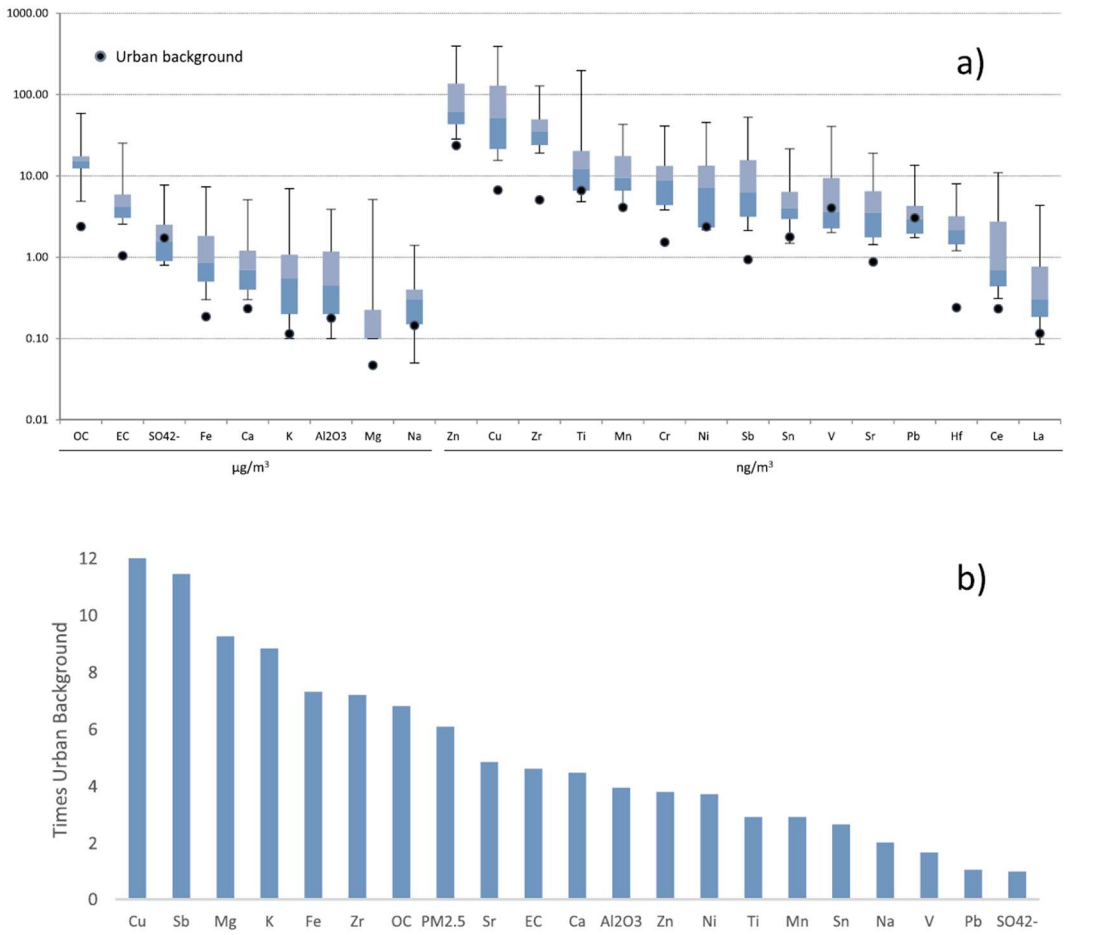

Fig. 1. Elemental concentrations measured inside Barcelona buses and urban background. 1a. Boxplot showing concentration median, lower and upper quartiles, and ranges (vertical "whisker" bar) of major and trace elements measured from $PM_{2.5}$ sampled in buses and compared to urban background (black dot); 1b. Histogram demonstrating the relative enrichments of elements measured from $PM_{2.5}$ sampled in buses relative to Barcelona urban background.

for "horizontal"), whether they operate across a considerable change of gradient between the coast and the northeast-southwest oriented hills that form the hinterland of Barcelona (prefix V: "vertical"), or whether the bus is neither H nor V but follows some more variable route through the city (buses 34, 39, 47, 19, and 60: "others" on Table 2). Vertical routes showed on average higher concentrations of carbon content (OC + EC = 25 for V vs. 18 µg/m^3 for H), and mineral dust (6.2 V vs 3.6 µg/m^3 H). Other elements also occur in higher concentrations in V routes, especially Cu, Sb, Mg and K which are >50% higher in buses running along V routes (Fig. 2c, Table 2) and presumably this is likely to reflect greater use of brakes on the routes with higher gradient.

3.4. Source apportionment calculations

Several PMF solutions were evaluated in terms of scaled residuals, G-space plots, profiles and contributions. The most-reliable solution provided 6 main factors responsible for the variability of $PM_{2.5}$ and its components (Fig. 3):

- The first factor comprises mainly OC although it also explains a significant share of some metals such as Ti, Pb, Na, Sr and Ca. Previous studies in Barcelona have related indoor sources of high OC concentrations (without EC) to the textile fibres and skin flakes of occupants (Amato et al., 2014; Rivas et al., 2014). This is the dominant source of $PM_{2.5}$ inside the bus (46%) increasing $PM_{2.5}$ levels by 39.6 µg/m^3 on average. In addition, this first factor is taken to include a Ca, Ti, Sr and Na grouping similar to that identified as linked to a cosmetic product source in a previous study in Barcelona (Minguillón et al., 2012). The largest contributions of this first factor were found in tourist buses, probably due to the higher occupancy.
- The second factor was traced by Cu, and mainly comprises OC and EC (OC/EC = 1.8). This factor was labelled as vehicle exhaust, although it likely involves a partial contribution from brake wear as well. It is the second most important source of $PM_{2.5}$, contributing 16.3 µg/m^3 (19%) on average. Interestingly the lowest contributions were obtained for electric buses, as already described for EC, Cu and Sb. The rest of fuel-types do not register significant differences.
- The third factor was traced by SO_4^{2-} and V (highest % of species) and was interpreted as secondary SO_4^{2-} and shipping. The mean

Table 3
Elemental Carbon concentrations (μg/m^3) in $PM_{2.5}$ sampled from bus pairs chosen for this study (see Table 1).

Bus pair	SUMMER		WINTER	
	Line	Elemental Carbon	Line	Elemental Carbon
Euro V vs Euro IV	V13	8.9 vs 9.5	V3	19.4 vs 2.6
Euro V vs HD	V13	6.8 vs 5.8	H4	4.9 vs 4.2
Euro V vs CNG	V3	4.5 vs 5.7	V3	4.1 vs 6.9
Euro V vs Electric	34	4.9 vs 7.2	–	–
Euro IV vs HD	47	3.5 vs 8.9	19	3.8 vs 2.9
Euro IV vs CNG	V17 vs V11	6.3 vs 3.8	V3	3.9 vs 4.7
Euro IV vs Electric	–	–	60	9.6 vs 4.9
HD vs CNG	H12	3.8 vs 3.1	H12	6.4 vs 6.4
HD vs Electric	34	3.1 vs 4.7	34	1.0 vs 0.3
CNG vs HCNG	39	3.8 vs 5.3	39	2.0 vs 4.2
CNG vs Electric	H16	2.7 vs 2.4	H16	2.7 vs 3.2
Tourist Inside vs outside	Blue	3.6 vs 6.1	Blue	2.4 vs 2.5
Tourist Inside vs outside	Red	3.8 vs 5.5	Red	1.9 vs 2.3

contribution to exposure in buses was 4.8 μg/m^3 (6%). Significant differences were observed between the winter (3 μg/m^3) and summer (7 μg/m^3) campaigns, as both oxidation processes and shipping emissions reach their maximum in summer months (Querol et al., 2001; Amato et al., 2009). The association of secondary sulphate and primary vanadium in the same factor has been reported in Barcelona before, as the ammonium sulphate particles are formed from SOx emissions which are often emitted by heavy oil combustion processes (notably by shipping) containing high amount of vanadium.

- The fourth factor was traced by Mg, Fe, K and Ca, with OC as main component. This factor had a contribution in only 2 bus pairs and was practically null for the rest of the campaigns. Since the 2 bus pairs included routes and vehicles used also in other days, we interpret this source as local urban dust, probably some minor building activities, which affected only 2 samples.
- The fifth factor was traced by Sb, Cu, Zn, Al_2O_3 and La and was interpreted as road dust resuspension. The main components are OC, EC and Fe, with an OC/EC ratio of 6.0. The lowest contributions of this factor were observed for electric and touristic buses, the reason for the latter remains unclear.
- The sixth factor was identified as metalliferous and accounts for most of the variance of metals originated from brake wear (Sn, Ba, Fe) and metallurgy (Mn, Pb and Zn) (Amato et al., 2009). The largest components are EC and Fe. The largest contributions were found in tourist buses, possibly due to their higher weight (higher braking emissions) and because they move mostly in the southern part of the city which is nearer to the metallurgical cluster of Baix Llobregat county.

3.5. Volatile organic compounds

A total of 44 VOCs were quantified inside 16 buses sampled during the winter campaign (Table S2, supplementary information). The overall VOC concentrations ranged from 69.9 to 173 μg/m^3. However, bus 34 hybrid diesel was a notable exception because of the much higher concentrations (851 μg/m^3). This bus is a special case in the context of the study because it was a brand new vehicle which was still degassing VOCs from the furnishing and coatings, including glues and other products.

Excluding the above mentioned bus, the VOC distributions in the studied buses are rather similar. The aromatic compounds are dominant (27.5–50.2%), being mainly constituted of benzene, toluene, ethylbenzene, xylenes and trimethylbenzenes, which involve 87% of the total aromatic compounds. Toluene (10–29 μg/m^3) and m-xylene (5–17 μg/m^3) are common in all samples (Table S2). The overall BTEX (Benzene, Toluene, Ethylbenzene and Xylene) signature of indoor air in the buses is remarkably similar. The typical distribution is predominated by toluene (10–30 μg/m^3) and followed by m-xylene (5–17 μg/m^3) > p-xylene (2–5 μg/m^3) > o-xylene (3–6 μg/m^3) > ethylbenzene (2–7 μg/m^3) and benzene (2–4 μg/m^3).

The alkanes (26.7–48.1%) constitute the second most abundant VOC group (Fig. 4). They are dominated by 2-methylbutane (14–36 μg/m^3) followed by n-pentane (5–15 μg/m^3) which are found in all samples (Table S2). With regard to the remaining VOCs detected, only the monoterpene compound d-Limonene was present in concentrations >10 μg/m^3 and this in only four buses, one of which registered 65 μg/m^3 (Table S2).

As mentioned above, bus 34 (a hybrid diesel) registered exceptionally high VOC concentrations that together totalled over 850 μg/m^3. In this case aromatic compounds were present in higher overall concentrations (497 μg/m^3: 58% of total VOCs) than the alkane/alkene subgroup (332 μg/m^3; 39%). Most outstanding in the aromatic subgroup are anomalously high concentrations of the three xylene (= dimethylbenzene) isomers (especially o-xylene: these compounds were found in concentrations of 160 μg/m^3). Ethylbenzene was also present in exceptional concentrations (95 μg/m^3) which, like Isopropylbenzene and sec-butylbenzene, registered levels well over tenfold those in any other bus sampled (Fig. 4). This bus shows a completely different BTEX hierarchy from normal, with o-xylene (160 μg/m^3) > ethylbenzene (95 μg/m^3) > p-xylene (91 μg/m^3) > toluene (44 μg/m^3) > m-xylene (43 μg/m^3) > benzene (5 μg/m^3). In the alkane/alkene sub-group the most abundant VOC was again 2-methylbutane (92 μg/m^3), as with the other buses. However, relative to levels in the other buses, the most striking alkane/alkene VOC increases were shown by cyclohexane (86 μg/m^3), n-decane (63 μg/m^3), n-octane (12 μg/m^3), and 2,3-dimethylpentane (10 μg/m^3). Other VOCs subgroups showed much lower concentrations, although relative to the other buses, there were unusually raised levels of the monoterpene p-cymene, the organochlorine 1,1,2-trichloroethane, as well as methyl methacrylate, tetrahydrofuran, and ethyl methacrylate (Table S2). As mentioned above, this bus was brand new and the high VOC concentrations presumably reflect significant offgassing from the interior components.

4. Discussion

The data presented in this paper can be viewed as "state-of-the-art" in the sense that it is currently technically difficult to obtain gravimetric samples of inhalable particles breathed by commuters in public transport in enough quantity to allow comprehensive chemical analysis. The limitations of the personal environmental monitor used in the study meant that the same filter had to be used for three journeys (on the same route and at approximately the same time) in order to obtain just one chemical analysis, so that each of the results listed on Table 1 are an average of 6 h, collected over three days. Such logistic limitations, added to the difficulties of negotiating permission with transport companies, have perhaps inevitably resulted in very few publications on the chemistry of indoor bus air. In this context, and despite these limitations, the information presented here represents by far the largest bus air chemical database publicly available to date, involving 132 days of direct sampling inside urban commuter buses under normal working conditions.

The design of the PM BUSAIR sampling programme was based on the expectation that several factors influence air quality inside buses, but that some of these factors are likely to be more influential than others. Thus, we sampled bus pairs powered by different engines in different seasons and following different routes through the city, adding the open-topped tourist buses as an interesting "extra" to compare with normal commuting routes. Given such variety, the number of buses sampled (48) is rather small, but it is enough to make several observations. The first of these is the distinct difference between interior bus air chemistry

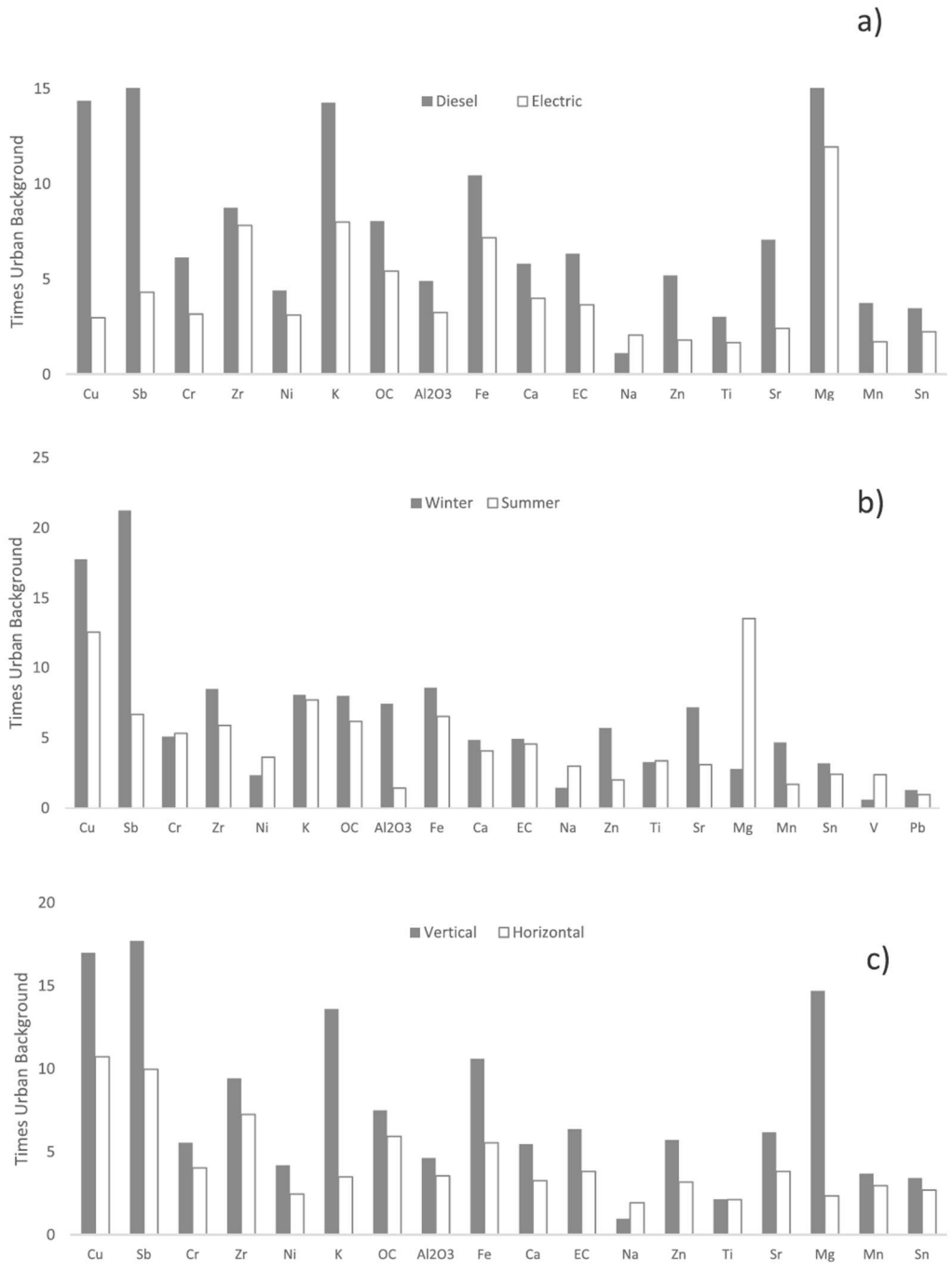

Fig. 2. Histograms comparing Barcelona BUSAIR data with urban background in: 1a. Diesel v electric buses; 2b. Winter v summer, 2c. "Vertical" (sea-to-mountain) v "Horizontal" (coast-parallel) routes. Note the consistent especial enhancement of Cu and Sb, interpreted as sourced from brake emissions.

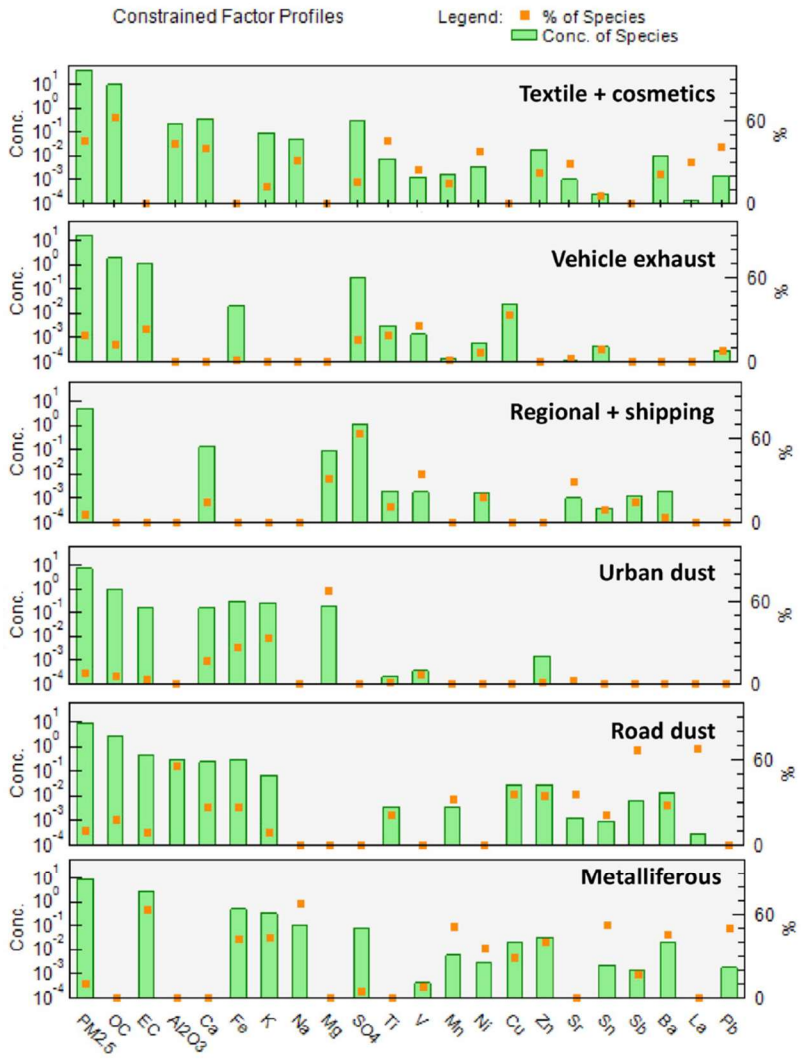

Fig. 3. Positive matrix factorization results showing the factor profiles identified.

of $PM_{2.5}$ in summer and winter (Fig. 2b). The air chemistry inside the buses sampled in summer is noticeably richer in Na, Mg, V, Ni, Cr and SO_4. Given the coastal position of Barcelona, a city with a large and active port catering especially for cruise ships, combined with more active landward-driven sea breezes in early summer, it seems likely that this seasonal difference in chemical signature is due to a greater influence of marine aerosols contaminated by shipping emissions and to the higher summer SO_2 oxidation (Querol et al., 2001; Amato et al., 2009). Another seasonal difference is registered in winter, when most $PM_{2.5}$ elemental concentrations are not only higher inside the buses, but the chemical mix is noticeably richer in several trace metals, including a quite spectacular enrichment in Cu and Sb.

The data presented here fail to reveal any great difference in major element chemistry between the chosen bus pairs following the same route one after another, even though the buses were driven always by different engine types. Thus, the differences between bus pairs of measured OC, EC and "mineral" concentrations were most commonly <5 μg/m^3, <2.5 μg/m^3, and <2 μg/m^3 respectively (Table S1). Taken overall, however, our data do suggest poorer interior bus air quality, measured as increased carbon and mineral content, is more likely to be associated with diesel buses when compared to, for example, electric buses (Fig. 2a). This implicates part of the PM contamination present inside the moving vehicle as being a result of emissions from the bus itself ("self-pollution"), a phenomenon well documented in previous publications (e.g. Fondelli et al., 2008; Zhang et al., 2013; Chernyshev et al., 2019).

Another, and stronger, indication of self-pollution affecting interior bus chemistry, however, emerges from a consideration of the trace element signature of the $PM_{2.5}$. One of the more striking observations repeatedly noted in this study is the ubiquity and abundance of Cu- and Sb-bearing fine particulates in bus air. Previous publications have demonstrated how these elements are good tracers for brake particles

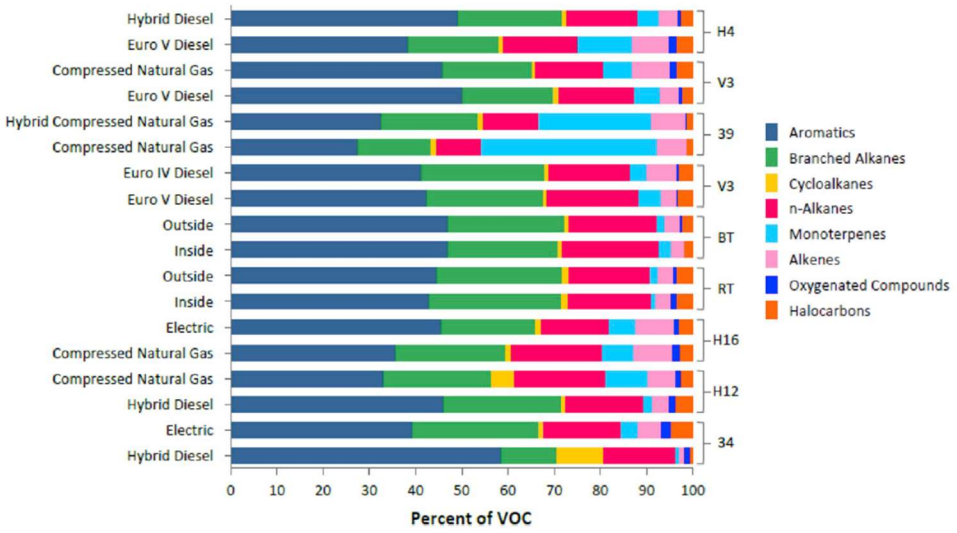

Fig. 4. Percentages of abundances of VOCs measured in 17 Barcelona buses and a brand new hybrid diesel bus (34) contaminated by severe interior offgassing. See Table S2 and text for details.

(Adamice et al., 2016; Amato et al., 2011; Grigoratus and Martini, 2015). In a previous publication on public transport air quality in Barcelona we published the results of a pilot study on just three buses, demonstrating the same enrichment in Sb and introducing a Mn, Ti, Sbx10 ternary diagram to show how bus air can be contrasted with $PM_{2.5}$ samples collected from subway and outdoor city air (Moreno et al., 2015). On Fig. 5 we plot our new BUSAIR database onto the same ternary diagram, adding the urban background data from the Palau Reial monitoring site during the sampling campaigns. The same relative enrichment in Sb and Cu inside the vehicle also strongly suggests that brake particles are more common in the buses operating along a significant slope, with the "vertical" buses (from coast line to the hills) recording concentrations >50% higher than the coast-parallel "horizontal" buses (Fig. 2c, Table 2). Even more interesting is the fact that electric buses do not show such enrichment (Fig. 2a), an observation that may reflect the fact that these buses have more hermetic closure and/or that they use regenerative braking and so emit fewer brake particles. Another conclusion arising from this difference in braking patterns is that it is the brake-contaminated PM plume generated by the bus itself ("self-pollution") that is infiltrating into the bus, presumably through open windows and when doors are opened after braking upon arrival at bus stops.

The open-topped tourist buses provide a special case in that upstairs they are open to the city highway air which also enters the lower floor of the bus. This higher degree of ventilation is reflected in the fact that the $PM_{2.5}$ mass represented by OC content is relatively low in the tourist buses (11 $\mu g/m^3$) when compared to all other bus types (17–23 $\mu g/m^3$) except electric (13 $\mu g/m^3$) (Table 2). We also observe that those passengers travelling in the open top upper floor of the tourist bus breathe higher levels of EC, Cu and Zr, presumably sourced from fresh traffic exhaust and brake emissions (Table 2).

Our source apportionment data indicates that although almost half of the particles inhaled when travelling in the bus are most probably related to vehicle passenger emissions such as textile fibres and skin flakes (Amato et al., 2014; Minguillón et al., 2012; Rivas et al., 2014), independently of the bus type. The infiltration from outdoor sources such as vehicle exhaust and brake wear particles both from the same bus (self-pollution) and from other vehicles, also represents an important source of pollution (19%).

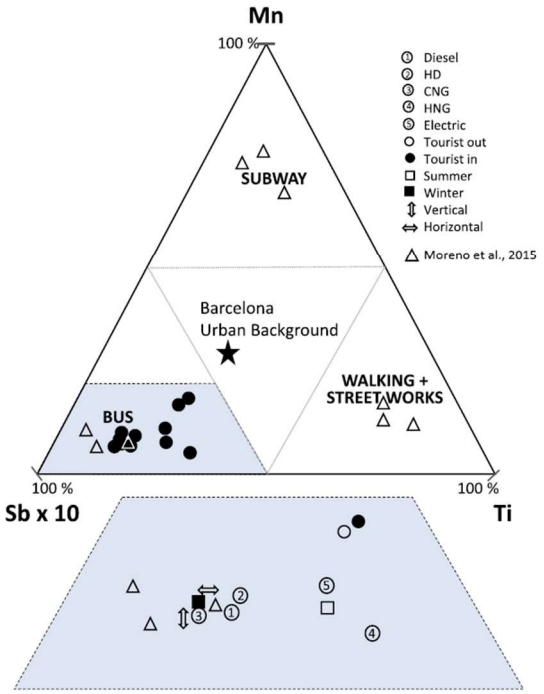

Fig. 5. MnTiSbx10 ternary plot comparing $PM_{2.5}$ measured inside Barcelona buses, showing enrichment in Sb typical of brake PM-contaminated air. Fields for subway, walking/streetworks, and bus from Moreno et al. (2015).

Concerning VOCs, comparison of the concentrations in the inner bus atmospheres with those in open air collected in the Route Blue and Red

Tourist buses, shows similar concentrations for gasoline vehicle pollutants such as benzene, toluene, ethylbenzene, xylenes, and trimethylbenzenes. Thus, the concentrations of toluene are 11–26 μg/m^3 in the external atmosphere and 10–29 μg/m^3 in the inner bus air, and total xylenes are 19–23 μg/m^3 and 11–28 μg/m^3, respectively. Traffic emissions infiltrating from outside will be also rich in alkanes, but also contain BTEX and other aromatic compounds as well as several alkanes (Yang et al., 2017). Evaporative emissions will normally favour aromatics over alkanes (Yue et al., 2017), whereas exhaust emissions of alkane and aromatic VOC are likely to be mostly toluene, 2-methylbutane and p- & m-xylenes derived from gasoline (petrol) combustion (Chin and Batterman, 2012; Montells et al., 2000).

The present Barcelona bus data confirm that the most common and typical VOCs measured in the vehicle interior are 2-methylpentane (14-36 μg/m3), toluene (10-30 μg/m3), xylenes (10-28 μg/m3, with m- >> o- > p-Xylene) and n-pentane (5-15 μg/m3). Total BTEX concentrations measured in our study were generally rather low (<70 μg/m3), with toluene being commonest, followed in turn by m-xylene, p-xylene, and o-xylene. Benzene (2-4 μg/m3) and ethylbenzene (2-7 μg/m3) were both consistently present in low concentrations. Such aromatic VOCs levels can be favourably compared to other studies, for example that by Chen et al. (2011) in Changsha city, China, where mean ΣBTEX values inside buses were 464 μg/m3 and included highly undesirable levels of benzene (69 μg/m3). A comparable study inside buses in Bangkok found ΣBTEX concentrations of 169 μg/m3, with 12 μg/m3 benzene (Ongwandee and Chavalparit, 2010). A study in Taegu, Korea, reported mean ΣBTEX levels of 131 μg/m3 inside buses and 195 μg/m3 inside taxis, including 22 μg/m3 and 33 μg/m3 benzene respectively (Jo and Yu 2001). However, not all studies of VOC levels in public transport have been conducted in busy, polluted cities, as demonstrated by measurements made inside public buses operating in the relatively small and uncongested Spanish city of Pamplona where ΣBTEX concentrations of 10-22 μg/m3 were recorded (Parra et al., 2008).

Pairwise comparison of the concentrations of the individual VOCs found in the buses compared in each route shows statistically significant correlations for the concentrations of aromatic compounds in all routes and alkanes in all routes except 34 (Hybrid Diesel and Electric) (Table 4). Despite these correlations significant statistical differences in the composition of aromatic compounds were observed in routes H4 (Hybrid and Euro V Diesel), V3 (Euro IV and V Diesel), H12 (compressed natural gas hybrid Diesel) and 34 (Hybrid Diesel, Electric). They also show significant differences when comparing between inner and external atmospheres (routes BT and RT) (Table 4).

The composition of alkanes shows significant differences in route V3 (Euro IV and V Diesel), H16 (Electric and CNG), H12 (CNG and Hybrid Diesel) and 34 (Hybrid Diesel and Electric), and significant differences between the inner and external atmospheres of route BT but not in route RT (Table 4).

With regard to the compounds related to personal care, such as the monoterpenes, these are present in higher concentrations in the inner bus atmospheres than in the external air. This is the case of p-cymene, 0.15–0.17 μg/m^3 in the outer atmosphere and 0.11–0.54 μg/m^3 in the inner atmosphere (Table S2), δ-limonene, 0.94–1.6 μg/m^3 and 0.49–65 μg/m^3, respectively, and β-ocimene, ND-0.03 μg/m^3 and ND-0.64 μg/m^3, respectively. The same is the case of VOCs exhaled from human breath such as isoprene (Marco and Grimalt, 2015), e.g. 0.78–1.3 μg/m^3 in the external atmosphere and 0.80–10 μg/m^3 in the inner bus air. Compounds that are commonly found in furniture tissues such as methyl methachrylate are also found in higher concentrations in the inner bus atmospheres, 0.12–0.19 μg/m^3 and <LOD-0.89 μg/m^3, respectively. The organochlorinated VOCs do not show a defined trend when comparing both atmospheres (Table S2).

The obvious exception to the general rule of relatively low VOCs concentrations inside buses in Barcelona is that of the brand new hybrid diesel bus sampled on 27 March and seriously contaminated by interior VOC off-gassing (Table S2). In this new bus many VOCs concentrations were much higher, and with a different distribution: o-xylene (160 μg/m^3), ethylbenzene (95 μg/m^3), 2-methybutane (92 μg/m^3), p-xylene (91 μg/m^3), and cyclohexane (86 μg/m^3). However, despite the fact that levels of BTEX approached 500 μg/m^3 in this bus (over x10 higher than normal), the benzene concentrations still remained relatively subdued at 4.5 μg/m^3, below the European Union limit value of 5 μg/m^3 (EU air quality directive 2008/EC/50; Kerchich and Kerbachi, 2012) because the occurrence of this compound is related to the inputs from external

Table 4
Statistical analysis in the composition of aromatic alkanes in all routes studied.

Route	Engine	Aromatics							Alkanes						
		Wilcoxon Signed Rank Test					Spearman's Correlation		Wilcoxon signed rank test					Spearman's correlation	
		25	Median	75	Z	p-Value	r_s	p-Value	25	Median	75	Z	p-Value	r_s	p-Value
H4	Hybrid Diesel	0.43	2.77	3.42	−2.856	0.004	0.996	0.000	0.95	2.04	5.18	−1.362	0.173	0.983	0.000
	Euro V Diesel	0.38	1.63	3.16					0.85	2.07	5.33				
V3	Compressed Natural Gas	0.22	1.38	2.54	−0.282	0.778	0.952	0.000	0.59	1.18	4.42	−0.533	0.594	0.917	0.001
	Euro V Diesel	0.24	1.31	2.82					0.66	1.25	4.13				
39	Hybrid Compressed Natural Gas	0.38	1.77	3.29	−1.961	0.050	0.974	0.000	0.91	1.72	5.72	−1.12	0.263	0.983	0.000
	Compressed Natural Gas	0.38	1.98	3.42					0.86	1.70	6.08				
V3	Euro IV Diesel	0.24	1.31	2.57	−2.919	0.004	1.000	.	0.81	1.45	3.96	−2.666	0.008	0.950	0.000
	Euro V Diesel	0.26	1.40	2.79					0.85	2.52	5.67				
BT	Outside	0.19	2.36	4.90	−2.856	0.004	0.991	0.000	1.13	2.76	9.16	−2.666	0.008	0.983	0.000
	Inside	0.20	2.53	6.20					1.22	2.96	10.94				
RT	Outside	0.16	1.66	4.25	−2.040	0.041	0.988	0.000	0.83	1.40	6.37	−1.244	0.214	0.939	0.000
	Inside	0.13	1.54	3.72					0.72	1.32	6.37				
H16	Electric	0.40	2.06	4.34	−0.943	0.345	0.996	0.000	0.93	1.92	7.18	−2.666	0.008	0.988	0.000
	Compressed Natural Gas	0.46	2.39	4.12					1.15	2.69	10.44				
H12	Compressed Natural Gas	0.31	2.30	3.97	−3.180	0.001	0.991	0.000	1.29	4.32	11.23	−2.666	0.008	0.77	0.009
	Hybrid Diesel	0.17	1.68	2.75					0.67	1.29	5.26				
34	Hybrid Diesel	0.27	1.64	3.32	−3.296	0.001	0.855	0.000	0.75	1.46	6.04	−2.666	0.008	0.491	0.150
	Electric	2.68	5.86	55.27					10.05	19.24	74.41				

air and the general pollution by traffic. Although our VOCs data from this bus are much higher than what is normal for a commuter bus in Barcelona, others studies have demonstrated that levels of interior BTEX in brand new passenger vehicles can be even higher. A study of newly built coaches less than a month from the production line in China reported BTEX levels that in some cases exceeded 8,000 $\mu g/m^3$, with the highest concentrations peaking at around 15 days after delivery (Lu et al., 2016).

It is also interesting to compare our BUSAIR chemical data with a recent study of air quality inside Barcelona taxis (Moreno et al., 2019). The taxi interiors recorded exactly the same "top-five" distribution of VOCs as observed inside the buses, although at significantly higher concentrations: 2-methylpentane (43–60 $\mu g/m^3$), toluene (37–56 $\mu g/m^3$), xylenes (32–50 $\mu g/m^3$, with m- » o- > p-xylene) and n-pentane (17–28 $\mu g/m^3$). This VOC signature is typical of Barcelona city roadside air and, although varying in concentration, is quite homogeneous in terms of composition. The observation that taxi interior air is higher in VOCs than bus air is consistent with the results of the Taegu study mentioned above (Jo and Yu, 2001), and likely reflects poorer air quality in the more confined breathing space inside smaller vehicles.

5. Conclusions

1. The chemistry of $PM_{2.5}$ measured inside Barcelona public buses is dominated by the presence of OC (typically 10–15 $\mu g/m^3$) and EC (usually 3–6 $\mu g/m^3$), followed by SO_4, Fe, Ca, K, Al_2O_3, Mg and Na. Average OC values are around x3 those of EC average (OC/EC = 3.4), and calculated mineral content is approximately one third that of total carbon content. Most bus pairs used in the study, following the same route but using differing bus models, show little difference in major element $PM_{2.5}$ chemistry, typically varying in EC, OC and mineral content by < 2.5 $\mu g/m^3$, <3 $\mu g/m^3$, and <2 $\mu g/m^3$ respectively. However, major element concentrations of $PM_{2.5}$ in bus interiors are typically 2–8 times higher than urban background levels, reflecting the compromised air quality of the traffic-contaminated city streets.
2. Enhanced concentrations of certain trace metals and metalloids, notably Cu and Sb, inside the buses are attributed to the presence of brake particles entering the bus through doors and windows. In extreme cases, Sb concentrations can exceed x20 that of urban background.
3. Interior bus PM chemistry is not especially affected by the type of fuel used by the bus (with the exception of the electric and diesel bus), and can be affected by seasonal changes in ambient outdoor air. In the case of Barcelona in summer bus $PM_{2.5}$ can contain relatively higher levels of Na, Mg, V, Ni, Cr and SO_4^{2-}, attributed to the ingress of outdoor marine aerosols contaminated by port emissions and the higher SO_2 summer oxidation ratio. In winter, when air conditioning is off and city air is commonly more contaminated, the air inside the bus can be richer in mineral particles, with enhanced levels of trace metals/metalloid such as Mn, Sr, Zn, Zr, Sb and Cu.
4. Interior bus air chemistry can be influenced by both route taken and bus model. Higher gradients favour the ingress of more brake particles and thus affect the chemistry of the PM being inhaled by passengers. In contrast, buses designed to use more engine-braking (such as the Barcelona electric buses) are less contaminated by their own brake PM, especially if the windows are kept closed. Open-topped double decker tourist buses are more directly exposed to fresh traffic emissions (especially on the upper floor) but enhanced air exchange rates maintain elemental PM concentrations slightly below that more typical of enclosed commuter buses.
5. Based on the chemical tracer, the two main sources of particles inside the bus are deduced to be from passenger emissions such as textile fibres and skin flakes (46%) and infiltrated vehicle exhaust and brake wear particles (19%). Other sources include road and urban dust, regional sulphate and shipping and industrial metalliferous particles.
6. The chemical signature of VOCs present in most Barcelona buses is remarkably uniform, irrespective of bus engine type, being dominated by alkanes and aromatics in the following order: 2-methylpentane (14–36 $\mu g/m^3$), toluene (10–30 $\mu g/m^3$), xylenes (10–28 $\mu g/m^3$, with m- » o- > p-xylene) and n-pentane (5–15 $\mu g/m^3$). This is the same mixture recorded inside Barcelona taxis (although inside buses VOC concentrations are usually lower than in taxis) and presumably records the ingress into the vehicle of mostly gasoline-sourced exhaust emissions from outside. Ambient benzene concentrations measured inside the buses were always <5 $\mu g/m^3$. A notable exception to this rule occurs in new buses which can exhibit a very different, and greatly enhanced, VOC signature due to offgassing of interior coatings and materials. In this study one such bus (HD34) recorded exceptionally high concentrations in particular of o-Xylene (160 $\mu g/m^3$), Ethylbenzene (95 $\mu g/m^3$), 2-Methybutane (92 $\mu g/m^3$), p-Xylene (91 $\mu g/m^3$), and Cyclohexane (86 $\mu g/m^3$).
7. BTEX concentrations in Barcelona buses typically range from 25 to 68 $\mu g/m^3$ in a hierarchy of Toluene (10–30 $\mu g/m^3$) > m-Xylene (5–17 $\mu g/m^3$) > p-Xylene (2–5 $\mu g/m^3$) > o-Xylene (3–6 $\mu g/m^3$) > Benzene (2–4 $\mu g/m^3$) and Ethylbenzene (2–7 $\mu g/m^3$). The exceptional levels of VOC offgassing recorded in the new hybrid diesel bus produced interior BTEX concentrations closely approaching 0.5 mg/m^3, although benzene levels still remained below the European Union limit value of 5 $\mu g/m^3$.

Author contributions section

Amaia Fernández-Iriarte: Investigation, data curation, validation. **Fulvio Amato**: Conceptualization, formal analysis. **Natalia Moreno**: Data curation. **Antonio Pacitto**: Data curation. **Cristina Reche**: Visualization. **Esther Marco**: Methodology. **Joan O. Grimalt**: Validation. **Xavier Querol**: Supervision. **Teresa Moreno**: Writing- Reviewing and Editing, project administration.

Declaration of competing interest

The authors declare that they have no known competing financial interests or personal relationships that could have appeared to influence the work reported in this paper.

Acknowledgements

This work is supported by the Spanish Ministry of Economy, Industry and Competitiveness with FEDER funds (BUSAIR CGL2016-79132-R) and by CSIC with the "Proyecto Intramural: Exposición a compuestos organicos volatiles en el interior de autobuses de transporte publico urbano" (201730I003). We are grateful to Transports Metropolitans de Barcelona (TMB) for their co-operation throughout the whole project. Funding from the Generalitat de Catalunya (AGAUR 2017 SGR41) is also acknowledged.

Appendix A. Supplementary data

Supplementary data to this article can be found online at https://doi.org/10.1016/j.atmosenv.2019.117234.

References

Adamice, E., Jarosz-Krzeminska, E., Wieszala, R., 2016. Heavy metals from non-exhaust vehicle emissions in urban and motorway road dusts. Environ. Monit. Assess. 188, 369.

Alameddine, I., Abi Esber, L., Bou Zeid, E., Hatzopoulou, M., El-Fadel, M., 2016. Operational and environmental determinants of in-vehicle CO and PM2.5 exposure. Sci. Total Environ. 551–552, 42–50.

Amato, F., Pandolfi, M., Escrig, A., Querol, X., Alastuey, A., Pey, J., Perez, N., Hopke, P. K., 2009. Quantifying road dust resuspension in urban environment by multilinear engine: a comparison with PMF2. Atmos. Environ. 43, 2770–2780.

Amato, F., Pandolfi, M., Moreno, T., Furger, M., Pey, J., Alastuey, A., Bukowiecki, N., Prevot, A.S.H., Baltensperger, U., Querol, X., 2011. Sources and variability of inhalable road dust particles in three European cities. Atmos. Environ. 45, 6777–6787.

Amato, F., Alastuey, A., de la Rosa, J., Gonzalez Castanedo, Y., Sanchez de la Campa, A., Pandolfi, M., Lozano, A., Contreras, J., Querol, X., 2014. Trends of road dust emissions contributions on ambient air particulate levels at rural, urban and industrial sites in southern Spain. Atmos. Chem. Phys. 14, 3533—3544.

Cepeda, M., Schoufour, J., Freak-Poli, R., Koolhaas, C., Dhana, K., Bramer, W., Franco, O., 2017. Levels of ambient air pollution according to mode of transport: a systematic review. The Lancet Public Health 2, 23–34.

Chen, X., Zhang, G., Zhang, Q., Chen, H., 2011. Mass concentrations of BTEX inside air environment of buses in Changsha, China. Build. Environ. 46, 421–427.

Chernyshev, V., Zakharenko, A., Ugay, S., Hien, T., Hai, L., Olesik, S., Kholodov, A., Zubko, E., Kokkinakis, T., Burykina, T., Stratidakis, A., Mezhuev, Ya, Sarigiannis, D., Tsatsakis, A., Golokhvast, K., 2019. Morphological and chemical composition of particulate matter in buses exhaust. Toxicology Reports 6, 120–125.

Chin, J.-Y., Batterman, S.A., 2012. VOC composition of current motor vehicle fuels and vapors, and collinearity analyses for receptor modeling. Chemosphere 86 (9), 951–958.

Fondelli, C., Chellini, E., Yli-Tuomi, T., Cenni, I., Gasparrini, A., Nava, S., Garcia-Orellana, S., Lupi, A., Daniele Grechi, D., Mallone, S., Jantunen, M., 2008. Fine particle concentrations in buses and taxis in Florence, Italy. Atmos. Environ. 42, 8185–8193.

Fruin, S., Hudda, N., Sioutas, C., Delfino, R.J., 2011. Predictive model for vehicle air exchange rates based on a large, representative sample. Environ. Sci. Technol. 45 (8), 3569–3575.

Grigoratus, T., Martini, G., 2015. Brake wear particle emissions: a review. Environ. Sci. Pollut. Res. 22, 2491–2504.

Haagen-Smit, A.J., 1966. Carbon monoxide levels in city driving. Archives of Environ. Health 12, 548–551.

Hudda, N., Kostenidou, E., Delfino, R., Sioutas, C., Fruin, S., 2011. Factors that determine ultrafine particle exposure in vehicles. Environ. Sci. Technol. 45 (20), 8691–8697.

Hudda, N., Eckel, S., Knibbs, L., Sioutas, C., Delfino, R., Fruin, S., 2012. Linking in-vehicle ultrafine particle exposures to on-road concentrations. Atmos. Environ. 59, 578–586.

Hudda, N., Fruin, S., 2018. Carbon dioxide accumulation inside vehicles: the effect of ventilation and driving conditions. Sci. Total Environ. 610–611, 1448–1456.

Jo, W., Yu, C., 2001. Public bus and taxicab drivers' work-time exposure to aromatic volatile organic compounds. Environ. Res. 86, 66–72.

Kerchich, Y., Kerbachi, R., 2012. Measurement of BTEX (benzene, toluene, ethylbenzene, and xylene) levels at urban and semirural areas of Algiers City using passive air samplers. J. Air Waste Manag. Assoc. 62, 1370–1379.

Leavey, A., Reed, N., Patel, S., Bradley, K., Kulkarni, P., Biswas, P., 2017. Comparing on-road real-time simultaneous in-cabin and outdoor particulate and gaseous concentrations for a range of ventilation scenarios. Atmos. Environ. 166, 130–141.

Lee, E., Stenstrom, M., Zhu, Y., 2015. Ultrafine particle infiltration into passenger vehicles. Part 1: experimental evidence. Transp. Res. Part D 38, 156–165.

Lu, Y., Lin, Y., Zhang, H., Ding, D., Sun, X., Huang, Q., Lin, L., Chen, Y., Chi, Y., Dong, S., 2016. Evaluation of volatile organic compounds and carbonyl compounds present in the cabins of newly produced, medium- and large-size coaches in China. Int. J. Environ. Res. Public Health 13, 596.

Madl, P., Majid, H., Kwasny, F., Hofmann, W., 2015. In-vehicle exposure to ultrafine particles while driving through a tunnel system and associated lung deposition calculations. Aerosol and Air Quality Res 15, 295–305.

Marco, E., Grimalt, J.O., 2015. A rapid method for the chromatographic analysis of volatile organic compounds in exhaled breath of tobacco cigarette and electronic cigarette smokers. J. Chromatogr. 1410, 51–59.

Minguillón, M.C., Schembari, A., Triguero-Mas, M., de Nazelle, A., Dadvand, P., Figueras, F., Salvado, J.A., Grimalt, J.O., Nieuwenhuijsen, M., Querol, X., 2012. Source apportionment of indoor, outdoor and personal PM2.5 exposure of pregnant women in Barcelona, Spain. Atmos. Environ. Times 59, 426–436.

Montells, R., Aceves, M., Grimalt, J.O., 2000. Sampling and analysis of volatile organic compounds emitted from leaded and unleaded gasoline powered motor vehicles. Environ. Monit. Assess. 62, 1–14.

Moreno, T., Reche, C., Rivas, I., Minguillón, M.C., Martins, V., Vargas, C., Buonanno, G., Parga, J., Pandolfi, M., Brines, M., Ealo, M., Fonseca, A., Amato, F., Sosa, G., Capdevila, M., de Miguel, E., Querol, X., Gibbons, W., 2015. Urban air quality comparison for bus, tram, subway and pedestrian commutes in Barcelona. Environ. Res. 142, 495–510.

Moreno, T., Pacitto, A., Fernández, A., Amato, F., Marco, E., Grimalt, J.O., Buonanno, G., Querol, X., 2019. Vehicle interior air quality conditions when travelling by taxi. Environ. Res. 172, 529–542.

Ongwandee, M., Chavalparit, O., 2010. Commuter exposure to BTEX in public transportation modes in Bangkok, Thailand. J. Environ. Sci. 22, 397–404.

Paatero, P., Tapper, U., 1994. Positive matrix factorization: a non-negative factor model with optimal utilization of error estimates of data values. Environmetrics 5, 111–126.

Paatero, P., Hopke, P.K., 2003. Discarding or downweighting high-noise variables in factor analytic models. Anal. Chim. Acta 490 (1–2), 277–289, 25.

Paatero, P., 2007. End User's Guide to Multilinear Engine Applications.

Parra, M., Elustondo, D., Bermejo, R., Santamaría, J.M., 2008. Exposure to volatile organic compounds (VOC) in public buses of Pamplona, Northern Spain. Sci. Total Environ. 404, 18–25.

Querol, X., Alastuey, A., Rodríguez, S., Plana, F., Mantilla, E., Ruiz, C.R., 2001. Monitoring of PM10 and PM2.5 around primary particulate anthropogenic emission sources. Atmos. Environ. 35, 845–858.

Rivas, I., Viana, M., Moreno, T., Pandolfi, M., Amato, F., Reche, C., Bouso, L., Àlvarez-Pedrerol, M., Alastuey, A., Sunyer, J., Querol, X., 2014. Child exposure to indoor and outdoor air pollutants in schools in Barcelona, Spain. Environ. Int. 69, 200–212.

Tartakovsky, L., Baibikov, V., Czerwinski, J., Gutmana, M., Kasper, M., Popescu, D., Veinblata, M., Zvirina, Y., 2013. In-vehicle particle air pollution and its mitigation. Atmos. Environ. 64, 320–328.

Xing, L., Wang, L., Zhang, R., 2018. Characteristics and health risk assessment of volatile organic compounds emitted from interior materials in vehicles: a case study from Nanjing, China. Environ. Sci. Pollut. Res. Int. 25 (15), 14789–14798.

Yang, F., Kaul, D., Wong, K., Westerdahl, D., Sun, L., Ho, K., Tian, L., Brimblecombe, P., Ning, Z., 2015. Heterogeneity of passenger exposure to air pollutants in public transport microenvironments. Atmos. Environ. 109, 42–51.

Yang, C., Brown, C.E., Hollebone, B., Yang, Z., Lambert, P., Fieldhouse, B., Landriault, M., Wang, Z., 2017. Chemical fingerprints of crude oils and petroleum products. In: Fingas, Mervin (Ed.), In Book: Oil Spill Science and Technology, second ed. Gulf Professional Publishing, Elsevier Inc., pp. 209–304. https://doi.org/10.1016/B978-0-12-809413-6.00004-7 Chapter: 4.

Yue, T., Yue, X., Chai, F., Hu, J., Lai, Y., He, L., Zhu, R., 2017. Characteristics of volatile organic compounds (VOCs) from the evaporative emissions of modern passenger cars. Atmos. Environ. 151, 62–69.

Zhang, Q., Fischer, H., Weiss, R., Zhu, Z., 2013. Ultrafine particle concentrations in and around idling school buses. Atmos. Environ. 69, 65–75.

Zhu, Y., Eiguren-Fernandez, A., Hinds, W., Miguel, A., 2007. In-cabin commuter exposure to ultrafine particles on Los Angeles freeways. Environ. Sci. Technol. 41, 2138–2145.

Article 2

Bioaerosols in public and tourist buses

Amaia Fernández-Iriarte, Caroline Duchaine, Jodelle Degois, Hamza Mbareche, Marc Veillette, Natalia Moreno, Fulvio Amato, Xavier Querol, Teresa Moreno
Aerobiologia 223, 117234
https://doi.org/10.1007/s10453-021-09704-9
2021

Aerobiologia
https://doi.org/10.1007/s10453-021-09704-9

ORIGINAL PAPER

Bioaerosols in public and tourist buses

Amaia Fernández-Iriarte · Caroline Duchaine · Jodelle Degois · Hamza Mbareche · Marc Veillette · Natalia Moreno · Fulvio Amato · Xavier Querol · Teresa Moreno

Received: 22 September 2020 / Accepted: 23 March 2021

Abstract Public bus system worldwide transports daily more than 34 million people; therefore, air quality inside buses is an important urban air pollution issue. Airborne microbiological composition and abundance was examined inside five different fuel type buses (diesel (EURO IV and EURO V), hybrid diesel (HD), compressed natural gas (CNG), hybrid natural gas (HCNG) and electric vehicle (EV)) from Barcelona bus system, inside and outside the tourist bus and different periods of campaigns (summer: May–September and winter: November–March). Quantitative PCR was used to quantify total bacteria, *Penicillium/Aspergillus* and *Cladosporium sp.* and Kinetic Chromogenic *Limulus Amebocyte Lysate* (LAL) Assay for endotoxins. The targeted 16S rRNA genes were amplified and sequenced to asses bacterial community composition and biodiversity. Regarding the targeted microorganisms, the results showed low bioaerosol concentrations, being fungi and endotoxins below the detection limit, although bacterial airborne has a geometric average of 10^3 equivalent *E. Coli* genomes/m^3. Airborne bacterial community biodiversity showed that *Actinobacteria* and *Proteobacteria* were the most abundant Phylum in the different sampled buses and in the two seasons (summer: May–September and winter: November–March). While regarding to genera taxonomic category, the different fuel type buses presented a high overlap degree, being *Cutibacterium* the most abundant and *Paracoccus* the one only detected inside. The different seasons showed that the different taxonomic genera decrease from summer: May–September to winter: November–March and in this case *Paracoccus* was the most abundant. Overall, biodiversity inside buses is greatly affected by the presence of humans inside, but also by the outdoor sources at the moment of the sampling, and the seasonal period, more than the type of bus.

Keywords Bioaerosols · Public buses · Indoor air quality · Tourist bus

Supplementary Information The online version contains supplementary material available at https://doi.org/10.1007/s10453-021-09704-9.

A. Fernández-Iriarte · N. Moreno · F. Amato · X. Querol · T. Moreno
Institute for Environmental Assessment and Water Studies (IDAEA), Spanish Research Council (CSIC), 18-26 Jordi Girona, 08034 Barcelona, Spain

A. Fernández-Iriarte
Department of Natural Resources and Environment, Industrial and TCI Engineering (EMIT), Universitat Politécnica de Catalunya (UPC), 08242 Manresa, Spain

C. Duchaine (✉) · J. Degois · H. Mbareche · M. Veillette
Centre de Recherche de L'Institut Universitaire de Cardiologie Et de Pneumologie de Québec (IUCPQ), Université Laval, Québec City, Québec G1V 4G5, Canada
e-mail: Caroline.Duchaine@bcm.ulaval.ca

C. Duchaine
Canada Research Chair On Bioaerosols, Quebec, Canada

Published online: 09 April 2021

1 Introduction

In the last two decades, indoor air quality has become a subject of major public concern because of its potential health effects, since people tend to stay most of their time in closed environments due to civilization development (Norback 2009; EEA 2018). Thus, many of us might spend up to 90% of our day indoors including time at home, work, school, shopping or commuting (Karanasiou et al. 2014).

In this sense, buses, as other commuting modes, are an important microenvironment for environmental exposure. In Barcelona, public transport is used every day by more than a half of the city commuters, almost 3 million, on journeys lasting from 30 to 60 min every working day. External weather conditions or technologies within the vehicle, such as brake and tire wear, road abrasion, fuel, interior coatings and materials, are also responsible for the indoor air quality (Nowakowicz-Dębek et al. 2017).

Several studies have already reported that air quality experienced by travellers when inside the bus could be affected by elevated concentrations of different pollutants, including BC, PM, UFP, CO_2, NO_2, VOCs or O_3 (de Nazelle et al. 2017; Kaur et al. 2005; Knibbs & de Dear, 2010; Lim et al. 2015; Molle et al. 2013). Rivas et al. (2017) found that travelling inside London transport buses provided the highest exposure levels of ultrafine particles (UFP) and black carbon (BC), compared to the rest of commuting modes. $PM_{2.5}$ mass concentration has also been reported to be higher inside buses than in taxis, with a mean value of 56 ± 15 μg/m^3 and 39 ± 15 μg/m^3, respectively, while the corresponding concentrations recorded simultaneously at the urban background were half (Fondelli et al. 2008). Kingham et al. (2013) showed that both PM_1 and UFP levels were higher in buses compared to the car, bike (on-road and off-road) and metro. Similar results have been reported in Barcelona (Moreno et al. 2015), Shanghai (Tan et al. 2017) and Sydney (Knibbs & de Dear, 2010), where buses were the most polluted commuting mode compared to metro, tram, walking, taxi, train, ferry or car.

In addition, the interior of the bus can also be considered a place of health risks due to the constant contact with passengers among whom some can be ill or disease carriers (Nowakowicz-Dębek et al. 2017). Bioaerosols including bacteria, fungi and endotoxins are airborne biological particulate matter that can affect living beings through infectious, allergic, toxic and irritating processes to which bus commuters can be exposed. Their diameters range from 0.3 to 100 μm, which is included within the breathable size of 1 to 10 μm (Cox & Wathes, 1995). Concentrations of bacterial bioaerosols indoors are strongly linked to human activities, as human presence and moving activities increase their concentrations, and they are related to human diseases, such as pneumonia and tuberculosis. Fungal bioaerosols can be agents of respiratory diseases, such as allergic rhinitis and asthma (Lee et al. 2016). A study of Priyamvada et al. (2018) in India showed that the origin of fungi in indoor air is mostly due to the penetration of outdoor air, dominated by *Cladosporium* and *Aspergillus,* while bacteria were released by human shedding and resuspension. Endotoxins are active lipopolysaccharide molecules which are cell wall components of the outer membrane of Gram-negative bacteria, and they are ubiquitous in indoor and outdoor environments. Endotoxin inhalation may cause dry cough and shortness of breath accompanied by decreased lung function, fever reactions and malaise, and sometimes headache and joint aches occurring within a few hours of exposure (Lehtinen et al. 2013).

Due to the relevance of bioaerosols to human diseases, their concentration in indoor environments can be an important parameter in predicting the occurrence of such diseases. To date, bioaerosols have been measured in several of these microenvironments, such as public restrooms, public hospitals, houses, subway commuting and workplaces (Gołofit-Szymczak & Górny, 2010; Ghosh et al. 2015; Lee et al. 2016; Triadó-Margarit et al. 2016). Commuting microenvironments play an important role in term of air pollutants exposure as we spent there a significant part of the day, with multiple variables affecting the quality of the air we breathe when we are travelling inside them. Thus, important factors that can modify bioaerosol concentrations inside a bus, as for the chemical pollutants, is the ventilation type and air-conditioning (AC) system (Sowiak et al. 2018). Thus, previous studies inside households, university rooms, cars and other indoor spaces, have probed that the use of AC systems when not well designed or maintained can become an additional source of fungal aerosols introduced into indoor air (Almoffarreh et al. 2016; Hamada & Fujita, 2002). It was shown that during the

first 10 min of AC powered on fungal concentrations were highest (Hamada & Fujita, 2002; Jo & Lee, 2008). However, Sowiak et al. (2018) evaluated ventilation differences between 30 same type buses (10 of them with natural ventilation and 20 with AC), and showed that there is no strong evidence that AC system is an additional source of indoor air contamination with fungi. Few buses in this study showed higher concentrations of fungi in AC buses. In both, AC buses and non-AC buses, the presence of allergenic fungi genera *Aspergillus, Penicillium and Cladosporium* section were confirmed.

The aim of this study is therefore to investigate the presence and nature of total (culture independent) bacterial and fungal bioaerosols and endotoxins in the interior of public buses, and the factors affecting their presence and concentrations. For this, two different campaigns were carried out where different fuel type buses including diesel (EURO IV and EURO V), hybrid diesel (HD), compressed natural gas (CNG), hybrid natural gas (HCNG) and electric vehicle (EV), were sampled while travelling through the urban environment of Barcelona. In addition, tourist (EUROIV) open top double-decker buses were also studied in both lower and upper deck.

2 Methodology

2.1 Sampling sites

Monitoring sampling was carried out between May 2017 and March 2018 in different buses from the Metropolitan Transports of Barcelona (TMB), Spain. It was divided in two different campaigns, "summer", from May 2017 to September 2017, and "winter", from November 2017 to March 2018, seasons being defined according to the TMB annual ventilation protocols. Different types of fuel buses and bus lines were chosen in order to have representative results from the whole fleet of the company, including diesel, HD, CNG, HCNG and EV buses. The Barcelona bus system comprises 101 lines built progressively since 1906 (https://www.tmb.cat/documents/20182/111197/NOTICIES-NOVA-XARXA-BUS-20120523-TRANSPORT.pdf/37f4bca7-d018-4e73-9da3-f9cee5842448). The system carries around 203 million passengers a year (2018) and its network length is of 829.68 km. Almost all the lines run from 5 am to 23 pm every day, and all buses are equipped with an AC system, which functioning starts on spring, until the end of the summer (this corresponding to the summer: May–September campaign). At the time of the campaigns passengers were allowed to open/close the windows upon their necessities in most of the buses, except for the electric buses, where the window system was hermetically closed and climate control was regulated by the driver.

All sampling was done each day by two commuters taking samples from two different fuel type buses from the same line. The route was a round trip for each line, which lasted approximately 2 h (the shortest trip was about 82 min, the largest 171 min, and the median 123 min), c. 2.8 km, and it was repeated two consecutive days. The same bus pair comparison was made in both, summer: May–September and in winter: November–March, campaigns. A total of 100 buses (fifty per campaign) were sampled, including diesel (EURO V and EURO IV), HD, CNG, HCNG and EV buses, and two open tourist bus lines (EURO IV). All kinds of fuel types were compared in pairs except from HCNG, due to the low availability of this type of bus (only possible to compare with CNG). The quantity of samples recollected per fuel type was: 15 EURO V, 14 EURO IV, 17 HD, 20 CNG, 4 HCNG, 14 eV and 8 inside and 8 outside the tourist bus. Table 1 summarizes all the comparisons that have been done for both campaigns, including line and date information. Measurements inside the buses were performed in the middle of the bus, where the space for a wheelchair and strollers is located. Notes were taken during the sampling, taking into account the number of passengers, if the AC was functioning or not, and if the windows were open.

Environmental conditions like temperature and relative humidity (RH) were measured. Temperature mean ranges were 19–27 °C in the summer: May–September campaign, with a mean media of 23.2 °C and 38–64% mean ranges of RH with a mean media of 50.41%. Winter: November–March campaign temperature mean ranged between 13.8–25.2 °C, with a mean media of 19 °C, and RH mean range of 28–45% and a means media of 35.38%.

2.2 Sampling equipment and preparation

Bioaerosol and endotoxin samples were collected in each bus in 37-mm glass-fibre filters of 0.8 µm pore size loaded in closed-faced cassettes (CFC, SKC),

Table 1 Comparisons achieved per campaign including bus line and date information. HD: Hybrid Diesel; CNG: Compressed Natural Gas; HCNG: Hybrid Natural Gas; EV: Electric Vehicle

Bus pair	Summer		Winter	
	Line	Date	Line	Date
EURO V versus EURO IV	V13	10, 11 May	V3	16, 17 Jan
EURO V versus HD	V13	16, 17 May	H4	14, 15 Nov
EURO V versus CNG	V3	30, 31 May	V3	1, 12 Dec
EURO V versus EV	34	14, 15 Sep	–	–
EURO IV versus HD	47	10, 12 July	19	14, 15 Dec
EURO IV versus CNG	V17 vs V11	20, 21 Sep	V3	23, 24 Nov
EURO IV versus EV	–	–	60	10, 12 April
HD versus CNG	H12	18, 19 Jul	H12	26 Feb., 1 Mar
HD versus EV	34	23, 24 May	34	27, 28 Mar
CNG versus HCNG	39	13, 14 Jun	39	10, 11 Jan
CNG versus EV	H16	8, 9 Jun	H16	19, 20 Feb
Tourist inside versus outside	Blue	20, 21 Jun	Blue	23, 24 Jan
Tourist inside versus outside	Red	26, 27 Jun	Red	30, 31 Jan

which were connected to personal air sampling pumps (Gilian GilAir-5, Sensidyne, LP) previously calibrated with DryCal DC-2 flowmeter (Bios). The sampling was done for 2 h/day two consecutive days at a flow rate of 2 L/min. Samples were kept in a 4 °C fridge until measurement. All samples were then sent to the University Institute of Cardiology and Pulmonology of Quebec—Laval University, for analysis of total bacteria and fungi concentrations and endotoxins.

2.3 Sample processing and analyses

The pre-treatment of the filters for downstream analysis was the same for all the study experiments (Fig. 1). First of all, the glass-fibre filter was placed in a 50 mL sterilized falcon tube that was eluted with 20 mL of the extraction solution (saline water, 0.9% NaCl, containing 0.025% of Tween 20, Sigma-Aldrich, P2287). After 60 min of vortexing at 4 °C (Multi-Pulse Vortexer, Glas-Col, Terre Haute, Ind.), each sample was centrifuged (Centrifuge 5810R, Eppendorf) for 10 min at 5000 rpm (2800 G-force or RCF) and 4 °C to pellet the debris. A volume of 1 mL of debris free aliquot was taken for endotoxin assay. The rest of the supernatant was filtered, to concentrate all the microbial cells as described in Mbareche et al. 2019, and was used to analyze total bacteria, *Penicillium/Aspergillus,* and *Cladosporium* fungi. Both aliquots were stored at -20 °C freezer, until their analysis.

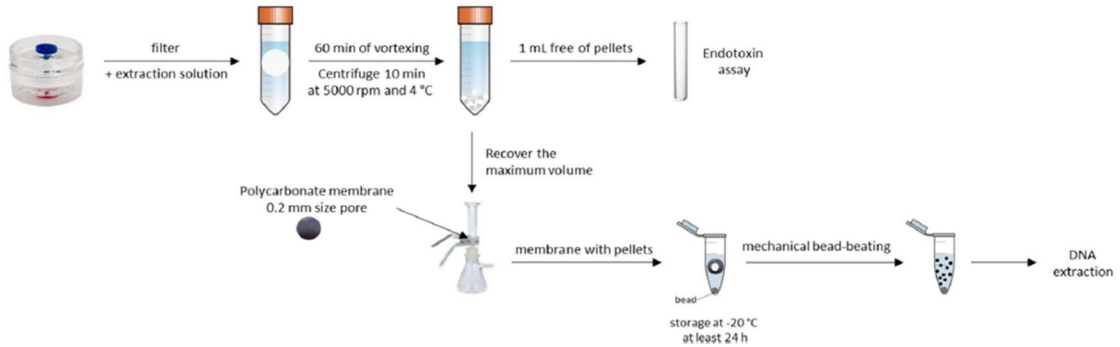

Fig. 1 Filter treatment diagram to obtain aliquots for endotoxin assay and DNA extraction, with its prior cells concentration protocol

2.3.1 Microbial concentration measurement by qPCR

DNA extraction was performed on pellets obtained from the previous step, using a Qiagen commercial DNasay kit (Qiagen, Mississauga, Ontario, Canada) according to the protocol established by the manufacturer. Concentrations of total bacteria, *Penicillium/Aspergillus and Cladosporium* sp. were assessed by qPCR. Primers, probes, master mix preparation and thermoprotocols are described in Table 2. All master mixes were prepared using iQ Supermix 1X (BioRad, Canada). Standard curves were prepared by diluting in series DNA from *Escherichia coli* (ATCC 25,922), *Aspergillus fumigatus* colonies (isolated from peatland/air samples) and *Cladosporium* sp. (colony isolated from indoor air) for total bacteria, *Penicillium/Aspergillus* and *Cladosporium sp.* qPCR respectively. All qPCR runs were performed using thermal cycler CFX96™ Real Time System (BioRad, Canada) for 40 cycles (Table 2). Data were analyzed using the

Table 2 Primers/probes, master mix composition and the thermoprotocol used for each analysis (total bacteria, *Penicillium/Aspergillus* and *Cladosporium* sp.)

Target	Primers/probe	Master mix composition	Temperature cycles	Reference
Total bacteria (16S rDNA)	EUBf: [5′-GGTAGTCYAYGCMSTAAACGT-3′] EUBr: [5′-GACARCCATGCASCACCTG-3′] EUBP: FAMa-5′-TKCGCGTTGCDTCGAATTAAWCCAC-3′ IBTMFQb]	Primers (F + R): 50 µM Probe: 10 µM iQ SuperMix: 10 µL DNA template: 5 µL Water: 4.5 µL Final volume: 20 µL	Initial denaturation: 95 °C, 3 min Denaturation: 95 °C, 20 s Hybridization and elongation: 62 °C, 60 s	Bach et al. 2002
Penicillium/Aspergillus (18S rDNA)	PenAspF1: 5′- CGG AAG GAT CAT TAC TGA GTG-3’ PenAspR1: 5′- GCC CGC CGA AGC AAC-3’ PenAspP1mgb: 5′-FAM-CCA ACC TCC CAC CCG TG-TAMRA-3’	Primers (F + R): 50 µM Probe: 10 µM iQ SuperMix: 10 µL DNA template: 5 µL Water: 4.5 µL Final volume: 20 µL	Initial denaturation: 94 °C, 3 min Denaturation: 94 °C, 15 s Hybridization and elongation: 60 °C, 60 s	EPA, 2019
Cladosporium sp. (18S rDNA)	Clado-TaqMan-PF: 5′-CCTCAACGTCAGTTATTACAT -3’ Clado-TaqMan-PR: 5′-ACCTAGACAGTATTTCTAGCCT -3’ Clado-TaqMan-PB: 5′-FAM-CTACTCCAATGGTTCTAATATTTTCCTCTC -BHQ-3’	Primers (F + R): 50 µM Probe: 10 µM iQ SuperMix: 10 µL DNA template: 2 µL Water: 7.5 µL Final volume: 20 µL	Initial denaturation: 95 °C, 5 min Denaturation: 95 °C, 10 s Hybridization and elongation: 60 °C, 60 s	Zeng et al. 2006

software CFX Manager version 3.1 (BioRad, Canada). Microbial concentrations were expressed in *E. coli* genome equivalent/m^3, *A. Fumi* genome equivalent/m^3, *Clado* genome equivalent/m^3 for total bacteria, *Penicilium/Aspergillus* sp. and *Cladosporium* sp. respectively.

2.3.2 MiSeq Illumina® sequencing

The amplification of targeted genes, equimolar pooling, and sequencing were performed at the Plateforme d'analyses génomiques (IBIS, Université Laval, Québec, QC, Canada). The 16S rRNA V6-V8 region was amplified using the sequence-specific regions described in Comeau et al. (2011) using a two-step dual-indexed PCR approach, specifically designed for Illumina® instruments, San Diego, California, United States. The gene-specific sequence was first fused to the Illumina® TruSeq sequencing primers and PCR was carried out in a total volume of 25 µL containing 1 × Q5 buffer (NEB, Ipswish, MA, USA), 0.25 µM of each primer, 200 µM of each of the dNTPs, 1 U of Q5 High-Fidelity DNA polymerase (NEB) and 1 µL of template DNA. PCR thermoprotocol began with an initial denaturation at 98 °C for 30 s followed by 35 cycles of denaturation at 98 °C for 10 s, annealing at 55 °C for 10 s, extension at 72 °C for 30 s and a final extension at 72 °C for 2 min. The PCR reaction was purified using the Axygen PCR cleanup kit (Axygen®, Waltham, MA, USA). The quality of the purified PCR product was checked on a 1% agarose gel. A fifty to 100-fold dilution of the purified product was used as a template for a second round of PCR in order to add barcodes (dual-indexed) and for missing sequences required for Illumina sequencing. The thermoprotocol for the second PCR was identical to the first one but with 12 cycles. PCR reactions were purified again in the same way as above, checked for quality on a DNA7500 Bioanalyzer chip (Agilent®, Santa Clara, CA, USA) and then quantified spectrophotometrically with the Nanodrop® 1000 (Thermo Fisher Scientific, Waltham, MA, USA). Barcoded amplicons were pooled in equimolar concentrations for sequencing on the Illumina® MiSeq machine. The oligonucleotide sequences that were used for PCR amplification are presented in Table 3.

Regarding Bioinformatics, it was applied to EURO IV, EURO V, HD and GNG, as they had enough bacterial concentration and EV and HCNG were excluded due to small number of samples with that bacterial load. Briefly, after de-multiplexing the raw FASTQ files, the reads generated from the paired end sequencing were combined using the *make.contigs* script from mothur (Schloss et al. 2009). Quality filtering was also performed with mothur, using the *screen.seqs* script to discard homopolymers, reads with ambiguous sequences, and reads with suspiciously short lengths (reads shorter than a 100 bp and longer than 500 pb were discarded to insure selection of overlapping paired-end reads). Similar sequences were gathered together in order to reduce the computational burden, and the number of copies of the same sequence was displayed to monitor the abundance of each sequence. This de-replication step was performed with VSEARCH (Rognes et al. 2016). The sequences were then aligned with the bacterial reference SILVA core alignment using the QIIME script *align_seqs.py* (Caporaso et al. 2011). Operational taxonomic units (OTUs), with a 97% similarity cut-off, were clustered using the UPARSE method implemented in VSEARCH. UCHIME was used to identify and remove the chimeric sequences (Edgar et al. 2011). QIIME was used to assign taxonomy to OTUs based on the SILVA v132 database reference training dataset for taxonomic assignment and to generate an OTU table. A metadata-mapping file was produced that includes information about air samples. The microbial diversity analyses, including statistical analyses, conducted in this study, were achieved using QIIME plugins in version 1.9.0 as described in QIIME scripts (http://qiime.org/scripts/). A total of 304,394 reads were obtained from 16 samples. The minimum number of reads per sample obtained was 14,447 and the maximum was 23,279 (average 19,024.63 – Std. dev. 2474.69). The reads clustered into 646 OTUs. The final reads were rarefied at a sequencing depth of 14,000 reads per sample.

Raw sequence reads of every sample used in this study and that support its findings have been deposited in the National Center for Biotechnology Information (NCBI) under the BioProject ID: PRJNA687990.

2.3.3 Endotoxin assay

The debris-free aliquot obtained from filter extraction was used for endotoxin quantification using a *Limulus Amebocyte Lysate* (LAL) Kinetic-QCL® kit Kinetic Chromogenic LAL Assay (Lonza, Walkersville,

Table 3 Primers used for PCR amplification of the 16S rRNA gene

Primers [a]	Sequences 5′ to 3′
First-PCR primers	Forward: 5′-ACACTCTTTCCCTACACGACGCTCTTCCGATCTACGCGHNRACCTTACC-3′
	Reverse: 5′-GTGACTGGAGTTCAGACGTGTGCTCTTCCGATCTACGGGCRGTGWGTRCA-3′
Second-PCR primers	Forward: 5′AATGATACGGCGACCACCGATCTACA[index1]ACACTCTTTCCCTACACGAC-3′
	Reverse: 5′CAAGCAGAAGACGGCATACGAGAT[index2]GTGACTGGAGTTCAGACGTGT-3′

[a]Primers used in this work contain Illumina® specific sequences protected by intellectual property (Oligonucleotide sequences © 2007–2013 Illumina, Inc. All rights reserved. Derivative works created by Illumina customers are authorized for use with Illumina instruments and products only. All other uses are strictly prohibited)

Maryland, USA) according to the protocol established by the manufacturer.

Endotoxins from *Escherichia coli* O55:B5 were used as a standard. An inhibition/enhancement test was performed prior to measurement (Hollander et al. 1993). Runs were performed using a plate reader (Synergy H1 Hybrid Multi-Mode Reader, BioTek, Winooski, VT, USA) and data were analyzed using the software Gene5 2.00 (BioTek, Winooski, NH, USA). Endotoxin concentrations were expressed as endotoxin units per cubic meter of air (EU/m^3).

2.4 Statistical analysis

The statistical analyses were run in Prism version 8.0 (GraphPad). Different tests were applied: Mann Whitney test to see if there were significant differences between both sampling campaigns, Kruskal–Wallis test for bus fuel type differences, Wilcoxon matched-pairs signed rank test for differences between inside and outside tourist bus.

For alpha diversity measures, the normality was verified using the D'Agostino and Pearson omnibus normality test. The assumption of data normality was not fulfilled. Nonparametric Mann–Whitney *U* tests (two-tailed) were performed to highlight that there are significant differences in diversity measures between the groups of samples. A p value ≤ 0.05 was considered statistically significant. All of the results were analyzed using the software GraphPad Prism 5.03 (GraphPad Software, Inc., San Diego, California, United States). Detailed information about the performance of the test is presented in the multivariate section of the results. The nonparametric Mann–Whitney *U* test was used to evaluate the significance of the relative abundance of taxa and to ascertain whether or not differences in OTU abundances were statistically significant between the group of samples. To test OTU differential abundance, the null hypothesis was that the populations of the two groups of samples were collected from have equal means.

3 Results and discussion

3.1 Total bacteria quantification

Of 100 bioaerosol samples, total bacteria were detected in 94, (46 of 50 in summer: May–September and 48 of 50 in winter: November–March). The detection limit of the sampling procedure was 2.5×10^0 equivalent *E. coli* genomes/m^3 of air, and the concentrations of samples that were below the detection limit were defined as 1.25×10^0 equivalent *E. coli* genomes/m^3 of air. Total bacteria concentrations in the summer: May–September campaign ranged between 1.25×10^0 and 3.49×10^4 equivalent *E. coli* genomes/m^3 of air, which correspond to a geometric average (GA) concentration of $9.63 \times 10^2 \pm 7.21 \times 10^0$ equivalent *E. coli* genomes/m^3 of air for the summer: May–September campaign (a total of 50 filters), whereas for winter: November–March total bacteria concentrations ranged between 1.25×10^0 and 2.28×10^4 equivalent *E. coli* genomes/m^3 of air, which correspond to a GA concentration of $2.63 \times 10^3 \pm 1.31 \times 10^1$ equivalent *E. coli* genomes/m^3 of air. Mann Whitney test confirmed that there are significant differences (P-value 0.0208) between the different campaigns. In addition, Kruskal–Wallis test confirmed that there is no significant difference (P-value 0.2733) between different types of fuel (this statistical analysis was

made for all the samples, taking both campaigns into account). No statistical significant difference was noted between inside (lower floor) or outside (upper floor) the tourist bus, as demonstrated by Wilcoxon matched-pairs signed rank test and Mann Whitney test. A ventilation system working efficiently help reduce contaminants in the inside air, which could explain why inside the tourist bus had similar concentration of equivalent *E. coli* genomes compared to the open upper floor.

Total airborne bacteria geometric average concentration was approximately 1.35×10^3 equivalent *E. coli* genomes/m^3 lower than the one detected in the Barcelona subway system (Triadó-Margarit et al. 2016). *E. coli* genome eq. median values were highest inside EURO V and HCNG buses, while the lowest value was found inside EV buses (Fig. 2). As EV buses do not allow opening windows, they always have the ventilation on, which can help reducing bacterial concentration entering inside the bus with passengers (Bonetta et al. 2010; Maestre et al. 2018). *E. coli* concentrations were also lower in the tourist bus when travelling outside in the open upper floor.

When analyzing the total concentration clustered by campaign (summer: May–September and winter: November–March, according to TMB ventilation protocols) the bacterial load was higher in winter: November–March (Fig. 3), as it was expected, due to less ventilation as the AC is not functioning, as opposed to summer: May–September. Nowakowicz-Dębek et al. (2017) have analyzed microorganisms inside public buses in winter, autumn and spring, in Lublin, Poland, and showed that the highest concentration of total bacteria was detected in winter, while the lowest in spring. In contrast, for Lee and Jo (2005) in a study in Daegu, Korea, total bacteria concentration inside buses was higher in summer than in winter, however these comparison must be taken with care as the "summer: May–September" and "winter: November–March" periods were not the same, and the

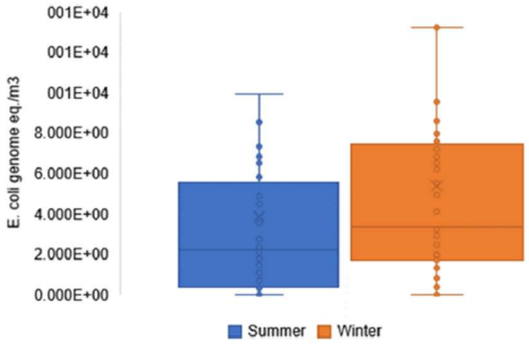

Fig. 3 Concentrations of airborne Bacterial 16S rDNA gene copies determined by qPCR analyses for different seasons

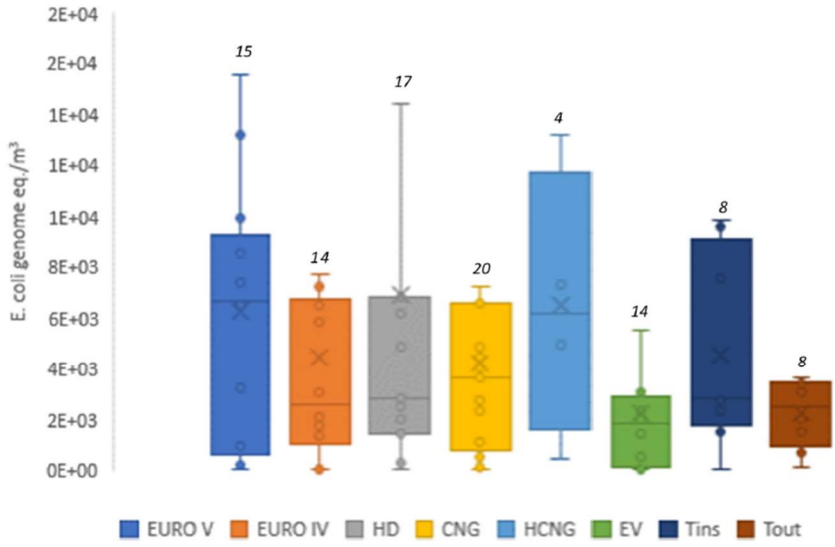

Fig. 2 Concentrations of airborne Bacterial 16S rDNA gene copies determined by qPCR analyses for different fuel/engine type and tourist buses. The number above each of the boxes refers to the number of samples taken in each kind of fuel bus

methodology for sampling was also different in each study.

3.2 Biodiversity analysis

3.2.1 Powertrain/fuel type bus differences

As in 94 of 100 samples bacterial load was detected, a biodiversity study was carried out in order to determine the microbial diversity present in different type of buses (excluding HCNG and EV due to small number of samples with enough bacterial concentration). In the case of samples taken in tourist buses, we can also see the differences between the inside and the outside.

CNG buses were the richest in terms of the number of observed OTUs, followed by HD, EURO V and EURO IV (Fig. 4). The slope of the curves shows sufficient sequencing depth and good bacterial coverage in all samples, as no more OTUs were identified even with a higher number of sequences per sample.

Chao1 is a richness estimator. The higher the number of unique OTUs in a sample, the higher the value of the Chao1 index. Shannon diversity index is a measure of diversity that takes into account the number of species present, as well as the relative abundance of each species. PD (Phylogenetic diversity) whole tree is a measure of biodiversity which incorporates phylogenetic difference between species. It is defined and calculated as the sum of all branch lengths of the OTUs in the group (Fig. 5). CNG buses were statistically the richest, the most diverse and the most branched (Mann–Whitney U p-value ≤ 0.05).

HD and EURO IV achieved similar results, but HD was richer and more diverse and EURO IV had more branches. The lowest, taking the median value into account, was the EURO V. It had a wide range, but the median values were lower than the rest of the buses.

Regarding the identified taxa at the phylum level (Fig. S1), almost 80% of the relative abundance was covered by *Actinobacteria* and *Proteobacteria* for all the buses. *Actinobacteria* are a phylum and class of Gram-positive bacteria that can be ubiquitously distributed in both terrestrial and aquatic ecosystems. They are able to produce two-thirds of all the antibiotics in current clinical use that came from natural sources, as well as many anticancer, anthelmintic, and antifungal compounds, that is why these bacteria are very important for biotechnology, medicine, and agriculture (Barka et al. 2016). *Proteobacteria* is the largest bacterial phylum, with six classes and over 116 families (Parte et al. 2020). Members are Gram-negative, and play a variety of roles in diverse microbial ecosystems (such as in aquatic, soil, plant, and animal niches). They can grow up on a variety of organic compounds: proteins, carbohydrates, and lipids; and contribute to the human gut microbiome functional variation (Bradley & Pollard, 2017).

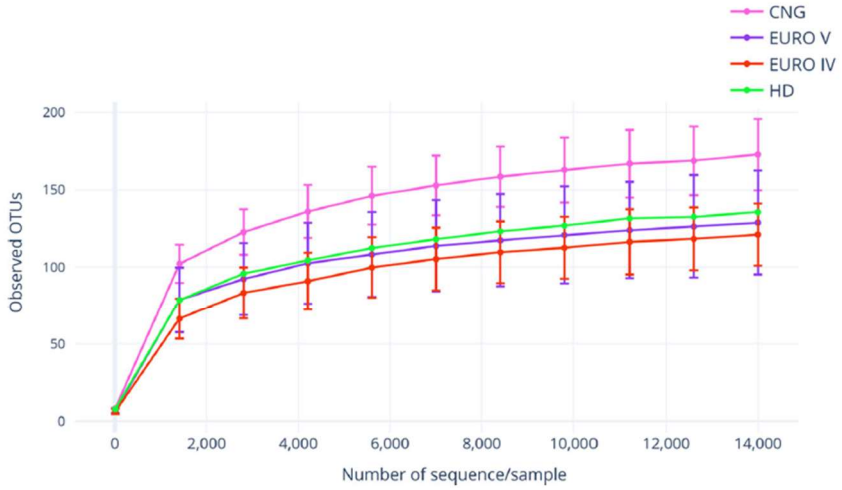

Fig. 4 Rarefaction curves obtained from the number of observed operational taxonomic units (OTUs) and the sequences per sample for air samples from four different fuelled buses. The plateau of the curves started around 2000 sequences

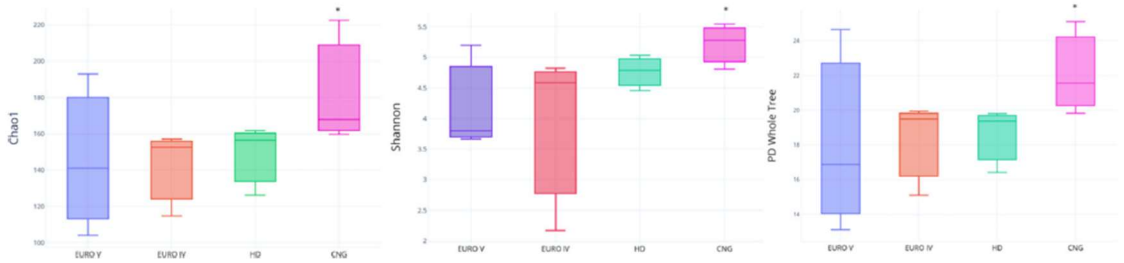

Fig. 5 Boxplots of bacterial richness (Chao 1), bacterial diversity (Shannon and PD whole tree) for different analyzed fuel type buses (EURO IV, EURO V, HD and CNG). Nonparametric Mann–Whitney *U* tests (two-tailed) were performed to highlight that there are significant differences in diversity measures between the groups of samples. Asterisk indicate a p-value ≤ 0.05

Amongst the differences that were found inside the different fuel type buses, the most obvious one was *Proteobacteria* being more abundant in EURO IV compared to the others (Mann–Whitney *U* p-value ≤ 0.05), and *Deinococcus-Thermus* being detected only in the inside of the four type of buses analyzed, and not present in the outside samples, which make it a potential useful marker.

Moving on to the genus level (Fig. S2), some substantial differences were noted. Airborne bacterial communities in Barcelona bus systems were largely dominated by a limited number of taxa, where *Cutibacterium* was the most abundant. The interior of the bus is a distinctive microenvironment where the concentration of pollutants from both outdoor environment and the ones generated internally can occur, that's why, variety of ubiquitously detected genus level taxa was regarded as the environment inside the bus can be a mixture of both, indoor and outdoor air. Six of 44 (14%) were found to overlap between all the different fuel type buses, where two of them were detected in the six scenarios above mentioned, *Cutibacterium* and *Bradyrhizobium*. However, looking to the ones that are overlapped at least in two different fuel type buses, the percentage gets to 48% (21 of 44). The ones encountered in all the different fuel type buses with a high relative abundance were from different sources as: human skin or body (*Cutibacterium, Corynebacterium, Prevotella*), environmental (*Paracoccus, Sphingomonas*) nitrogen atmospheric fixator (*Bradyrhizobium*), organic matter recycling (*Burkholderia*) (Collins et al. 2004; Larsen, 2017).

Related to human microbiota, *Staphylococcus* and *Neisseria* were detected in 3 of the different fuel type buses and outside the tourist bus. The relative abundance of *Staphylococcus* was higher outside and *Neisseria* was higher inside CNG buses (Mann–Whitney *U* p-value ≤ 0.05). The main source of contamination of bacteria inside the buses is human, as 19 of 44 (43%) genera taxa are related to human beings (presence in the human body, in the skin microbiota, dental plaque, blood among other human scenarios.). Note that the mentioned taxa herein are ubiquitous and can be found in other terrestrial and atmospheric environments.

It is interesting to see that *Paracoccus* and *Prevotella* were detected inside all the buses, and *Sediminibacterium* and *Micrococcus* only in some of them. *Paracoccus* is the one with the highest relative abundance, representing 40% of genera detected inside EURO IV buses (Mann–Whitney *U* p-value ≤ 0.05). Some other taxa that were detected with high richness or abundance were *Streptococcus, Brevundimonas, Massilia (O), Enhydrobacte, Dermacoccaceae (O) and Pseudomonas* (Mann–Whitney *U* p-value ≤ 0.05). Most of them are related to human skin and some of them are opportunistic pathogens for humans.

Figure 6 shows the top five taxa that were differentially more abundant in each one of the four buses type compared to the others. The highest mean number of sequences of differentially abundant bacteria was found in the inside buses. *Stomatobaculum* had a mean count of sequences of 320 inside tourist buses, which doubles the highest of any of the other scenario. This bacterium is isolated from the human dental plaque (Sizova et al. 2013). *Nocardia* had a mean count of sequences of 270; these taxa are encountered in soils around the world rich in organic matter. Some species can be pathogenic causing pneumonia and

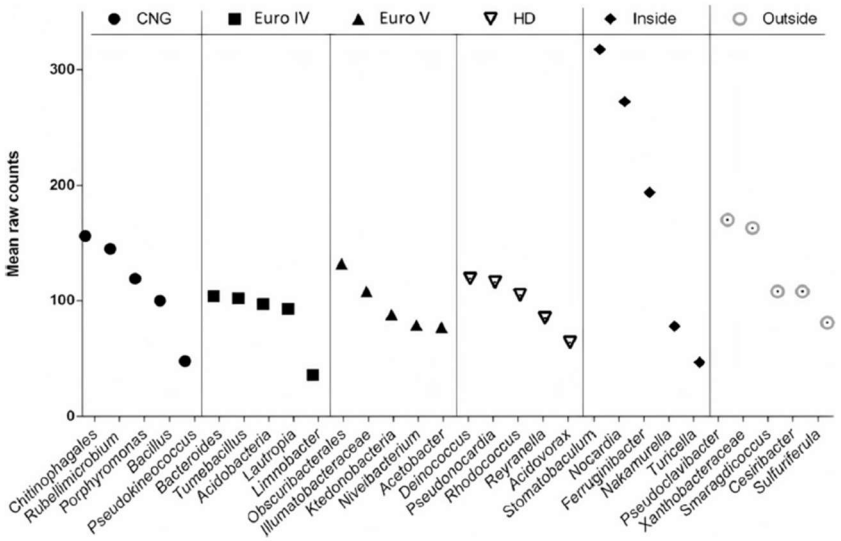

Fig. 6 Differential abundance analysis of five taxa detected in a specific type of bus but not in the others. The mean raw counts represent the mean number of sequences identified to a particular taxa in the different groups of samples. The inside and outside bars include data from samples collected only in touristic buses

nocardiosis, among other diseases (Ryan & Ray, 2004). *Ferruginibacter* also had a high mean count of sequences of 200. It is a genus of bacteria from the family of *Chitinophagaceae* which is isolated from freshwater sediment (Lim et al. 2009).

In summary, the biodiversity inside buses is greatly affected by the presence of humans inside, but also by the outdoor sources at the moment of the sampling more than the fuel type.

3.2.2 *Seasonal differences*

It is important to consider that in this work seasonal campaigns were defined according to TMB ventilation protocols, thus summer: May–September having air conditioning functioning (windows closed) compared to winter: November–March without it. The main determinants for bacterial growth are the environment, meteorological conditions, including variability between cities and seasons (Gandolfi et al. 2008). Looking at the 2 different seasons in the bus study, summer: May–September samples were the richest, and most branched. For Shannon diversity index, although the median values were close for the two seasons, summer: May–September samples were statistically richer than winter: November–March (Fig. 7). This is in agreement with previous studies showing spring and winter: November–March climatic conditions to be unfavorable for bacterial growth in air samples (Chakrawarti et al. 2020; Tignat-Perrier et al. 2020).

The observed seasonality could be a combination between changes in meteorological conditions and changes in the contributions of individual source environments (Bowers et al. 2013; Uetake et al. 2019). Nuñez et al., 2019 suggested that the variability of airborne diversity in urban areas is mostly influenced by environmental changes, in agreement with other studies (Bertolini et al., 2013; Franzetti et al., 2011; Innocente et al., 2017) and in a less extent due to the characteristics of the local microenvironment, indicating that air temperature also has a strong influence on the composition of bacteria. Bowers et al. (2013) and Genitsaris et al. (2017) agreed in that the only meteorological variable found to be correlated with airborne bacteria composition was the temperature, but that it does not have direct control in it. Temperature was measured inside buses in the present study (not showed due to be very similar between both seasons), but it was not measured outside, where temperatures are more different between summer and winter in Barcelona. Apart from the temperature, seasonal variability is also affected by different environmental source contributions. And human

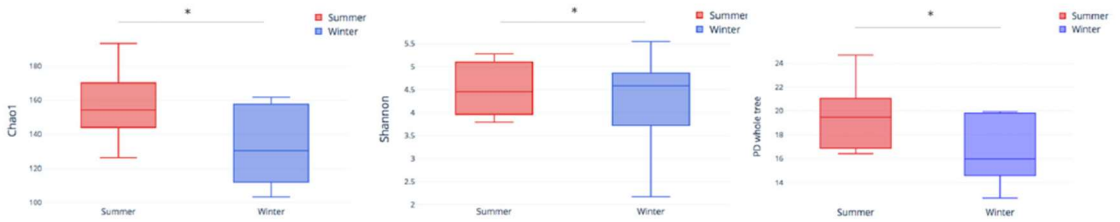

Fig. 7 Boxplots of bacterial richness (Chao 1), bacterial diversity (Shannon and PD whole tree) for different analyzed seasons (summer and winter)

pathogens that could cause respiratory diseases could be transported by the air (Abd Aziz et al., 2018; Fan et al., 2019). The bus routes in where measurements have been done are distributed all over Barcelona, going through sea environments to mountain and urban areas, which may have affected the airborne bacteria composition.

Proteobacteria and *Actinobacteria* were the most abundant Phylum as observed in the different fuel type buses achieving more than the 80% of relative abundance in the two seasons (Fig. 8). *Proteobacteria* were more abundant in winter: November–March and *Firmicutes* more abundant in summer: May–September (Mann–Whitney U p-value ≤ 0.05). Some Phylum were exclusively detected in summer: May–September and others only in the winter: November–March, like *Fibrobacteres* that was the only one identified only in winter: November–March. *Fibrobacteres* are a small bacterial Phylum that includes many of the ruminant animal stomach bacteria that

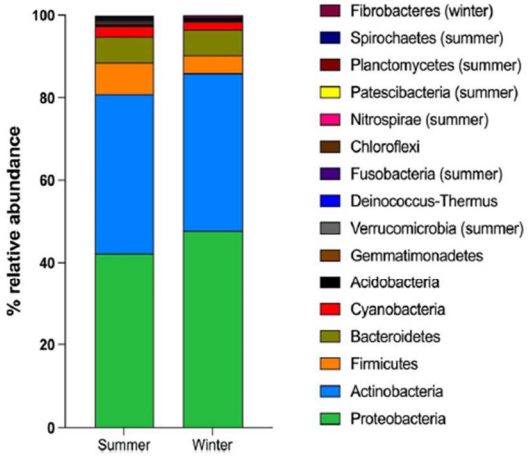

Fig. 8 Relative abundance of Phylum taxonomic category for each season

allow degradation of plant-based cellulose (Ransom-Jones et al. 2012). The ones detected only in summer: May–September were *Verrucomicrobia, Fusobacteria, Nitrospirae, Patescibacteria, Planctomycetes* and *Spirochaetes*, most of them related with aquatic ecosystem, but also with human oral microbiome, or widespread in the environment (Chiang et al. 2018; Dewhirst et al. 2010; Gupta et al. 2013; Pollet et al. 2014; Tian et al. 2020; Zecchin et al. 2017).

Moving on to the genus level (Fig. 9), some substantial differences were noted between the two seasons. *Corynebacterium, Bradyrhizobium, Paracoccus* and *Streptococcus* were identified in both seasons, summer: May–September and winter: November–March, but summers' relative abundance was higher (Mann–Whitney U p-value ≤ 0.05). Bonetta et al. 2010 identified that bacterial counts increased in summer: May–September. This study could be helpful in order to see if the season affects the existing taxonomic genera. Some genera were exclusively detected in summer: May–September and others only in winter: November–March. Airborne bacterial communities in Barcelona bus systems were largely dominated by a limited number of taxa, where *Corynebacterium, Bradyrhizobium* and *Paracoccus* were the most abundant genera in summer: May–September (Mann–Whitney U p-value ≤ 0.05), whereas *Paracoccus* and *Cutibacterium* were only detected in winter: November–March with a 20% of relative abundance (Mann–Whitney U p-value ≤ 0.05). *Cutibacterium* is a taxonomic genera related to skin microbiota (Corvec, 2018) and *Paracoccus* is an environmental genus. Half of the genera, 13 of 26, were detected in the two seasons, being almost the 80% of the genera in summer: May–September and almost 70% in winter: November–March. It can be observed that the relative abundance of the different

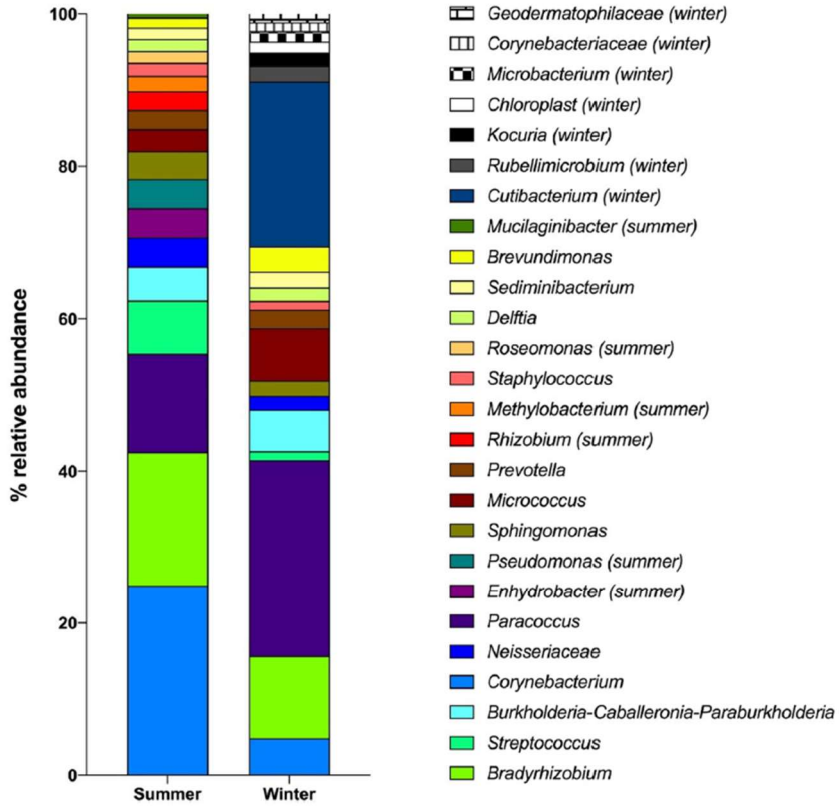

Fig. 9 Relative abundance of Genus taxonomic category Genera taxonomic category for each season. The taxa that were specific to each season, controls are specified in parentheses

taxonomic genera decreases from summer: May–September to winter: November–March.

Enhydrobacter, Pseudomonas, Rhizobium, Methylobacterium, Roseomonas and *Mucilaginibacter* were only detected in summer: May–September. These genera were related to human skin microbiota, plants, environmental bacteria and some of them can be opportunistic pathogen for human (Indra Dé et al. 2004; Leung et al. 2015; González et al. 2019; Lai et al. 2020). *Cutibacterium, Rubellimicrobium, Kocuria, Chloroplast, Microbacterium, Corynebacteriaceae* and *Geodermatophilaceae* were the ones identified only in winter: November–March, which are ubiquitous, related to wide range of environments (soil, human commensals, plants) (Collins et al. 1983; Dastager et al. 2008; Kandi et al. 2016; Sun et al. 2015).

3.3 Penicillium/Aspergillus and Cladosporium quantification

Quantification of *Penicillium/Aspergillus sp.* and *Cladosporium sp.* concentrations was performed in bioaerosols to assess fungi contamination in buses. Concentrations were below detection limit for both targets in all samples. Detection limit was between 9 and 16 for *A. fumigatus* genome equiv/m^3 (median = 19 *A. fumigatus* genome equiv/m^3 for *Aspergillus/Penicillium* sp. and between 4 and 66 *Cladosporium* sp. genome equiv/m^3 (median = 8 *Cladosporium* genome equiv/m^3) for *Cladosporium* sp. depending on sample.

Penicillium and *Aspergillus* sp. are very close genetically, and are markers of water damages (flood), condensation and humidity. *Cladosporium sp.* is a good marker for outdoor contamination and is a common indoor fungus. This suggests that the air

quality inside the buses in terms of the studied fungi is good.

In contrast to what was identified in the present study, Nowakowicz-Dębek et al. 2017 and Prakash et al. (2014) identified *Aspergillus sp.* as the most frequently represented fungi genera inside buses. Similar results were shown by Priyamvada et al. (2018) and Sowiak et al. (2018)..

Lee and Jo (2005) have also indicated that the growth medium used in the measurement, the vehicle type and the season are related to microorganism concentration. Indeed, it could be due to the cleanliness of the bus, AC maintenance, the method of sampling, and sample treatment. All these factors can affect the concentration of the microorganism measured. However, the cited studies used culture methods, which make the comparison of concentrations with our work not valid.

It would be necessary to make a study more focused on the detection of fungi using different methods, including culture and sequencing methods. The moment in which the AC is turned on, and the exact moment in which the windows are open could be considered as variables for future studies.

3.4 Endotoxins

Taking total bacteria results into account, three samples were analyzed to perform an inhibition/enhancement test, including those with the highest and lowest total bacteria concentration, and one with an intermediate value. All three samples concentrations were below detection limit, with a value of 0.004 EU/m^3 and 4.445 EU/m^3. Therefore, no other samples were analyzed. In addition, inhibition was detected in the suggesting an underestimation of endotoxin content (Hollander et al. 1993). However, given the relatively low sample volume (240 L of air) and the relatively low bacterial concentration and the importance of Gram-positive taxa, this result is not surprising.

4 Conclusions

Total airborne bacteria inside buses was detected in low concentrations. Actinobacteria and Proteobacteria were the most abundant phyla inside all the fuel type buses and also in both floors of tourist buses, achieving almost 80% of relative abundance in all the buses. In relation to genus level, *Cutibacterium* was the most abundant one followed by *Paracoccus*, which was only detected inside buses. The main source of contamination of bacteria inside the buses is the presence of humans inside, as 19 of 44 (43%) genera taxa are related to human being, but also by the outdoor sources at the moment of the sampling. The different type of fuel did not seem to affect airborne microbes. However, the seasons affect inside buses, both, qualitatively and quantitatively. It can be observed that the relative abundance of the different taxonomic genera decreases from summer: May–September to winter: November–March. Fungi and endotoxins couldn't be detected in any sample.

Bus routes in Barcelona are long enough to cross different areas in the city attributed to different airborne bacterial sources. When comparing summer: May–September and winter: November–March samples, where all types of routes were taken into account, the seasonal comparison was a mix of different sources, per each season. This could explain why most abundant airborne bacteria are the same in both seasons.

Even if humans are the main source of bacteria inside buses, the air exchange in this microenvironment should be always optimized in order to reduce commuters' exposure to potentially harmful microbes.

Acknowledgements This work is supported by the Spanish Ministry of Economy, Industry and Competitiveness with FEDER funds (BUSAIR CGL2016-79132-R). We are grateful to Transports Metropolitans de Barcelona (TMB) for their cooperation throughout the whole project. Funding from the Generalitat de Catalunya (AGAUR 2017 SGR41) is also acknowledged. Laboratory analyses for bioaerosols (PCR, sequencing, endotoxins) as well as some travel expenses for A FI were provided through CD Discovery Grant (National Sciences and Engineering Council of Canada-NSERC). HM is supported by a postdoctoral fellowship from Fondde Recherche du Québec Nature et Technologie and is the recipient of the Lab Exchange Visitor Program Award from the Canadian Society for Virology. CD is holder of Tier-1 Canada Research Chair on Bioaerosols.

References

Abd Aziz, A., Lee, K., Park, B., Park, H., Park, K., Choi, I.-G., et al. (2018). Comparative study of the airborne microbial communities and their functional composition in fine particulate matter (PM2.5) under non-extreme and extreme

PM2.5 conditions. *Atmospheric Environment, 194*, 82–92. https://doi.org/10.1016/j.atmosenv.2018.09.027.

Almoffarreh, H. K., Alsaleh, F. M., & Alruwaili, M. S. (2016). Bacterial and fungal contamination of air conditioners filters and carpets. *International Journal of Environment, Agriculture and Biotechnology, 3*, 399–404. https://doi.org/10.22161/ijeab/1.3.14.

Bach, H. J., Tomanova, J., Schloter, M., & Munch, J. C. (2002). Enumeration of total bacteria and bacteria with genes for proteolytic activity in pure cultures and in environmental samples by quantitative PCR mediated amplification. *Journal of Microbiological Methods, 49*(3), 235–245. https://doi.org/10.1016/S0167-7012(01)00370-0.

Barka, E. A., Vatsa, P., Sanchez, L., Gaveau-Vaillant, N., Jacquard, C., Klenk, H.-P., et al. (2016). Taxonomy, physiology, and natural products of Actinobacteria. *Microbiology and Molecular Biology Reviews, 80*(1), 1–43. https://doi.org/10.1128/mmbr.00019-15.

Bertolini, V., Gandolfi, I., Ambrosini, R., Bestetti, G., Innocente, E., Rampazzo, G., et al. (2013). Temporal variability and effect of environmental variables on airborne bacterial communities in an urban area of Northern Italy. *Applied Microbiology and Biotechnology, 97*, 6561–6570. https://doi.org/10.1007/s00253-012-4450-0.

Bonetta, S., Bonetta, S., Mosso, S., Sampò, S., & Carraro, E. (2010). Assessment of microbiological indoor air quality in an Italian office building equipped with an HVAC system. *Environmental Monitoring and Assessment, 161*(1–4), 473–483. https://doi.org/10.1007/s10661-009-0761-8.

Bowers, R. M., Clements, N., Emerson, J. B., Wiedinmyer, C., Hannigan, M. P., & Fierer, N. (2013). Seasonal variability in bacterial and fungal diversity of the near-surface atmosphere. *Environmental Science and Technology, 47*(21), 12097–12106. https://doi.org/10.1021/es402970s.

Bradley, P. H., & Pollard, K. S. (2017). Proteobacteria explain significant functional variability in the human gut microbiome. *Microbiome, 5*(1), 1–23. https://doi.org/10.1186/s40168-017-0244-z.

Caporaso, J. G., Kuczynski, J., Stombaugh, J., Bittinger, K., Bushman, F. D., Costello, E. K., et al. (2011). *NIH Public Access, 7*(5), 335–336. https://doi.org/10.1038/nmeth.f.303.QIIME.

Chakrawarti, M. K., Singh, M., Yadav, V. P., & Mukhopadhyay, K. (2020). Temporal dynamics of air bacterial communities in a university health centre using illumina miseq sequencing. *Aerosol and Air Quality Research, 20*(5), 966–980. https://doi.org/10.4209/aaqr.2019.11.0613.

Chiang, E., Schmidt, M. L., Berry, M. A., Biddanda, B. A., Burtner, A., Johengen, T. H., et al. (2018). Verrucomicrobia are prevalent in north-temperate freshwater lakes and display class-level preferences between lake habitats. *PLoS ONE*. https://doi.org/10.1371/journal.pone.0195112.

Collins, M. D., Jones, D., & Kroppenstedt, R. M. (1983). Reclassification of Brevibacterium imperiale (Steinhaus) and "Corynebacterium laevaniformans" (Dias and Bhat) in a Redefined Genus Microbacterium (Orla-Jensen), as Microbacterium imperiale comb. nov. and Microbacterium laevaniformans nom rev.; comb. nov. *Systematic and Applied Microbiology, 4*, 65–78.

Collins, M. D., Hoyles, L., Foster, G., & Falsen, E. (2004). Corynebacterium caspium sp. nov., from a Caspian seal (Phoca caspica). *International Journal of Systematic and Evolutionary Microbiology, 54*(3), 925–928.

Comeau, A. M., Li, W. K. W., Tremblay, J. É., Carmack, E. C., & Lovejoy, C. (2011). Arctic ocean microbial community structure before and after the 2007 record sea ice minimum. *PLoS ONE*. https://doi.org/10.1371/journal.pone.0027492.

Corvec, S. (2018). *Clinical and Biological Features of Cutibacterium (Formerly Propionibacterium) avidum, an Underrecognized Microorganism*. Retrieved from 10

Cox, C. S., & Wathes, C. M. (1995). *Bioaerosol Handbook*. . Lewis Publishers.

Dastager, S. G., Lee, J. C., Ju, Y. J., Park, D. J., & Kim, C. J. (2008). Rubellimicrobium mesophilum sp. nov., a mesophilic, pigmented bacterium isolated from soil. *International Journal of Systematic and Evolutionary Microbiology, 58*(8), 1797–1800. https://doi.org/10.1099/ijs.0.65590-0.

de Nazelle, A., Bode, O., & Orjuela, J. P. (2017). Comparison of air pollution exposures in active versus passive travel modes in European cities: A quantitative review. *Environment International, 99*, 151–160. https://doi.org/10.1016/j.envint.2016.12.023.

Dewhirst, F. E., Chen, T., Izard, J., Paster, B. J., Tanner, A. C. R., Yu, W. H., et al. (2010). The human oral microbiome. *Journal of Bacteriology, 192*(19), 5002–5017. https://doi.org/10.1128/JB.00542-10.

Edgar, R. C., Haas, B. J., Clemente, J. C., Quince, C., & Knight, R. (2011). UCHIME improves sensitivity and speed of chimera detection. *Bioinformatics, 27*(16), 2194–2200. https://doi.org/10.1093/bioinformatics/btr381.

EEA, European Environment Agency, 2018. Air Quality in Europe—2018 report. Available from: https://www.eea.europa.eu/publications/air-quality-in-europe-2018 (accessed March 2019).

EPA, 2019. Available from: http://www.epa.gov/nerlcwww/moldtech.htm (accessed March 2019)

Fan, C., Li, Y., Liu, P., Mu, F., Xie, Z., Lu, R., et al. (2019). Characteristics of airborne opportunistic pathogenic bacteria during autumn and winter in Xi'an China. *Science of the Total Environment, 672*, 834–845. https://doi.org/10.1016/j.scitotenv.2019.03.412.

Franzetti, A., Gandolfi, I., Gaspari, E., Ambrosini, R., & Bestetti, G. (2011). Seasonal variability of bacteria in fine and coarse urban air particulate matter. *Applied Microbiology and Biotechnology, 90*, 745–753.

Fondelli, M. C., Chellini, E., Yli-Tuomi, T., Cenni, I., Gasparrini, A., Nava, S., et al. (2008). Fine particle concentrations in buses and taxis in Florence Italy. *Atmospheric Environment, 42*(35), 8185–8193. https://doi.org/10.1007/s00253-014-6348-5.

Gandolfi, I., Bertolini, V., Bestetti, G., Ambrosini, R., Innocente, E., Rampazzo, G., et al. (2015). Spatio-temporal variability of airborne bacterial communities and their correlation with particulate matter chemical composition across two urban areas. *Applied Microbiology and Biotechnology, 99*(11), 4867–4877. https://doi.org/10.1007/s00253-014-6348-5.

Genitsaris, S., Stefanidou, N., Katsiapi, M., Kormas, K. A., Sommer, U., & Moustaka-Gouni, M. (2017). Variability of airborne bacteria in an urban Mediterranean area

(Thessaloniki, Greece). *Atmospheric Environment, 157*, 101–110. https://doi.org/10.1016/j.atmosenv.2017.03.018.

Ghosh, B., Lal, H., & Srivastava, A. (2015). Review of bioaerosols in indoor environment with special reference to sampling, analysis and control mechanisms. *Environment International, 85*, 254–272. https://doi.org/10.1016/J.ENVINT.2015.09.018.

Gołofit-Szymczak, M., & Górny, R. L. (2010). Bacterial and Fungal Aerosols in Air-Conditioned Office Buildings in Warsaw, Poland—The Winter Season. *International Journal of Occupational Safety and Ergonomics, 16*(4), 465–476. https://doi.org/10.1080/10803548.2010.11076861.

González, V., Santamaría, R. I., Bustos, P., Pérez-Carrascal, O. M., Vinuesa, P., Juárez, S., et al. (2019). Phylogenomic Rhizobium species are structured by a continuum of diversity and genomic clusters. *Frontiers in Microbiology*. https://doi.org/10.3389/fmicb.2019.00910.

Gupta, R. S., Mahmood, S., & Adeolu, M. (2013). A phylogenomic and molecular signature based approach for characterization of the phylum spirochaetes and its major clades: Proposal for a taxonomic revision of the phylum. *Frontiers in Microbiology*. https://doi.org/10.3389/fmicb.2013.00217.

Hamada, N., & Fujita, T. (2002). Effect of air-conditioner on fungal contamination. *Atmospheric Environment, 36*(35), 5443–5448. https://doi.org/10.1016/S1352-2310(02)00661-1.

Hollander, A., Douwes, J., & Heederik, D. (1993). Inhibition and enhancement in the analysis of airborne endotoxin levels in various occupational environments. *American Industrial Hygiene Association Journal, 54*(11), 647–653. https://doi.org/10.1080/15298669391355189.

https://www.tmb.cat/documents/20182/111197/NOTICIES-NOVA-XARXA-BUS-20120523-TRANSPORT.pdf/37f4bca7-d018-4e73-9da3-f9cee5842448

Indra Dé, Kenneth V.I. Rolston, and X. Y. H. (2004). *Clinical Significance of Roseomonas Species Isolated from Catheter and Blood Samples: Analysis of 36 Cases in Patients with Cancer*. Retrieved from https://academic.oup.com/cid/article/38/11/1579/285332

Innocente, E., Squizzato, S., Visin, F., Facca, C., Rampazzo, G., Bertolini, V., et al. (2017). Influence of seasonality, air mass origin and particulate matter chemical composition on airborne bacterial community structure in the Po Valley, Italy. *Science of The Total Environment, 593–594*, 677–687.

Jo, W. K., & Lee, J. H. (2008). Airborne fungal and bacterial levels associated with the use of automobile air conditioners or heaters, room air conditioners, and humidifiers. *Archives of Environmental and Occupational Health, 63*(3), 101–107. https://doi.org/10.3200/AEOH.63.3.101-107.

Kandi, V., Palange, P., Vaish, R., Bhatti, A. B., Kale, V., Kandi, M. R., & Bhoomagiri, M. R. (2016). Emerging Bacterial Infection: Identification and clinical significance of Kocuria Species. *Cureus*. https://doi.org/10.7759/cureus.731.

Karanasiou, A., Viana, M., Querol, X., Moreno, T., & de Leeuw, F. (2014). Assessment of personal exposure to particulate air pollution during commuting in European cities—Recommendations and policy implications. *Science of The Total Environment, 490*, 785–797. https://doi.org/10.1016/J.SCITOTENV.2014.05.036.

Kaur, S., Nieuwenhuijsen, M., & Colvile, R. (2005). Personal exposure of street canyon intersection users to PM2.5, ultrafine particle counts and carbon monoxide in Central London. *UK. Atmospheric Environment, 39*(20), 3629–3641. https://doi.org/10.1016/j.atmosenv.2005.02.046.

Kingham, S., Longley, I., Salmond, J., Pattinson, W., & Shrestha, K. (2013). Variations in exposure to traffic pollution while travelling by different modes in a low density, less congested city. *Environmental Pollution, 181*, 211–218. https://doi.org/10.1016/j.envpol.2013.06.030.

Knibbs, L. D., & de Dear, R. J. (2010). Exposure to ultrafine particles and PM2.5 in four Sydney transport modes. *Atmospheric Environment, 44*(26), 3224–3227. https://doi.org/10.1016/J.ATMOSENV.2010.05.026.

Lai, K., Nguyen, N. T., Miwa, H., Yasuda, M., Nguyen, H. H., & Okazaki, S. (2020). Diversity of methylobacterium spp. in the rice of the vietnamese mekong delta. *Microbes and Environments*. https://doi.org/10.1264/jsme2.ME19111.

Larsen, J. M. (2017). The immune response to Prevotella bacteria in chronic inflammatory disease. *Immunology*. https://doi.org/10.1111/imm.12760.

Uk Lee, B., Lee, G., & Joon Heo, K. (2016). Concentration of culturable bioaerosols during winter. *Journal of Aerosol Science, 94*, 1–8. https://doi.org/10.1016/J.JAEROSCI.2015.12.002.

Lee, J. H., & Jo, W. K. (2005). Exposure to airborne fungi and bacteria while commuting in passenger cars and public buses. *Atmospheric Environment, 39*(38), 7342–7350. https://doi.org/10.1016/j.atmosenv.2005.09.013.

Lehtinen, J., Tolvanen, O., Nivukoski, U., Veijanen, A., & Hänninen, K. (2013). Occupational hygiene in terms of volatile organic compounds (VOCs) and bioaerosols at two solid waste management plants in Finland. *Waste Management, 33*(4), 964–973. https://doi.org/10.1016/j.wasman.2012.11.010.

Leung, M. H. Y., Wilkins, D., & Lee, P. K. H. (2015). Insights into the pan-microbiome: Skin microbial communities of Chinese individuals differ from other racial groups. *Scientific Reports*. https://doi.org/10.1038/srep11845.

Lim, J. H., Baek, S. H., & Lee, S. T. (2009). Ferruginibacter alkalilentus gen. nov, sp nov and ferruginibacter lapsinanis sp nov novel members of the family 'chitinophagaceae' in the phylum Bacteroidetes isolated from freshwater sediment. International Journal of Systematic and Evolutionary Microbiology 59(10), 2394–2399. https://doi.org/10.1099/ijs.0.009480-0

Lim, S., Dirks, K. N., Salmond, J. A., & Xie, S. (2015). Determinants of spikes in ultrafine particle concentration whilst commuting by bus. *Atmospheric Environment, 112*, 1–8. https://doi.org/10.1016/j.atmosenv.2015.04.025.

Maestre, J. P., Jennings, W., Wylie, D., Horner, S. D., Siegel, J., & Kinney, K. A. (2018). Filter forensics: Microbiota recovery from residential HVAC filters. *Microbiome*. https://doi.org/10.1186/s40168-018-0407-6.

Mbareche, H., Veillette, M., Bilodeau, G. J., & Duchaine, C. (2019). Fungal aerosols at dairy farms using molecular and culture techniques. *Science of The Total Environment, 653*,

253–263. https://doi.org/10.1016/J.SCITOTENV.2018.10.345.

Molle, R., Mazoué, S., Géhin, É., & Ionescu, A. (2013). Indoor-outdoor relationships of airborne particles and nitrogen dioxide inside Parisian buses. *Atmospheric Environment, 69*, 240–248. https://doi.org/10.1016/j.atmosenv.2012.11.050.

Moreno, T., Reche, C., Rivas, I., Cruz Minguillón, M., Martins, V., Vargas, C., et al. (2015). Urban air quality comparison for bus, tram, subway and pedestrian commutes in Barcelona. *Environmental Research, 142*, 495–510. https://doi.org/10.1016/j.envres.2015.07.022.

Norbäck, D. (2009). An update on sick building syndrome. *Current Opinion in Allergy and Clinical Immunology, 9*(1), 55–59. https://doi.org/10.1097/ACI.0b013e32831f8f08.

Nowakowicz-Dębek, B., Pawlak, H., Wlazło, Ł, Maksym, P., Kapica, J., Chmielowiec-Korzeniowska, A., & Trawińska, B. (2017). Evaluating bioaerosol exposure among bus drivers in the public transport sector. *Journal of Occupational and Environmental Hygiene, 14*(11), D169–D172. https://doi.org/10.1080/15459624.2017.1339165.

Núñez A., Amo de Paz G., Rastrojo A., Ferencova Z., Gutiérrez-Bustillo A.M., Alcamí A., et al. (2019). Temporal patterns of variability for prokaryotic and eukaryotic diversity in the urban air of Madrid (Spain), Atmospheric Environment, 217 116972 ISSN: 1352–2310, https://doi.org/10.1016/j.atmosenv.2019.116972.

Parte, A. C., Sardà Carbasse, J., Meier-Kolthoff, J. P., Reimer, L. C., & Göker, M. (2020). List of Prokaryotic names with Standing in Nomenclature (LPSN) moves to the DSMZ. *International Journal of Systematic and Evolutionary Microbiology*. https://doi.org/10.1099/ijsem.0.004332.

Pollet, T., Humbert, J. F., & Tadonléké, R. D. (2014). Planctomycetes in lakes: Poor or strong competitors for phosphorus? *Applied and Environmental Microbiology, 80*(3), 819–828. https://doi.org/10.1128/AEM.02824-13.

Prakash, N. (2014). A Study on the Prevalence of Indoor Mycoflora in Air Conditioned Buses. *British Microbiology Research Journal, 4*(3), 282–292. https://doi.org/10.9734/bmrj/2014/5380.

Priyamvada, H., Priyanka, C., Singh, R. K., Akila, M., Ravikrishna, R., & Gunthe, S. S. (2018). Assessment of PM and bioaerosols at diverse indoor environments in a southern tropical Indian region. *Building and Environment, 137*(March), 215–225. https://doi.org/10.1016/j.buildenv.2018.04.016.

Ransom-Jones, E., Jones, D. L., McCarthy, A. J., & McDonald, J. E. (2012). An important phylum of cellulose-degrading bacteria. *Microbial Ecology*. https://doi.org/10.1007/s00248-011-9998-1.

Rivas, I., Kumar, P., Hagen-Zanker, A., de Andrade, M., & F., Slovic, A. D., Pritchard, J. P., & Geurs, K. T. . (2017). Determinants of black carbon, particle mass and number concentrations in London transport microenvironments. *Atmospheric Environment, 161*, 247–262. https://doi.org/10.1016/J.ATMOSENV.2017.05.004.

Rognes, T., Flouri, T., Nichols, B., Quince, C., & Mahé, F. (2016). VSEARCH: A versatile open source tool for metagenomics. *Peer Journal*. https://doi.org/10.7717/peerj.2584.

Ryan, K. J., & Ray, C. G. (2004). *Sherris Medical Microbiology*. . McGraw-Hill.

Schloss, P. D., Westcott, S. L., Ryabin, T., Hall, J. R., Hartmann, M., Hollister, E. B., et al. (2009). Introducing mothur: Open-source, platform-independent, community-supported software for describing and comparing microbial communities. *Applied and Environmental Microbiology, 75*(23), 7537–7541. https://doi.org/10.1128/AEM.01541-09.

Sizova, M. V., Muller, P., Panikov, N., Mandalakis, M., Hohmann, T., Hazen, A., et al. (2013). Stomatobaculum longum gen. nov., sp. nov., an obligately anaerobic bacterium from the human oral cavity. *International Journal of Systematic and Evolutionary Microbiology, 63*(PART4), 1450–1456. https://doi.org/10.1099/ijs.0.042812-0.

Sowiak, M., Kozajda, A., Jeżak, K., & Szadkowska-Stańczyk, I. (2018). Does the air condition system in busses spread allergic fungi into driver space? *Environmental Science and Pollution Research, 25*(5), 5013–5023. https://doi.org/10.1007/s11356-017-0830-4.

Sun, H. M., Zhang, T., Yu, L. Y., Sen, K., & Zhang, Y. Q. (2015). Ubiquity, diversity and physiological characteristics of Geodermatophilaceae in Shapotou National Desert Ecological Reserve. *Frontiers in Microbiology*. https://doi.org/10.3389/fmicb.2015.01059.

Tan, S. H., Roth, M., & Velasco, E. (2017). Particle exposure and inhaled dose during commuting in Singapore. *Atmospheric Environment, 170*, 245–258. https://doi.org/10.1016/J.ATMOSENV.2017.09.056.

Tian, R., Ning, D., He, Z., Zhang, P., Spencer, S. J., Gao, S., et al. (2020). Small and mighty: Adaptation of superphylum Patescibacteria to groundwater environment drives their genome simplicity. *Microbiome*. https://doi.org/10.1186/s40168-020-00825-w.

Tignat-Perrier, R., Dommergue, A., Thollot, A., Magand, O., Amato, P., Joly, M., et al. (2020). Seasonal shift in airborne microbial communities. *Science of the Total Environment*. https://doi.org/10.1016/j.scitotenv.2020.137129.

Triadó-Margarit, X., Veillette, M., Duchaine, C., Talbot, M., Amato, F., Minguillón, M. C., et al. (2016). Bioaerosols in the Barcelona subway system. *Indoor Air*. https://doi.org/10.1111/ina.12343.

Uetake, J., Tobo, Y., Uji, Y., Hill, T. C. J., DeMott, P. J., Kreidenweis, S. M., & Misumi, R. (2019). Seasonal changes of airborne bacterial communities over Tokyo and influence of local meteorology. *Frontiers in Microbiology*. https://doi.org/10.3389/fmicb.2019.01572.

Zecchin, S., Mueller, R. C., Seifert, J., Stingl, U., Anantharaman, K., von Bergen, M., et al. (2017). Rice paddy nitrospirae carry and express genes related to sulfate respiration: Proposal of the New Genus "Candidatus Sulfobium." *Applied and Environmental Microbiology, 84*(5), e02224-e2317. https://doi.org/10.1128/AEM.02224-17.

Zeng, Q.-Y., Westermark, S.-O., Rasmuson-Lestander, A., & Wang, X.-R. (2006). Detection and quantification of Cladosporium in aerosols by real-time PCR. *Journal of Environmental Monitoring, 8*, 153–160.

Research publications contributions

Article 1

Vehicle interior air quality conditions when travelling by taxi

Teresa Moreno, Antonio Pacitto, **Amaia Fernández**, Fulvio Amato, Esther Marco, Joan O. Grimalt, Giorgio Buonanno, Xavier Querol

Environmental Research 172, 529–542

https://doi.org/10.1016/j.envres.2019.02.042

2019

Environmental Research 172 (2019) 529–542

Contents lists available at ScienceDirect

Environmental Research

journal homepage: www.elsevier.com/locate/envres

Vehicle interior air quality conditions when travelling by taxi

Teresa Moreno[a,*], Antonio Pacitto[b], Amaia Fernández[a], Fulvio Amato[a], Esther Marco[a], Joan O. Grimalt[a], Giorgio Buonanno[b,c], Xavier Querol[a]

[a] Institute for Environmental Assessment and Water Studies (IDAEA), CSIC, 18-26 Jordi Girona, Barcelona 08034, Spain
[b] Dept. of Civil and Mechanical Engineering, University of Cassino and Southern Lazio, Italy
[c] International Laboratory for Air Quality and Health, Queensland University of Technology, Brisbane, Australia

ARTICLE INFO

Keywords:
Indoor air quality
Commuting
Taxi
Ultrafine particles
Occupational exposure

ABSTRACT

Vehicle interior air quality (VIAQ) was investigated inside 14 diesel/non-diesel taxi pairs operating simultaneously and under normal working conditions over six weekday hours (10.00–16.00) in the city of Barcelona, Spain. Parameters measured included PM_{10} mass and inorganic chemistry, ultrafine particle number (N) and size, lung surface deposited area (LDSA), black carbon (BC), CO_2, CO, and a range of volatile organic compounds (VOCs). Most taxi drivers elected to drive with windows open, thus keeping levels of CO_2 and internally-generated VOCs low but exposing them to high levels of traffic-related air pollutants entering from outside and confirming that air exchange rates are the dominant influence on VIAQ. Median values of N and LDSA (both sensitive markers of VIAQ fluctuations and likely health effects) were reduced to around 10^4 #/cm^3 and < 20 μm^2/cm^3 respectively under closed conditions, but more than doubled with windows open and sometimes approached 10^5 #/cm^3 and 240 μm^2/cm^3. In exceptional traffic conditions, transient pollution peaks caused by outside infiltration exceeded N = 10^6 #/cm^3 and LDSA = 1000 μm^2/cm^3. Indications of self-pollution were implicated by higher BC and CO levels, and larger UFP sizes, measured inside diesel taxis as compared to their non-diesel pair, and the highest concentrations of CO (> 2 ppm) were commonly associated with older, high-km diesel taxis. Median PM_{10} concentrations (67 μg/m^3) were treble those of urban background, mainly due to increased levels of organic and elemental carbon, with source apportionment calculations identifying the main pollutants as vehicle exhaust and non-exhaust particles. Enhancements in PM_{10} concentrations of Cr, Cu, Sn, Sb, and a "High Field Strength Element" zircon-related group characterised by Zr, Hf, Nb, Y and U, are attributed mainly to the presence of brake-derived PM. Volatile organic compounds display a mixture which reflects the complexity of traffic-related organic carbon emissions infiltrating the taxi interior, with 2-methylbutane and n-pentane being the most abundant VOCs, followed by toluene, m-xylene, o-xylene, 1,2,4-trimethylbenzene, ethylbenzene, p-xylene, benzene, and 1,3,5-trimethylbenzene. Internally sourced VOCs included high monoterpene concentrations from an air freshener, and interior off-gassing may explain why the youngest taxi registered the highest content of alkanes and aromatic compounds. Carbon dioxide concentrations quickly climbed to undesirable levels (> 2500 ppm) under closed ventilation conditions and could stay high for much of the working day. Taxi drivers face daily occupational exposure to traffic-related air pollutants and would benefit from a greater awareness of VIAQ issues, notably the use of ventilation, to encourage them to minimise possible health effects caused by their working environment.

1. Introduction

Traffic is the main source of air pollutants in cities, and with urban inhabitants already accounting for a majority of the total global population (https://data.worldbank.org/indicator/SP.URB.TOTL.IN.ZS, UN Population Division) the effects of breathing vehicular gas and particle emissions have grown to become one of our most challenging environmental health problems (e.g. Cepeda et al., 2017; Hoek et al., 2013; Kelly and Zhu, 2016; Heal et al., 2012; Rivas et al., 2014). Traffic-related air pollutants (TRAPs) source from both exhaust and non-exhaust (such as brakes: Amato et al., 2011) emissions and their distribution is typically highly variable in time and space (e.g; Kaur et al., 2005; Krecl et al., 2015; Kumar et al., 2011; Nikolova et al., 2011; Ragettli et al., 2014; Vu et al., 2015). There are consequently notable differences in the exposure of individual city commuters to TRAPs during their travel through the city. For the traveller outdoors the most

* Corresponding author.
E-mail address: teresa.moreno@idaea.csic.es (T. Moreno).

https://doi.org/10.1016/j.envres.2019.02.042
Received 24 January 2019; Received in revised form 26 February 2019; Accepted 27 February 2019
Available online 28 February 2019

important of these factors is proximity to the sources of traffic emissions, whereas for the commuter inside a road vehicle exposure to TRAPs will depend primarily on air exchange rates (e.g. Zhu et al., 2002; Durant et al., 2010; Fruin et al., 2011; Leavey et al., 2017; Lee et al., 2015). In a previous contribution to this subject we compared pollutant exposure when travelling by different public transport options (bus, tram, subway) in Barcelona to improve our understanding of how real-time air pollutant concentrations regularly inhaled by urban commuters vary depending on how they choose to travel (Moreno et al., 2015). In the paper presented here we turn our attention to variations in air quality experienced when travelling across Barcelona by taxi, a key transport mode used in the city and one that has been described as "bridging the gap between private and other public transport" (An et al., 2011).

The published literature on vehicular interior air quality (VIAQ) has already demonstrated that car commuters can be exposed to significantly enhanced levels of inhalable particles (PM_{10}, $PM_{2.5}$ and PM_1: particles in suspension with diameter less than 10, 2.5 and 1 μm respectively) and gases (CO, CO_2, NO, NO_2, VOCs) (e.g. Alameddine et al., 2016; Fruin et al., 2008; Hudda et al., 2011, 2012; Hudda and Fruin, 2018; Joodatnia et al., 2013; Leavey et al., 2017; Lee et al., 2015; Madl et al., 2015; Tartakovsky et al., 2013; Xing et al., 2018; Yang et al., 2015; Zhu et al., 2007). Taxi drivers offer a special case in that they are chronically exposed to TRAPs as an occupational hazard (Shu et al., 2015), and this transport mode is additionally interesting in that current taxi fleets utilise various fuel options that include both hybrid and electric vehicles, which generate different patterns of pollutant emissions. While most city taxi fleets are still dominated by traditional gasoline- or diesel-powered engines, this is changing rapidly. In 2017 for example already one third of the 10,523 taxis operating in the city of Barcelona used alternative fuels, with the fleet composition being 67% diesel, 26% hybrid, 6% liquefied petroleum gas (LPG, mainly propane and butane), 0.4% compressed natural gas (CNG, methane and ethane) and 0.3% electric. Our aim was to study the VIAQ inside taxis including all these vehicle types and involved simultaneous collection (tracked by GPS) of air quality data on inhalable particle mass, number, and chemistry, as well as gaseous contaminants (CO, CO_2 and VOCs). The data recorded everyday VIAQ conditions breathed by taxi drivers and passengers during 6-h of a working day (10.00–16.00) and involved the co-operation of taxi drivers who consented to collect the equipment in the morning and carry it in the car with them as they went about their business. Considering there is relatively little literature documenting on-roadway/in-vehicle PM composition, and that most studies focus on collecting samples at locations in the vicinity of the roadway, the novelty of this manuscript is emphasised by the extensive effort made to collect "true" in-vehicle on-roadway PM that infiltrates into vehicles.

2. Methodology

The study was carried out in the metropolitan area of Barcelona with the collaboration of the Barcelona Metropolitan Taxi Institute (IMET) which gave permission and helped with the logistics of organising the sampling campaign that lasted from 4th–31st of October 2017 (weekdays only). On each day two taxis carried an identical set of measuring equipment, one vehicle always being diesel, and the other non-diesel (gasoline-hybrid, LPG, CNG or electric). The equipment was carried all together, usually in the boot (trunk) kept with roof open to the taxi interior. Both taxis started their journey together at the IDAEA-CSIC institute at 10.00 a.m. avoiding the height of the rush hour (although the city is by then extremely busy), and returned the equipment to the same location six hours later after working normally in the city. Note was taken of mileages covered plus any special variables such as the use of air conditioning, air fresheners, and whether the windows were open or closed, although the number of passengers during the 6-h monitoring period was not recorded. The range of taxi models and engine types that participated in the study are listed in Table 1.

Table 1
List of vehicles that participated in the Barcelona Taxi Air Quality Monitoring Campaign. For hybrid, CNG and electric the same taxi was used for repeated experiments.

Model	Number days	km on odometer	Year of purchase	Fuel type	Euro stage
Skoda Octavia	1	690,000	2006	Diesel	E4
	1	575,000	2009		E5
	1	780,000	2010		E5
	1	650,000	2010		E6
	1	560,000	2010		
	1	550,000	2010		
	1	256,000	2010		
	1	255,000	2014		
Seat Toledo	1	300,000	2014	Diesel	E5
	1	150,000	2016		E6
Seat Altea	1	737,000	2010	Diesel	E5
	1	572,000	2010		E6
	1	614,000	2011		
	1	575,000	2011		
	1	542,000	2011		
Toyota Prius	4	387,000	2012	Hybrid (petrol)	E6
Citroen C-Elysée	1	165,000	2016	LPG	E5
	3	153,000	2016		
Volkswagen Caddy	3	47,000	2017	CNG	E6
Nissan Evalia	4	160,000	2014	Electric	E6

Air quality measurements were registered every 10 s with the following equipments:

- Mini-aethalometer (Magee Scientific) to measure black carbon (BC) (only in the diesel taxis).
- DiSCmini (Matter Aerosol AG, Wohlen AG, Swiss) to monitor particle number concentrations (N, expressed in #/cm^3) and size mode in the size range of 30–700 nm, as well as lung deposited surface area (LDSA $\mu m^2/cm^3$).
- IAQ-track (Model 7545, TSI) to register levels of CO_2, CO, temperature and humidity.
- GPS to monitor the routes taken by each taxi during the working day.

Furthermore, the set was also equipped with a personal Environmental Monitor (PEM) to collect PM_{10} with a flow rate of 10 L/min on previously weighed 63 mm quartz microfiber filters (this allowing both measurement of average PM concentration and also a full chemical analysis of the particles being breathed during 6 h), and a low-volume VOC collector Markes International Ltd for later analysis using gas chromatography.

Given that the data were collected over a period of 4 weeks, they were deseasonalised to remove temporal fluctuations when comparing the levels of pollutants between the taxis. This was done with reference to the "Palau Reial" Urban Background station (termed UB-PR), where the same pollutants were monitored throughout the sampling period (Rivas et al., 2014). This station is located in the garden of the IDAEA-CSIC building (41°23′14″ N, 02°06′56″E, 78 m.a.s.l) and is exposed to road traffic emissions from the Diagonal Avenue (200 m away), one of the largest thoroughfares in Barcelona (100,000 cars/day). The adjusted concentration $(C_i^j)_k^*$ of the i^{th} pollutant for the k^{th} day at the taxi j^{th} was calculated as shown in Eq. (1):

$$(C_i^j)_k^* = (C_i^j)_k / [(C_i^{PR})_k / (\overline{C_i^{PR}})] \quad (1)$$

where $(C_i^j)_k$ is the concentration measured at the taxi, $(C_i^{PR})_k$ and $(\overline{C_i^{PR}})$ are the 6 h average corresponding to day k^{th} and campaign averages at UB-PR, respectively. The range of quotients to deseasonalised varied

between 0.53 and 1.39, except for the 19th of October that was 2.35 due to heavy rain.

A total of 30 PM_{10} gravimetric samples collected using the PEM were chemically analysed using ICP-AES and ICP-MS for major and trace elements respectively. A sample was collected for each of the daily trips in each taxi. After sampling, filters were dried for 24 h at room temperature, (20–25 °C and 25% humidity), before being chemically analysed. SiO_2 and CO_3^{2-} were indirectly determined on the basis of empirical factors (Alx1.89 = Al3xAl_2O_3 = SiO_2 and (1.5xCa) + (2.5xMg) = CO_3^{2-}, see Querol et al. (2001)). A portion of each filter was digested in acidic environment (5 mL HF, 2.5 mL HNO_3, 2.5 mL $HClO_4$) for the determination of major and trace elements. A sub-sample measuring 1.5 cm^2 was taken from each filter to allow the determination of Organic Carbon (OC) and Elemental Carbon (EC) content by thermo-optical transmission using a Sunset Laboratory OCEC Analyzer. Blank filters were used for every stock purchased for sampling (one blank filter for each 12 filter stock). A few milligrams of the NIST 1633b reference material were added to blank filters to check the precision of the data obtained. Regarding the precision of the analyses, most of the elements showed an analytical error < 10%, except for P and K which had a 15% error.

Volatile organic compounds (VOC) in 5 (one per type of fuel) air samples were collected using stainless steel cartridges (89 mm length x 6.4 mm O.D. x 5 mm I.D, Markes International Ltd., Llantrisant, UK) custom packed with 3 successive sections of activated graphitized BC adsorbents, 150 mg Carbotrap C 20–40 mesh, 150 mg of Carbotrap 20–40 mesh and 150 mg of Carbotrap X 40–60 mesh (Supelco, Sigma-Aldrich, St. Louis, USA). The cartridges were pre-conditioned at 320 °C with helium (5 N quality) flow at 100 mL/min for 2 h and conditioned before each sampling at 335 °C with same helium flow for 30 min. The clean cartridges were capped with ¼ inch brass long-term storage caps with ¼ PTFE ferrules and storage in free-VOC ambient until its use. For active sampling the cartridges were coupled to a low-flow pump through a single air inlet port of Pocket Pump Air (SKC Ltd., Blandford Forum, UK) with constant flow compensation at 20 mL/min for 6 h. The pump was calibrated before and after each air intake with the Defender 510-L primary flow calibrator (Bios Drycal, NJ, USA). The VOC trapped in the cartridges were analysed by the thermal desorption equipment Ultra 50:50 Multi-tube Auto-sampler/Thermal Desorber Unity Series 2 (Markes International Ltd, Llantrisant, UK) coupled to a gas chromatograph with mass spectrometry detector. External calibration method was used for quantification of target VOC using multi-point reference stock solutions at different concentration in the range of 0.25–200 µg/mL in methanol from different commercial solutions: FIA Paraffin Standard (Accustandard Inc., New Haven, USA), Special Mix 6 compounds (CPAchem Ltd., Bulgaria), 8260B Calibration Mix #1 (Restek Corporation, Bellefonte, USA) and Cannabis Terpenes Standard #1 (Restek Corporation, Bellefonte, USA). 1 µL reference stock solution was injected onto clean cartridge through the injector port of Calibration Solution Loading Ring (CSLR, Markes International Ltd, Llantrisant, UK) using a standard syringe and purged for 3 min with helium (5 N quality) at 50 mL/min to remove the solvent. Carbon disulfide, ethyl methacrylate, iodomethane, methyl acrylate, 2-nitropropane, methylene chloride, acetonitrile, 2-chloroethanol, (-)-alpha-bisabolol, linalool and geraniol from commercial solution could not be determined. Calibration for most these targets showed excellent linearity (R2 ≥ 0.99). Clean cartridges were spiked at low different concentration levels to determine the limit of detection, ranged 0.03–1.5 ng/cartridge.

For the PM_{10} source apportionment, the Positive Matrix Factorization (PMF, Paatero and Tapper, 1994) model was run by means of the EPA PMF v5 software. The input data uncertainty estimates were based on the approach of Amato et al. (2009) and provided a criterion to separate the 22 species which retain a significant signal from the remaining ones with higher noise. This criterion is based on the signal-to-noise S/N ratio defined by Paatero and Hopke (2003). As an additional criterion, we used the percentage of data above detection limit. The combination of both criteria permitted to select for the PMF analysis 21 strong species and 1 weak species (Cr). Given the low number (30) of PM_{10} samples obtained in the taxis, the PMF was run to an extended matrix where we added 90 additional ambient air PM_{10} samples collected at the above referenced UB-PR site. This data assembling showed the most satisfactory results for factor profiles since it allowed exploring a larger area of the N-dimensional source contributions space. The data matrix was uncensored, i.e. negative, zero and below detection limit values were included as such in the analyses to avoid a bias in the results (Paatero, 2007). Given that samplings in different taxi engine types were performed in different days, resolved source contributions were deseasonalized using simultaneous data from the continuously running monitoring station, following the same method described above.

3. Results

3.1. Concentrations of major pollutants

Concentration ranges and median values for pollutant concentrations are presented in Table 2 and demonstrate considerable variation in vehicular interior air quality (VIAQ). Diesel and LPG vehicle interiors registered highest median values of PM_{10} (75–81 µg/m^3), OC (26 µg/

Table 2
Median (MD), maximum (max) and minimum (min) values for selected parameters measured at different fuel-type taxis. n: number of taxis. LPG: liquefied petroleum gas, CNG: compressed natural gas.

	n	PM_{10} (µg/m^3)			OC (µg/m^3)			EC (µg/m^3)			BC (µg/m^3)		
		MD	max	min	MD	max	min	MD	max	min	MD	max	min
Diesel	14	75.2	106.3	41.8	25.6	40.3	10.8	9.4	28.2	3.2	6.5	17.2	2.22
Hybrid	4	49.6	61.2	43.8	18.6	21.0	14.9	7.4	10.9	5.5			
LPG	4	81.0	94.6	64.5	26.3	32.0	18.1	10.5	13.3	4.2			
CNG	3	51.0	54.2	47.8	15.0	15.18	15.0	8.3	9.4	7.3			
Electric	4	49.8	75.4	35.0	21.7	40.8	12.4	4.6	7.3	2.5			

	Number (#/cm^3)			Size (nm)			LDSA (µm^2/cm^3)			CO (ppm)			CO_2 (ppm)		
	MD	max	min	MD	max	min	MD	max	min	MD	max	min	MD	max	min
Diesel	32138	88257	7938	46	59	31	104	233	45	2.1	3.7	1.2	418	2052	364
Hybrid	48436	58153	31900	34	36	33	55	66	29	1.2	1.4	0.7	398	529	346
LPG	38614	65778	7017	38	46	35	53	91	17	1.5	2.4	1.1	410	2139	361
CNG	45701	46208	45194	32	33	31	46	47	45	1.0	1.1	0.8	391	424	358
Electric	10614	13214	7329	34	40	34	12	13	12	0.1	0.5	0.1	2395	3478	1724

m^3), and EC (9–11 μg m^3). Diesel cars also recorded the highest median levels of CO (2.1 ppm) and LDSA (104 $\mu m^2/cm^3$) and largest sizes (46 nm) of UFP, but registered lower concentrations of particle numbers (median N < 33,000 #/cm^3) than hybrid, natural gas (CNG) or LPG car interiors (39–46,000 #/cm^3). Previous studies have already shown higher number of particles emitted by CNG buses than diesel buses, in accelerating mode (Hallquist et al., 2013). In contrast, electric and hybrid operated taxis recorded the lowest interior PM_{10} values (50 μg/m^3). The interiors of electric powered taxis driven with closed windows showed the lowest median values in EC (4.6 μg/m^3), number of UFP (N = 10,614 #/cm^3), LDSA (12 $\mu m^2/cm^3$), and CO (0.1 ppm). The CO_2 data demonstrate clearly that concentrations of this gas are strongly influenced by whether windows are open for much of the day (< 570 ppm) or kept closed (> 1700 ppm): the electric taxi used in the study for example was driven all day with closed windows, producing median CO_2 values of 2395 ppm. A closer look at the data is presented below, focusing on individual 6-h journeys and daily pairings, and emphasising the effects on VIAQ of driving with windows open or closed.

Opening windows during road travel allows direct entry of outside traffic contaminants into the vehicle, whereas a closed system will encourage the build-up of internally-generated pollutants. This contrast between interior and exterior contaminants is demonstrated by Fig. 1 which compares particle number concentrations (N: in the size range of 30–700 nm) with levels of CO_2. Taxis circulating with windows closed recorded low N values across a limited range (7–13,000 #/cm^3), whereas those driving in the city with windows open showed median interior N levels always above 20,000 #/cm^3 and in extreme cases exceeding 80,000 #/cm^3. Conversely, open-window taxis record VIAQ ambient CO_2 concentrations similar to outdoor levels of around 400 ppm, whereas when the taxi interior becomes a closed system CO_2 concentrations rise substantially, depending on the number of passengers being carried. The highest median CO_2 value recorded in the study (3478 ppm) was measured in a closed electric car, with peaks occasionally exceeding 4500 ppm during the 6-h monitoring period.

Further comparison between VIAQ in taxis with windows open and closed is provided by the box plot on Fig. 2. The pattern of higher N with a much greater concentration range in open window vehicles is also shown by both PM_{10} and LDSA values. The results for both N and LDSA are strikingly lower in the closed taxi interiors, and contrast with median particle size values which show little variation irrespective of whether windows are open or closed (around 40 nm).

Ambient concentrations of carbon monoxide measured inside the taxis during this study were low, although there was considerable variation, with values ranging between 0.1 and 3.7 ppm. Fig. 3 plots CO levels against kilometer age (thousands of km driven) and tax models employed in the study. It is apparent from the figure that, with one exception (4LPG), the highest interior CO values (> 2 ppm) were reached in diesel vehicles, irrespective of whether the windows are open or closed. Of the different models used in this study the highest CO levels (2.5 ppm or above) were measured in Skoda Octavia taxis that had over 500,000 km on the odometer. In contrast, median concentrations of CO inside the hybrid taxi used in the study (a Toyota Prius) remained below 1.5 ppm despite the car having nearly 400,000 km on the odometer. The lowest CO concentrations measured in the study (< 0.5 ppm) were recorded inside an electric powered Nissan Evalia (160,000 km), this comparing with median CO levels of 2.2 ppm inside a Skoda Octavia (650,000 km) even though both taxis were driven with windows closed and a/c on.

With regard to ultrafine particle size measured in the taxi interior, as previously mentioned Table 2 demonstrates that those vehicles using diesel fuel registered larger median particle sizes than in the non-diesel vehicles. This difference is recorded in *every* daily pairing, irrespective of whether the non-diesel partner taxi was LPG, NG, hybrid or electric (Fig. 4). Diesel interior median UFP sizes ranged from 31 to 59 nm (median 46 nm) as compared to 31–46 nm (median 34 nm) for non-diesels.

The GPS-Route data obtained during this study confirm the highly

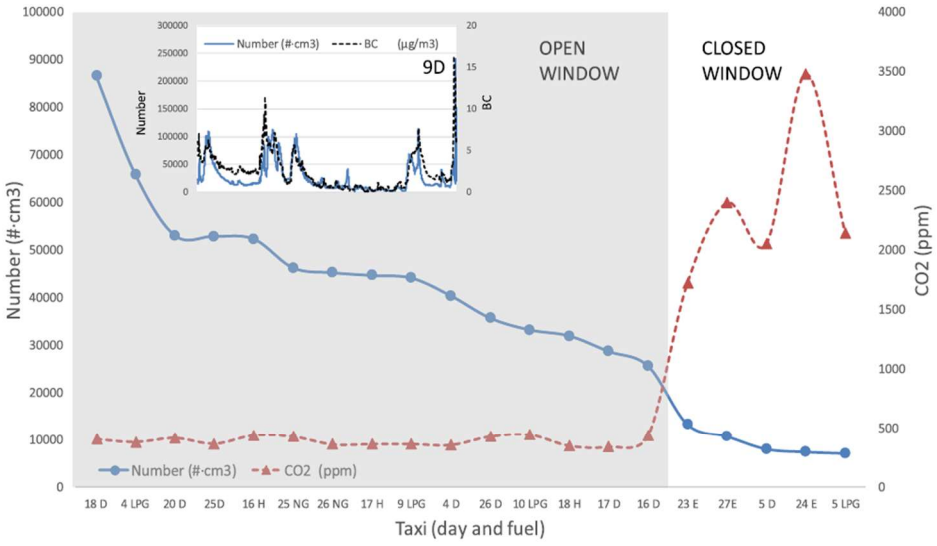

Fig. 1. Median values of particle numbers (N, in blue, expressed in #/cm^3 in the size range of 30–700 nm) measured inside taxis compared to CO_2 concentrations (in red) for conditions of either open (CO_2 = 330–440 ppm) or closed (CO_2 = 1700–3500 ppm) windows over 6-h daytime period. Lowest values of N, and highest values of CO_2, were recorded when windows were closed. The number on the horizontal axis refers to the date in October 2017 (all dry days without precipitation), and the letter refers to the fuel type (D = diesel; E = electric; H = hybrid; LPG = liquefiedd petroleum gas; NG = natural gas). Five taxis (9D, 10D, 23D, 27D, 20 H: not shown on this figure) recorded CO_2 values between 450 and 600 ppm due to windows being opened occasionally, and in one taxi (31D) the CO_2 equipment malfunctioned. The inset shows an example of how N and black carbon peaks can be positively correlated (diesel taxi 9th October with windows open), as demonstrated in previous publications (e.g. Krecl et al., 2017).

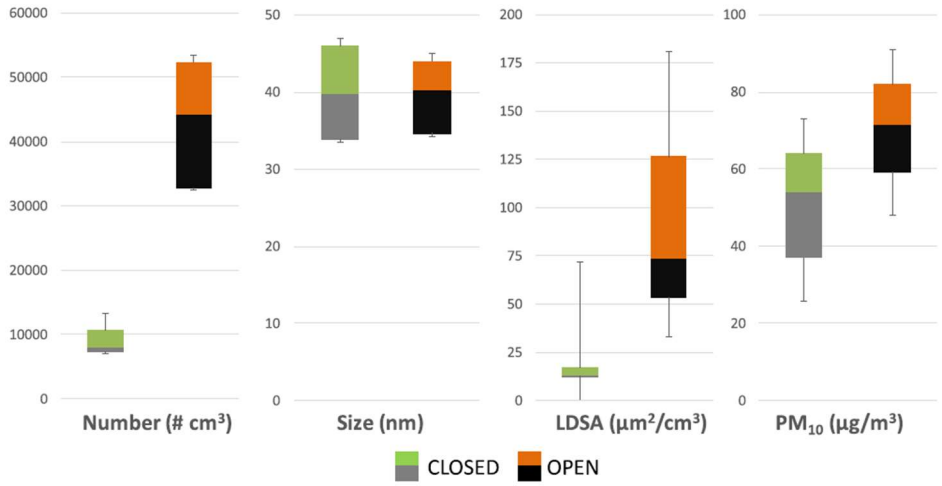

Fig. 2. Box plot comparing VIAQ parameters particle number, size, lung deposited surface area (LDSA) and PM_{10} mass inside taxis with windows open and closed (median values over 6-h daytime period). The coloured box defines the interquartile range, and the median is represented by the horizontal line separating the two colours. Particulate number, LDSA and mass levels are lower in the protected environment of a taxi interior with closed windows.

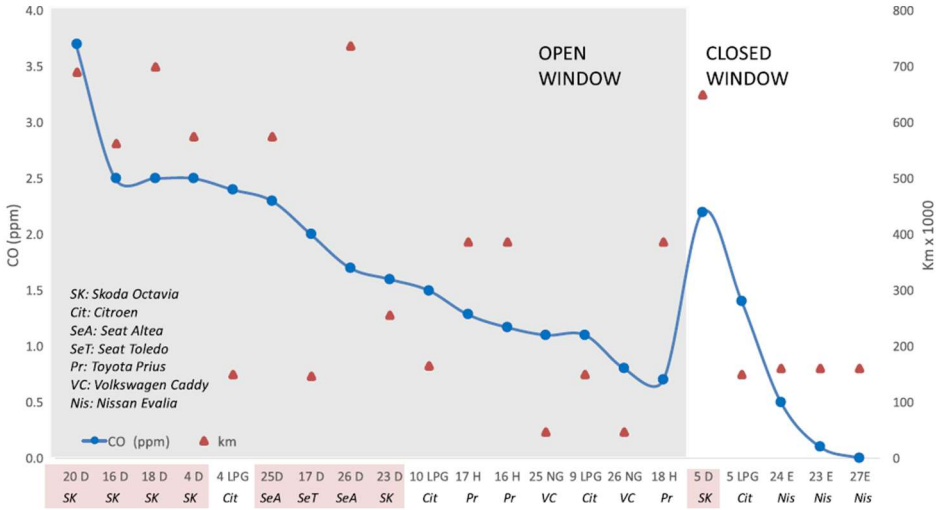

Fig. 3. Median 6-h daytime values of carbon monoxide levels in taxi interiors with windows open (CO_2 = 330–570 ppm) and closed (CO_2 = 1700–3500 ppm). Higher levels of CO are mostly associated with diesel taxis (pink shading), notably the high-km Skoda Octavia. Lowest CO levels were recorded in electric-powered taxis driving with windows closed. Note the difference between closed-window diesel and electric vehicles. The number on the horizontal axis refers to the date in October 2017, and the letter refers to the fuel type (D = diesel (pink background); E = electric; H = hybrid; LPG = liquid petroleum gas; NG = natural gas). All diesel cars were different (this being the most common taxi type in Barcelona), whereas for other fuel types the same car was used more than once except in the case of LPG where two different vehicles were used.

polluted nature of the Barcelona city centre road system, especially the grid plan area known as L'Eixample (the Enlargement) built to the west and north of the mainly pedestrianized medieval core. Taxis circulating with open windows through L'Eixample consistently show poor VIAQ (Fig. 5a–b). The routes illustrated by Fig. 5a and b for example compare concentrations of UFP numbers and black carbon (BC) breathed inside a Skoda Octavia diesel taxi with 700,000 km on the odometer during a 6-h daytime period mostly confined within L'Eixample and the equally congested central tourist route from Via Laetana to the sea front. The comparison not only graphically demonstrates the poor air quality ($N > 75{,}000$ #/cm^3; BC > 12 µg/m^3 for much of the time) but also reaffirms the positive correlation between N and BC in the VIAQ of diesel taxis (Fig. 1). In contrast Fig. 5c and d compare ultrafine particle numbers inside diesel and electric taxis driving with windows closed. Under these conditions the interior concentration of UFP is kept low (usually $N < 25{,}000$ #/cm^3 and for most of the time driving in the city centre, especially inside the electric vehicle, $N < 10{,}000$ #/cm^3).

The routes driven by the diesel and electric taxis recorded in Fig. 5c and d respectively include journeys away from the city centre, both to the airport (southwest of the city) and to the Besòs River estuary on the

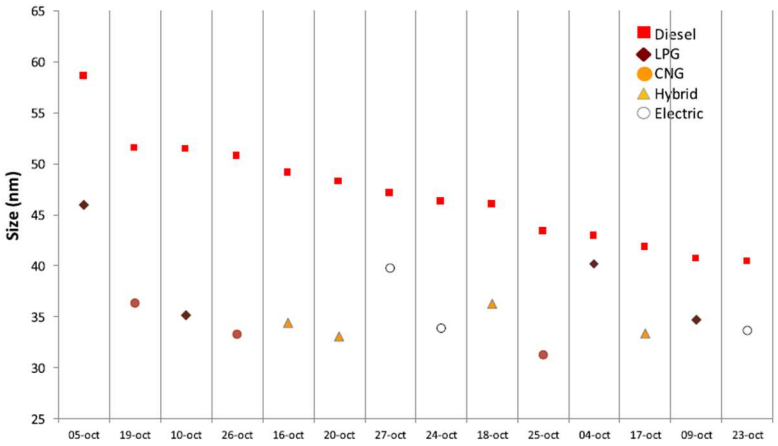

Fig. 4. Median ultrafine particle sizes (nm) inside taxi pairings over 6-h daytime working period. Diesel taxi VIAQ consistently shows larger median particle sizes than other engine types.

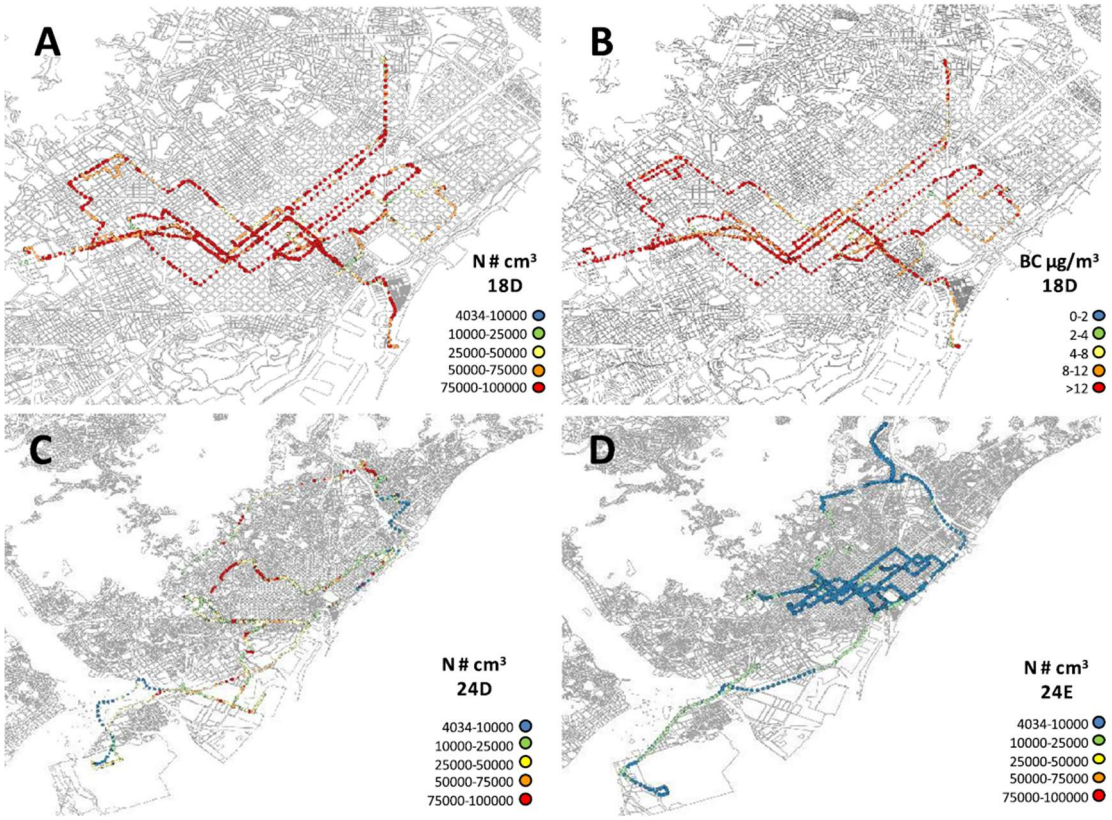

Fig. 5. Examples of pollutant concentrations inside taxis driving through the Barcelona area during the 6-h daytime monitoring period (10.00–16.00). The route taken by the open-window diesel taxi on 18th October was restricted to the city centre, especially the traffic-choked grid-plan L'Eixample area, and records generally very high levels of both UFP number (N: 5a) and black carbon (BC: 5b). In contrast the two taxis represented in Fig. 5c and d drove with windows closed and A/C on, spending much of the time in the city centre but also making excursions out of the city to the southwest and the northeast. Levels of UFP numbers inside the closed taxis remained very low except when the windows were opened briefly (see text for discussion).

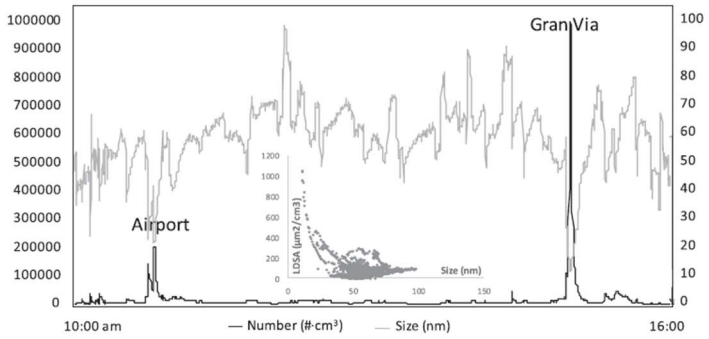

Fig. 6. Comparison of median UFP number (N) and particle size (nm) during the 6-h monitoring period inside taxi 24D (Fig. 5c). Generally low levels of N (< 10,000 #/cm^3) were maintained during the day by keeping windows closed, with the notable exception of two pollution events in the airport area and when driving along the congested Gran Via, when N rose rapidly and particle size decreased. The insert diagram shows the scatter between size and LDSA to reinforce the inverse correlation between size and number concentration.

northeast side of the city, as well as use of the urban ring road system. Excursions such as those out to the airport involve motorway driving conditions, usually at higher speeds that favour the infiltration of outside contaminants even into cars driving with windows closed so that interior N rises above 10,000 #/cm^3. Thus both closed taxis 24D (Fig. 5c) and 24E (Fig. 5d) recorded lowest interior particulate levels when driving slowly in the city centre, but demonstrated increasing entry of external pollutants into the car when driven out to the airport. A comparison between the VIAQ of these two taxis (24D and 24E) further reveals that whereas the driver of the electric taxi 24E ensured that windows were kept closed (with 6-h median CO_2 levels consequently rising to 3478 ppm), this was not the case for taxi 24D which recorded two VIAQ pollution events (Fig. 6). One of these was in the airport area and resulted in N rising to a peak around 200,000 #/cm^3, whereas the other occurred when driving along the extremely congested and canyon-like enclosed Gran Via 6-lane urban motorway leading northeast out of the city, when N levels suddenly spiked to 1000,000 #/cm^3 (Figs. 5 c and 6). Note also on Fig. 6 how peaks in N are accompanied by troughs in particle size.

3.2. PM chemistry and VOCs speciation

Chemical data from the PM_{10} filter samples collected from vehicle interiors during the Barcelona taxi experiment are listed in Table 3. Average values for all taxis (28 samples) are accompanied by two subgroups selected to compare (1) taxis with open windows all day (as recorded by the driver and confirmed by median interior CO_2 levels below 450 ppm: 8 diesel and 8 non-diesel); (2) taxis with windows closed all or most of the day (as recorded by the driver and confirmed by median CO_2 levels between 1700 and 3500 ppm: 1 diesel, 1 LPG; 4 electric). Levels of PM_{10} inside the taxis were on average around 3 times higher (67 µg/m^3) than urban background (22 µg/m^3), although once again there was considerable variation (35–106 µg/m^3). Elemental and organic carbon were the particle types most notably enriched inside all taxis, especially EC in vehicles with open windows, these registering concentrations > x10 urban background (Table 3). Interior levels of EC in open-window taxis (9–11 µg/m^3) were also notably higher than those with closed windows (3–5 µg/m^3), presumably reflecting the ingress of vehicle exhaust fumes from outside. In contrast, concentrations of OC in the closed electric vehicle were only slightly lower than those in openly ventilated diesel taxis (Table 3), implicating the greater influence of indoor sources, as will be discussed below.

The relative enrichment in urban air of carbonaceous particles and a range of traffic-emission-related trace metals such as Cu, Sn and Sb is shown by the histograms on Fig. 7 which compares the taxi interior PM chemistry with that from the Barcelona outdoor urban background. These metals, already noticeably enriched in background urban air, rise to concentrations exceeding PM_{10}Cu 100 ng/m^3, PM_{10}Sn 15 ng/m^3, PM_{10}Sb 8 ng/m^3 within the taxi interiors. Another metal showing notable enrichment is Zr, accompanied by other similarly enriched high field strength elements (HFSE) such as Hf, Nb, Y and U.

With regard to the **source apportionment** results, we identified six main sources of PM_{10} (Fig. 8a). The sum of the source contributions explained on average 66% of PM_{10} mass with the unexplained mass attributed mainly to a combination of ammonium nitrate particles and humidity. The six sources were labelled as vehicle wear, vehicle exhaust, industrial (mainly metallurgy), sea salt, mineral and regional. On average the main impacting source was vehicle exhaust (31%, 20 µg/m^3), which resulted about twice the contribution from vehicle wear (14%, 9 µg/m^3) (Fig. 8a,b), although the two factors seem not perfectly separated due to the relatively high share of Sb, Sn, Cr, Cu and Ba in the vehicle exhaust profile. This result may suggest a relatively higher efficiency of the air conditioning filter for supermicron particles rather than submicron particles. The third source by importance (excluding ammonium nitrate) was the regional source (10%, 6 µg/m^3), followed by industrial (5%, 3 µg/m^3), mineral and sea salt (both 3%, 2 µg/m^3). Given that about 80% of NOx urban ambient levels in the city have been attributed to road traffic (Querol et al., 2012), the total impact of traffic as a source for air pollutants breathed by taxi drivers and their passengers is estimated to be around 72%.

With regard to the analysis of **Volatile Organic Compounds** (VOCs) sampled in the taxi interiors, out of a total of 99 VOCs investigated 47 were detected and quantified (Table 4: another 60 compounds were analysed for but found to be below detection limit). These compounds included nine C_5-C_{10} alkanes and four C_5 alkenes (45–47% of total), thirteen C_6-C_{10} aromatic hydrocarbons (37–52%), eleven monoterpenes (0.7–15%), seven C_1-C_6 organochlorines (1–1.7%), two C_4 ethers and one C_5 ester (0.2–1.8%) (Table 4; Fig. 9). In addition several compounds, such as 4-methyl-1-pentene naphthalene, isobutanol, 1,1,1-trichloroethane, 1,4-dioxane, dibromochloromethane, chlorobenzene, bromoform, α-terpinene, were found in some taxi vehicles but at the limit of detection.

The most abundant compound of the alkane/alkene group was 2-methylbutane (43–60 µg/m^3) followed by n-pentane (17–28 µg/m^3) in all taxi models, whereas in the aromatic hydrocarbon group toluene was the most abundant compound (37–56 µg/m^3). All three of these VOCs are well documented as products of hydrocarbon fuel emissions. Other abundant VOCs were m-xylene, o-xylene, 1,2,4-trimethylbenzene, ethylbenzene, p-xylene, benzene, and 1,3,5-trimethylbenzene, all of which are also products of hydrocarbon fuel emissions (e.g. Chin and Batterman, 2012; Faber et al., 2013; Tsai et al., 2006; Yao et al., 2015). Several of these compounds are also known to be emitted by off-gassing of interior vehicle components (e.g. Brodzik et al., 2014). The dominance of aliphatic and aromatic hydrocarbons conforms to what is known from other studies of VOCs inside passenger cars (Faber and Brodzik, 2017).

The concentrations of benzene found in the taxi vehicles of the present study, 5.3–10 µg/m^3, were lower than those found in taxis of

Table 3
Average concentrations of major and trace components of PM_{10} sampled from taxi interiors and of ambient air PM_{10} sampled simultaneously at UB-PR (urban background). In addition to all taxis analysed (28 analyses) there are 5 subgroups depending on whether windows were kept open or closed, and on how the vehicle was powered.

	Urban	ALL TAXIS (AT)		open windows (CO_2 < 450 ppm)		Closed windows		
µg/m³	Background (UB)	(No. = 28)	AT/UB	Diesel (8)	Non Diesel (8)	Diesel (1)	LPG (1)	Electric (4)
PM_{10}	21.9	66.9	3.1	72.3	62.5	53.7	64.5	52.5
OC	2.5	21.7	8.7	25.6	20.8	14.6	18.1	24.2
EC	0.9	9.4	10.4	11.1	9.2	3.2	4.2	4.7
Al_2O_3	0.4	0.8	2.0	0.8	0.7	0.8	0.9	0.5
Ca	0.5	1.5	3.0	1.5	1.7	2.0	2.1	1.6
Fe	0.5	1.7	3.4	1.5	1.8	2.1	2.9	2.2
K	0.2	0.2	1.0	0.2	0.2	0.3	0.1	0.3
Na	0.6	0.5	0.8	0.5	0.8	0.7	1.1	0.7
Mg	0.1	0.1	1.0	0.1	0.3	0.3	0.3	0.2
P	< 0.05	0.1		0.1	0.1	0.1	0.2	0.1
S	1.0	0.5	0.5	0.5	1.0	0.4	0.7	1.1
ng/m³								
Ti	14.4	23.6	1.6	28.6	27.9	23.6	8.3	16.1
Cr	4.8	14.7	3.1	16.3	15.3	< 0.5	< 0.5	< 0.5
Cu	17.9	90.0	5.0	88.8	106.5	40.7	90.0	53.5
Zn	25.3	63.7	2.5	59.2	79.3	58.9	69.4	36.9
Mn	7.9	12.9	1.6	14.7	19.3	11.8	10.4	3.6
Sr	2.2	4.1	1.9	4.5	5.5	3.1	4.7	1.5
Y	0.1	1.9	19.0	2.0	1.7	< 0.5	< 0.5	< 0.5
Zr	8.8	49.7	5.6	56.6	63.5	69.2	57.2	31.2
Nb	0.1	0.7	7.0	0.6	1.4	< 0.5	< 0.5	< 0.5
Sn	3.9	14.8	3.8	18.6	19.5	11.3	14.2	5.5
Sb	2.0	5.8	2.9	6.5	8.6	1.2	5.4	2.4
Hf	0.4	2.4	6.0	2.5	3.0	2.8	2.7	1.4
Pb	3.2	4.3	1.3	5.1	5.6	1.1	1.3	1.8
Th	0.1	0.3	3.0	0.3	0.3	< 0.5	< 0.5	< 0.5
U	0.1	1.0	10	1.0	0.8	< 0.5	< 0.5	< 0.5

Guangzhou, 34 µg/m³ (Chan et al., 2003) and those found in the inner atmospheres of patrol cars from North Carolina, 13 µg/m³ (Riediker et al., 2003). The concentrations of toluene in the taxis of the present study, 37–56 µg/m³, were lower than those found in the taxis of Guangzhou, 110 µg/m³ (Chan et al., 2003) and similar to those found in the patrol cars of North Carolina, 39 µg/m³ (Riediker et al., 2003). The taxis of Guangzhou also have higher concentrations of ethylbenzene, 20 µg/m³, than those observed in the taxis of the present study, 6.5–11 µg/m³. However, the concentrations of xylenes, m/p-xylenes and o-xylene in Guangzhou, 20 µg/m³ and 17 µg/m³, respectively, are similar to those of the present study, 23–37 µg/m³ and 8.5–13 µg/m³, respectively. In contrast, a study of VIAQ in Hong Kong taxis fuelled by LPG recorded much lower levels of aromatic hydrocarbons (Guo et al., 2011).

Normality testing of the concentration of these compounds inside each taxi under different fuel-engine models using the Shapiro-Wilk test showed non-normal distribution ($p < 0.001$). The Kruskal-Wallis test for non-parametric ANOVA indicated that the indoor taxi VOC concentrations of the different powered models were not significantly different for the compounds related with fuel emissions ($p = 0.322$). High correlations between the concentrations of alkanes/alkenes and aromatics in the air of each taxi model were observed showing a predominance of the same emission sources.

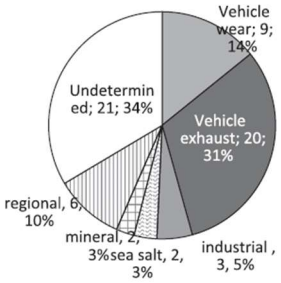

Fig. 8. a. Average mass contributions (in µg/m³ and %) of aerosol sources in the interior of the taxis determined by PMF. b: Chemical profiles of the aerosol sources resolved by PMF.

Four of the five taxis used to sample VOCs were driven with windows open and therefore exposed to traffic pollutants infiltrating from outside. The only taxi driven with windows closed was the electric vehicle which recorded the lowest concentrations of n-pentane, 2-

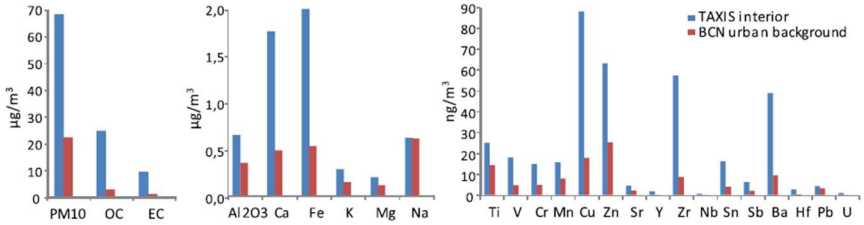

Fig. 7. Comparisons between the chemistry of PM_{10} measured inside taxis with data from the Barcelona urban background air monitoring site in Palau Reial.

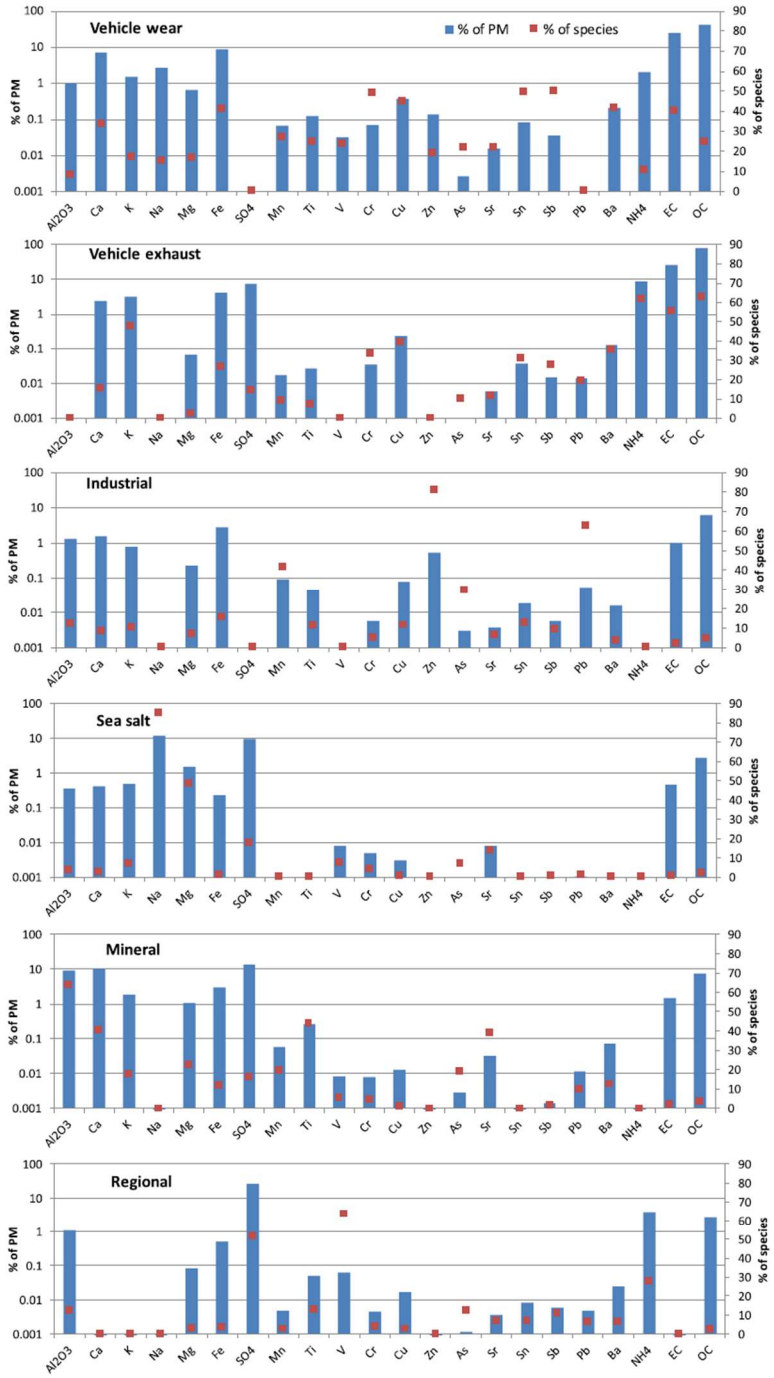

Fig. 8. (*continued*)

Table 4
Concentrations of VOCs inside the studied taxi cars. LPG: liquefied petroleum gas; CNG: compressed natural gas.

	Concentration inside taxi (μg/m³)				
Group/Compound	LPG	Diesel	Hybrid	Electric	CNG
Alkanes/Alkenes					
n-Pentane	21	20	18	17	28
n-Heptane	5.9	4.9	2.9	6.0	7.5
n-Hexane	5.0	4.8	3.8	5.6	5.4
n-Octane	3.1	2.6	2.1	2.3	3.4
n-Decane	5.1	0.8	0.6	1.0	1.7
2-Methylbutane (i-pentane)	53	50	47	43	60
2,3-Dimethylpentane	2.2	2.0	1.6	2.3	2.4
Isooctane	0.3	0.7	0.5	2.2	1.3
Cyclohexane	2.2	2.1	1.6	2.6	3.2
Isoprene	11	4.1	2.0	31	5.7
1-Pentene	1.2	1.1	0.8	1.0	1.5
cis-Pentene	1.2	1.0	0.9	1.0	1.7
trans – 2-Pentene	3.5	2.9	2.2	2.9	5.1
Total	*115*	*97*	*84*	*118*	*127*
Aromatics					
Benzene	8.6	6.8	6.8	5.3	10
Toluene	51	39	37	40	56
Ethylbenzene	10	8.0	6.5	7.1	11
m-Xylene	26	20	17	18	26
p-Xylene	9.9	7.8	6.5	6.8	11
o-Xylene	13	10	8.5	8.6	13
1,2,4-Trimethylbenzene	11	8.7	6.4	7.7	10
1,3,5-Trimethylbenzene	2.3	1.8	1.4	1.7	2.2
n-Propylbenzene	1.1	0.9	0.7	0.9	1.2
Styrene	1.0	0.7	0.8	0.5	1.0
Isopropylbenzene	0.4	0.3	0.3	0.3	0.4
n-Butylbenzene	0.3	0.2	0.2	< 0.1	0.3
sec-Butylbenzene	0.1	0.1	0.1	< 0.1	0.1
Total	*135*	*104*	*92*	*97*	*142*
Monoterpenes					
d-Limonene	4.5	0.8	0.9	30	4.4
Camphene	0.6	< 0.1	< 0.1	0.1	0.1
α-Pinene	0.4	0.2	0.3	1.8	0.6
(-)-β-Pinene/β-Myrcene	0.5	0.1	0.1	1.8	0.2
p-Cymene	0.6	0.3	0.2	0.6	0.4
δ-Terpinene	0.3	< 0.1	< 0.1	0.4	0.1
β-Ocimene	0.4	0.1	0.1	1.2	0.1
α-Ocimene	0.2	< 0.1	0.1	0.6	< 0.1
γ-Terpinene	0.1	< 0.1	< 0.1	1.3	0.1
δ3-Carene	0.1	0.1	0.1	0.2	0.1
Total	*7.7*	*1.5*	*1.7*	*38.2*	*5.9*
Organochlorines					
Tetrachloroethylene	0.8	0.8	0.9	0.5	2.3
1,2,2-Trichlorotrifluoroethane	0.7	0.7	0.7	0.6	0.8
Carbon Tetrachloride	0.6	0.6	0.6	0.6	0.6
Chloroform	0.4	0.2	0.4	0.1	0.3
1,2-Dichloroethane	0.2	0.2	0.2	0.5	0.2
Trichloroethylene	0.1	< 0.1	0.1	0.1	0.2
1,4-Dichlorbenzene	< 0.1	0.06	< 0.1	< 0.1	0.1
Total	*2.7*	*2.6*	*3.1*	*2.5*	*4.6*
Others					
Methyl methacrylate	0.2	0.2	0.3	0.5	0.5
Tetrahydrofuran	0.2	0.2	0.2	0.3	0.5
Diethyl ether	0.1	0.1	0.1	3.9	0.1
Total	*0.4*	*0.5*	*0.6*	*4.7*	*1.0*

methybutane (both strongly associated with hydrocarbon fuel emissions) but the highest concentrations of isoprene and most monoterpenes. In particular, isoprene recorded concentrations of 31 μg/m³ in the electric vehicle whereas in the others it ranged between 2 and 11 μg/m³. A similar difference was observed for all monoterpenes (except camphene) which were found in higher concentration in the electric vehicle, e.g. δ-limonene, 30 μg/m³, whereas in the atmospheres of the other cars it ranged between 0.8 and 4.5 μg/m³ (Table 4). An obvious cause for this difference is the use of an air freshener in this vehicle. The high concentration of diethyl ether in the electric taxi model is probably also due to the use of the air freshener under closed window conditions.

Another factor proven to influence the VOC content of car interior air is the age of the vehicle (You et al., 2007; Xu et al., 2016). The youngest vehicle used in this study was that powered by natural gas (1-year old; < 50,000 km on the odometer). The sample analysed from this vehicle showed the highest overall concentrations of alkanes/alkenes, aromatics, and organochlorines (Table 4), which we attribute to an extra VOC contribution by continued in-cabin degassing from a relatively young vehicle.

4. Discussion

The results summarised above offer insight into the controls on VIAQ inside a taxi driven through a busy city. They confirm the importance of air exchange rates (AER), the dominant influence of which has been noted by other publications dealing with VIAQ (e.g. Joodatnia et al., 2013; Knibbs and de Dear, 2010; 2011; Shu et al., 2015; Zhu et al., 2007). The concentration of UFP provides a sensitive indicator of AER inside a road vehicle, rapidly responding to variations in ventilation, traffic conditions, car speed, and cabin pressure which together influence particle infiltration from outside (e.g. Knibbs et al., 2009; Lee et al., 2015). Our data indicate that in taxis driven with windows and air circulation systems closed to outside air, the UFP number concentration can be expected to be limited to relatively small variations above and below median values of 10,000 #/cm³ during the working day. In contrast, driving the vehicle through the city with windows open exposes the occupants to substantial and highly erratic increases in UFP numbers, with median values ranging from 20 to 90,000 #/cm³, and with transient peak concentrations at times exceeding one million #/cm³.

Most of the UFP infiltrating the taxi cabin from outdoors will derive from the burning of hydrocarbon fuels, a process that produces nucleation mode particles that most commonly lie in the size range 10–20 nm. The rapid transformation of these fresh emissions to coarser accumulation mode particles by processes such as coagulation, especially in the confined microenvironment of a vehicle interior where dilution effects are impeded, is reflected by median UFP size values of 30–60 nm in our data. Our observation that median UFP size is always larger (usually by 10–15 nm) inside diesel vehicles as compared to taxis powered by other fuel systems suggests the influence of self-pollution inside the diesel cars, given the fact that PM emitted from diesel engines lie in a broader size range (20–130 nm) than those from gasoline engines (20–60 nm) (Morawska et al., 2008 and references therein). This suggestion is reinforced by data on black carbon (BC) concentrations measured in a taxi pair (diesel v. hybrid: this was only done on one day). The results from this pair recorded almost twice as much BC inside the diesel vehicle (16 October, diesel BC 17 μg/m³/CO_2 433 ppm v. hybrid BC 9 μg/m³/CO_2 435 ppm) even though both were driven around the city with open windows and with the equipment placed in the open boot (trunk). Similarly in all cases where CO was measured simultaneously in taxi pairs, concentrations of this gas were higher in the diesel (average 2.1 ppm) as opposed to the non-diesel (0.1–1.5 ppm) vehicle, again indicating a component of self-pollution.

Median concentrations of LDSA measured in our study were highly variable (12–233 μm²/cm³), although once again diesel vehicles recorded generally higher levels than in non-diesel taxis (with two exceptions, in LPG taxis, which were similar to their diesel pair). All median values > 100 μm²/cm³ were recorded only in diesel vehicles whereas, at the other extreme, LDSA values in the closed electric vehicle lay in the range 12–13 μm²/cm³. Lung deposited surface area values (for particles in the size range 20–400 nm) are likely to be a better predictor for pulmonary inflammation than number concentration and, especially, PM mass (Sager and Castranova, 2009; Buonanno et al., 2012). Our data confirm how LDSA concentrations present inside the cabin of a road vehicle are very sensitive to influxes of traffic pollutants from outside (see also Geiss et al., 2016). In the transient peak

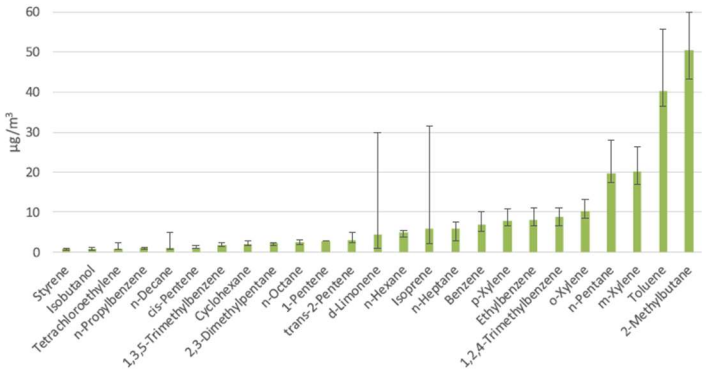

Fig. 9. Histogram ranking the relative abundances of VOCs measured inside taxis.

example described previously (taxi 24D, Figs. 5c and 6), for example, the dramatic increase in UFP numbers from 10,491 #/cm^3 to 973,696 #/cm^3 was matched by a rise in LDSA over the same 3-min period from 132 µm^2/cm^3 to 1052 µm^2/cm^3, whilst simultaneously median particle size dropped from 54 nm to 11 nm in response to the entry of fresh traffic emissions.

Most studies of inhalable particle mass inside road vehicles have reported on concentrations of $PM_{2.5}$ rather than PM_{10}, placing emphasis on the dominant numbers of fine and ultrafine exhaust-generated particles in traffic emissions (e.g. Fondelli et al., 2008; Fruin et al., 2008; Quiros et al., 2013). In contrast we chose to measure PM_{10} on the basis of the fact that a large percentage of inhalable traffic-related particles derive from non-exhaust sources and are therefore abundantly present in the $PM_{2.5–10}$ size fraction. It has been shown for example that although particles emitted from brake wear range down to nanometric sizes (Nosko et al., 2017), they commonly measure 2–6 µm and can contribute over 50% to the mass of traffic-related PM_{10} (Amato et al., 2014; Grigoratos and Martini, 2015; Thorpe and Harrison, 2008). Our data demonstrate that PM_{10} concentrations inside Barcelona taxis were variable but averaged 67 µg/m^3, which is more than treble the urban background for the same period (Table 3). Much of this difference in PM mass is attributable to increased levels of organic and elemental carbon, both of which are around x10 urban background inside taxi driven with windows open (Table 3) and source from both exhaust and non-exhaust traffic emissions. Our source apportionment data indicate the main impacting source of PM_{10} measured inside the taxis was vehicle exhaust (31%), with an additional 14% apportioned to vehicle wear (Fig. 8a,b).

The enrichment by a factor of x3 to x7 shown by a range of trace metals (Cr, Cu, Sn, Sb) in taxi interior air as compared to urban background is attributed mainly to the presence of particles abraded from brakes. The metalliferous nature of brake particles (which also contribute OC to traffic-contaminated air) has been well documented, with Cu and Sb being perhaps the most quoted classic markers of this source (Adamice et al., 2016; Amato et al., 2011; Grigoratus and Martini, 2015). To this list however we would add an "HFSE group" comprising mainly Zr and the associated High Field Strength Elements of Hf, Nb, Y and U. The likely origin for these HFSE enrichment anomalies in traffic-contaminated air is their concentration in the mineral zircon ($ZrSiO_4$) used as an abrasive in road vehicle brakes. Such abrasive minerals can comprise up to 10% of the brake lining and are employed to increase friction and limit the build-up of transfer films (Cho et al., 2008; Grigoratus and Martini, 2015).

The unusual trace metal signature of brake-particle contaminated aerosol loadings breathed at roadsides and inside vehicles is graphically displayed in the ternary plot of Fig. 10 and introduced in a previous publication (Moreno et al., 2015). This triangular diagram uses Mn, Ti

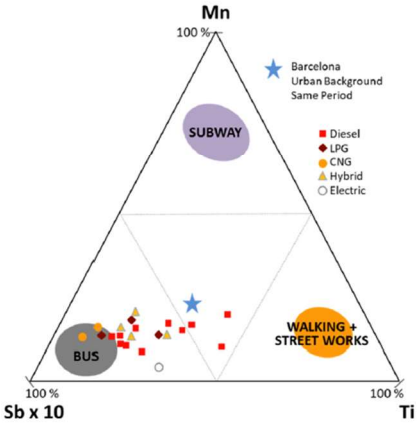

Fig. 10. Ternary plot comparing PM_{10} measured inside Barcelona taxis with the compositions of $PM_{2.5}$ collected from bus, subway and outdoor roadside microenvironments (see Moreno et al., 2015). The relative enrichment in Sb is attributed to brake particle emissions. The blue star marks the composition of Barcelona urban background PM_{10} during the October 2017 VIAQ taxi measurement campaign.

and Sbx10 to highlight the composition of particles produced by frictional movement of steel wheels and rails (subway), silicate-rich crustal (or "geological") particles (walking and street works), and those produced by Sb-rich brake emissions and breathed inside buses. Plotting our taxi data on this diagram demonstrates a clear affinity for the brake-contaminated apex, moving progressively away from a more crustal signature. For comparison the composition of Barcelona urban background for October 2017 is also plotted (blue star).

Our VIAQ data on VOCs inside taxi vehicles reveal a mix of compounds which reflects the complexity of traffic-related organic carbon emissions. The observation that the C_4-C_5 alkanes 2-methylbutane and n-pentane together comprise over half of the VOCs measured implicates the strong presence of light-hydrocarbon fuel emissions (gasoline, natural gas) (Montells et al., 2000; Watson et al., 2001; Liu et al., 2008). Given the fact that purely gasoline vehicles were not used in our study we can assume that most of these alkanes are infiltrating the taxi from outside, although note the content of n-pentane recorded inside the compressed natural gas vehicle (28 µg/m^3) was 7–11 µg/m^3 higher than all other vehicle types, suggesting an additional component of self-pollution. Over half the cars currently driven in Barcelona have diesel engines, so it is likely that many of the VOCs measured derive from

diesel combustion. Separating diesel from gasoline emissions however is not simple as they share several species (Hong et al., 2017) and fuels vary in composition, although it is probable that compounds such as m-xylene, trimethylbenzene and toluene derive at least in part from diesel engines (Tsai et al., 2006). Another complicating factor involves the well-documented effect of VOC off-gassing from interior materials, an influence that is most obvious in newer cars (Brodzik et al., 2014; Chien, 2007; Faber et al., 2013; Xu et al., 2016). This may explain why the youngest car (1-year old and with the lowest km: Volkswagen Caddy CNG) recorded the highest concentrations of a majority of alkane/alkene and aromatic compounds (Table 4). Finally, the influence on VIAQ of introducing VOC-emitters such as air-fresheners can be dramatic. Our case of δ-limonene reaching median values of 30 $\mu g/m^3$ inside a closed electric taxi provides a good example, although it is eclipsed by the study of Fedoruk and Kerger (2003) who recorded nearly 600 $\mu g/m^3$ of 2-butoxyethanol released by a deodoriser inside a used Ford Taurus.

Another result of operating taxis under closed ventilation conditions will be a rise in CO_2 concentrations. The maximum CO_2 level recorded in our study was 4600 ppm, reached inside a closed electric vehicle (24E). The taxi began work that day recording interior CO_2 concentrations of 400 ppm, this rising to 3000 ppm in 45 min and staying above this level for over 4 h before a sudden drop (over 3 min) to 2000 ppm when the car was ventilated. This brief ventilation episode was accompanied by a jump in N from 10,000 to 20,000 $\#/cm^3$ and in LDSA from 10 to 20 $\mu m^2/cm^3$, before closed conditions were re-established and CO_2 rose again. The rapidity (less than 1 h to reach several thousand ppm) with which CO_2 concentrations can climb inside a taxi is a cause for concern. Although CO_2 is listed as a toxic contaminant workplace exposure to which should be kept below a 8-h time-weighted average of 5000 ppm, various studies have demonstrated that concentrations lower than this, and certainly within the range of the example given above, can have a detectable effect on both mental performance and physical condition (Kajtár and Herczeg, 2012; Zhang et al., 2015). A recent exercise in modelling CO_2 accumulation inside vehicles has emphasised the sagacity of ventilating the vehicle when CO_2 levels reach 2500 ppm, a threshold considered to be "consistently linked to detrimental cognitive effects" (Hudda and Fruin, 2018). In the Barcelona electric taxi example described above, this threshold of 2500 ppm CO_2 was exceeded for 4.5 h of the 6 h monitoring period.

Taxi drivers work at the coalface of modern transport-related urban air pollution. During their working day they are continuously exposed to enhanced mass and number concentrations of particles derived from vehicle exhaust and non-exhaust sources. Yet there seems to be only limited awareness of the risks associated with breathing poor quality air, as demonstrated by the fact that a majority of the taxi drivers in our study chose to drive through the busy city with open windows, thus unwittingly breathing UFP concentrations that, during extreme transient peaks, can exceed one million $\#/cm^3$. A recent survey of taxi drivers in New York reflected this lack of awareness with 74% of respondents claiming they were not very worried about being exposed to air pollution while driving (Gany et al., 2017). Presumably this situation applies not just to the hazard of pollutants infiltrating from outside but also to the problem of contaminants such as CO_2 that are generated within the taxi interior and need to be briefly but regularly ventilated, preferably in relatively clean air outside conditions. The taxi driver community would clearly benefit from awareness initiatives designed to help them better understand the value of good practice regarding VIAQ, and thus encourage them to take measures to reduce air pollutant exposure to themselves and their passengers.

5. Conclusions

i. Our study reveals real air quality conditions experienced by taxi drivers and their passengers travelling day-to-day through a traffic-congesting city such as Barcelona, and reinforces the critical importance of air exchange rates to vehicular interior air quality (VIAQ).
ii. Both ultra-fine particle numbers (N) in the size range of 10–700 nm and lung deposited surface area (LDSA) measurements offer sensitive indicators of VIAQ and the likelihood of negative health effects. Despite the high city centre traffic volumes, and even with a dominance of diesel vehicles on the road, taxis driven under closed ventilation conditions can suppress median levels of UFP to around N = 10,000 $\#/cm^3$ or less. Such levels are considerably lower than N values reported for UFP breathed when travelling by public transport (bus, metro, tram) in the same city (Moreno et al., 2015). In contrast, if taxi windows are left open then median N values will rise above 20,000 and can approach 100,000 $\#/cm^3$, with transient peak exposures capable of exceeding N = 1,000,000 $\#/cm^3$. Similarly, median LDSA levels can rise from < 20 $\mu m^2/cm^3$ under closed conditions to > 200 $\mu m^2/cm^3$ with windows open and with transient peak levels exceeding 1000 $\mu m^2/cm^3$.
iii. Median UFP sizes of 36 nm (non-diesel) and 46 nm (diesel) reflect the presence of accumulation mode particles undergoing processes such as coagulation within the confined and relatively undiluted microenvironment of the vehicle interior.
iv. Evidence for the presence of exhaust contaminants generated by the vehicle being driven ("self-pollution") is implicated by higher BC and CO levels, and larger UFP sizes, measured inside the diesel taxi as compared to their non-diesel pair. Higher concentrations of CO (> 2 ppm) are most commonly associated with older diesel taxis with > 500,000 km on the odometer.
v. PM_{10} concentrations measured inside the taxis were variable but averaged 67 $\mu g/m^3$, which is more than treble the urban background for the same period and mostly attributable to increased levels of organic and elemental carbon. Source apportionment calculations indicate the main source of PM_{10} measured inside the taxis was vehicle exhaust followed by non-exhaust particles emitted by vehicle wear.
vi. The trace metal signature of PM_{10} collected within the taxis shows significant enhancements in Cr, Cu, Sn, Sb and a "High Field Strength Element" group characterised by Zr accompanied by Hf, Nb, Y and U. This signature is attributed mainly to the presence of brake PM and, in the case of the HFSE group, to the abrasive mineral zircon.
vii. Volatile organic compounds measured inside the taxi are dominated by 2-methylbutane and n-pentane, both of which are presumably sourced from the combustion of light hydrocarbon fuels. Other common VOCs include toluene, m-xylene, o-xylene, 1,2,4-trimethylbenzene, ethylbenzene, p-xylene, benzene, and 1,3,5-trimethylbenzene, all interpreted as exhaust emissions sourced from a mix of fuels. The youngest taxi (fuelled by natural gas) registered the highest content of alkanes and aromatics (possibly due at least in part to off-gassing), and the VOC composition inside a closed electric taxi was strongly influenced by the presence of an air freshener.
viii. Carbon dioxide concentrations stayed at around ambient levels (400 ppm) with taxi windows open, but quickly climbed to undesirable levels under closed ventilation conditions. In one example it took just 33 min to reach a CO_2 concentration of 2500 ppm and stayed above that level for 4.5 h of the 6-h monitoring period.
ix. Taxi drivers (and their passengers) would benefit from greater awareness of the known hazards associated with breathing traffic pollutants. Such knowledge would encourage them to make intelligent use of interior ventilation to reduce both the infiltration of outside contaminants and the build-up of indoor-generated pollutants.

Appendix

Acknowledgements

This work was supported by the ACS Foundation contributing to the dissemination of good environmental practices and environmental protection activities, the Spanish Ministry of Economy and Competitiveness and FEDER funds within the I+D Project CGL2016–79132 (BUSAIR), and the IMPROVE LIFE project (LIFE13ENV/ES/000263). We thank the Barcelona Metropolitan Taxi Institute (IMET) for their enthusiastic help and collaboration in this project.

References

Adamice, E., Jarosz-Krzeminska, E., Wieszala, R., 2016. Heavy metals from non-exhaust vehicle emissions in urban and motorway road dusts. Environ. Monit. Assess. 188, 369.

Alameddine, I., Abi Esber, L., Bou Zeid, E., Hatzopoulou, M., El-Fadel, M., 2016. Operational and environmental determinants of in-vehicle CO and $PM_{2.5}$ exposure. Sci. Total Environ. 551–552, 42–50.

Amato, F., Pandolfi, M., Escrig, A., Querol, X., Alastuey, A., Pey, J., Perez, N., Hopke, P.K., 2009. Quantifying road dust resuspension in urban environment by multilinear engine: a comparison with PMF2. Atmos. Environ. 43, 2770–2780.

Amato, F., Pandolfi, M., Moreno, T., Furger, M., Pey, J., Alastuey, A., Bukowiecki, N., Prevot, A.S.H., Baltensperger, U., Querol, X., 2011. Sources and variability of inhalable road dust particles in three European cities. Atmos. Environ. 45, 6777–6787.

Amato, F., Cassee, F.R., Denier van der Gon, H.A., Gehrig, R., Gustafsson, M., Hafner, W., Harrison, R.M., Jozwicka, M., Kelly, F.J., Moreno, T., Prevot, A.S., Schaap, M., Sunyer, J., Querol, X., 2014. Urban air quality: the challenge of traffic non-exhaust emissions. J. Hazard. Mater. 275, 31–36.

An, S., Hu, X., Wang, J., 2011. Urban taxis and air pollution: a case study in Harbin, China. J. Trans. Geogr. 19, 960–967.

Brodzik, K., Faber, J., Łomankiewicz, D., Gołda-Kopek, A., 2014. In-vehicle VOCs composition of unconditioned, newly produced cars. J. Environ. Sci. 26, 1052–1061.

Buonanno, G., Marini, S., Morawska, L., Fuoco, F.C., 2012. Individual dose and exposure of Italian children to ultrafine particles. Sci. Total Environ. 438, 271–277.

Cepeda, Magda, Schoufour, Josje, Freak-Poli, Rosanne, Koolhaas, Chantal M., Dhana, Klodian, Bramer, Wichor M., Franco, Oscar H., 2017. Levels of ambient air pollution according to mode of transport: a systematic review. Lancet Public Health 2 (1), 23–34.

Chan, L.Y., Lau, W.L., Wang, X.M., Tang, J.H., 2003. Preliminary measurements of aromatic VOCs in public transportation modes in Guangzhou, China. Environ. Int. 29, 429–435.

Chien, Y.-C., 2007. Variations in amounts and potential sources of volatile organic chemicals in new cars. Sci. Total Environ. 382, 228–239.

Chin, J.-Y., Batterman, S.A., 2012. VOC composition of current motor vehicle fuels and vapors, and collinearity analyses for receptor modelling. Chemosphere 86, 951–958.

Cho, K.-W., Jang, H., Hong, Y.-S., Fash, J.W., 2008. The size effect of zircon particles on the friction characteristics of brake lining materials. Wear 264, 291–297.

Durant, J.,L., Ash, C.A., Wood, E.C., Herndon, S.C., Jayne, J.T., Knighton, W.B., Canagaratna, M.R., Trull, J.B., Brugge, D., Zamore, W., Kolb, C.E., 2010. Short-term variation in near-highway air pollutant gradients on a winter morning. Atmos. Chem. Phys. 10 (2), 5599–5626.

Faber, J., Brodzik, K., 2017. Air quality inside passenger cars. Environ. Sci. 4, 112–133.

Faber, J., Brodzik, K., Golda-Kopek, A., Lomankiewicz, D., 2013. Benzene, toluene and xylenes in new and used vehicles of the same model. J. Environ. Sci. 25, 2324–2330.

Fedoruk, M.J., Kerger, B.D., 2003. Measurement of volatile organic compounds inside automobiles. J. Exp. Anal. Environ. Epidemiol. 13, 31–41.

Fondelli, M. Cristina, Chellini, Elisabetta, Yli-Tuomi, Tarja, Cenni, Isabella, Gasparrini, Antonio, Nava, Silvia, Garcia-Orellana, Isabel, Lupi, Andrea, Grechi, Daniele, Mallone, Sandra, Jantunen, Matti, 2008. Fine particle concentrations in buses and taxis in Florence, Italy. Atmos. Environ. 42 (35), 8185–8193.

Fruin, S., Westerdahl, D., Sax, T., Sioutas, C., Fine, P.F., 2008. Measurements and predictors of on-road ultrafine particle concentrations and associated pollutants in Los Angeles. Atmos. Environ. 42 (2), 207–219.

Fruin, S., Hudda, N., Sioutas, C., Delfino, R.J., 2011. Predictive model for vehicle air exchange rates based on a large, representative sample. Environ. Sci. Technol. 45 (8), 3569–3575.

Gany, F., Bari, S., Prasad, L., Leng, J., Lee, T., Thurston, G.D., Gordon, T., Acharya, S., Zelikoff, J., 2017. Perception and reality of particulate matter exposure in New York City taxi drivers. J. Expo. Sci. Environ. Epidemiol. 27 (2), 221–226.

Geiss, Otmar, Bianchi, Ivana, Barrero-Moreno, Josefa, 2016. Lung-deposited surface area concentration measurements in selected occupational and non-occupational environments. J. Aerosol Sci. 96, 24–37.

Grigoratus, T., Martini, G., 2015. Brake wear particle emissions: a review. Environ. Sci. Pol. Res. 22, 2491–2504.

Guo, H., Zou, S.C., Tsai, W.Y., Chan, L.Y., Blake, D.R., 2011. Emission characteristics of nonmethane hydrocarbons from private cars and taxis at different driving speeds. Atmos. Environ. 45, 2711–2721.

Hallquist, A.M., Jerksjo, M., Fallgren, H., Westerlund, J., Sjödin, A., 2013. Particle and gaseous emissions from individual diesel and CNG buses. Atmos. Chem. Phys. 13, 5337–5350.

Heal, M.R., Kumar, P., Harrison, R.M., 2012. Particles, air quality, policy and health. Chem. Soc. Rev. 41, 6606–6630.

Hoek, G., Krishnan, R.M., Beelen, R., Peters, A., Ostro, B., Brunekreef, B., Kaufman, J.D., 2013. Long-term air pollution exposure and cardio-respiratory mortality: a review. Environ. Health 12, 43.

Hudda, N., Fruin, S., 2018. Carbon dioxide accumulation inside vehicles: the effect of ventilation and driving conditions. Sci. Total Environ. 610–611, 1448–1456.

Hudda, N., Kostenidou, E., Delfino, R., Sioutas, C., Fruin, S., 2011. Factors that determine ultrafine particle exposure in vehicles. Environ. Sci. Technol. 45 (20), 8691–8697.

Hudda, N., Eckel, S., Knibbs, L., Sioutas, C., Delfino, R., Fruin, S., 2012. Linking in-vehicle ultrafine particle exposures to on-road concentrations. Atmos. Environ. 59, 578–586.

Joodatnia, P., Kumara, P., Robins, A., 2013. Fast response sequential measurements and modelling of nanoparticles inside and outside a car cabin. Atmos. Environ. 71, 364–375.

Kajtár, L., Herczeg, L., 2012. Influence of carbon-dioxide concentration on human well-being and intensity of mental work. Q. J. Hungari. Meteor. Serv. 116, 145–169.

Kaur, S., Nieuwenhuijsen, M., Colvile, R., 2005. Pedestrian exposure to air pollution along a major road in Central London, UK. Atmos. Environ. 39, 7307–7320.

Kelly, F., Zhu, T., 2016. Transport solutions for cleaner air. Science 352, 934–936.

Knibbs, Luke D., de Dear, Richard J., Morawska, Lidia, Mengersen, Kerrie L., 2009. On-road ultrafine particle concentration in the M5 East road tunnel, Sydney, Australia. Atmos. Environ. 43 (22–23), 3510–3519.

Knibbs, Luke D., de Dear, Richard J., 2010. Exposure to ultrafine particles and $PM_{2.5}$ in four Sydney transport modes. Atmos. Environ. 44 (26), 3224–3227.

Kreci, A., Targino, C., Johansson, C., Ström, J., 2015. Characterisation and source apportionment of submicron particle number size distributions in a busy street canyon. Aerosol Air Qual. Res. 15, 220–233.

Kreci, P., Johansson, C., Créso, A., Johan, S., Burman, L., 2017. Trends in black carbon and size-resolved particle number concentrations and vehicle emission factors under real-world conditions. Atmos. Environ. 165, 155–168.

Kumar, P., Ketzel, M., Vardoulakis, S., Pirjola, L., Britter, R., 2011. Dynamics and dispersion modelling of nanoparticles from road traffic in the urban atmospheric environment – a review. J. Aerosol Sci. 42, 580–603.

Leavey, A., Reed, N., Patel, S., Bradley, K., Kulkarni, P., Biswas, P., 2017. Comparing on-road real-time simultaneous in-cabin and outdoor particulate and gaseous concentrations for a range of ventilation scenarios. Atmos. Environ. 166, 130–141.

Lee, E., Stenstrom, M., Zhu, Y., 2015. Ultrafine particle infiltration into passenger vehicles. Part 1: experimental evidence. Transp. Res. Part D 38, 156–165.

Liu, Y., Shao, M., Fu, L., Lu, S., Zeng, L., Tang, D., 2008. Source profiles of volatile organic compounds (VOCs) measured in China: Part I. Atmos. Environ. 42, 6247–6260.

Madl, P., Majid, H., Kwasny, F., Hofmann, W., 2015. In-vehicle exposure to ultrafine particles while driving through a tunnel system and associated lung deposition calculations. Aerosol Air Qual. Res. 15, 295–305.

Montells, R., Aceves, M., Grimalt, J.O., 2000. Sampling and analysis of volatile organic compounds emitted from leaded and unleaded gasoline powered motor vehicles. Environ. Monit. Assess. 62, 1–14.

Morawska, L., Ristovski, Z., Jayaratne, R., Keogh, D., Ling, X., 2008. Ambient nano and ultrafine particles from motor vehicle emissions: characteristics, ambient processing and implications on human exposure. Atmos. Environ. 42 (35), 8113–8138.

Moreno, T., Reche, C., Rivas, I., Minguillón, M.C., Martins, V., Vargas, C., Buonanno, G., Parga, J., Pandolfi, M., Brines, M., Ealo, M., Fonseca, A., Amato, F., Sosa, G., Capdevila, M., de Miguel, E., Querol, X., Gibbons, W., 2015. Urban air quality comparison for bus, tram, subway and pedestrian commutes in Barcelona. Environ. Res. 142, 495–510.

Nikolova, I., Janssen, S., Vos, P., Vrancken, K., Mishra, V., Berghmans, P., 2011. Dispersion modelling of traffic induced ultrafine particles in a street canyon in Antwerp, Belgium and comparison with observations. Sci. Total Environ. 412, 336–343.

Nosko, O., Vanhanen, J., Olofsson, U., 2017. Emission of 1.3–10 nm airborne particles from brake materials. Aerosol Sci. Technol. 51 (1), 91–96.

Paatero, P., 2007. End User's Guide to Multilinear Engine Applications.

Paatero, P., Hopke, P.K., 2003. Discarding or downweighting high-noise variables in factor analytic models. Anal. Chim. Acta 490 (1–2, 25), 277–289.

Paatero, P., Tapper, U., 1994. Positive matrix factorization: a non-negative factor model with optimal utilization of error estimates of data values. Environmetrics 5, 111–126.

Querol, X., Alastuey, A., Rodríguez, S., Plana, F., Mantilla, E., Ruiz, C.R., 2001. Monitoring of PM_{10} and $PM_{2.5}$ around primary particulate anthropogenic emission sources. Atmos. Environ. 35, 845–858.

Quiros, David C., Lee, Eon S., Wang, Rui, Zhu, Yifang, 2013. Ultrafine particle exposures while walking, cycling, and driving along an urban residential roadway. Atmos. Environ. 73, 185–194.

Ragettli, M., Tsai, M., Braun-Fahrländer, C., de Nazelle, A., Schindler, C., Ineichen, A., Ducret-Stich, R., Perez, L., Probst-Hensch, N., Künzli, N., Phuleria, H., 2014. Simulation of population-based commuter exposure to NO_2 using different air pollution models. Int. J. Environ. Res. Public Health 11 (5), 5049–5068.

Riediker, M., Williams, R., Devlin, R., Griggs, T., Bromberg, P., 2003. Exposure to particulate matter, volatile organic compounds, and other air pollutants inside patrol cars. Environ. Sci. Technol. 37, 2084–2093.

Rivas, I., Viana, M., Moreno, T., Pandolfi, M., Amato, F., Reche, C., Bouso, L., Àlvarez-Pedrerol, M., Alastuey, A., Sunyer, J., Querol, X., 2014. Child exposure to indoor and outdoor air pollutants in schools in Barcelona, Spain. Environ. Int. 69, 200–212.

Sager, T.M., Castranova, V., 2009. Surface area of particle administered versus mass in determining the pulmonary toxicity of ultrafine and fine carbon black: comparison to ultrafine titanium dioxide. Part. Fibre Toxicol. 6, 6–15.

Shu, S., Yu, N., Wang, Y., Zhu, Y., 2015. Measuring and modeling air exchange rates inside taxi cabs in Los Angeles, California. Atmos. Environ. 122, 626–635.

Tartakovsky, L., Baibikov, V., Czerwinski, J., Gutmana, M., Kasper, M., Popescu, D.,

Veinblata, M., Zvirina, Y., 2013. In-vehicle particle air pollution and its mitigation. Atmos. Environ. 64, 320–328.
Thorpe, A., Harrison, R.M., 2008. Sources and properties of non-exhaust particulate matter from road traffic: a review. Sci. Total Environ. 400 (1–3), 270–282.
Tsai, W.Y., Chan, L.Y., Blake, D.R., Chui, K.W., 2006. Vehicular fuel composition and atmospheric emissions in South China: Hong Kong, Macau, Guangzhou, and Zhuhai. Atmos. Chem. Phys. 6, 3281–3288.
Vu, T., Delgado-Saborit, J.M., Harrison, R., 2015. Review: particle number size distributions from seven major sources and implications for source apportionment studies. Atmos. Environ. 122, 114–132.
Watson, J.G., Chow, J.C., Fujita, E.M., 2001. Review of volatile organic compound source apportionment by chemical mass balance. Atmos. Environ. 35, 1567–1584.
Xing, L., Wang, L., Zhang, R., 2018. Characteristics and health risk assessment of volatile organic compounds emitted from interior materials in vehicles: a case study from Nanjing. China Environ. Sci. Pol. Res. Int. 25 (15), 14789–14798.
Xu, B., Wu, Y., Gong, Y., Wu, S., Wu, Z., Zhu, S., Liu, T., 2016. Investigation of volatile organic compounds exposure inside vehicle cabins in China. Atmos. Pol. Res. 7, 215–220.
Yang, F., Kaul, D., Wong, K., Westerdahl, D., Sun, L., Ho, K., Tian, L., Brimblecombe, P., Ning, Z., 2015. Heterogeneity of passenger exposure to air pollutants in public transport microenvironments. Atmos. Environ. 109, 42–51.
Yao, Z., Shen, X., Ye, Y., Cao, X., Jiang, X., Zhang, Y., 2015. On-road emission characteristics of VOCs from diesel trucks in Beijing, China. Atmos. Environ. 103, 87–93.
You, K.W., Ge, Y.S., Hu, B., Ning, Z.W., Zhao, S.T., Zhang, Y.N., Xie, P., 2007. Measurement on in-vehicle volatile organic compounds under static conditions. J. Environ. Sci. China 19, 1208–1213.
Zhang, Xiaojing, Wargocki, Pawel, Lian, Zhiwei, 2015. Effects of exposure to carbon dioxide and human bioeffluents on cognitive performance. Procedia Eng. 121, 138–142.
Zhu, Y., Hinds, W., Kim, S., Shen, S., Sioutas, C., 2002. Study of ultrafine particles near a major highway with heavy-duty diesel traffic. Atmos. Environ. 36, 4323–4335.
Zhu, Y., Eiguren-Fernandez, A., Hinds, W., Miguel, A., 2007. In-cabin commuter exposure to ultrafine particles on Los Angeles freeways. Environ. Sci. Tech. 41, 2138–2145.

Research publications contributions

Article 2

Using miniaturised scanning mobility particle sizers to observe size distribution patterns of quasi-ultrafine aerosols inhaled during city commuting

Teresa Moreno, Cristina Reche, Kang-Ho Ahn, Hee-Ram Eun, Woo Young Kim, Hee-Sang Kim, **Amaia Fernández-Iriarte**, Fulvio Amato, Xavier Querol

Environmental Research 191 109978

https://doi.org/10.1016/j.envres.2020.109978

2020

Environmental Research 191 (2020) 109978

Contents lists available at ScienceDirect

Environmental Research

journal homepage: www.elsevier.com/locate/envres

Using miniaturised scanning mobility particle sizers to observe size distribution patterns of quasi-ultrafine aerosols inhaled during city commuting

Teresa Moreno [a,*], Cristina Reche [a], Kang-Ho Ahn [b], Hee-Ram Eun [b], Woo Young Kim [b], Hee-Sang Kim [b], Amaia Fernández-Iriarte [a,c], Fulvio Amato [a], Xavier Querol [a]

[a] Institute of Environmental Assessment and Water Research (IDAEA-CSIC), Barcelona, 08034, Spain
[b] Department of Mechanical Engineering, Hanyang University, Seoul, Republic of Korea
[c] Department of Natural Resources and Environment, Industrial and TIC Engineering (EMIT-UPC), 08242, Manresa, Spain

ARTICLE INFO

Keywords:
Commuting air quality
SMPS
Ultrafine
Nanoparticles
New particle formation
Nucleation
Road traffic

ABSTRACT

Portable miniaturised scanning mobility particle sizer (SMPS) instruments measuring atmospheric particles within the 10–241 nm size range were used to track particle number size distributions and concentrations during near-simultaneous pedestrian, bicycle, bus, car, tram and subway commuting journeys in Barcelona, Spain on 4th-6th July 2018. The majority of particles in this size range were <100 nm, with *k*-means cluster analysis identifying peaks at 15–22 nm, 30–40 nm, and 45–75 nm. Around 10–25% of the particles measured however were >100 nm (especially in the subway environment) and so lie outside the commonly defined range of "ultrafine" particles (UFP, or <100 nm particles). The study demonstrated in detail how personal exposure to quasi-UFP (QUFP, <241 nm), most of which present in the city streets are produced by road traffic, varies greatly depending on the transport mode and route chosen. Proximity to fresh traffic exhaust sources, such as in a car with open windows, on-road cycling, walking downwind of busy roads, or in a subway station contaminated by roadside air, enhances commuter exposure to particles <30 nm in size. In contrast, travelling inside air-conditioned bus or tram offers greater protection to the commuter from high concentrations of fresh exhaust. Ultrafine number size distributions in traffic-contaminated city air typically peak in the size range 30–70 nm, but they can be shifted to finer sizes not only by increased content of fresh proximal exhaust emissions but also by bursts of new particle formation (NPF) events in the city. One such afternoon photochemical nucleation NPF event was identified during our Barcelona study and recognised in different transport modes, including underground in the subway system. The integration of static urban background air monitoring station information with particle number concentration and size distribution data obtained from portable miniaturised SMPS instruments during commuting journeys opens new approaches to investigating city air quality by offering a level of detail not previously available.

1. Introduction

There is by now a huge body of scientific evidence demonstrating that the human population is suffering a self-inflicted environmental health crisis in which urban air quality is being severely compromised by road transport emissions (e.g. Morawska et al., 2008; Kumar et al., 2014, 2018; Kelly and Fussel, 2015; Steiner et al., 2016; Nieuwenhuijsen et al., 2018; Pope, 2020). Current estimates of the effects of air pollution on human longevity (e.g. Lelieveld et al., 2020) calculate millions of deaths worldwide annually brought forward, a health insult similar in scale to smoking-related diseases, with road traffic being the main culprit. These health effects are most commonly associated with particles measuring around 100 nm or less (defined as 'ultrafine' particles or UFP; Kumar et al., 2014; Krecl et al., 2017). Indeed, key to understanding the pervasiveness of our 21st century urban air pollution problem is that the extremely fine size of most inhaled traffic aerosols means that they can translocate from the lung to the systemic circulation so that "air pollution can harm nearly every organ in the body, and

* Corresponding author.
E-mail address: teresa.moreno@idaea.csic.es (T. Moreno).

https://doi.org/10.1016/j.envres.2020.109978
Received 25 June 2020; Received in revised form 18 July 2020; Accepted 19 July 2020
Available online 19 August 2020

particulate matter (PM) is the main offender" (Schraufnagel, 2020). In this size range the particles are low in mass (PM) but high in in number (PN) concentrations, and most are small enough (<100 nm) to enter cells by endocytosis and express their toxicity by impacting on intracellular redox state and disrupting cellular processes (Burello and Worth, 2011; Familiari et al., 2019). Intracellular particles <40 nm in size have even been shown to be capable of passing from the cell cytoplasm into the nucleus (Panté and Kann, 2002), with their elevated surface/volume ratio offering greatly enhanced biological reactivity (Auffan et al., 2009). The very smallest particle sizes approach atomic scales, the so-called "ultrasmall nanoparticles" of Hewitt et al. (2020) and including the traffic "nanocluster aerosols" of Rönkkö et al. (2017), giving them the ability to mimic biological macromolecules and so potentially interfere with cell machinery. In the context of traffic pollutants then, increasing recognition of the complexities of particle bioreactivity at UFP size levels demands improved understanding of the patterns of particle size ranges being inhaled.

The technical challenge of measuring the particle size distributions of UFPs has been met primarily by the development of differential and scanning mobility particle sizers (DMPS and SMPS). The SMPS in particular is considered a reference instrument for measuring particle number size distributions (PNSD) in the submicron range (Giechaskiel et al., 2013; Xue et al., 2015) and is widely employed to analyse air quality at static and mobile monitoring stations (e.g. Pirjola et al., 2012; Brines et al., 2014, 2015; Harrison et al., 2011, 2019). A limited number of experiments have used more portable versions of these spectrometers to measure nanometric PNSD at roadsides (e.g Al-Dabbous and Kumar, 2014) and inside moving motor vehicles (e.g. Giechaskiel et al., 2005; Zhu et al., 2007; Joodatnia et al., 2012). In this paper we move a significant step forward by experimenting with a newly developed miniaturised portable SMPS instrument whilst commuting through a traffic-congested city. The data collected examine the size distribution of particles in the range 10–241 nm and thus offer the opportunity to compare quasi-UFP (QUFP, <241 nm) PNSD commuting exposure patterns encountered by individuals moving through the city. Using these state-of-the-art instruments we were able to simultaneously collect data on return journeys from the suburbs to the city centre using contrasting transport modes.

2. Methodology

2.1. Instruments

The Barcelona SMPS commuting campaign used six custom-built miniaturised scanning mobility particle sizers (Hy-SMPS) developed by Hanyang University (Lee et al., 2015). These instruments are capable of measuring PNSD in the diameter range of 9.5–241.4 nm (QUFP), separated in 91 size bins, with a time resolution of 80 s and an inlet flow rate of 0.13 L min^{-1}, working on a battery lasting for 4 h. The equipment has previously been successfully employed in tethered balloon and hexacopter experiments investigating atmospheric vertical profiles (Querol et al., 2017, 2018; Carnerero et al., 2018; Zhu et al., 2019). Given the extreme portability of the Hy-SMPS, which weighs <2 kg and measures 250 mm^3 (Lee et al., 2015), it is potentially well suited for the study of the complexities of PNSD in the traffic-contaminated urban environment.

2.2. Commuting routes

Hy-SMPS instruments placed in ventilated backpacks were carried with a GPS through the streets and city transport systems of Barcelona, Spain from the suburbs to the city centre and back using different transport modes, expanding on a similar approach adopted by Moreno et al. (2015). The transport modes compared were walking, cycling, car, bus, tram and subway (see information on sampling times and data recovery in Table S1). The commute chosen is 8.4–9 km long (4.2–4.5 km each way depending on route) from the IDAEA-CSIC Institute (in suburban Pedralbes 300 m north of Palau Reial subway/tram stops) to the Diagonal subway stop on La Rambla in the city centre (Fig. 1), taking between 1 and 2 h depending on the transport mode. All above-ground commuting routes made use of the wide, straight multilane arterial route known as the Diagonal (which is one of the main highways of the city, with >60,000 vehicles per day), to access the city centre at least as far as the large nodal roundabout at Francesc Macia (Fig. 1). Urban background (UB) measurements were recorded in the official monitoring site of Palau Reial located in the southwestern side of the city 250 m north of the Diagonal Avenue, (41°23′24.01″N 02°6′58.06″E, 80 m a.s.l.).

The *walking route* followed the north side of the Diagonal east-northeastwards from Palau Reial, past the Francesc Macia roundabout and on to the intersection with the semi-pedestrianised Rambla de Catalunya which was followed southeast for 200 m to the Diagonal subway station exit (Fig. 1). Return was made by the same route but using the south side of the Diagonal. The *bicycle route* used the 2-way cycle lanes on the north side of the Diagonal as far as Francesc Macia but then zigzagged through the chamfered grid plan city central area known as L'Eixample (the distinctive 19th century city "Enlargement" designed by Ildefons Cerdà) to the Diagonal subway exit. This route mostly involves one-way, two-lane roads with few (and very narrow) cycle lanes, and there is no effective barrier between the cyclist and adjacent traffic (Fig. 1). The return journey by bicycle was made via the Rambla/Diagonal intersection and back along the bicycle lane on the north side of the Diagonal. The *car route* was the road-users equivalent of the cycle route, using a Kangoo diesel-engined van. Windows were open on the outward journey to the centre, but closed (air recirculation mode) on the way back. The *tram route* used the amalgamated T1/T2/T3 line running from Palau Reial down to the terminus at Francesc Macia then involved walking a regular zigzag through L'Eixample somewhat different from that described for the bike route (Fig. 1). The *bus route* used the 33 line which ran hybrid diesel buses from the terminus directly outside IDAEA then along the Diagonal to the intersection with La Rambla, after which the commuter walked to the Diagonal subway exit then returned the same way. Finally, the *subway route* used Line 3 from Palau Reial, changing underground at Sants station to connect with Line 5 to the Diagonal station street exit, then returning by the same route.

2.3. Sampling runs, conditions and methodological limitations

The sampling took place on the morning and afternoon of 4th and 5th of July, 2018 and the morning of 6th July 2018 under dry, sunny, anticyclonic Mediterranean summer conditions, with light winds (<5 m/s) blowing from directions varying from E to SW, temperatures at 28–30 °C, and a humidity of 63–73%. A total of 24 commuting journeys were successfully completed (5 walking; 4 bicycle; 4 bus; 3 tram; 4 car; 4 subway). On another two journeys (1 bicycle; 1 tram) only a partial Hy-SMPS dataset was retrieved, and in four other cases (1 bus; 1 tram; 1 car; 1 subway) no useful data were recovered, probably due to the effect on these sensitive prototype instruments of high temperature and sudden movement while being carried through the city in a soft backpack. Urban background monitoring data at the official site of Palau Reial where all commuting trips started, including BC, PM (PM10, PM2.5 and PM1), particle number concentration, as well as meteorological data (wind direction and speed, T and HR) are shown in supplementary information (Table S2; Figures S1 and S2).

A quality assurance/quality control (QA/QC) was developed to ensure reliable results. For this the HySMPS equipments were previously compared with a scanning mobility particle sizer (SMPS, 10–478 nm), composed of a differential mobility analyser (DMA, TSI 3081) coupled with a CPC (TSI 3772) (Hy-SMPS = 0.71 ·Reference SMPS + 999, R2 = 0.88). HySMPS equipments were also intercompared at the end of the campaign. We view the design of the sampling campaign and consequent data collections are subject to the following limitations. Firstly, intercomparisons between the portable Hy-SMPS instruments with each

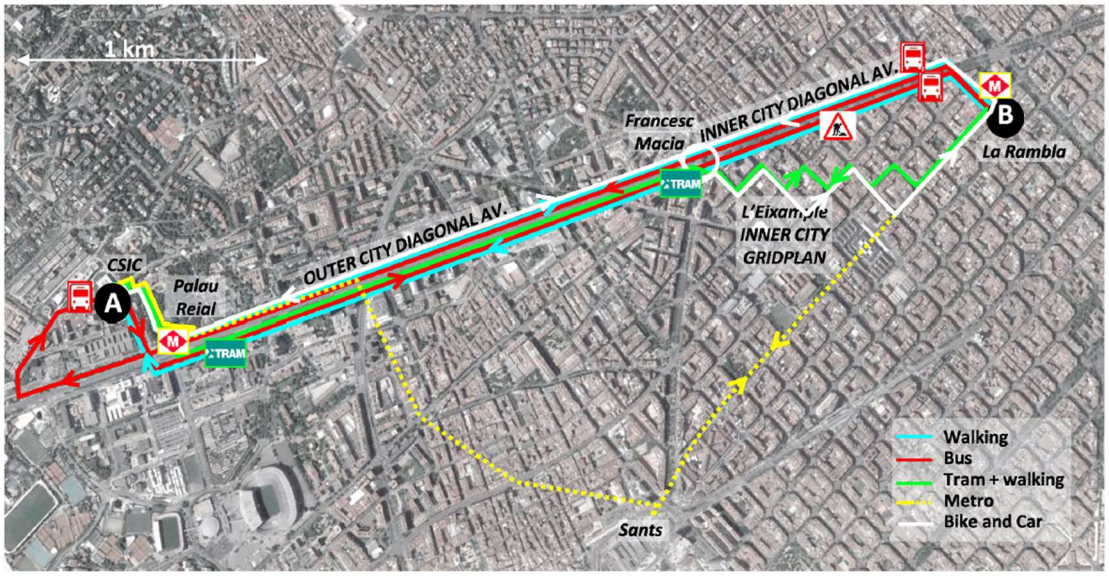

Fig. 1. Location of commuting routes for UFP exposure measurements in this study.

other were performed at the end of the sampling period and although these showed good agreement in terms of particle sizes (Figures S3 and S4), there were differences in terms of total particle number concentrations (±20% on average). For this reason we have focussed more on the shape of the size distribution spectra and mean particle size rather than absolute number concentrations. A second point here is that this was a brief, experimental campaign taking advantage of the fact that we had access to several of the Hy-SMPS instruments being used for a larger study of vertical atmospheric profiling elsewhere in Spain. Thus, given the time constraints, the sample size for some transport modes and routes is limited, and therefore the applied statistical analysis could be subjected to biases that may have influenced our estimates. This has been considered and described within the text where appropriate.

3. Results

The Hy-SMPS PN and PNSD obtained during the various morning commuting journeys show considerable variability, although consistent key patterns emerge and these are encapsulated under the following subheadings and in Figs. 2–5.

3.1. Unimodal size distribution of >10 nm roadside QUFP

The first of these key patterns observed is the repetition of a unimodal distribution of particle sizes between 10 and 200 nm, with a peak within the range 30–70 nm. This characteristic PNSD pattern of QUFP has been demonstrated in both laboratory and on-road studies of "accumulation mode" vehicle emissions (e.g. Kittelson et al., 2006; Asbach et al., 2009; Xue et al., 2015) and is viewed as typical of what city roadside commuters are breathing during their journey. This is demonstrated in Fig. 2 which reveals the broad similarity of data obtained during all morning walking journeys undertaken on 4–6th July 2018, splitting them into outward and return segments. The most polluted conditions were recorded on the outward journey on 4th July which took place earlier in the morning (09:35 LT) when peak-time traffic flow was still high and with ESE winds blowing at low angles across the highway. Despite such variations in PN concentrations, however, the particle size distributions for all commuting journeys consistently define a broadly symmetric curve serrated by a series of minor peaks, with most particles (75–80%) being UFP in size (Fig. 2). Plotted on a log scale, the PNSDs rise rapidly from 10 nm to 25–45 nm

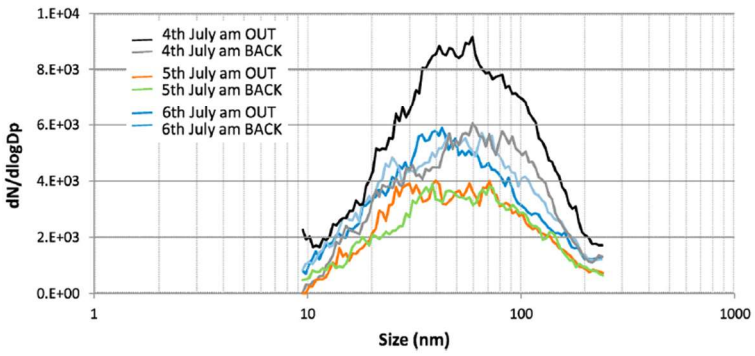

Fig. 2. Particle number size distributions measured by portable Hy-SMPS on three morning return walking commutes out and back from IDAEA to the city centre on 4–6th July 2018. Curves shown are median values. Note the slight displacement of the peak area on the return journey of all measured distributions per particle size. when fewer fine-sized (<30 nm) fresh traffic aerosols were encountered (see text for discussion). The times for collection and number of data points are shown in Table S1.

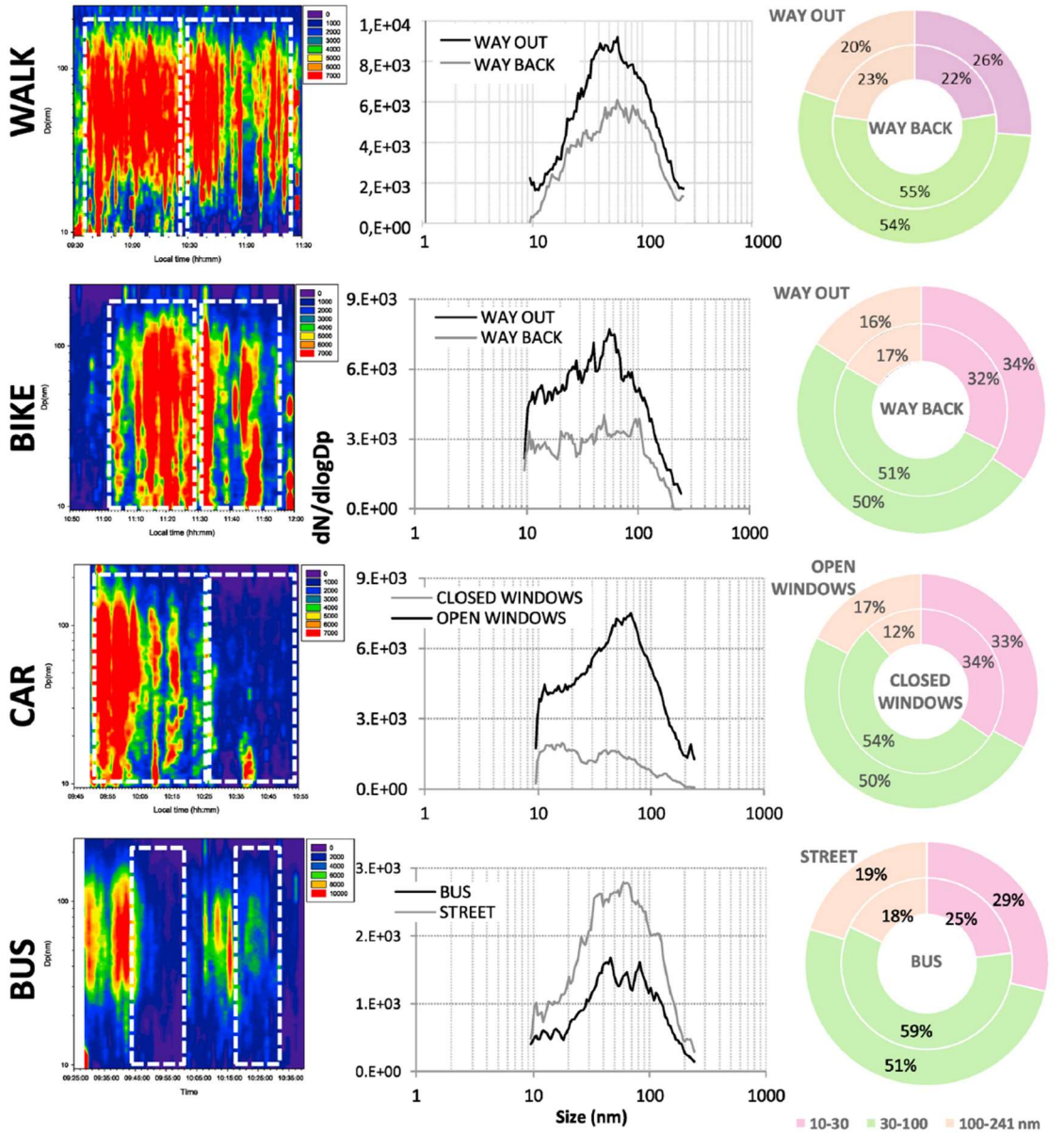

Fig. 3. Particle number size distributions measured by portable Hy-SMPS comparing four different transport mode commutes into Barcelona on the morning of Wednesday July 4th, 2018 (see Fig. 1). Note the higher particle number concentrations of finer particles (<20 nm) during the bicycle and car journeys (see text for discussion).

before flattening out then falling towards the 200 nm line (Fig. 2). The distribution of the main concentration peaks on these PNSDs is wider for some than others but most data plot within 30–100 nm. In all three cases the outward journey PNSD is shifted more towards finer particle sizes than on the return journey, this likely reflecting the fact that the commuter was exposed to fresher traffic emissions when walking to the city on the north side of the Diagonal, which lay immediately downwind of the road traffic (Fig. 2) and at a time closer to the morning peak vehicle-flow.

3.2. Comparing PNSDs from pedestrian, bicycle, bus and car commuting

Having observed a broadly repeated pattern of Hy-SMPS results for the morning walking journey into Barcelona via the Diagonal, we can compare this with PN and PNSD data obtained from using different commuting modes. The key PNSD patterns observed here are again

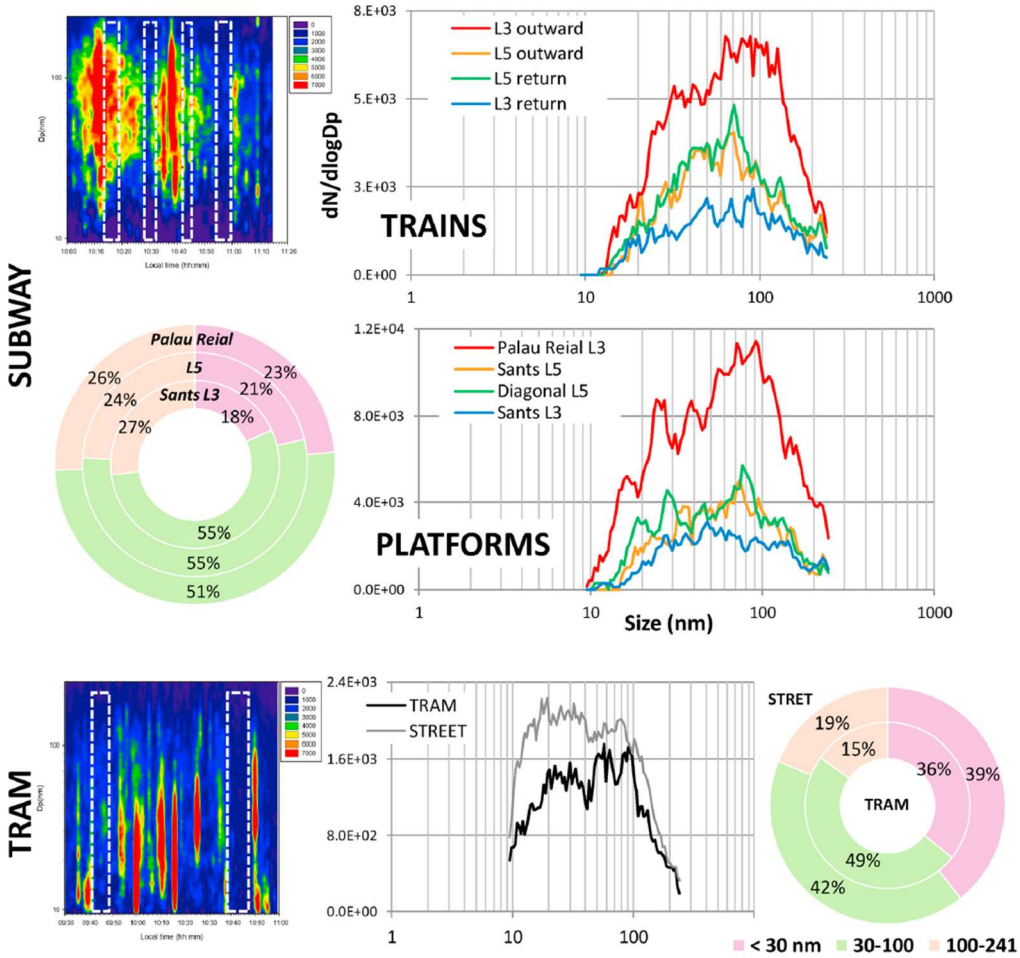

Fig. 4. Particle number size distributions measured by portable Hy-SMPS comparing subway and tram commutes on the morning of Thursday July 5th, 2018. The subway data are split into the four train journeys and the three station platforms involved. Note the higher particle number concentrations on the platform and outward train journey from Palau Reial station, and the rise of a second finer size mode (20–30 nm) in the tram data (see text for discussion).

characterised by a dominant peak typically at 50–70 nm, but journeys most exposed to fresh exhaust (bicycle and car with windows open) showed an enhancement of finer particles (<30 nm). Another observation well demonstrated by the SMPS dN/dLogDp plot is how the microenvironment inside an air conditioned bus was significantly protected from the levels of roadside UFP pollution outdoors.

These points are demonstrated by Fig. 3 which compares the four commuting journeys potentially most exposed to traffic emissions, namely walking, bicycle, bus and car (with open windows) during the first of the three morning excursions (July 4th). As stated above, the outward journey on foot (inside the white dashed rectangles on coloured dN/dLogDp plot) started out early and under the poorest air quality conditions when exposure to traffic pollutants was at a maximum, in this case with headwinds of 2-4 m s^{-1} blowing at a low angle across the busy highway (the wind later rotated into a more SE direction as the journey progressed). The red colours on Fig. 3 (WALK) reflect these conditions by demonstrating high PN initially across a broad size range (10–140 nm). The return journey on foot down the south (upwind) side of the

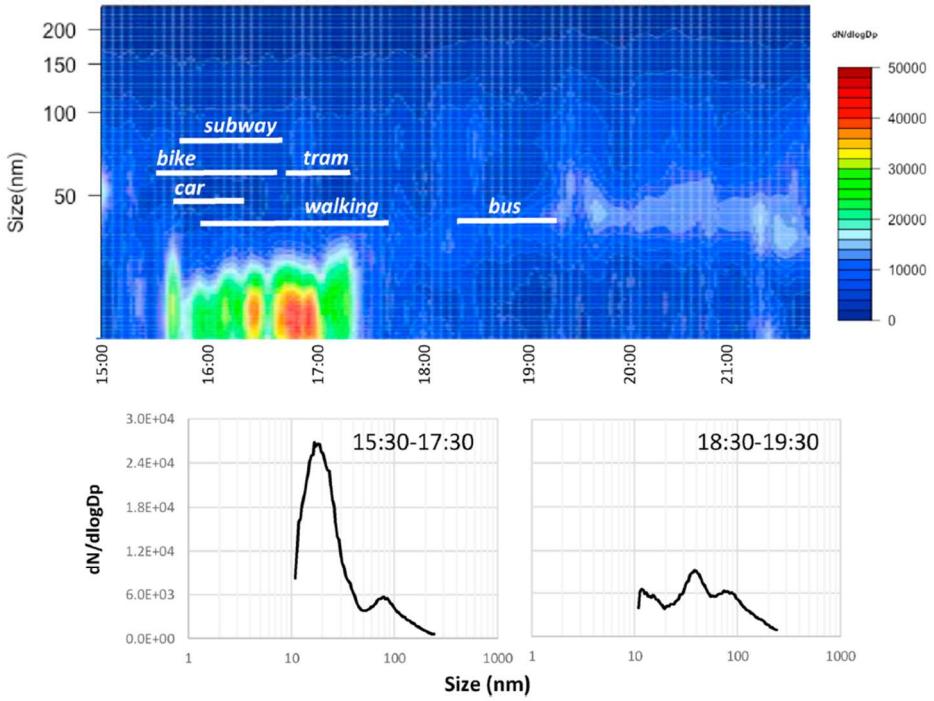

Fig. 5. SMPS data recorded at the Palau Reial urban monitoring station on the afternoon and evening of 5th July. Note the new particle formation event in the afternoon which produced a strong peak at 17–19 nm but by 18:30 had collapsed to leave a residual peak at c.40 nm rising above the aged traffic particle peak of 70–90 nm which remained unchanged (see text for discussion).

Diagonal bears greater similarity to the other morning PNSDs registered on the subsequent 2 days (Fig. 2).

The bicycle journey on Fig. 3 (BIKE) started 90 min later (when winds had rotated SE) and initially followed the bike lane which is spatially slightly further from the roadside than the walking route. The dataset (again within the white dashed rectangle) record mostly cleaner air conditions on the bike lane until encountering the Francesc Macia traffic hotspot and entering the more street canyon-like roads of the Eixample, when PNs rose across a 10–140 nm size range. The return bicycle journey did not include entering the Eixample and mostly stayed on cycle lanes that were spatially further from the roadside than during the outward journey, a less polluted combination which resulted in a lower PN (Fig. 3).

With regard to the car commuting, the outward journey was made with the windows open and once again we see highly contaminated conditions associated with the Diagonal highway that morning, with particle sizes ranging from 10 to 140 nm (Fig. 3). Despite a difference in smoothness, there is striking similarity between the outward BIKE and CAR PNSDs. Both these PNSDs record higher concentrations of the finest particle sizes (10–15 nm) than when walking, presumably due to closer proximity to fresh road emissions (Fig. 3). The return journey was made with windows and ventilation closed/recirculating, resulting in a marked improvement in vehicle interior air quality (Fig. 3), although note smaller particles sizes (<20 nm) are prevalent and suggest the presence of fresh exhaust derived from self-pollution within the vehicle (an effect noted in a previous study within Barcelona taxis by Moreno et al., 2019).

In contrast to the bicycle and car data, the journey down the Diagonal by air conditioned bus (within the white dashed rectangles in Fig. 3) recorded the lowest PN, with size range peaks between 40 and 80 nm. The outdoor short walk from the Diagonal down the semi-pedestrianised Rambla demonstrated more polluted conditions than inside the bus, although with lower concentrations than those measured walking alongside the Diagonal (compare WALK and BUS PNSDs on Fig. 3). Note how all walking and bus data recorded similar PNSDs, less influenced by the finer-sized fresher exhaust particles recorded during the bicycle and car journeys (Fig. 3).

Grouping the particle size ranges into smallest (10–30 nm), largest (100–240 nm) and those in between (30–100 nm) we see very similar overall distribution patterns (doughnut charts on Fig. 3). In all journeys 77–88% of particles measured <100 nm in size, with 50–59% lying within the 30–100 nm range. In both the bicycle and car journeys one third of the PN measured belonged to the finest 10–30 nm group (32–34%), whereas in contrast the walking and bus journeys recorded lower 10–30 nm (22–29%) but slightly higher >100 nm (18–23%: most of which lay within the 100–200 nm range) PNs. These data imply greater relative and absolute exposure to fresh exhaust emissions (particles measuring <30 nm, Brines et al., 2015) when travelling by bicycle and car rather than inside an air conditioned bus (Fig. 3).

3.3. Tram and subway PNSDs

The key observation of a relatively protected indoor transport microenvironment seen in the bus data is repeated inside the tram. In contrast QUFP air quality inside subway trains and on platforms is far more variable, as demonstrated in this section which presents Hy-SMPS data from subway and tram commuting on the morning of 5th July 2018 (Fig. 4).

The data obtained from inside the subway system are shown split into train interior and platform environments, with the four train journeys marked by white dashed lines on the coloured dN/dLogDp square (Fig. 4). This figure provides an excellent illustration of the detail that can be achieved with the portable Hy-SMPS instrument. It is immediately clear from Fig. 4 that the L3 platform at Palau Reial was much more polluted by QUFP-sized particles than that at Sants station. A similar difference was measured inside the outward and return L3 trains: compare the red and blue PNSDs on Fig. 4 TRAINS. In contrast, the data from L5 recorded similar PNs on both outward and return journeys (green and yellow lines on Fig. 4). Compared to the nanoparticle data from above ground in the city, the PNSDs for the subway environment reveal a broadly similar shape although with a higher proportion of coarser (>100 nm) aerosols, as has been noted in previous publications on subway air quality (e.g. Moreno et al., 2015).

The higher PNs at Palau Reial platform are most likely linked to significant infiltration of QUFPs from the Diagonal highway above (Moreno et al., 2017). In this initial part of the L3 route the trains run immediately beneath the Diagonal for a length 1.5 km at a maximum depth of 14 m and there is air exchange via pavement grills and subway exits on both side of the highway. The pattern of dN/dLogDp red colouration for platform and train records how PN dissipated inside the subway carriage as the train moved further down the line from Palau Reial, curving away from the Diagonal highway towards the interchange at Sants station. This lessening of PN is especially marked in the finest size fractions (<40 nm: see left hand white rectangle on Fig. 4 SUBWAY). The other notable "red zone" recorded by the dN/dLogDp square, at the halfway point of the commute, records emergence into the street at the Diagonal subway exit.

The Palau Reial subway PNSD is similar in shape to that recorded inside the tram (also leaving from Palau Reial, where the tram stop lies alongside the Diagonal highway and immediately above the subway). However the tram interior records PNs to have been much lower than in the subway (Fig. 4) and instead similar to those recorded inside the bus the previous day (Fig. 3). One clear difference between the interior of these two vehicles is that the tram data on July 5th, 2018 reveal a distinctly a bimodal pattern, with a second mode emerging at finer sizes (Fig. 4). An even more marked finer mode, peaking at 17–20 nm, is shown by the city centre (Eixample) walking data on Fig. 4 (STREET). This extremely fine PN mode is further reflected in the doughnut charts, with a higher relative proportion of 10–30 nm particles in both street and tram (36–39%: Fig. 4) as compared to the street and bus data of the previous day (22–29%: Fig. 3). The reason for the occurrence of this enhanced finer mode on July 5th 2018 will be discussed in the next sub-section.

According to the above results, outdoors in the streets of Barcelona within the aerosol particle size range of 10–241 nm we observed dominant PNSD peaks typically at 40–70 nm. In some commuting journeys there is also a notable enhancement of finer particles (<30 nm), most obviously in journeys which involve direct proximal exposure to road vehicle exhaust emissions (car and bicycle). The coarsest particles measured (100–241 nm) are relatively least abundant inside road vehicles (12–18%) and most abundant in the subway platform (24–27%). The commuting environments registering lowest PNs are those recorded inside air conditioned buses, trams and cars relatively protected from outside air entry. Finally, the street and tram data from 5th July 2018 indicate that the PNs of the finest aerosol fraction measured by the Hy-SMPS instrument (10–30 nm) sometimes rises to produce a bimodal PNSD in which the finer mode can become dominant.

3.4. City commuting through new particle formation events

The bimodal PNSD emerging from the morning TRAM commuting in Fig. 4 coincided with the early development of a new particle formation (NPF) event registered that day at the nearby Palau Reial urban background monitoring station. Such photochemically-driven NPF events are common during the Barcelona summer months (Dall'Osto et al., 2012, 2013; Brines et al., 2014, 2015; Minguillión et al., 2015; Brean et al., 2020). On the July 5, 2018 the longest and most prominent NPF burst occurred after 15:30 LT (13:30 UTC) and lasted for around 100 min, reaching maximum PNs at 16:20–17:10 (14:20–15:10 UTC), producing particles <30 nm in size and peaking at 14–20 nm. The ability to integrate static urban background air monitoring station information with PSDN data obtained synchronously during commuting journeys through the city provides another demonstration of the new approaches to city air quality made possible by the portable miniaturised Hy-SMPS. In this case the timing of this major NPF event coincided with our commuting Hy-SMPS sampling programme that afternoon (Fig. 5), although the return walking journey finished after the nucleation event had suddenly dissipated, and the bus journey missed the event altogether (having been repeated after equipment malfunction the first time).

The urban background PNSDs presented on Fig. 5 compare patterns recorded during and after this NPF event. The data captured at 15:30–17:30 (13:30–15:30 UTC) shows the nucleation event as a sharp peak in the size range 16–19 nm, with a secondary peak at 70–90 nm (Fig. 5). In contrast, the post-burst PNSD curve recorded for 18:30–19:30 shows a collapse of the <20 nm peak, the maintenance of the 70–90 nm peak, and the appearance of a new peak at around 35–40 nm (Fig. 5). This new peak reflects the presence of an evening particle concentration band that can be discerned in pale blue on the coloured dN/dLogDp plot to the right of the "bus" white line on Fig. 5. Interestingly, the colour contours faintly indicate a bridge back in time from 19:00 LT to the particle size ceiling at the end of the nucleation burst at 17:30 (15:30 UTC), linking the afternoon NPF event and the evening concentration of aged particles in the 35–40 nm size range (Fig. 5).

Fig. 6 demonstrates how the Hy-SMPS commuting data captured the main afternoon NPF on 5 th July 2018, with a dominant concentration peak at <30 nm particle sizes in all cases except for the late bus commute and the return walking journey. The finest size peaks reflect the commuting routes most directly exposed to road traffic, namely open car (12 nm), bicycle (16 nm) and outward walking (19 nm), with 57–69% of particle sizes measured lying in the 10–30 nm range (Fig. 6). This is around double the relative proportion of 10–30 nm particles recorded just the previous day, when no daytime nucleation bursts occurred. The walking route records the sudden weakening of the main nucleation event around 17:00 LT, with the consequent collapse of the fine particle peak which coarsened to 25–30 nm (Fig. 6 WALK WAY BACK). Around 1 h later the fine particle peak was merely residual, as recorded by the bus data in which the dominant peaks >40 nm had reasserted themselves (Fig. 6 BUS).

This nucleation event peak in the <20 nm particle size range also dominates the PSNDs recorded both inside the tram and outside in the street while walking through the Eixample (Fig. 6 TRAM), although the PNs are lower. This suggests that the NPF event in the city atmosphere was not strictly confined to the Diagonal area. The same 17–20 nm PNSD peak was by the afternoon also clearly prominent in Palau Reial subway station platform and train, again emphasising the likely connection between Diagonal outdoor air and the subway line beneath. Remarkably, even the L5 line platforms and trains running between Sants and the Diagonal subway stations recorded the same bimodal PNSD with

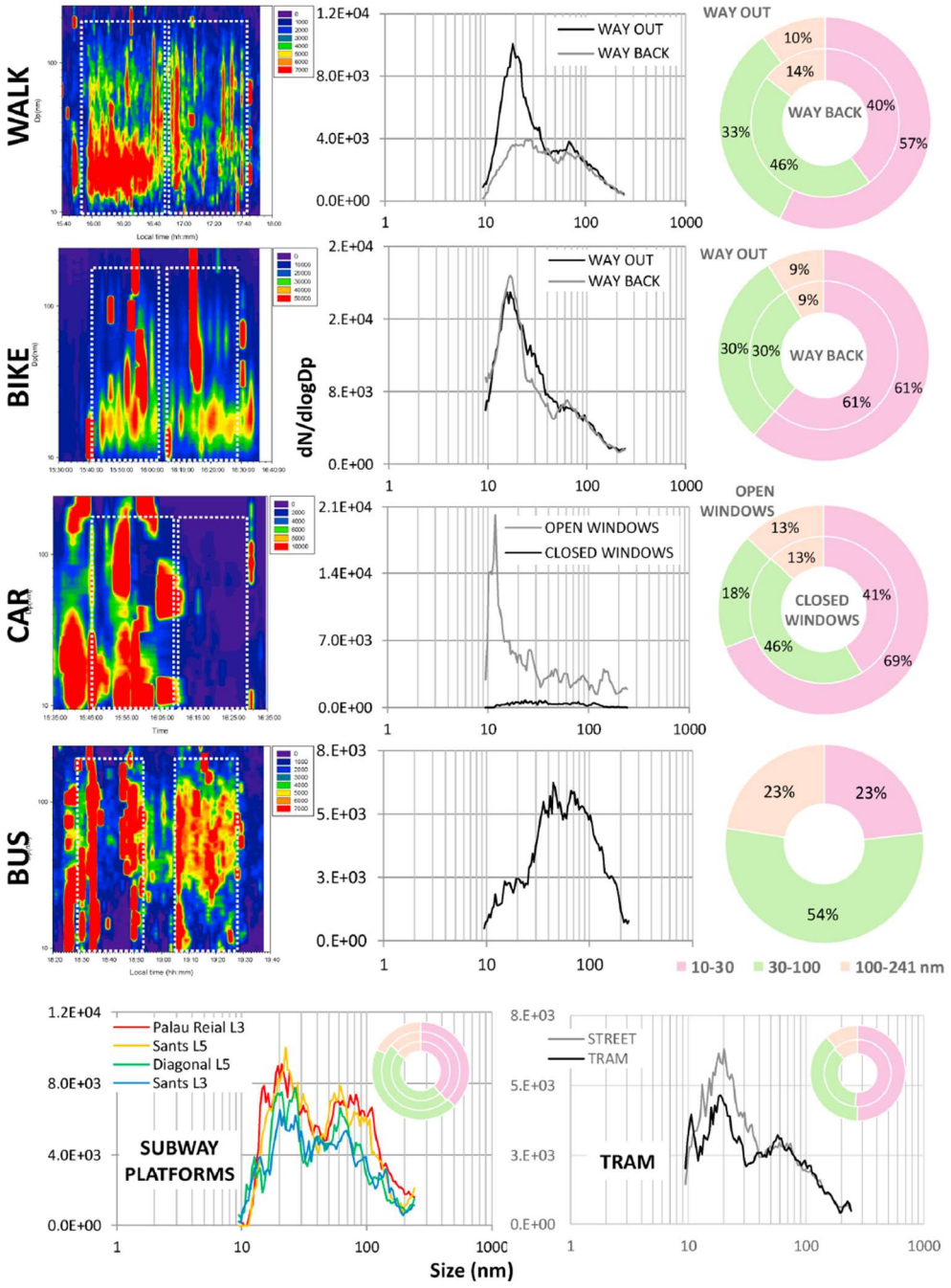

Fig. 6. Particle number size distributions measured by portable Hy-SMPS comparing six different transport mode commutes into Barcelona on the afternoon of Thursday July 5, 2018 (see Fig. 1 and text for discussion). Note how the bicycle, open-window car, tram and even subway journeys captured the new particle formation event recorded in Fig. 5, as did the outward walking commute. The return walking journey occurred after the sudden collapse of the afternoon particle nucleation burst, and the bus journey took place later in the early evening (see text for discussion).

peaks at 20–30 nm, indicating that the afternoon nucleation burst was penetrating extensively into the underground subway system (Fig. 6 SUBWAY PLATFORMS).

4. Discussion

It is by now well established that the dominant source of UFP in typical roadside city environments such as the ones sampled in this study is motor vehicle traffic (e.g. Hussein et al., 2004; Rodriguez and Cuevas, 2007; Morawska et al., 2008; Pirjola et al., 2012; Charron and Harrison, 2013; Al-Dabbous and Kumar, 2014; Brines et al., 2014; Kumar et al., 2014; Ma and Birmili, 2015; Strasser et al., 2018; Rönkkö and Timonen, 2019; Harrison et al., 2019; Dinoi et al., 2020). It is also clear that the general term "traffic emissions" encompasses a complex mix of exhaust (primary and secondary) and non-exhaust particle types produced by a range of processes. In terms of PN these traffic emission particles are nearly all <300 nm in size (Kumar et al., 2010) so that our Hy-SMPS size distribution patterns from Barcelona reflect real exposure to inhalable QUFP aerosols in the city streets. The roadside exhaust particles measured by the Hy-SMPS in Barcelona include (1) high temperature primary aerosols sourced from the internal combustion engine (Kittelson, 1998); (2) secondary particles generated from the cooling and dilution of hot exhaust gases seconds after emission (Robinson et al., 2007; see also the concept of "delayed primary particles" of Rönkkö et al., 2017). Mixed with these rapidly diluting locally emitted traffic-sourced particles will be aged regional and urban background UFP and secondary aerosols resulting from reactions driven by atmospheric photochemistry (Brines et al., 2015). Thus the city commuter moves through a continuously replenished deeply inhalable pollution cloud rich in hydrocarbon combustion-sourced elemental and organic carbonaceous materials and inorganic compounds, mixed with particles released from vehicle wear (such as brakes and tyres), resuspended road dust, and aerosols derived from elsewhere in the city and beyond.

Extensive research into the size distribution patterns of aerosol PNSD has included the application of apportionment methods such as Positive Matrix Factorisation and *k*-means cluster analysis to identify sub-groups and attribute likely sources of particles in traffic-contaminated urban air (Al-Dabbous and Kumar, 2014; Beddows et al., 2009, 2015; Beddows and Harrison, 2019; Brines et al., 2015; Dall'Osto et al., 2012; Friend et al., 2012; Hussein et al., 2004; Keuken et al., 2015; Kim et al., 2004; Lingard et al., 2006; Liu et al., 2014; Pey et al., 2008, 2009; Rivas et al., 2020; Squizzato et al., 2019; Yue et al., 2008; Zhou et al., 2004; Zhu et al., 2002a,b). In the case of our Hy-SMPS commuting results the low number of data points has limited our ability to apply a statistical source apportionment approach successfully to all transport modes, although for the walking and cycling data the results from *k*-means cluster analysis are promising (Fig. 5). The PNSDs for these two commuting modes can be classified into cluster types (related to an emission, formation process or proximity to a source, etc.), aiming to optimally assess the trends of the PNSD during commuting.

The clusters obtained from the walking data averaged over the five return commuting journeys are shown in Fig. 7 WALK. Four size distribution clusters define peaks at 30–40 nm (cluster A), 85–100 nm (cluster B), 15–22 nm (cluster C, with a second, lower peak at 65–70 nm), and 45–75 nm (cluster D). The data from the four completed bicycle journeys (Fig. 7 BIKE) were similar to that from walking, although cluster B could not be distinguished, and particle concentrations for the main two clusters (A and C) were generally higher than those for walking.

Fig. 7 also compares published PNSD data from similarly traffic-contaminated urban air at urban background and roadside monitoring sites (Al-Dabbous and Kumar 2014; Beddows et al., 2015; Dall'Osto, 2012; Friend et al., 2012; Hussein et al., 2004; Lingard et al., 2006; Liu et al., 2014; Rivas et al., 2020; Squizzato et al., 2019; Zhu et al., 2002a, b). All these studies have identified 10–30 nm size modes, with most authors choosing to label these variously as "nucleation mode", "fresh traffic" and/or "photochemical/nucleation", depending on the co-occurrence with other air pollutants or meteorological conditions, as well as timing. Furthermore, 30–100 nm size modes are commonly interpreted as "traffic", "aged traffic", or "Aitken mode". However, a collation of such data immediately demonstrates the difficulty in comparing modes within the 10–100 nm size range in traffic-contaminated air at different monitoring stations. The PNSDs alongside a highway will be in a state of constant flux, with UFPs changing their sizes and PN with time, in space and in response to traffic flow and ambient atmospheric conditions. Zhu et al. (2002 a,b) for example measured UFPs 30 m away from a highway in Los Angeles and reported PNSD modes at 13 nm, 27 nm, and 65 nm, noting how the finest size mode (13 nm) increased to 16 nm at 60 m, and disappeared by 90 m. Furthermore, 300 m downwind from the highway "ultrafine particle number concentration … was indistinguishable from upwind background concentration" (Zhu et al., 2002b). Similarly, Barone and Zhu (2008) observed an on-road PNSD peak at 14 nm, which increased to 36 nm 90 m from the road. In this context, our data presented on Fig. 3 demonstrate how road users travelling by bicycle and open car were breathing higher numbers of the finest particles measured in our study (10–20 nm) as compared for example to roadside pedestrians. Similarly, the data on Fig. 6 suggest a coarsening of nucleation mode peaks which shifted from 12 nm on-road (car), to 16 nm on route dominated by bicycle lanes, to 19 nm for roadside walking. Such size changes presumably reflect the rapid ageing of the fresh traffic pollution cloud as it disperses into the surrounding urban air, although the health effects of breathing these different size fractions of UFP depending on transport microenvironment remain unknown.

The data presented in this paper represent to our knowledge the first attempt to capture real-time urban commuting exposure to QUFP and PNSD in city transport microenvironments (the TME's of Kumar et al., 2018) at the level of sophistication offered by a portable SMPS instrument. Clear patterns for roadside and vehicle interior conditions emerge that demonstrate number concentration peaks in ageing traffic emissions rising rapidly from 20 nm to define a curve that peaks at <100 nm then falls rapidly towards 200 nm (Fig. 2). Under normal roadside conditions in Barcelona at least 50% of particles in the range 10–241 nm will be 30–100 nm in size (Fig. 3) although this % figure can fall much lower when moving through clouds of freshly nucleating particles and fresh primary traffic QUFP emissions. The results provide a detailed confirmation of how road and roadside users most exposed to fresh traffic emissions and NPF events will inhale larger numbers of QUFP and that, conversely, commuters in closed vehicles (buses, trams, cars) can be significantly more protected from these pollutants.

Finally, perhaps the most striking aspect of this experimental campaign using the Hy-SMPS developed at Hanyang University was the amount of additional detail suddenly available to the study of urban air quality whilst moving through the city. Thus we observe subtle increases in UFP sizes modes from car to bike to walking, and marked differences existed between walking or cycling using different city routes, including different sides of the road. Other observations noted the effect of self-pollution inside private vehicles with closed windows and air recirculation, the recognition that some subway stations are wide open to the ingress of abundant road vehicle emissions, and that city-wide outside pollution episodes, such as NPF events, can be detected penetrating the underground commuting system. With enhanced miniaturisation and portability of robustly built high-tech air quality monitoring instruments such data will presumably become increasingly available to the urban commuter, offering more informed choices of how to recognise and avoid polluted hotspots in the city.

5. Conclusions

- The commuter in Barcelona is constantly exposed to high number concentrations of traffic-sourced primary and secondary particles, the majority of which are <100 nm in size (ultrafine particles, UFP).

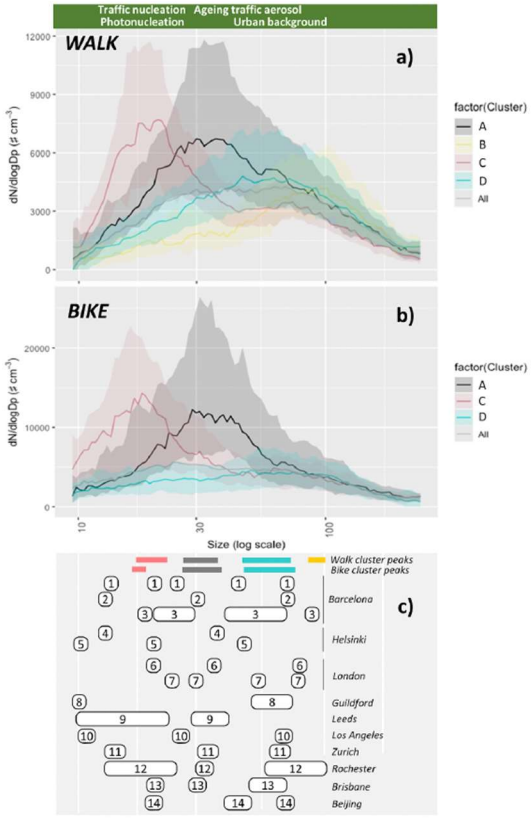

Fig. 7. Cluster analysis for return a) walking (WALK) and b) bicycle (BIKE) commuting journeys to Barcelona city centre. The times for collection and number of data points are shown in Table S1. The method classifies spectra with the highest degree of similarity into the same category or cluster, therefore reducing the number of spectra to analyse. Data were previously normalized, with the analysis being applied to the shape of the size distribution, not the magnitude, and performed on 2-min intervals. Data management and descriptive statistics and plots were made using the R statistical software (RStudio Version February 1, 5033) and the package cluster (Maechler et al., 2019). Cluster validation indices (silhouette width and Dunn Index) were used to choose the optimum number of spectra to divide the data, a purely statistical optimization, followed by refinement of clustering taking into account the scientific context in which the data were collected. c) The lower chart presents the coloured peak size ranges of these clusters and compares them with previously published particle number concentration major peaks between 10 and 100 nm identified in similarly traffic-contaminated urban air (R = roadside; UB = urban background): 1. Barcelona UB: 16 nm nucleation; 26 nm traffic 1; 48 nm traffic 2; 75 nm traffic 3 (Brines et al., 2015); 2. Barcelona UB: 13 nm photonucleation; 31 nm fresh traffic + photonucleation; 76 nm urban, mostly traffic (Rivas et al., 2020); 3. Barcelona UB: 18–20 nm photochemical; 22–29 nm traffic nucleation mode; 41–62 nm Aitken mode; 90 nm urban/regional background (Dall'Osto et al., 2012); 4. Helsinki UB (2 locations): 11.7 & 13.8 nm "aged" nucleation mode; 37.3 & 42.5 nm Aitken mode (Hussein et al., 2004); 5. Helsinki UB: 11 nm nucleation; 22 nm fresh traffic; 50 nm urban (Rivas et al., 2020); 6. London UB: 21 nm nucleation; 34 nm fresh traffic; 67 nm urban (Rivas et al., 2020); 7. London UB: 25 nm nucleation; 30 nm traffic; 55 nm woodsmoke; 80 nm secondary (Beddows et al., 2015); 8. Guildford, UK R: 10 nm "fresh" nucleation mode; 55–75 nm (Al-Dabbous and Kumar, 2014); 9. Leeds, UK R: <10–24.8 nm nucleation mode; 28.2–41.4 nm Aitken mode (Lingard et al., 2006); 10. Los Angeles 30 m from R: 12.6 nm, 27.3 nm, 65.3 nm (Zhu et al., 2002b); 11. Zurich UB: 15 nm nucleation; 33 nm fresh traffic; 67 nm urban (Rivas et al., 2020); 12. Rochester, USA UB: 14–25 nm nucleation; 30–35 nm fresh traffic; 58–104 nm aged traffic (Squizzato et al., 2019); 13. Brisbane R: 20 nm local traffic; 30 nm traffic; 50–70 nm traffic (Friend et al., 2012); 14. Beijing UB: 20 nm traffic nucleation; 40–50 nm aged traffic; 70 nm aged coal power plant (Liu et al., 2014).

A significant proportion of particles in the size range 10–241 nm (typically 10–25%) are >100 nm in size (quasi-ultrafine), especially in the subway environment.

- Comparisons between different commuting transport modes using a portable SMPS instrument reveal what can be large and rapidly fluctuating differences in exposure to PN and PN size distribution (PNSD) depending on the route chosen and time of the day. Those closer to fresh traffic exhaust sources (such as in an open window car, on bicycle, walking downwind of busy roads, or on a subway platform contaminated by highway air) will breathe higher PN than those choosing enclosed environments such inside an air conditioned bus or tram. Our PNSD data identified subtle differences in size modes of freshly nucleated traffic-related-particles when travelling by open car, bicycle or roadside walking, which we view as a snapshot of the rapid maturation of the fresh traffic pollution cloud as it begins the ageing process.
- The ability to integrate static urban background air monitoring station information with PSDN data obtained synchronously from portable miniaturised SMPS instruments during commuting journeys opens new approaches to investigating city air quality by offering a level of detail not previously available. An example of how to use this opportunity to discover "the devil in the detail" was provided by our identification of a <20 nm roadside aerosol PN mode that could be traced to a photochemically-driven afternoon new particle formation

(NPF) event recorded by the local urban background air quality station.

- Application of *k*-means cluster analysis to the 10–241 nm PNSD pedestrian and cycling commuting data identified modes at relatively fine (15–22 nm), medium (30–40 nm), and coarse (45–75 nm) particle size ranges. Previously published applications of statistical apportionment methods to the nanometric particle signature of traffic-contaminated city air have similarly identified peaks within the UFP size spectrum, usually interpreting the finer sizes as "nucleation mode" or "fresh traffic", and the coarser sizes as "aged traffic" or "Aitken mode". Such studies on QUFP typically capture uni- or bimodal PNSD patterns within a multi-sourced aerosol mixture in constant flux in response to traffic flow and ambient atmospheric conditions. The city commuter moves through this chemically complex and reactive pollution cloud that is continuously replenished by fresh traffic emissions which immediately begin ageing as they disperse away from their source and merge into the urban background.

Credit author statement

Teresa Moreno, Conceptualization, Writing, Supervision, Editing, Cristina Reche, Data curation, Editing, Kang-Ho Ahn, Data curation. Hee-Ram Eun, Data curation. Woo Young Kim, Data curation. Hee-sang Kim, Data curation. Amaia Fernández-Iriarte, Methodology, Validation, Fulvio Amato: Validation, Xavier Querol, Conceptualization, Reviewing.

Declaration of competing interest

The authors declare that they have no known competing financial interests or personal relationships that could have appeared to influence the work reported in this paper.

Acknowledgements

The authors thank the following colleagues who helped carry the Hy-SMPS instrument on the commuting journeys: Andrés Alastuey, Cristina Carnerero, Miguel Escudero, Maria Izquierdo, Alessia Mancuso, Antonio Pacitto, Marco Pandolfi, Anna Ripoll, Apostolos Salmatonidis, Mar Viana, Jesus Yus. This work was supported by the Spanish Ministry of Economy and Competitiveness and FEDER funds within the I + D Projects CGL 2016-78594-R (HOUSE) and CGL 2016–79132 (BUSAIR), and the Catalan Research Agency (AGAUR 2017 SGR41) of the Generalitat de Catalunya.

Appendix A. Supplementary data

Supplementary data to this article can be found online at https://doi.org/10.1016/j.envres.2020.109978.

References

Al-Dabbous, A., Kumar, P., 2014. The influence of roadside vegetation barriers on airborne nanoparticles nanoparticles and pedestrians exposure under varying wind conditions. Atmos. Environ. 90, 113–124.
Asbach, C., Kaminski, H., Fissan, H.J., Monz, C., 2009. Comparison of four mobility particle sizers with different time resolution for stationary exposure measurements. J. Nanoparticle Res. 11, 1593–1609.
Auffan, M., Rose, J., Wiesnera, M., Bottero, J.Y., 2009. Chemical stability of metallic nanoparticles: a parameter controlling their potential cellular toxicity in vitro. Environ. Pol. 157, 1127–1133.
Barone, T.L., Zhu, Y., 2008. The morphology of ultrafine particles on and near major freeways. Atmos. Environ. 42, 6749–6758.
Beddows, D., Dall'Osto, M., Harrison, R.M., 2009. Cluster Analysis of rural, urban, and curbside atmospheric particle size data. Environ. Sci. Technol. 43 (13), 4694–4700.
Beddows, D., Harrison, R.M., Green, D., Fuller, G.W., 2015. Receptor modelling of both particle composition and size distribution from a background site in London, UK. Atmos. Chem. Phys. 15, 10107–10125.
Beddows, D., Harrison, R.M., 2019. Receptor modelling of both particle composition and size distribution from a background site in London, UK – a two-step approach. Atmos. Chem. Phys. 19, 4863–4876.
Brean, J., Beddows, D.C.S., Zongbo, S., Temime-Roussel, B., Marchand, N., Querol, X., Alastuey, A., Minguillón, M., Harrison, R.M., 2020. Molecular insights into new particle formation in Barcelona, Spain. Atmos. Chem. Phys. 20, 10029–10045.
Brines, M., Dall'Osto, M., Beddows, D.C.S., Harrison, R.M., Gómez-Moreno, F., Núñez, L., Artíñano, B., Costabile, F., Gobbi, G.P., Salimi, F., Morawska, L., Sioutas, C., Querol, X., 2014. Frequency of new particle formation events in the urban Mediterranean climate. Atmos. Chem. Phys. 14, 26463–26494.
Brines, M., Dall'Osto, M., Beddows, D., Harrison, R., Gómez-Moreno, F., Núñez, L., Artíñano, B., Costabile, F., Gobbi, G., Salimi, F., Morawska, L., Sioutas, C., Querol, X., 2015. Traffic and nucleation events as main sources of ultrafine particles in high-insolation developed world cities. Atmos. Chem. Phys. 15, 5929–5945.
Burello, E., Worth, A.P., 2011. A theoretical framework for predicting the oxidative stress potential of oxide nanoparticles. Nanotoxicology 5 (2), 228-235.
Carnerero, C., Pérez, N., Reche, C., Ealo, M., Titos, G., Lee, H.-K., Eun, H.-R., Park, Y.-H., Lubna, D., Paasonen, P., Kerminen, V.M., Mantilla, E., Escudero, M., Gómez-Moreno, F.J., Alonso-Blanco, E., Coz, E., Saiz-Lopez, A., Temime-Roussel, B., Marchand, N., Beddows, D.C.S., Harrison, R.M., Petäjä, T., Kulmala, M., Ahn, K.-H., Alastuey, A., Querol, X., 2018. Vertical and horizontal distribution of regional new particle formation events in Madrid. Atmos. Chem. Phys. 18, 16601–16618.
Charron, A., Harrison, R., 2003. Primary particle formation from vehicle emissions during exhaust dilution in the roadside atmosphere. Atmos. Environ. 37, 4109–4119.
Dall'Osto, M., Beddows, D.C.S., Pey, J., Rodriguez, S., Alastuey, A., Harrison, R.M., Querol, X., 2012. Urban aerosol size distributions over the Mediterranean city of Barcelona, NE Spain. Atmos. Chem. Phys. 12, 10693–10707.
Dall'Osto, M., Querol, X., Alastuey, A., O'Dowd, C., Harrison, R.M., Wenger, J., Gómez-Moreno, F.J., 2013. On the spatial distribution and evolution of ultrafine particles in Barcelona. Atmos. Chem. Phys. 13, 741–759.
Dinoi, A., Conte, M., Grasso, F., Contini, D., 2020. Long-term characterization of submicron atmospheric particles in an urban background site in southern Italy. Atmosphere 11, 334. https://doi.org/10.3390/atmos11040334.
Familari, M., Naav, A., Erlandsson, L., de Iongh, R.U., Isaxon, C., Strandberg, B., Lundh, T., Hansson, S.R., Malmqvist, E., 2019. Exposure of trophoblast cells to fine particulate matter air pollution leads to growth inhibition, inflammation and ER stress. PloS One 14 (7), e0218799. https://doi.org/10.1371/journal.pone.0218799.
Friend, A.J., Ayoko, G.A., Jayaratne, E.R., Jamriska, M., Hopke, P.K., Morawska, L., 2012. Source apportionment of ultrafine and fine particle concentrations in Brisbane, Australia. Environ. Sci. Pollut. Res. 19, 2942–2950.
Giechaskiel, B., Maricq, M., Ntziachristos, L., Dardiotis, C., Wang, X., Axmann, H., Bergmann, A., Schindler, W., 2014. Review of motor vehicle particulate emissions sampling and measurement: from smoke and filter mass to particle number. J. Aero. Sci. 67, 48–86.
Giechaskiel, B., Ntziachristos, L., Samaras, Z., Scheer, V., Casati, R., Vogt, R., 2005. Formation potential of vehicle exhaust nucleation mode particles on-road and in the laboratory. Atmos. Environ. 39, 3191–3198.
Harrison, R.M., Beddows, D.C., Dall'Osto, M., 2011. PMF analysis of wide-range particle size spectra collected on a major highway. Environ. Sci. Technol. 45 (13), 5522–5528.
Harrison, R.M., Beddows, D.C.S., Alam, M.S., Singh, A., Brean, J., Xu, R., Kotthaus, S., Grimmond, S., 2019. Interpretation of particle number size distributions measured across an urban area during the FASTER campaign. Atmos. Chem. Phys. 19, 39–55.
Hewitt, R., Chappell, H., Powell, P., 2020. Small and dangerous? Potential toxicity mechanisms of common exposure particles and nanoparticles. Current Opinion in Toxicology 19, 93–98.
Hussein, T., Puustinen, A., Aalto, P.P., Mäkelä, J.M., Hämeri, K., Kulmala, M., 2004. Urban aerosol number size distributions. Atmos. Chem. Phys. 4, 391–411.
Joodatnia, P., Kumara, P., Robins, A., 2013. Fast response sequential measurements and modelling of nanoparticles inside and outside a car cabin. Atmos. Environ. 71, 364–375.
Kelly, F., Fussell, J., 2015. Air pollution and public health: emerging hazards and improved understanding of risk. Environ. Geochem. Health 37, 631–649.
Keuken, M.P., Moerman, M., Zandveld, P., Henzing, J.S., Hoek, G., 2015. Total and size resolved particle number and black carbonconcentrations in urban areas near Schiphol airport (The Netherlands). Atmos. Environ. 104, 132–142.
Kim, E., Hopke, P.K., Larson, T.V., Covert, D.S., 2004. Analysis of ambient particle size distributions using unmix and positive matrix factorization. Environ. Sci. Technol. 38, 202–209.
Kittelson, D., 1998. Engines and nanoparticles: a review. J. Aerosol Sci. 29, 575–588.
Kittelson, D.B., Watts, W.F., Johnson, J.P., Schauer, J.J., Lawson, D.R., 2006. On-road and laboratory evaluation of combustion aerosols—Part 2: summary of spark ignition engine results. J. Aerosol Sci. 37, 931–949.
Krecl, P., Johansson, C., Targino, A., Ström, J., Burman, L., 2017. Trends in black carbon and size-resolved particle number concentrations and vehicle emission factors under real-world conditions. Atmos. Environ. 165, 155–168.
Kumar, P., Robins, A., Vardoulakis, S., Britter, R., 2010. A review of the characteristics of nanoparticles in the urban atmosphere and the prospects for developing regulatory controls mode particles in an urban street canyon. Atmos. Environ. 44, 5035–5052.
Kumar, P., Morawska, L., Birmili, W., Paasonen, P., Hu, M., Kulmala, M., Harrison, R.M., Norford, L., Britter, R., 2014. Ultrafine particles in cities. Environ. Int. 66, 1–10.
Kumar, P., Patton, A.P., Durant, J.L., Frey, H.C., 2018. A review of factors impacting exposure to PM2.5, ultrafine particles and black carbon in Asian transport microenvironments. Atmos. Environ. 187, 301–316.
Lee, E., Stenstrom, M., Zhu, Y., 2015. Ultrafine particle infiltration into passenger vehicles. Part 1: experimental evidence. Transp Res Part D 38, 156–165.

Lelieveld, J., Pozzer, A., Pöschl, U., Fnais, M., Haines, A., Münzel, A., 2020. Loss of life expectancy from air pollution compared to other risk factors: a worldwide perspective. Cardiovasc. Res. 116, 1910–1917. https://doi.org/10.1093/cvr/cvaa025.

Lingard, J.J., Agus, E.L., Young, D.T., Andrews, G.E., Tomlin, A.S., 2006. Observations of urban airborne particle number concentrations during rush-hour conditions: analysis of the number based size distributions and modal parameters. Journal of environmental monitoring. JEM 8 (12), 1203–1218.

Liu, Z.R., Hu, B., Liu, Q., Sun, Y., Wang, Y.S., 2014. Source apportionment of urban fine particle number concentration during summertime in Beijing. Atmos. Environ. 96, 359–369.

Ma, N., Birmili, W., 2015. Estimating the contribution of photochemical particle formation to ultrafine particle number averages in an urban atmosphere. Sci. Total Environ. 512–3, 154–166.

Maechler, M., Rousseeuw, P., Struyf, A., Hubert, M., Hornik, K., 2019. Cluster Analysis Basics and Extensions. R Package Version 2.1.0.

Morawska, L., Ristovski, Z., Jayaratne, E., Keogh, D., Ling, X., 2008. Ambient nano and ultrafine particles from motor vehicle emissions: characteristics, ambient processing and implications on human exposure. Atmos. Environ. 42, 8113–8138.

Minguillón, M.C., Brines, M., Pérez, N., Reche, C., Reche, C., Pandolfi, M., Fonseca, A.S., Amato, F., Alastuey, A., Lyasota, A., Codina, B., Lee, H.-K., Eun, H.-R., Ahn, K.-H., Querol, X., 2015. New particle formation at ground level and in the vertical column over the Barcelona area.

Moreno, T., Reche, Cr, Rivas, I., Minguillón, M.C., Martins, V., Vargas, C., Buonanno, G., Parga, J., Pandolfi, M., Brines, M., Ealo, M., Fonseca, A., Amato, F., Sosa, G., Capdevila, M., de Miguel, E., Querol, X., Gibbons, W., 2015. Urban air quality comparison for bus, tram, subway and pedestrian commutes in Barcelona. Environ. Res. 142, 495–510.

Moreno, T., Pacitto, A., Fernández, A., Amato, F., Marco, E., Grimalt, J.O., Buonanno, G., Querol, X., 2019. Vehicle interior air quality conditions when travelling by taxi. Environ. Res. 172, 529–542.

Moreno, T., Reche, C., Minguillon, M.C., Querol, X., Martins, V., Amato, F., Perez, N., Bartolí, R., Cabañas, M., Martínez, S., Vasconcelos, C., De Miguel, E., Capdevila, M., Centelles, S., Pellot, M., 2017. In: Moreno, T. (Ed.), Improving Air Quality in the Subway Environment: Technical Guide, ISBN 978-84-697-5167-1, 48 pp.

Nieuwenhuijsen, M.J., Gascon, M., Martinez, D., Ponjoan, A., Blanch, J., Garcia-Gil, M., Ramos, R., Foraster, M., Mueller, N., Espinosa, A., Cirach, M., Khreis, H., Dadvand, P., Basagaña, X., 2018. Air pollution, noise, blue space, and green space and premature mortality in Barcelona: a mega cohort. Int. J. Environ. Res. Publ. Health 15, 2405.

Panté, N., Kann, M., 2002. Nuclear pore complex is able to transport macromolecules with diameters of ~39 nm. Mol. Biol. Cell 13, 425–434.

Pey, J., Rodríguez, S., Querol, X., Alastuey, A., Moreno, T., Putaud, J.P., Van Dingenen, R., 2008. Variations of urban aerosols in the western mediterranean. Atmos. Environ. 42, 9052–9062.

Pey, J., Querol, X., Alastuey, A., Rodríguez, S., Putaud, J.P., 2009. Source apportionment of urban fine and ultra-fine particle number concentration in a western Mediterranean city. Atmos. Environ. 43, 4407–4415.

Pirjola, L., Lähde, T., Niemi, J.V., Kousa, A., Rönkkö, T., Karjalainen, P., Keskinen, J., Frey, A., Hillamo, R., 2012. Spatial and temporal characterization of traffic emissions in urban microenvironments with a mobile laboratory. Atmos. Environ. 63, 156–167.

Pope, C., Coleman, N., Pond, Z., Burnett, R., 2020. Fine particulate air pollution and human mortality: 25+ years of cohort studies. Environ. Res. 183, 108924. https://doi.org/10.1016/j.envres.2019.108924.

Querol, X., Gangoiti, G., Mantilla, E., Alastuey, A., Minguillón, M.C., Amato, F., Reche, C., Viana, M., Moreno, T., Karanasiou, A., Rivas, I., Pérez, N., Ripoll, A., Brines, M., Ealo, M., Pandolfi, M., Lee, H.-K., Eun, H.-R., Park, Y.-H., Escudero, M., Beddows, D., Harrison, R.M., Bertrand, A., Marchand, N., Lyasota, A., Codina, B., Olid, M., Udina, M., Jiménez-Esteve, B., Soler, M.R., Alonso, L., Millán, M., Ahn, K.-H., 2017. Phenomenology of high-ozone episodes in NE Spain. Atmos. Chem. Phys. 17, 2817–2838.

Querol, X., Alastuey, A., Gangoiti, G., Perez, N., Lee, H.K., Eun, H.R., Park, Y., Mantilla, E., Escudero, M., Titos, G., Alonso, L., Temime-Roussel, B., Marchand, N., Moreta, J.R., Revuelta, M.A., Salvador, P., Artiñano, B., García dos Santos, S., Anguas, M., Notario, A., Saiz-Lopez, A., Harrison, R.M., Millán, M., Ahn, K.-H., 2018. Phenomenology of summer ozone episodes over the madrid metropolitan area, central Spain. Atmos. Chem. Phys. 18, 6511–6533. https://doi.org/10.5194/acp18-6511-2018.

Rivas, I., Beddows, D., Amato, F., Green, D.C., Järvi, L., Hueglin, C., Reche, C., Timonen, H., Fuller, G.W., Niemi, J.V., Pérez, N., Aurela, M., Hopke, P.K., Alastuey, A., Kulmala, M., Harrison, R.M., Querol, X., Kelly, F.J., 2020. Source apportionment of particle number size distribution in urban background and traffic stations in four European cities. Environ. Int. 135, 105345.

Robinson, A.L., Donahue, N.M., Shrivastava, M.K., Weitkamp, E.A., Sage, A.M., Grieshop, A.P., Lane, T.E., Pierce, J.R., Pandis, S.N., 2007. Rethinking organic aerosols: semivolatile emissions and photochemical aging. Science 315, 1259.

Rodriguez, S., Cuevas, E., 2007. The contributions of "minimum primary emissions" and "new particle formation enhancements" to the particle number concentration in urban air. Aerosol Science 38, 1207–1219.

Rönkkö, T., Timonen, H., 2019. Overview of sources and characteristics of nanoparticles in urban traffic-influenced areas. J. Alzheim. Dis. 72, 15–28.

Rönkkö, T., Kuuluvainen, H., Karjalainen, P., Keskinen, J., Hillamo, R., Niemi, J.V., Pirjola, L., Timonen, H.J., Saarikoski, S., Saukko, E., Järvinen, A., Silvennoinen, H., Rostedt, A., Olin, M., Yli-Ojanperä, J., Nousiainen, P., Kousa, A., Dal Maso, M., 2017. Traffic is a major source of atmospheric nanocluster aerosol. Proc. Natl. Acad. Sci. U. S.A. 114, 7549–7554.

Schraufnagel, D., 2020. The health effects of ultrafine particles. Exp. Mol. Med. 52, 311–317.

Squizzato, S., Masiol, M., Emami, F., Chalupa, D.C., Utell, M.J., Rich, D.Q., Hopke, P.K., 2019. Long-term changes of source apportioned particle number concentrations in a metropolitan area of the northeastern United States. Atmosphere 10. https://doi.org/10.3390/atmos10010027.

Steiner, S., Bisig, C., Petri-Fink, A., Rothen-Rutishauser, B., 2016. Diesel exhaust: current knowledge of adverse effects and underlying cellular mechanisms. Arch. Toxicol. 90 (7), 1541–1553.

Strasser, G., Hiebaum, S., Neuberger, M., 2018. Commuter exposure to fine and ultrafine particulate matter in Vienna. Wien Klin. Wochenschr. 130 (1–2), 62–69.

Xue, J., Li, Y., Wang, X., Durbin, T., Johnson, K., Karavalakis, G., Asa-Awuku, A., Villela, M., Quiros, D., Hu, S., Huai, T., Ayala, A., Heejung, S., 2015. Comparison of vehicle exhaust particle size distributions measured by SMPS and EEPS during steady-state conditions. Aerosol Sci. Technol. 49, 984–996.

Yue, W., Stölzel, M., Cyrys, J., Pitz, M., Heinrich, J., Kreyling, W.G., Wichmann, H.E., Peters, A., Wang, S., Hopke, P.K., 2008. Source apportionment of ambient fine particle size distribution using positive matrix factorization in Erfurt, Germany. Sci. Total Environ. 398, 133–144. https://doi.org/10.1016/j.scitotenv.2008.02.049.

Zhou, L., Kim, E., Hopke, P.K., Stanier, C.O., Pandis, S., 2004. Advanced factor analysis on Pittsburgh particle size-distribution data. Aerosol Sci. Technol. 38, 118–132.

Zhu, Y., Eiguren-Fernandez, A., Hinds, W., Miguel, A., 2007. In-cabin commuter exposure to ultrafine particles on Los Angeles freeways. Environ. Sci. Technol. 41, 2138–2145.

Zhu, Y., Hinds, W., Kim, S.H., Sioutas, C., 2002a. Concentration and size distribution of ultrafine particles near a major highway. J. Air Waste Manag. Assoc. 52 (9), 1032–1042. https://doi.org/10.1080/10473289.2002.10470842.

Zhu, Y., Hinds, W.C., Kim, S., Shen, S., Sioutas, C., 2002b. Study of ultrafine particles near a major highway with heavy-duty diesel traffic. Atmos. Environ. 36, 4323–4335.

Zhu, Y., Wu, Z., Park, Y., Fan, X., Bai, D., Zong, P., Qin, B., Cai, X., Ahn, K.H., 2019. Measurements of atmospheric aerosol vertical distribution above North China Plain using hexacopter. Sci. Total Environ. 665, 1095–1102.

CHAPTER 6: REFERENCES

6. REFERENCES

Abd Aziz, A., Lee, K., Park, B., Park, H., Park, K., Choi, I.-G., et al. (2018). Comparative study of the airborne microbial communities and their functional composition in fine particulate matter ($PM_{2.5}$) under non-extreme and extreme $PM_{2.5}$ conditions. *Atmospheric Environment*, 194, 82–92. https://doi.org/10.1016/j.atmosenv.2018.09.027.

Adamice, E., Jarosz-Krzeminska, E., and Wieszala, R. (2016). Heavy metals from non-exhaust vehicle emissions in urban and motorway road dusts. *Environ. Monit. Assess*. 188,369.

Adams, H. S., Nieuwenhuijsen, M. J., Colvile, R. N., McMullen, M. A. S., and Khandelwal, P. (2001). Fine particle ($PM_{2.5}$) personal exposure levels in transport microenvironments, London, UK. *Science of The Total Environment*, *279*(1–3), 29–44. https://doi.org/10.1016/S0048-9697(01)00723-9

Adar, S. D., Davey, M., Sullivan, J. R., Compher, M., Szpiro, A., and Sally Liu, L. J. (2008). Predicting airborne particle levels aboard Washington State school buses. *Atmospheric Environment*, *42*(33), 7590–7599. https://doi.org/10.1016/j.atmosenv.2008.06.041

Alameddine, I., Abi Esber, L., Bou Zeid, E., Hatzopoulou, M. and El-Fadel, M. (2016). Operational and environmental determinants of in-vehicle CO and $PM_{2.5}$ exposure. *Sci. Total Environ*. 551–552, 42–50.

Almoffarreh, H. K., Alsaleh, F. M., and Alruwaili, M. S. (2016). Bacterial and Fungal Contamination of Air conditioners filters and Carpets. *International Journal of Environment, Agriculture and Biotechnology*, *3*, 399–404. https://doi.org/10.22161/ijeab/1.3.14

Amato, F., Pandolfi, M., Viana, M., Querol, X., Alastuey, A., and Moreno, T. (2009). Spatial and chemical patterns of PM_{10} in road dust deposited in urban environment. *Atmospheric Environment*, *43*(9), 1650–1659. https://doi.org/10.1016/j.atmosenv.2008.12.009

Amato, F., Pandolfi, M., Moreno, T., Furger, M., Pey, J., Alastuey, A., Bukowiecki, N., Prevot, A.S.H., Baltensperger, U., and Querol, X. (2011). Sources and variability of inhalable road dust particles in three European cities. *Atmos. Environ*. 45, 6777–6787.

Amato, F., Karanasiou, A., Cordoba, P., Alastuey, A., Moreno, T., Lucarelli, F., Nava, S., Calzolai, G., and Querol, X. (2014). Effects of road dust suppressants on PM levels in a mediterranean urban area. *Environmental Science and Technology*, *48*(14), 8069–8077. https://doi.org/10.1021/es502496s

Amato, F., Escrig, A., Sanfelix, V., Celades, I., Reche, C., Monfort, E., and Querol, X. (2016). Effects of water and CMA in mitigating industrial road dust resuspension. *Atmospheric Environment*, *131*, 334–340. https://doi.org/10.1016/j.atmosenv.2016.02.018

Anjaneyulu, M. V. L. R., Harikrishna, M., and Chenchuobulu, S. (2006). Modeling ambient carbon monoxide pollutant due to road traffic. *World Academy of Science, Engineering and Technology*, 17, 103-106.

Asmi, E., Antola, M., Yli-Tuomi, T., Jantunen, M., Aarnio, P., Mäkelä, T., Hillamo, R., and Hämeri, K. (2009). Driver and passenger exposure to aerosol particles in buses and trams in Helsinki, Finland. *Science of The Total Environment*, *407*(8), 2860–2867. https://doi.org/10.1016/J.SCITOTENV.2009.01.004

Auffan, M., Rose, J., Wiesner, M.R., and Bottero, J.Y. (2009). Chemical stability of metallic nanoparticles: a parameter controlling their potential cellular toxicity in vitro. *Environ. Pollut.* 157 (4), 1127–1133.

Bach, H. J., Tomanova, J., Schloter, M., and Munch, J. C. (2002). Enumeration of total bacteria and bacteria with genes for proteolytic activity in pure cultures and in environmental samples by quantitative PCR mediated amplification. *Journal of Microbiological Methods*, 49(3), 235–245.https://doi.org/10.1016/S0167-7012(01)00370-0.

Badami, M. G. (2005). Transport and urban air pollution in India. *Environmental Management*, *36*(2), 195–204. https://doi.org/10.1007/s00267-004-0106-x

Banzhaf, E., De La Barrera, F., Kindler, A., Reyes-Paecke, S., Schlink, U., Welz, J., and Kabisch, S. (2014). A conceptual framework for integrated analysis of environmental quality and quality of life. *Ecological Indicators*, *45*, 664–668. https://doi.org/10.1016/j.ecolind.2014.06.002

Barka, E. A., Vatsa, P., Sanchez, L., Gaveau-Vaillant, N., Jacquard, C., Klenk, H.-P., et al. (2016). Taxonomy, physiology, and natural products of Actinobacteria. *Microbiology and Molecular Biology Reviews*, 80(1), 1–43. https://doi.org/10.1128/mmbr.00019-15.

Bauer, K., Bosker, T., Dirks, K. N., and Behrens, P. (2018). The impact of seating location on black carbon exposure in public transit buses: Implications for vulnerable groups. *Transportation Research Part D: Transport and Environment*, *62*, 577–583. https://doi.org/10.1016/J.TRD.2018.04.009

Behrentz, E., Fitz, D. R., Pankratz, D. V., Sabin, L. D., Colome, S. D., Fruin, S. A., and Winer, A. M. (2004). Measuring self-pollution in school buses using a tracer gas technique. *Atmospheric Environment*, *38*(23), 3735-3746.

Bertolini, V., Gandolfi, I., Ambrosini, R., Bestetti, G., Innocente, E., Rampazzo, G., et al. (2013). Temporal variability and effect of environmental variables on airborne bacterial communities in an urban area of Northern Italy. *Applied Microbiology and Biotechnology*, 97, 6561–6570. https://doi.org/10.1007/s00253-012-4450-0.

Blais-Lecours, P., Perrott, P., and Duchaine, C. (2015). Non-culturable bioaerosols in indoor settings: Impact on health and molecular approaches for detection. *Atmospheric Environment*, *110*, 45-53. https://doi.org/10.1016/j.atmosenv.2015.03.039

Bonetta, S., Bonetta, S., Mosso, S., Sampò, S., and Carraro, E. (2010). Assessment of microbiological indoor air quality in an Italian office building equipped with an HVAC system. *Environmental Monitoring and Assessment*, 161(1–4), 473–483. https://doi.org/10.1007/s10661-009-0761-8.

Borghi, F., Fanti, G., Cattaneo, A., Campagnolo, D., Rovelli, S., Keller, M., Spinazzè, A., and Cavallo, D. M. (2020). Estimation of the Inhaled Dose of Airborne Pollutants during Commuting: Case Study and Application for the General Population. *International journal of environmental research and public health*, *17*(17), 6066. https://doi.org/10.3390/ijerph17176066

Bradley, M. J., and Jones, B. M. (2002). Reducing global NOx emissions: developing advanced energy and transportation technologies. *Ambio: A journal of the Human Environment*, *31*(2), 141-149. https://doi.org/10.1579/0044-7447-31.2.141

Bowers, R. M., Clements, N., Emerson, J. B., Wiedinmyer, C., Hannigan, M. P., and Fierer, N. (2013). Seasonal variability in bacterial and fungal diversity of the near-surface atmosphere. *Environmental Science and Technology*, 47(21), 12097–12106. https://doi.org/10.1021/es402970s.

Bradley, P. H., and Pollard, K. S. (2017). Proteobacteria explain significant functional variability in the human gut microbiome. *Microbiome*, 5(1), 1–23. https://doi.org/10.1186/s40168-017-0244-z.

Bragoszewska, E., Mainka, A., and Pastuszka, J. S. (2017). Concentration and size distribution of culturable bacteria in ambient air during spring and winter in Gliwice: A typical urban area. *Atmosphere*, *8*(12). https://doi.org/10.3390/atmos8120239

Brunekreef, B., Künzli, N., Pekkanen, J., Annesi-Maesano, I., Forsberg, B., Sigsgaard, T., Keuken, M., Forastiere, F., Barry, M., Querol, X., and Harrison, R. M. (2015). Clean air in Europe: Beyond the horizon? In *European Respiratory Journal* (Vol. 45, Issue 1, pp. 7–10). https://doi.org/10.1183/09031936.00186114

Burello, E., and Worth, A. P. (2011). A theoretical framework for predicting the oxidative stress potential of oxide nanoparticles. *Nanotoxicology*, *5*(2), 228-235.

Caporaso, J. G., Kuczynski, J., Stombaugh, J., Bittinger, K., Bushman, F. D., Costello, E. K., Fierer, N., Peña, A. G., Goodrich, K., Gordon, J. I., Huttley, G. A., Kelley, S. T., Knights, D., Jeremy, E., Ley, R. E., Lozupone, C. A., Mcdonald, D., Muegge, B. D., Reeder, J., … Walters, W. A. (2011). *NIH Public Access*. *7*(5), 335–336. https://doi.org/10.1038/nmeth.f.303.QIIME

Casati, R., Scheer, V., Vogt, R., and Benter, T. (2007). Measurement of Nucle-ation and Soot Mode Particle Emission from a Diesel Passenger Car in RealWorld and Laboratory In-Situ Dilution. *Atmos. Environ*. 41:2125–2135.

Cepeda, M., Schoufour, J., Freak-Poli, R., Koolhaas, C. M., Dhana, K., Bramer, W. M., and Franco, O. H. (2017). Levels of ambient air pollution according to mode of transport: a systematic review. *The Lancet Public Health*, *2*(1), e23–e34. https://doi.org/10.1016/S2468-2667(16)30021-4

Chakrawarti, M. K., Singh, M., Yadav, V. P., and Mukhopadhyay, K. (2020). Temporal dynamics of air bacterial communities in a university health centre using illumina miseq sequencing. *Aerosol and Air Quality Research*, 20(5), 966–980. https://doi.org/10.4209/aaqr.2019.11.0613.

Chaney, R. A., Sloan, C. D., Cooper, V. C., Robinson, D. R., Hendrickson, N. R., McCord, T. A., and Johnston, J. D. (2017). Personal exposure to fine particulate air pollution while commuting: An examination of six transport modes on an urban arterial roadway. *PLoS ONE*, *12*(11). https://doi.org/10.1371/journal.pone.0188053

Chen, X., Zhang, G., Zhang, Q., and Chen, H. (2011). Mass concentrations of BTEX inside air environment of buses in Changsha, China. *Build. Environ*. 46, 421–427.

Chernyshev, V., Zakharenko, A., Ugay, S., Hien, T., Hai, L., Olesik, S., Kholodov, A., Zubko, E., Kokkinakis, T., Burykina, T., Stratidakis, A., Mezhuev, Ya, Sarigiannis, D., and Tsatsakis, A., Golokhvast, K. (2019). Morphological and chemical composition of particulate matter in buses exhaust. *Toxicology Reports* 6, 120–125.

Chiang, E., Schmidt, M. L., Berry, M. A., Biddanda, B. A., Burtner, A., Johengen, T. H., et al. (2018). Verrucomicrobia are prevalent in north-temperate freshwater lakes and display class-level preferences between lake habitats. *PLoS ONE*. https://doi.org/10.1371/journal.pone.0195112.

Chin, J.-Y. and Batterman, S.A. (2012). VOC composition of current motor vehicle fuels and vapors, and collinearity analyses for receptor modeling. *Chemosphere* 86 (9), 951–958.

Collins, M. D., Jones, D., and Kroppenstedt, R. M. (1983). Reclassification of Brevibacterium imperiale (Steinhaus) and ‘‘Corynebacterium laevaniformans’’ (Dias and Bhat) in a Redefined Genus Microbacterium (Orla-Jensen), as Microbacterium imperiale comb. nov. and Microbacterium laevaniformans nom rev.; comb. nov. *Systematic and Applied Microbiology*, 4, 65–78.

Collins, M. D., Hoyles, L., Foster, G., and Falsen, E. (2004). Corynebacterium caspium sp. nov., from a Caspian seal (Phoca caspica). *International Journal of Systematic and Evolutionary Microbiology*, 54(3), 925–928.

COM (2019). The European Green Deal COM/2019/640 Final. *Brussels*, *11*(12), 2019.

COM (2021). Pathway to a Healthy Planet for All EU Action Plan: 'Towards Zero Pollution for Air, Water and Soil'. COM/2021/400 Final. *Brussels,* 2021.

COM (2021) 44. Europe’s Beating Cancer Plan COM/2021/44. *Brussels*, 2021

Comeau, A. M., Li, W. K. W., Tremblay, J. É., Carmack, E. C., and Lovejoy, C. (2011). Arctic ocean microbial community structure before and after the 2007 record sea ice minimum. *PLoS ONE*, *6*(11). https://doi.org/10.1371/journal.pone.0027492

Corvec, S. (2018). *Clinical and Biological Features of Cutibacterium (Formerly Propionibacterium) avidum, an Underrecognized Microorganism*. Retrieved from 10

Cox, C. S., and Wathes, C. M. (Eds.). (1995). *Bioaerosols handbook*. crc press.

Dades bàsiques-Basic data, (2019). https://www.tmb.cat/documents/20182/94438/Dades+viatgers+bus+metro+2019_CA_EN/3f6c014d-4dd3-46d0-b688-26989e763677

Dades bàsiques-Basic data, (2020). https://www.tmb.cat/documents/20182/94438/Dades+viatgers+bus+metro+2020_CA_EN/41aa4b84-420e-4fb0-adc9-3f3e3f87eb65

Dastager, S. G., Lee, J. C., Ju, Y. J., Park, D. J., and Kim, C. J. (2008). Rubellimicrobium mesophilum sp. nov., a mesophilic, pigmented bacterium isolated from soil. *International Journal of Systematic and Evolutionary Microbiology*, 58(8), 1797–1800. https://doi.org/10.1099/ijs.0.65590-0.

de Nazelle, A., Fruin, S., Westerdahl, D., Martinez, D., Ripoll, A., Kubesch, N., and Nieuwenhuijsen, M. (2012). A travel mode comparison of commuters' exposures to air pollutants in Barcelona. *Atmospheric Environment*, *59*, 151–159. https://doi.org/10.1016/J.ATMOSENV.2012.05.013

de Nazelle, A., Bode, O., and Orjuela, J. P. (2017). Comparison of air pollution exposures in active vs. passive travel modes in European cities: A quantitative review. *Environment International*, *99*, 151–160. https://doi.org/10.1016/j.envint.2016.12.023

Dewhirst, F. E., Chen, T., Izard, J., Paster, B. J., Tanner, A. C. R., Yu, W. H., et al. (2010). The human oral microbiome. *Journal of Bacteriology*, 192(19), 5002–5017. https://doi.org/10.1128/JB.00542-10.

Di, Q., Wang, Y., Zanobetti, A., Wang, Y., Koutrakis, P., Choirat, C., Dominici, F., and Schwartz, J. D. (2017). Air pollution and mortality in the medicare population. *New England Journal of Medicine*, *376*(26), 2513–2522. https://doi.org/10.1056/NEJMoa1702747

Dons, E., Panis, L. I., Van Poppel, M., Theunis, J., Willems, H., Torfs, R., and Wets, G. (2011). Impact of time–activity patterns on personal exposure to black carbon. *Atmospheric Environment*, *45*(21), 3594-3602.

Dons, E., Int Panis, L., Van Poppel, M., Theunis, J., and Wets, G. (2012). Personal exposure to Black Carbon in transport microenvironments. *Atmospheric Environment*, *55*, 392–398. https://doi.org/10.1016/j.atmosenv.2012.03.020

Duce, R. A. (1995). Sources, distributions, and fluxes of mineral aerosols and their relationship to climate. *Aerosol forcing of climate*, *6*, 43-72.

Durant, J.L., Ash, C.A., Wood, E.C., Herndon, S.C., Jayne, J.T., Knighton, W.B., Canagaratna, M.R., Trull, J.B., Brugge, D., Zamore, W. and Kolb, C.E. (2010). Short-term variation in near-highway air pollutant gradients on a winter morning. *Atmos. Chem. Phys*. 10 (2), 5599–5626.

EC (2008). Council Directive 2008/50/EC of the European Parliament and of the Council of 21 May 2008 on ambient air quality and cleaner air for Europe. Official Journal of the European Union. L152, 11.6.2008, 1-44.

Economic cost of the health impact of air pollution in Europe. (2015).

Edgar, R. C., Haas, B. J., Clemente, J. C., Quince, C., and Knight, R. (2011). *UCHIME improves sensitivity and speed of chimera detection*. *27*(16), 2194–2200. https://doi.org/10.1093/bioinformatics/btr381

EEA - European Environment Agency. (2019). Air quality in Europe — 2018 report. In *Report* (Issue 5). https://doi.org/10.2800/777411

Engling, G. and Gelencsér, A. (2010). Atmospheric particles: atmospheric brown clouds: From local air pollution to climate change. *Elements* 6, 223–228. doi:10.2113/gselements.6.4.223.

EPA, 2019. Available from: http://www.epa.gov/nerlcwww/moldtech.htm (accessed March 2019)

EPA, 2022. Available from: https://www.epa.gov/indoor-air-quality-iaq/volatile-organic-compounds-impact-indoor-air-quality#Health_Effects (accessed May 2023)

Escrig, A., Monfort, E., Celades, I., Querol, X., Amato, F., Minguillón, M.C. and Hopke, P.K. (2009). Application of optimally scaled target factor analysis for assessing source contribution of ambient PM_{10}. *J. Air Waste Manage. Assoc*. 59, 1296–1307. doi:10.3155/1047-3289.59.11.1296.

Eze, I. C., Schaffner, E., Fischer, E., Schikowski, T., Adam, M., Imboden, M., Tsai, M., Carballo, D., von Eckardstein, A., Künzli, N., Schindler, C., and Probst-Hensch, N. (2014). Long-term air pollution exposure and diabetes in a population-based Swiss cohort. *Environment International*, *70*, 95–105. https://doi.org/10.1016/j.envint.2014.05.014

Fan, C., Li, Y., Liu, P., Mu, F., Xie, Z., Lu, R., et al. (2019). Characteristics of airborne opportunistic pathogenic bacteria during autumn and winter in Xi'an China. *Science of the Total Environment*, 672, 834–845. https://doi.org/10.1016/j.scitotenv.2019.03.412.

Fang, Z., Ouyang, Z., Zheng, H., Wang, X., and Hu, L. (2007). Culturable airborne bacteria in outdoor environments in Beijing, China. *Microbial Ecology*, *54*, 487-496.

Fernández-Iriarte, A., Amato, F., Moreno, N., Pacitto, A., Reche, C., Marco, E., … Moreno, T. (2020). Chemistry and sources of $PM_{2.5}$ and volatile organic compounds breathed inside urban commuting and tourist buses. *Atmospheric Environment*, 223, 117234. doi:10.1016/j.atmosenv.2019.117234

Fernández-Iriarte, A., Duchaine, C., Degois, J., Mbareche, H., Veillette, M., Moreno, N., … Moreno, T. (2021). *Bioaerosols in public and tourist buses. Aerobiologia, 37(3), 525–541.* doi:10.1007/s10453-021-09704-9

Finlayson-Pitts, B.J. and Pitts, J.N. (2000). Chemistry of the upper and lower atmosphere: theory, experiments, and applications. *Academic Press*, San Diego.

Fondelli, M. C., Chellini, E., Yli-Tuomi, T., Cenni, I., Gasparrini, A., Nava, S., Garcia-Orellana, I., Lupi, A., Grechi, D., Mallone, S., and Jantunen, M. (2008). Fine particle concentrations in buses and taxis in Florence, Italy. *Atmospheric Environment*, *42*(35), 8185–8193. https://doi.org/10.1016/J.ATMOSENV.2008.07.054

Forouzanfar, M. H., Alexander, L., Bachman, V. F., Biryukov, S., Brauer, M., Casey, D., Coates, M. M., Delwiche, K., Estep, K., Frostad, J. J., Astha, K. C., Kyu, H. H., Moradi-Lakeh, M., Ng, M., Slepak, E., Thomas, B. A., Wagner, J., Achoki, T., Atkinson, C., … Zhu, S. (2015). Global, regional, and national comparative risk assessment of 79 behavioural, environmental and occupational, and metabolic risks or clusters of risks in 188 countries, 1990-2013: A systematic analysis for the Global Burden of Disease Study 2013. *The Lancet*, *386*(10010), 2287–2323. https://doi.org/10.1016/S0140-6736(15)00128-2

Forouzanfar, M. H., Afshin, A., Alexander, L. T., Anderson, H. R., Bhutta, Z. A., Biryukov, S., Brauer, M., Burnett, R., Cercy, K., Charlson, F. J., Cohen, A. J., Dandona, L., Estep, K., Ferrari, A. J., Frostad, J. J., Fullman, N., Gething, P. W., Godwin, W. W., Griswold, M., … Murray, C. J. L. (2016). Global, regional, and national comparative risk assessment of 79 behavioural, environmental and occupational, and metabolic risks or clusters of risks, 1990–2015: a systematic analysis for the Global Burden of Disease Study 2015. *The Lancet*, *388*(10053), 1659–1724. https://doi.org/10.1016/S0140-6736(16)31679-8

Fox, K., Fox, A., Elßner, T., Feigley, C., and Salzberg, D. (2010). MALDI-TOF mass spectrometry speciation of staphylococci and their discrimination from micrococci isolated from indoor air of schoolrooms. *Journal of Environmental Monitoring*, *12*(4), 917–923. https://doi.org/10.1039/b925250a

Franzetti, A., Gandolfi, I., Gaspari, E., Ambrosini, R., and Bestetti, G. (2011). Seasonal variability of bacteria in fine and coarse urban air particulate matter. *Applied Microbiology and Biotechnology*, 90, 745–753.

Fruin, S., Hudda, N., Sioutas, C. and Delfino, R.J. (2011). Predictive model for vehicle air exchange rates based on a large, representative sample. *Environ. Sci. Technol*. 45 (8), 3569–3575.

Gandolfi, I., Bertolini, V., Bestetti, G., Ambrosini, R., Innocente, E., Rampazzo, G., et al. (2015). Spatio-temporal variability of airborne bacterial communities and their correlation with particulate matter chemical composition across two urban areas. *Applied Microbiology and Biotechnology*, 99(11), 4867–4877. https://doi.org/10.1007/s00253-014-6348-5.

Genitsaris, S., Stefanidou, N., Katsiapi, M., Kormas, K. A., Sommer, U., and Moustaka-Gouni, M. (2017). Variability of airborne bacteria in an urban Mediterranean area (Thessaloniki, Greece). *Atmospheric Environment*, 157, 101–110. https://doi.org/10.1016/j.atmosenv.2017.03.018.

Ghosh, B., Lal, H., and Srivastava, A. (2015). Review of bioaerosols in indoor environment with special reference to sampling, analysis and control mechanisms. In *Environment International* (Vol. 85, pp. 254–272). *Elsevier Ltd*. https://doi.org/10.1016/j.envint.2015.09.018

GuideBook - Measures to improve urban air quality, (2017). AIRUSE LIFE Project (LIFE11 ENV/ES/584)

Giere, R., and Querol, X. (2010). Solid particulate matter in the atmosphere. *Elements* 6, 215–222. doi:10.2113/gselements.6.4.215.

Grigoratus, T. and Martini, G. (2015). Brake wear particle emissions: a review. *Environ. Sci. Pol. Res*. 22, 2491–2504.

Goel, R., Gani, S., Guttikunda, S. K., Wilson, D., and Tiwari, G. (2015). On-road $PM_{2.5}$ pollution exposure in multiple transport microenvironments in Delhi. *Atmospheric Environment*, *123*, 129–138. https://doi.org/10.1016/J.ATMOSENV.2015.10.037

Gołofit-Szymczak, M., and Górny, R. L. (2010). Bacterial and Fungal Aerosols in Air-Conditioned Office Buildings in Warsaw, Poland—The Winter Season. *International Journal of Occupational Safety and Ergonomics*, *16*(4), 465–476. https://doi.org/10.1080/10803548.2010.11076861

González, V., Santamaría, R. I., Bustos, P., Pérez-Carrascal, O. M., Vinuesa, P., Juárez, S., et al. (2019). Phylogenomic Rhizobium species are structured by a continuum of diversity and genomic clusters. *Frontiers in Microbiology*. https://doi.org/10.3389/fmicb.2019.00910.

Grobéty, B., Gieré, R., Dietze, V., and Stille, P. (2010). Atmospheric particles: airborne particles in the urban environment. *Elements* 6, 229–234. doi:10.2113/gselements.6.4.229.

Gupta, R. S., Mahmood, S., and Adeolu, M. (2013). A phylogenomic and molecular signature based approach for characterization of the phylum spirochaetes and its major clades: Proposal for a taxonomic revision of the phylum. *Frontiers in Microbiology*. https://doi.org/10.3389/fmicb.2013.00217.

Haagen-Smit, A.J. (1966). Carbon monoxide levels in city driving. *Archives of Environ. Health* 12, 548–551.

Ham, W., Vijayan, A., Schulte, N., and Herner, J. D. (2017). Commuter exposure to $PM_{2.5}$, BC, and UFP in six common transport microenvironments in Sacramento, California. *Atmospheric Environment*, *167*, 335–345. https://doi.org/10.1016/J.ATMOSENV.2017.08.024

Hama, S., Ouchen, I., Wyche, K. P., Cordell, R. L., and Monks, P. S. (2022). Carbonaceous aerosols in five European cities: Insights into primary emissions and secondary particle formation. Atmospheric Research, 274, 106180.

Hamada, N., and Fujita, T. (2002). Effect of air-conditioner on fungal contamination. *Atmospheric Environment*, *36*(35), 5443–5448. https://doi.org/10.1016/S1352-2310(02)00661-1

Hammond, D., Jones, S. and Lalor, M. (2007). In-vehicle Measurement of Ultrafine Particles on Compressed Natural Gas, Conventional Diesel, and Oxidation-catalyst Diesel Heavy-duty Transit Buses. *Environ Monit Assess* 125, 239–246. https://doi.org/10.1007/s10661-006-9515-z

Harrison, R. M., Shi, J. P., Xi, S., Khan, A., Mark, D., Kinnersley, R., and Yin,J. (2000). Measurement of Number, Mass and Size Distribution of Particles in the Atmosphere, in Philosophical Transactions: Mathematical, Physical and Engineering Sciences, Vol. 358, No. 1775, Ultrafine Particles in the Atmosphere, pp. 2567–2580. *The Royal Society*.

Harrison R. M. and Yin J. (2008). Sources and processes affecting carbonaceous aerosol in central England. *Atmospheric Environment* 42, 1413–1423.

Heal, M. R., Kumar, P., and Harrison, R. M. (2012). Particles, air quality, policy and health. *Chemical Society Reviews*, *41*(19), 6606. https://doi.org/10.1039/c2cs35076a

Hertel, O., Hvidberg, M., Ketzel, M., Storm, L., and Stausgaard, L. (2008). A proper choice of route significantly reduces air pollution exposure — A study on bicycle and bus trips in urban streets. *Science of The Total Environment*, *389*(1), 58–70. https://doi.org/10.1016/J.SCITOTENV.2007.08.058

Hewitt, R. E., Chappell, H. F., and Powell, J. J. (2020). Small and dangerous? Potential toxicity mechanisms of common exposure particles and nanoparticles. *Current opinion in toxicology*, *19*, 93-98.

Hinds, W.C., (1999). Aerosol technology: properties, behaviour, and measurement of airborne particles. *John Wiley and Sons, Inc*., New York, USA.

Hoek, G., Krishnan, R. M., Beelen, R., Peters, A., Ostro, B., Brunekreef, B., and Kaufman, J. D. (2013). Long-term air pollution exposure and cardio-respiratory mortality: a review. *Environmental health*, *12*(1), 1-16.

Hollander, A., Douwes, J., and Heederik, D. (1993). Inhibition and Enhancement in the Analysis of Airborne Endotoxin Levels in Various Occupational Environments. *American Industrial Hygiene Association Journal*, 54(11), 647–653. https://doi.org/10.1080/15298669391355189

Hudda, N. and Fruin, S. (2018). Carbon dioxide accumulation inside vehicles: the effect of ventilation and driving conditions. *Sci. Total Environ*. 610–611, 1448–1456.

Hudda, N., Kostenidou, E., Sioutas, C., Delfino, R. J., and Fruin, S. A. (2011). Vehicle and Driving Characteristics That Influence In-Cabin Particle Number Concentrations. *Environmental Science* and *Technology*, *45*(20), 8691–8697. https://doi.org/10.1021/es202025m

ICRP, 1994. Human Respiratory Tract Model for Radiological Protection. International Commission on Radiological Protection, Pergamon.

Indra Dé, Kenneth V.I. Rolston, and X. Y. H. (2004). Clinical Significance of Roseomonas Species Isolated from Catheter and Blood Samples: Analysis of 36 Cases in Patients with Cancer. Retrieved from https://academic.oup.com/cid/article/38/11/1579/285332

Innocente, E., Squizzato, S., Visin, F., Facca, C., Rampazzo, G., Bertolini, V., et al. (2017). Influence of seasonality, air mass origin and particulate matter chemical composition on airborne

bacterial community structure in the Po Valley, Italy. *Science of The Total Environment*, 593–594, 677–687.

IPCC, (2001). Climate Change 2001: The Scientific Basis. Contribution of Working Group I to the Third Assessment Report of the Intergovernmental Panel on Climate Change. Houghton J.T., Ding Y., Griggs D.J., Noguer M., van der Linden P.J., Dai X., Maskell K. and Johnson C.A. (eds.). Cambridge University Press.

Jo, W. K., and Lee, J. H. (2008). Airborne Fungal and Bacterial Levels Associated With the Use of Automobile Air Conditioners or Heaters, Room Air Conditioners, and Humidifiers. *Archives of Environmental and Occupational Health*, *63*(3), 101–107. https://doi.org/10.3200/AEOH.63.3.101-107

Jo, W. and Yu, C. (2001). Public bus and taxicab drivers' work-time exposure to aromatic volatile organic compounds. *Environ. Res*. 86, 66–72.

Johnson, G. R., and Morawska, L. (2009). The mechanism of breath aerosol formation. *Journal of aerosol medicine and pulmonary drug delivery*, *22*(3), 229-237. https://doi.org/10.1089/jamp.2008.0720

Kelly, F. J., and Zhu, T. (2016). Transport solutions for cleaner air. *Science*, *352*(6288), 934-936.

Kampa, M. and Castanas, E., (2008). Human health effects of air pollution. *Environ. Pollut*. 151, 362–367. doi:10.1016/j.envpol.2007.06.012.

Kandi, V., Palange, P., Vaish, R., Bhatti, A. B., Kale, V., Kandi, M. R., and Bhoomagiri, M. R. (2016). Emerging Bacterial Infection: Identification and clinical significance of Kocuria Species. *Cureus*. https://doi.org/10.7759/cureus.731.

Karagulian, F., Belis, C. A., Dora, C. F. C., Prüss-Ustün, A. M., Bonjour, S., Adair-Rohani, H., and Amann, M. (2015). Contributions to cities' ambient particulate matter (PM): A systematic review of local source contributions at global level. In *Atmospheric Environment*. https://doi.org/10.1016/j.atmosenv.2015.08.087

Karanasiou, A., Viana, M., Querol, X., Moreno, T., and de Leeuw, F. (2014). Assessment of personal exposure to particulate air pollution during commuting in European cities—Recommendations and policy implications. *Science of the Total Environment*, *490*, 785-797.

Kaur, S., Nieuwenhuijsen, M., and Colvile, R. (2005a). Personal exposure of street canyon intersection users to $PM_{2.5}$, ultrafine particle counts and carbon monoxide in Central

London, UK. *Atmospheric Environment*, *39*(20), 3629–3641. https://doi.org/10.1016/j.atmosenv.2005.02.046

Kaur, S., Nieuwenhuijsen, M. J., and Colvile, R. N. (2005b). Pedestrian exposure to air pollution along a major road in Central London, UK. *Atmospheric Environment*, *39*(38), 7307–7320. https://doi.org/10.1016/J.ATMOSENV.2005.09.008

Kaur, S., Clark, R. D. R., Walsh, P. T., Arnold, S. J., Colvile, R. N., and Nieuwenhuijsen, M. J. (2006). Exposure visualisation of ultrafine particle counts in a transport microenvironment. *Atmospheric Environment, 40(2), 386–398.* doi:10.1016/j.atmosenv.2005.09.047

Kaur, S., Nieuwenhuijsen, M. J., and Colvile, R. N. (2007). Fine particulate matter and carbon monoxide exposure concentrations in urban street transport microenvironments. *Atmospheric Environment*, *41*(23), 4781–4810. https://doi.org/10.1016/j.atmosenv.2007.02.002

Kelly, F. J., and Fussell, J. C. (2015). Air pollution and public health: emerging hazards and improved understanding of risk. *Environmental geochemistry and health*, *37*, 631-649.

Kerchich, Y. and Kerbachi, R. (2012). Measurement of BTEX (benzene, toluene, ethylbenzene, and xylene) levels at urban and semirural areas of Algiers City using passive air samplers. *J. Air Waste Manag. Assoc*. 62, 1370–1379.

Kingham, S., Longley, I., Salmond, J., and Pattinson, W. (2013). Variations in exposure to traffic pollution while travelling by different modes in a low density, less congested city. *Environmental Pollution*, *181*, 211–218. https://doi.org/10.1016/j.envpol.2013.06.030

Knibbs, L. D., and de Dear, R. J. (2010). Exposure to ultrafine particles and $PM_{2.5}$ in four Sydney transport modes. In *Atmospheric Environment* (Vol. 44, Issue 26). https://doi.org/10.1016/j.atmosenv.2010.05.026

Knibbs, L. D., Cole-Hunter, T., and Morawska, L. (2011). A review of commuter exposure to ultrafine particles and its health effects. *Atmospheric Environment*, *45*(16), 2611–2622. https://doi.org/10.1016/j.atmosenv.2011.02.065

Krecl, P., Johansson, C., Targino, A. C., Ström, J., and Burman, L. (2017). Trends in black carbon and size-resolved particle number concentrations and vehicle emission factors under real-world conditions. *Atmospheric Environment*, *165*, 155-168.

Kulmala, M., Laakso, L., Lehtinen, K.E.J., Riipinen, I., Dal Maso, M., Anttila, T., Kerminen, V.-M., Hõrrak, U., Vana, M. and Tammet, H., (2004). Initial steps of aerosol growth. *Atmos. Chem. Phys*. 4, 2553–2560. doi:10.5194/acp-4-2553-2004.

Kumar, P., Fennell, P. and Britter, R., (2008). Effect of wind direction and speed on the dispersion of nucleation and accumulation mode particles in an urban street canyon. *Sci. Total Environ*. 402, 82–94.

Kumar, P., Morawska, L., Birmili, W., Paasonen, P., Hu, M., Kulmala, M., Harrison, R. M., Norford, L., and Britter, R. (2014). Ultrafine particles in cities. *Environment International*, *66*, 1–10. https://doi.org/10.1016/J.ENVINT.2014.01.013

Kumar, P., Patton, A. P., Durant, J. L., and Frey, H. C. (2018). A review of factors impacting exposure to $PM_{2.5}$, ultrafine particles and black carbon in Asian transport microenvironments. *Atmospheric Environment*, *187*, 301–316. https://doi.org/10.1016/J.ATMOSENV.2018.05.046

Kupiainen, K. (2007). Road dust from pavement wear and traction sanding. Monographs of the Boreal Environment Research, 26. Finnish Environment Institute, Finland. 50 p. Doctoral Dissertation.

Lai, K., Nguyen, N. T., Miwa, H., Yasuda, M., Nguyen, H. H., and Okazaki, S. (2020). Diversity of methylobacterium spp. In the rice of the vietnamese mekong delta. *Microbes and Environments*. https://doi.org/10.1264/jsme2.ME19111.

Larsen, J. M. (2017). The immune response to Prevotella bacteria in chronic inflammatory disease. *Immunology*. https://doi.org/10.1111/imm.12760.

Leavey, A., Reed, N., Patel, S., Bradley, K., Kulkarni, P. and Biswas, P. (2017). Comparing on-road real-time simultaneous in-cabin and outdoor particulate and gaseous concentrations for a range of ventilation scenarios. *Atmos. Environ*. 166, 130–141.

Lee, J. H., and Jo, W. K. (2005). Exposure to airborne fungi and bacteria while commuting in passenger cars and public buses. *Atmospheric Environment*, 39(38), 7342–7350. https://doi.org/10.1016/j.atmosenv.2005.09.013.

Lee, B., Lee, G., and Joon Heo, K. (2016). Concentration of culturable bioaerosols during winter. *Journal of Aerosol Science*, *94*, 1–8. https://doi.org/10.1016/j.jaerosci.2015.12.002

Lee, E., Stenstrom, M. and Zhu, Y. (2015). Ultrafine particle infiltration into passenger vehicles. Part 1: experimental evidence. *Transp. Res. Part* D 38, 156–165.

Lehtinen, J., Tolvanen, O., Nivukoski, U., Veijanen, A., and Hänninen, K. (2013). Occupational hygiene in terms of volatile organic compounds (VOCs) and bioaerosols at two solid waste management plants in Finland. *Waste Management*, *33*(4), 964–973. https://doi.org/10.1016/j.wasman.2012.11.010

Lelieveld, J., Pozzer, A., Pöschl, U., Fnais, M., Haines, A., and Münzel, T. (2020). Loss of life expectancy from air pollution compared to other risk factors: a worldwide perspective. *Cardiovascular research*, *116*(11), 1910-1917.

Leung, M. H. Y., Wilkins, D., and Lee, P. K. H. (2015). Insights into the pan-microbiome: Skin microbial communities of Chinese individuals differ from other racial groups. *Scientific Reports*. https://doi.org/10.1038/srep11845

Lim, J. H., Baek, S. H., and Lee, S. T. (2009). Ferruginibacter alkalilentus gen. nov, sp nov and ferruginibacter lapsinanis sp nov novel members of the family 'chitinophagaceae' in the phylum Bacteroidetes isolated from freshwater sediment. *International Journal of Systematic and Evolutionary Microbiology* 59(10), 2394–2399. https://doi.org/10.1099/ijs.0.009480-0

Lim, J.-M., Lee, J.-H., Moon, J.-H., Chung, Y.-S. and Kim, K.-H., (2010). Source apportionment of PM_{10} at a small industrial area using Positive Matrix Factorization. *Atmos. Res*. 95, 88–100. doi:10.1016/j.atmosres.2009.08.009.

Lim, S., Salmond, J. A., and Dirks, K. N. (2015). Influence of Differing Microenvironments on Personal Carbon Monoxide Exposure in Auckland, New Zealand. *The Open Atmospheric Science Journal*, *8*(1), 1–8. https://doi.org/10.2174/1874282301509010001

Lim, S., Dirks, K. N., Salmond, J. A., and Xie, S. (2015). Determinants of spikes in ultrafine particle concentration whilst commuting by bus. *Atmospheric Environment*, 112, 1–8. https://doi.org/10.1016/j.atmosenv.2015.04.025.

Lonati G., Giugliano M., Butelli P., Romele L. and Tardivo R. (2005). Major chemical components of $PM_{2.5}$ in Milan (Italy). *Atmospheric Environment* 39, 1925-1934.

Lu, Y., Lin, Y., Zhang, H., Ding, D., Sun, X., Huang, Q., Lin, L., Chen, Y., Chi, Y. and Dong, S. (2016). Evaluation of volatile organic compounds and carbonyl compounds present in the cabins of

newly produced, medium- and large-size coaches in China. *Int. J. Environ. Res. Public Health* 13, 596.

Madl, P., Majid, H., Kwasny, F. and Hofmann, W. (2015). In-vehicle exposure to ultrafine particles while driving through a tunnel system and associated lung deposition calculations. *Aerosol and Air Quality Res* 15, 295–305.

Maestre, J. P., Jennings, W., Wylie, D., Horner, S. D., Siegel, J., and Kinney, K. A. (2018). Filter forensics: Microbiota recovery from residential HVAC filters. *Microbiome*. https://doi.org/10.1186/s40168-018-0407-6.

Mancinelli, R. L., and Shulls, W. A. (1978). Airborne bacteria in an urban environment. *Applied and Environmental Microbiology*, *35*(6), 1095-1101.

Matti Maricq, M. (2007). Chemical characterization of particulate emissions from diesel engines: A review. *Journal of Aerosol Science*, 38(11), 1079–1118. https://doi.org/10.1016/j.jaerosci.2007.08.001

Mbareche, H., Veillette, M., Bilodeau, G. J., and Duchaine, C. (2019). Fungal aerosols at dairy farms using molecular and culture techniques. *Science of The Total Environment*, *653*, 253–263. https://doi.org/10.1016/J.SCITOTENV.2018.10.345

McNabola, A., Broderick, B. M., and Gill, L. W. (2008). Relative exposure to fine particulate matter and VOCs between transport microenvironments in Dublin: Personal exposure and uptake. *Atmospheric Environment,* 42(26), 6496–6512. doi:10.1016/j.atmosenv.2008.04.015

Mészáros, E. (1999). Fundamentals of atmospheric aerosol chemistry. Akademiai Kiadó, Budapest.

Minguillón, M.C., Schembari, A., Triguero-Mas, M., de Nazelle, A., Dadvand, P., Figueras, F., Salvado, J.A., Grimalt, J.O., Nieuwenhuijsen, M. and Querol, X. (2012). Source apportionment of indoor, outdoor and personal $PM_{2.5}$ exposure of pregnant women in Barcelona, Spain. *Atmos. Environ. Times* 59, 426–436.

Molina, L. T., Kolb, C. E., De Foy, B., Lamb, B. K., Brune, W. H., Jimenez, J. L., Ramos-Villegas, R., Sarmiento, J., Paramo-Figueroa, V. H., Cardenas, B., Gutierrez-Avedoy, V., and Molina, M. J. (2007). Air quality in North America's most populous city-overview of the MCMA-2003 campaign. In *Atmos. Chem. Phys* (Vol. 7). www.atmos-chem-phys.net/7/2447/2007/

Molina, L. T. and Molina, M. J. (Eds.) (2002) Air Quality in the Mexico Megacity: An Integrated Assessment, Kluwer Academic Publishers, Dordrecht, The Netherlands.

Molle, R., Mazoué, S., Géhin, É., and Ionescu, A. (2013). Indoor-outdoor relationships of airborne particles and nitrogen dioxide inside Parisian buses. *Atmospheric Environment*, *69*, 240–248. https://doi.org/10.1016/j.atmosenv.2012.11.050

Montells, R., Aceves, M. and Grimalt, J.O. (2000). Sampling and analysis of volatile organic compounds emitted from leaded and unleaded gasoline powered motor vehicles. *Environ. Monit. Assess*. 62, 1–14.

Morawska, L., Ristovski, Z., Jayaratne, E. R., Keogh, D. U., and Ling, X. (2008). Ambient nano and ultrafine particles from motor vehicle emissions: Characteristics, ambient processing and implications on human exposure. *Atmospheric Environment*, *42*(35), 8113–8138. https://doi.org/10.1016/j.atmosenv.2008.07.050

Morawska, L. and Salthammer, T., (2003). Indoor Environment - Airborne Particles and Settled Dust. WILEY-VCH Verlag GmbH and Co. KGaA, Weinheim.

Moreno, T., Reche, C., Rivas, I., Cruz Minguillón, M., Martins, V., Vargas, C., Buonanno, G., Parga, J., Pandolfi, M., Brines, M., Ealo, M., Sofia Fonseca, A., Amato, F., Sosa, G., Capdevila, M., de Miguel, E., Querol, X., and Gibbons, W. (2015). Urban air quality comparison for bus, tram subway and pedestrian commutes in Barcelona. *Environmental Research*, *142*, 495–510. https://doi.org/10.1016/j.envres.2015.07.022

Moreno, T., Pacitto, A., **Fernández-Iriarte, A.**, Amato, F., Marco, E., Grimalt, J. O., Buonanno, G., and Querol, X. (2019). Vehicle interior air quality conditions when travelling by taxi. *Environmental Research*, *172*, 529–542. https://doi.org/10.1016/J.ENVRES.2019.02.042

Moreno T., Reche C., Ahn K.H., Eun H.R., Kim W.Y., Kim H.S., **Fernández-Iriarte A.**, Amato F. and Querol X. (2020). Using miniaturised scanning mobility particle sizers to observe size distribution patterns of quasiultrafine aerosols inhaled during city commuting. *Environ Res* 109978. doi: 10.1016/j.envres.2020.109978.

Nieuwenhuijsen, M. J. (2018). Influence of urban and transport planning and the city environment on cardiovascular disease. *Nature reviews cardiology*, *15*(7), 432-438.

Nowakowicz-Dębek, B., Pawlak, H., Wlazło, Ł., Maksym, P., Kapica, J., Chmielowiec-Korzeniowska, A., and Trawińska, B. (2017). Evaluating bioaerosol exposure among bus drivers in the

public transport sector. *Journal of Occupational and Environmental Hygiene*, *14*(11), D169–D172. https://doi.org/10.1080/15459624.2017.1339165

Núñez A., Amo de Paz G., Rastrojo A., Ferencova Z., Gutiérrez-Bustillo A.M., Alcamí A., et al. (2019). Temporal patterns of variability for prokaryotic and eukaryotic diversity in the urban air of Madrid (Spain), *Atmospheric Environment*, 217 116972 ISSN: 1352–2310, https://doi.org/10.1016/j.atmosenv.2019.116972.

OECD. (2017). Health at a glance 2017: OECD Indicators. In *OECD Publishing*. https://doi.org/10.1787/health_glance-2013-en

Olivares G., Johansson C., Ström J. and Hansson H.C. (2007). The role of ambient temperature for particle number concentrations in a street canyon. *Atmospheric Environment* 41, 2145–2155.

Paatero, P. and Tapper, U., (1994). Positive matrix factorization: A non-negative factor model with optimal utilization of error estimates of data values. *Environmetrics* 5, 111–126. doi:10.1002/env.3170050203.

Pan, Y.P. and Wang, Y.S. (2015). Atmospheric wet and dry deposition of trace elements at 10 sites in Northern China. *Atmos. Chem. Phys*. 15, 951–972. doi:10.5194/acp-15-951-2015.

Panté, N., and Kann, M. (2002). Nuclear pore complex is able to transport macromolecules with diameters of~ 39 nm. *Molecular biology of the cell*, *13*(2), 425-434.

Parra, M., Elustondo, D., Bermejo, R. and Santamaría, J.M., (2008). Exposure to volatile organic compounds (VOC) in public buses of Pamplona, Northern Spain. *Sci. Total Environ*. 404, 18–25.

Parte, A. C., Sardà Carbasse, J., Meier-Kolthoff, J. P., Reimer, L. C., and Göker, M. (2020). List of Prokaryotic names with Standing in Nomenclature (LPSN) moves to the DSMZ. *International Journal of Systematic and Evolutionary Microbiology*. https://doi.org/10.1099/ijsem.0.004332.

Pollet, T., Humbert, J. F., and Tadonléké, R. D. (2014). Planctomycetesin lakes: Poor or strong competitors for phosphorus? *Applied and Environmental Microbiology*, 80(3), 819–828. https://doi.org/10.1128/AEM.02824-13.

Pope, C., Coleman N., Pond, Z. and Burnett, R. (2020). Fine particulate air pollution and human mortality: 25+ years of cohort studies. *Environ. Res*. 183, 108924. https://doi.org/10.1016/j.envres.2019.108924

Pöschl, U. (2005). Atmospheric aerosols: composition, transformation, climate and health effects. *Angew. Chemie Int*. Ed. 44, 7520–7540. doi:10.1002/anie.200501122.

Prakash, N. (2014). A Study on the Prevalence of Indoor Mycoflora in Air Conditioned Buses. *British Microbiology Research Journal*, 4(3), 282–292. https://doi.org/10.9734/bmrj/2014/5380.

Priyamvada, H., Priyanka, C., Singh, R. K., Akila, M., Ravikrishna, R., and Gunthe, S. S. (2018). Assessment of PM and bioaerosols at diverse indoor environments in a southern tropical Indian region. *Building and Environment*, 137(March), 215–225. https://doi.org/10.1016/j.buildenv. 2018.04.016.

Prospero, J.M., Ginoux, P., Torres, O., Nicholson, S.E. and Gill, T.E. (2002). Environmental characterization of global sources of atmospheric soil dust identified with the Nimbus 7 Total Ozone Mapping Spectrometer (TOMS) absorbing aerosol product. *Rev. Geophys*. 40, 2–31. doi:10.1029/2000RG000095.

PTEG (2009). Reducing emissions from PTE/SPT bus fleets – study report. *Transport* and *Travel Research Ltd*

Putaud, J.-P., Van Dingenen, R., Alastuey, A., Bauer, H., Birmili, W., Cyrys, J., Flentje, H., Fuzzi, S., Gehrig, R., Hansson, H.C., Harrison, R.M., Herrmann, H., Hitzenberger, R., Hüglin, C., Jones, A.M., Kasper-Giebl, A., Kiss, G., Kousa, A., Kuhlbusch, T.A.J., Löschau, G., Maenhaut, W., Molnar, A., Moreno, T., Pekkanen, J., Perrino, C., Pitz, M., Puxbaum, H., Querol, X., Rodriguez, S., Salma, I., Schwarz, J., Smolik, J., Schneider, J., Spindler, G., ten Brink, H., Tursic, J., Viana, M., Wiedensohler, A. and Raes, F., (2010). A European aerosol phenomenology – 3: Physical and chemical characteristics of particulate matter from 60 rural, urban, and kerbside sites across Europe. *Atmos. Environ*. 44, 1308–1320. doi:10.1016/j.atmosenv.2009.12.011.

Querol, X., Alastuey, A., Rodriguez, S., Plana, F., Ruiz, C. R., Cots, N., ... and Puig, O. (2001). PM_{10} and $PM_{2.5}$ source apportionment in the Barcelona Metropolitan area, Catalonia, Spain. *Atmospheric Environment*, *35*(36), 6407-6419.

Querol, X., Viana, M., Alastuey, A., Amato, F., Moreno, T., Castillo, S., Pey, J., de la Rosa, J., Sánchez de la Campa, A., Artíñano, B., Salvador, P., García Dos Santos, S., Fernández-Patier, R.,

Moreno-Grau, S., Negral, L., Minguillón, M.C., Monfort, E., Gil, J.I., Inza, A., Ortega, L.A., Santamaría, J.M. and Zabalza, J. (2007). Source origin of trace elements in PM from regional background, urban and industrial sites of Spain. *Atmos. Environ*. 41, 7219–7231. doi:10.1016/j.atmosenv.2007.05.022.

Querol, X., Gangoiti, G., Mantilla, E., Alastuey, A., Minguillón, M.C., Amato, F., Reche, C., Viana, M., Moreno, T., Karanasiou, A., Rivas, I., Pérez, N., Ripoll, A., Brines, M., Ealo, M., Pandolfi, M., Lee, H.-K., Eun, H.-R., Park, Y.-H., Escudero, M., Beddows, D., Harrison, R.M., Bertrand, A., Marchand, N., Lyasota, A., Codina, B., Olid, M., Udina, M., Jim´enez-Esteve, B., Soler, M.R., Alonso, L., Millán, M. and Ahn, K.- H., (2017). Phenomenology of high-ozone episodes in NE Spain. *Atmos. Chem. Phys*. 17, 2817–2838.

Raes, F., Dingenen, R. V., Vignati, E., Wilson, J., Putaud, J.-P., Seinfeld, J. H., and Adams, P. (2000). Formation and cycling of aerosols in the global troposphere. *Atmospheric Environment, 34(25), 4215–4240.* doi:10.1016/s1352-2310(00)00239-9

Ragettli, M. S., Corradi, E., Braun-Fahrländer, C., Schindler, C., de Nazelle, A., Jerrett, M., Ducret-Stich, R. E., Künzli, N., and Phuleria, H. C. (2013). Commuter exposure to ultrafine particles in different urban locations, transportation modes and routes. *Atmospheric Environment*, *77*, 376–384. https://doi.org/10.1016/j.atmosenv.2013.05.003

Ransom-Jones, E., Jones, D. L., McCarthy, A. J., and McDonald, J. E. (2012). An important phylum of cellulose-degrading bacteria. *Microbial Ecology*. https://doi.org/10.1007/s00248-011-9998-1.

Rivas, I., Kumar, P., Hagen-Zanker, A., Andrade, M. de F., Slovic, A. D., Pritchard, J. P., and Geurs, K. T. (2017). Determinants of black carbon, particle mass and number concentrations in London transport microenvironments. *Atmospheric Environment*, *161*, 247–262. https://doi.org/10.1016/J.ATMOSENV.2017.05.004

Rivas, I., Mazaheri, M., Viana, M., Moreno, T., Clifford, S., He, C., Bischof, O.F., Martins, V., Reche, C., Alastuey, A., Alvarez-Pedrerol, M., Sunyer, J., Morawska, L., Querol, X., 2017. Identification of technical problems affecting performance of DustTrak DRX aerosol monitors. Sci. Total Environ. 584–585, 849–855. https://doi.org/10.1016/j.scitotenv.2017.01.129

Rivas, I., Viana, M., Moreno, T., Pandolfi, M., Amato, F., Reche, C., Bouso, L., Àlvarez-Pedrerol, M., Alastuey, A., Sunyer, J., and Querol, X. (2014). Child exposure to indoor and outdoor air pollutants in schools in Barcelona, Spain. *Environment International*, *69*, 200–212. https://doi.org/10.1016/j.envint.2014.04.009

Robertson, S., Douglas, P., Jarvis, D., and Marczylo, E. (2019). Bioaerosol exposure from composting facilities and health outcomes in workers and in the community: A systematic review update. *International journal of hygiene and environmental health*, *222*(3), 364-386. https://doi.org/10.1016/j.ijheh.2019.02.006

Rodríguez S., Querol X., Alastuey A. and Mantilla E. (2002). Origin of high summer PM_{10} and TSP concentrations at rural sites in Eastern Spain. *Atmospheric Environment* 36(19):3101-3112.

Rodríguez, S., Querol, X., Alastuey, A., and de la Rosa, J. (2007). Atmospheric particulate matter and air quality in the Mediterranean: A review. In *Environmental Chemistry Letters* (Vol. 5, Issue 1, pp. 1–7). https://doi.org/10.1007/s10311-006-0071-0

Rognes, T., Flouri, T., Nichols, B., Quince, C., and Mahé, F. (2016). *VSEARCH : a versatile open source tool for metagenomics*. 1–22. https://doi.org/10.7717/peerj.2584

R Rönkkö, T., Kuuluvainen, H., Karjalainen, P., Keskinen, J., Hillamo, R., Niemi, J. V., Pirjola, L., Timonen, H.J., Saarikoski, S., Saukko, E., Järvinen, A., Silvennoinen, H., Rostedt, A., Olin, M., Yli-Ojanperä, J., Nousiainen, P., Kousa, A. and Dal Maso, M., (2017). Traffic is a major source of atmospheric nanocluster aerosol. *Proc. Natl. Acad. Sci*. 114, 7549–7554. https://doi.org/10.1073/pnas.1700830114

Ryan, K. J., and Ray, C. G. (2004). *Sherris Medical Microbiology*. McGraw-Hill.

Sabin, L. D., Behrentz, E., Winer, A. M., Jeong, S., Fitz, D. R., Pankratz, D. V., … Fruin, S. A. (2005). Characterizing the range of children's air pollutant exposure during school bus commutes. *Journal of Exposure Science* and *Environmental Epidemiology,* 15(5), 377–387. doi:10.1038/sj.jea.7500414

Schaechter, M. (2009). Encyclopedia of microbiology. *Academic Press*.

Schauer, J. J., Lough, G. C., Shafer, M. M., Christensen, W. F., Arndt, M. F.,DeMinter, J. T., and Park, J. S. (2006). Characterization of Metals Emittedfrom Motor Vehicles. *Health Effects Institute Research report* No. 133

Schraufnagel, DE (2020). Los efectos en la salud de las partículas ultrafinas. *Medicina experimental y molecular*, 52 (3), 311-317.

Seinfeld, J.H. and Pandis, S.N., (2006). Atmospheric Chemistry and Physics: From Air Pollution to Climate Change (2nd Ed.). *John Wiley and Sons, Inc*., New York, USA.

Shaffer, B. and Lighthart, B. (1997). Survey of Culturable Airborne Bacteria at Four Diverse Locations in Oregon: Urban, Rural, Forest, and Coastal. *Microb Ecol,* 34, 167–177. https://doi.org/10.1007/s002489900046

Schloss, P. D., Westcott, S. L., Ryabin, T., Hall, J. R., Hartmann, M., Hollister, E. B., Lesniewski, R. A., Oakley, B. B., Parks, D. H., Robinson, C. J., Sahl, J. W., Stres, B., Thallinger, G. G., Horn, D. J. Van, and Weber, C. F. (2009). *Introducing mothur: Open-Source, Platform-Independent, Community-Supported Software for Describing and Comparing Microbial Communities*. *75*(23), 7537–7541. https://doi.org/10.1128/AEM.01541-09

Singh, V., Sahu, S. K., Kesarkar, A. P., and Biswal, A. (2018). Estimation of high resolution emissions from road transport sector in a megacity Delhi. *Urban Climate*, *26*, 109–120. https://doi.org/10.1016/J.UCLIM.2018.08.011

Sizova, M. V., Muller, P., Panikov, N., Mandalakis, M., Hohmann, T., Hazen, A., et al. (2013). Stomatobaculum longum gen. nov., sp. nov., an obligately anaerobic bacterium from the human oral cavity. *International Journal of Systematic and Evolutionary Microbiology*, 63(PART4), 1450–1456. https://doi.org/10.1099/ijs.0.042812-0.

Sowiak, M., Kozajda, A., Jeżak, K., and Szadkowska-Stańczyk, I. (2018). Does the air condition system in busses spread allergic fungi into driver space? *Environmental Science and Pollution Research*, *25*(5), 5013–5023. https://doi.org/10.1007/s11356-017-0830-4

Squizzato, S., Masiol, M., Brunelli, A., Pistollato, S., Tarabotti, E., Rampazzo, G. and Pavoni, B. (2013). Factors determining the formation of secondary inorganic aerosol: a case study in the Po Valley (Italy). *Atmos. Chem. Phys*. 13, 1927–1939. doi:10.5194/acp-13-1927-2013.

Steiner, S., Bisig, C., Petri-Fink, A., and Rothen-Rutishauser, B. (2016). Diesel exhaust: current knowledge of adverse effects and underlying cellular mechanisms. *Archives of toxicology*, *90*, 1541-1553.

Sternbeck, J., Sjödin, Å. and Andréasson, K., (2002). Metal emissions from road traffic and the influence of resuspension—results from two tunnel studies. *Atmos. Environ*. 36, 4735–4744. doi:10.1016/S1352-2310(02)00561-7.

Strasser, G., Hiebaum, S. and Neuberger, M. (2018). Commuter exposure to fine and ultrafine particulate matter in Vienna. Wien Klin. *Wochenschr*. 130 (1–2), 62–69.

Sun, H. M., Zhang, T., Yu, L. Y., Sen, K., and Zhang, Y. Q. (2015). Ubiquity, diversity and physiological characteristics of Geodermatophilaceae in Shapotou National Desert Ecological Reserve. *Frontiers in Microbiology*. https://doi.org/10.3389/fmicb.2015.01059.

Sunyer, J., Esnaola, M., Alvarez-Pedrerol, M., Forns, J., Rivas, I., López-Vicente, M., Suades-González, E., Foraster, M., Garcia-Esteban, R., Basagaña, X., Viana, M., Cirach, M., Moreno, T., Alastuey, A., Sebastian-Galles, N., Nieuwenhuijsen, M., and Querol, X. (2015). Association between Traffic-Related Air Pollution in Schools and Cognitive Development in Primary School Children: A Prospective Cohort Study. *PLoS Medicine*, *12*(3). https://doi.org/10.7307/ptt.v30i2.2989

Tan, S. H., Roth, M., and Velasco, E. (2017). Particle exposure and inhaled dose during commuting in Singapore. *Atmospheric Environment*, 170, 245–258. https://doi.org/10.1016/J.ATMOSENV.2017.09.056.

Tartakovsky, L., Baibikov, V., Czerwinski, J., Gutmana, M., Kasper, M., Popescu, D., Veinblata, M. and Zvirina, Y. (2013). In-vehicle particle air pollution and its mitigation. *Atmos. Environ*. 64, 320–328.

Thorpe, A. and Harrison, R.M. (2008). Sources and properties of non-exhaust particulate matter from road traffic: A review. *Sci. Total Environ*. 400, 270–282. doi:10.1016/j.scitotenv.2008.06.007.

Tian, R., Ning, D., He, Z., Zhang, P., Spencer, S. J., Gao, S., et al. (2020). Small and mighty: Adaptation of superphylum Patescibacteria to groundwater environment drives their genome simplicity. *Microbiome*. https://doi.org/10.1186/s40168-020-00825-w.

Tignat-Perrier, R., Dommergue, A., Thollot, A., Magand, O., Amato, P., Joly, M., et al. (2020). Seasonal shift in airborne microbial communities. *Science of the Total Environment*. https://doi.org/10.1016/j.scitotenv.2020.137129.

TMB, 2018. https://www.tmb.cat/documents/20182/111197/NOTICIES-NOVA-XARXA-BUS-20120523-TRANSPORT.pdf/37f4bca7-d018-4e73-9da3-f9cee5842448

Triadó-Margarit, X., Veillette, M., Duchaine, C., Talbot, M., Amato, F., Minguillón, M. C., Martins, V., de Miguel, E., Casamayor, E. O., and Moreno, T. (2016). Bioaerosols in the Barcelona subway system. *Indoor Air*, *May*, 1–12. https://doi.org/10.1111/ina.12343

Uk Lee, B., Lee, G., and Joon Heo, K. (2016). Concentration of culturable bioaerosols during winter. *Journal of Aerosol Science*, *94*, 1–8. https://doi.org/10.1016/j.jaerosci.2015.12.002

Uetake, J., Tobo, Y., Uji, Y., Hill, T. C. J., DeMott, P. J., Kreidenweis, S. M., and Misumi, R. (2019). Seasonal changes of airborne bacterial communities over Tokyo and influence of local meteorology. *Frontiers in Microbiology*. https://doi.org/10.3389/fmicb.2019.01572.

United Nations, Department of Economic and Social Affairs (UN DESA) (2019) The World Urbanization Prospects: The 2018 Revisions, New York

Veillette, M., Knibbs, L. D., Pelletier, A., Charlebois, R., Blais Lecours, P., He, C., ... and Duchaine, C. (2013). Microbial contents of vacuum cleaner bag dust and emitted bioaerosols and their implications for human exposure indoors. *Applied and Environmental Microbiology*, *79*(20), 6331-6336. https://doi.org/10.1128/AEM.01583-13

Viana M., Chi X., Maenhaut W., Querol X., Alastuey A., Mikuška P. and Vecera Z. (2006). Organic and elemental carbon concentrations during summer and winter sampling campaigns in Barcelona, Spain. *Atmospheric Environment* 40, 2180-2193.

Vouitsis, I., Taimisto, P., Kelessis, A., and Samaras, Z. (2014). Microenvironment particle measurements in Thessaloniki, Greece. *Urban Climate,* 10, 608–620. doi:10.1016/j.uclim.2014.03.009

Wåhlin, P., Berkowicz, R., and Palmgren, F. (2006). Characterisation of Traffic-Generated Particulate Matter in Copenhagen. *Atmos. Environ*.40:2151–2159.

Wang, H., Fu, L., Zhou, Y., Du, X., and Ge, W. (2010). Trends in vehicular emissions in China's mega cities from 1995 to 2005. *Environmental Pollution*, *158*(2), 394–400. https://doi.org/10.1016/j.envpol.2009.09.002

Warneck, P. (1988). Chemistry of the natural atmosphere, 2nd ed, Chemistry of the Natural Atmosphere. *Academic Press*, San Diego, California.

Wehner, B., and Wiedensohler, A. (2003). Long term measurements of submicrometer urban aerosols: statistical analysis for correlations with meteorological conditions and trace gases. *Atmos. Chem. Phys* 3, 867–879, https://doi.org/10.5194/acp-3-867-2003

Wehner B., Uhrner U., von Löwis S., Zallinger M. and Wiedensohler A. (2009). Aerosol number size distributions within the exhaust plume of a diesel and a gasoline passenger car under

on-road conditions and determination of emission factors. *Atmospheric Environment* 43, 6, 1235-1245.

Weichenthal, S., Van Ryswyk, K., Kulka, R., Sun, L., Wallace, L., and Joseph, L. (2014). In-Vehicle Exposures to Particulate Air Pollution in Canadian Metropolitan Areas: The Urban Transportation Exposure Study. *Environmental Science and Technology*, 49(1), 597–605. doi:10.1021/es504043a

White, W.H. (2008). Chemical markers for sea salt in IMPROVE aerosol data. *Atmos. Environ*. 42, 261–274. doi:10.1016/j.atmosenv.2007.09.040.

WHO (2013). Review of evidence on health aspects of air pollution – REVIHAAP Project. Copenhagen, Denmark.

WHO (2016). Ambient Air Pollution: A global assessment of exposure and burden of disease. In *World Health Organization*. https://doi.org/9789241511353

WHO (2021). WHO global air quality guidelines. Particulate matter ($PM_{2.5}$ and PM_{10}), ozone, nitrogen dioxide, sulfur dioxide and carbon monoxide. Geneva: World Health Organization; 2021.

Williams, R. D., and Knibbs, L. D. (2016). Daily personal exposure to black carbon: A pilot study. *Atmospheric Environment,* 132, 296–299. doi:10.1016/j.atmosenv.2016.03.023

Xing, L., Wang, L. and Zhang, R. (2018). Characteristics and health risk assessment of volatile organic compounds emitted from interior materials in vehicles: a case study from Nanjing, China. *Environ. Sci. Pollut. Res. Int*. 25 (15), 14789–14798.

Yang, F., Kaul, D., Wong, K., Westerdahl, D., Sun, L., Ho, K., Tian, L., Brimblecombe, P. and Ning, Z. (2015). Heterogeneity of passenger exposure to air pollutants in public transport microenvironments. *Atmos. Environ*. 109, 42–51.

Yang, C., Brown, C.E., Hollebone, B., Yang, Z., Lambert, P., Fieldhouse, B., Landriault, M. and Wang, Z. (2017). Chemical fingerprints of crude oils and petroleum products. In: Fingas, Mervin (Ed.), In Book: Oil Spill Science and Technology, second ed. Gulf Professional Publishing, *Elsevier* Inc., pp. 209–304. https://doi.org/ 10.1016/B978-0-12-809413-6.00004-7 Chapter: 4.

Yu, S., Zhu, Y. G., and Li, X. D. (2012). Trace metal contamination in urban soils of China. *Science of the total environment*, *421*, 17-30. https://doi.org/10.1016/j.scitotenv.2011.04.020

Yue, T., Yue, X., Chai, F., Hu, J., Lai, Y., He, L. and Zhu, R. (2017). Characteristics of volatile organic compounds (VOCs) from the evaporative emissions of modern passenger cars. *Atmos. Environ*. 151, 62–69.

Zecchin, S., Mueller, R. C., Seifert, J., Stingl, U., Anantharaman, K., von Bergen, M., et al. (2017). Rice paddy nitrospirae carry and express genes related to sulfate respiration: Proposal of the New Genus ‘‘Candidatus Sulfobium.’’ *Applied and Environmental Microbiology*, 84(5), e02224-e2317. https://doi.org/10.1128/AEM.02224-17.

Zeng, Q.-Y., Westermark, S.-O., Rasmuson-Lestander, A., and Wang, X.-R. (2006). Detection and quantification of Cladosporium in aerosols by real-time PCR. *Journal of Environmental Monitoring*, 8, 153–160.

Zhang, Q., and Zhu, Y. (2010). Measurements of ultrafine particles and other vehicular pollutants inside school buses in South Texas. *Atmospheric Environment*, *44*(2), 253–261. https://doi.org/10.1016/J.ATMOSENV.2009.09.044

Zhang, Q., Fischer, H., Weiss, R. and Zhu, Z. (2013). Ultrafine particle concentrations in and around idling school buses. *Atmos. Environ*. 69, 65–75.

Zhu, Y., Eiguren-Fernandez, A., Hinds, W. and Miguel, A. (2007). In-cabin commuter exposure to ultrafine particles on Los Angeles freeways. *Environ. Sci. Technol*. 41, 2138–2145.

Zhu, Y., Wu, Z., Park, Y., Fan, X., Bai, D., Zong, P., Qin, B., Cai, X. and Ahn, K.H. (2019). Measurements of atmospheric aerosol vertical distribution above North China Plain using hexacopter. *Sci. Total Environ*. 665, 1095–1102.

Zuurbier, M., Hoek, G., Oldenwening, M., Lenters, V., Meliefste, K., van den Hazel, P. and Brunekreef, B. (2010). Commuters’ exposure to particulate matter air pollution is affected by mode of transport, fuel type, and route. *Environmental Health Perspectives*, 118(6), 783–789. https://doi.org/10.1289/ehp.0901622